Haem scavenging by pathogenic *Neisseriaceae* bacteria through haemoglobin receptor HpuAB

By
Daniel Oluwatosin Akinbosede

Thesis submitted for the degree of Doctor of Philosophy

Biochemistry and Biomedicine

School of Life Sciences

University of Sussex Falmer

UK

July 2022

Declaration

I hereby declare that this thesis has not been and will not be, submitted in whole or in part to another University for the award of any other degree.

Signature: .....

Acknowledgements

I would like to dedicate this thesis to my late friend and supervisor, Dr Stephen Hare. Over the years, Stephen's compassion, empathy and friendship were some of the most important and steadfast parts of my studies and my life. There is no doubt that Stephen was exceptional in many ways. He was a principled man who was as committed to his family and his faith as he was to his science. So it is of no surprise that in the lab, he always treated his people like family too. In our research endeavours, Stephen constantly showed himself as an intelligent, patient and kind supervisor. In the lowest moments of my time at Sussex, he reassured me that I was capable and always did everything he could to help me succeed. For this, I will always be indebted to him. He will live forever in my heart and mind.

I am also grateful to the rest of our 2C corridor family. To Mark, thank you for stepping in to get me over the finish line. To Pascale, thank you for your patience, skill, and perseverance as a microscopy teacher to a beginner microscopist. To Frankie, Hayley and Ali, I literally wouldn't be here without you. To Tracy, Simon and Zahid, your encouragement and support have been invaluable and your humour uplifting.

To my family, this achievement is more yours than it is mine. To my mum (Felicia) and dad (Taiwo), every experiment, every micrograph, and every word written was only possible because of the unconditional love and support you have blessed me with my whole life. To my siblings (Darius and Anu), you man have to call me Dr now, hold that. To all my aunties, uncles, cousins, and grandparents, you're the best family anyone could ask for and I hope this thesis makes you all proud.

To my friends, I'll always be grateful for the emotional support you've all provided over a very difficult four years. To Kanekwa, thank you for being there and encouraging me the whole way. To Meena and Dami, thank you for always making the time for me. No man is an island, and more people have contributed to the completion of this thesis than is possible to name here. I am so incredibly lucky to have you all and the love and support you continue to provide me. Thank you, thank you, thank you.

A kì í gbé àwòrán gàgàrà ká má fi ọwó ẹ ti nnkan.
One does not carve a tall statue without resting their hand on something
(Yoruba Proverb)

Dr Stephen Hare
12.03.1981 – 13.12.2021

Contents

List of figures

List of tables

Abbreviations

ABC – ATP binding cassette

CD – Circular dichroism

CF – Cystic fibrosis

CMC – Critical micelle concentration

DM – n-decyl-b-D-maltopyranoside

DMM – dodecyl-b-D-maltomaltpyranoside

DPPC – Dipalmitoylphosphatidylcholine

EM – Electron microscopy

GFP – Green fluorescence protein

Hal – Haem-acquisition leucine-rich repeat

Hb – Haemoglobin

Hb: Hp – Haemoglobin Haptoglobin complex

HID – Haemoglobin interacting domains

HmBP – Haemin binding protein

Hp – Haptoglobin

IB – Inclusion bodies

IEX – Ion exchange chromatography

IM – Inner membrane

IMAC – Immobilised Metal Affinity Chromatography

IMD – Invasive meningococcal disease

Isd – Iron-regulated surface determinant

ITC – Isothermal titration calorimetry

LDAO – Lauryl dimethylamine oxide

met-Hb – met-haemoglobin

MP – Membrane protein

MSP – Membrane Scaffold Protein

MST – Microscale thermophoresis

NEAT – NEAr Transporter

NICE – National Institute of Health and Care Excellence

NMR – Nuclear magnetic resonance

NHS – N – Hydroxysuccinimide

NSEM – Negative stain electron microscopy

NTHI – Non-typable strains of *H. influenzae*

OG – n-octyl-b-D-glucopyranoside

OM – Outer membrane

ORF – Open reading frame

oxy-Hb – oxy-haemoglobin

PCR – Polymerase Chain Reaction

PFA – Paraformaldehyde

PHE – Public Health England

POI – Protein of interest

POPC – 1-palmitoyl-2-oleoyl-glycerol-3-phosphocholine

PVDF – Polyvinylidene fluoride

ROSET – Rational surveillance and energy transfer

SANS – Small-angle neutron scattering

SAXS – Small-angle X-ray scattering

SEC – Size Exclusion Chromatography

Shp – Surface exposed haem binding protein

Shr – Streptococcal haemoprotein receptor

SMA – Styrene maleic acid

SMALP – Styrene Maleic Acid Lipid Particles

TBDT – Ton-B dependent transporter

WHO – World Health Organisation

WT – Wild type

Abstract

The *Neisseriaceae* family of bacteria is home to the genus of *Neisseria* which contain two relevant pathogens in humans, Neisseria meningitidis and *Neisseria gonorrhoeae*. *N. meningitidis* is responsible for bacterial meningitis and a death toll of tens of thousands globally per annum. *N. gonorrhoeae* is responsible for the sexually transmitted infection gonorrhoea, classed by the World Health Organisation amongst the 'HIGH' priority bacterial pathogens, where new therapies are urgently needed to fight antibiotic resistance. Key to developing new therapies is the understanding and exploitation of bacterial nutrient acquisition systems within the host. *Neisseria* can utilise haemoglobin and the haemoglobin-haptoglobin complex as an additional iron source through the haemoglobin-binding TonB-dependent receptor HpuAB. The specifics of HpuAB functionality on a structural level is poorly understood. Significant progress was made by Wong et al. (2015) who described the structure and binding capabilities of HpuA, an extracellular lipoprotein that works in partnership with HpuB to facilitate the iron acquisition. For this system to be completely understood, similar structural and functional analysis must also be carried out for HpuB.

In this project, HpuB was recombinantly produced in *E. coli* then extracted, solubilised, and reconstituted into a range of membrane memetics to facilitate downstream studies. Through pull down assays, recombinantly produced HpuB was shown to bind Hb and mutagenic analysis of HpuB's flexible extracellular loops demonstrated that they are key to Hpub's Hb binding capabilities. Electron microscopy (EM) was used for structural characterisation of HpuB in nanodiscs, peptidiscs and amphipols. Amphipol solubilised HpuB particles revealed interesting structural insights through 2D and 3D averaging and reconstruction. This sample was taken forward for cryo-EM screening.

In this work, optimisation and development of methodologies to express, purify and reconstitute HpuB for downstream studies was undertaken resulting a pathway to cryoEM structure utilising amphipols as a workable membrane memetic.

CHAPTER 1: GENERAL INTRODUCTION

1.1 – *Neisseriaceae*

Neisseriaceae are a group of mostly non-pathogenic Gram-negative and aerobic bacteria that are often found as a part of mammalian flora. Within the family of *Neisseriaceae* lies the genus of *Neisseria,* which is comprised of mostly non-pathogenic bacteria that form a significant part of the human microbiome (G. Liu et al., 2015). The genus includes at least eleven species that colonise humans, two of which are pathogenic. Whilst their respective infections present very different symptoms, *Neisseria meningitidis* and *Neisseria gonorrhoeae* are closely related, with DNA sequence identity of between 80 and 90% (Tinsley & Nassif, 1996). *N. meningitidis* is able to colonise the nasopharynx and can lead to rapidly fatal symptoms such as high fever, inflammation of the meninges and sepsis if not promptly treated with appropriate antibiotics (Coureuil et al., 2012). *N. gonorrhoeae* is the pathogen responsible for the sexually transmitted infection gonorrhoea and infects via the mucosal membranes of the reproductive tract. Where present, symptoms of gonorrhoea include discharge from infected genitalia, however, the infection is often asymptomatic, particularly in female patients. If undetected and untreated, *N. gonorrhoeae* infections may ascend the reproductive tract and develop into pelvic inflammatory disease and potentially cause infertility (Kamwendo et al., 1996). There is currently growing concern about the rise of antibiotic resistance in *N. gonorrhoeae* (Bodie et al., 2019)

1.1.1 - *Neisseria meningitidis*

N. meningitidis can be accurately described as a 'fastidious, encapsulated, aerobic Gram-negative diplococcus'. It infects hosts by colonising their mucosal surfaces with an assortment of mechanisms utilising its pili, lipooligosaccharides, other surface proteins and twitching motility (Rouphael & Stephens, 2014). *N. meningitidis* has twelve identified serogroups, six of which (A, B, C, W, X, and Y) have been responsible for virtually all invasive disease cases (Guedes et al., 2022). Data regarding the epidemiology of meningococcal infections always draws an unusual picture as its prevalence is often uneven and presents itself as a periodic and epidemic disease. Based on previous World Health Organisation (WHO) data, there are around 1.2 million meningococcal infections worldwide per annum, proving fatal around 10-15% of the time, with a death toll of approximately 135,000/yr. The 20th-century incidence rate in Europe was two per 100,000, and an increase to five per 100,000 prompted the United Kingdom (UK) to be the first country in the world to adopt a vaccine for the meningococcal serogroup C in 1999 (Rouphael & Stephens, 2014). More recent data from Public Health England (PHE) shows that the incidence rate of invasive meningococcal disease (IMD) in England stayed stable at one per 100,000 in 2017/2018, although incidence amongst infants increased from 11 per 100,000 population in 2016/2017 to 16 per 100,000 in 2017/2018 (Public Health England, 2017). Even when meningococcal diseases do not result in death, they can leave the surviving patient with serious impairments such as limb loss, hearing loss, visual impairment, educational difficulties, developmental delays, motor nerve deficits and behavioural problems (Whittaker et al., 2017). A recent review on the epidemiology of invasive meningococcal disease and sequelae in the United Kingdom during the period 2008 to 2017 by Guedes et al concluded that despite the availability of routine vaccination programs, meningococcal disease continues to pose a significant burden in the UK healthcare system. Optimization of vaccination programs may be required to reduce the disease burden (Guedes et al., 2022).

1.1.2 - *Neisseria gonorrhoeae*

N. gonorrhoeae is the pathogen responsible for the sexually transmitted infection (STI) gonorrhoea, colloquially referred to as 'the clap'. A global and ancient disease attested with biblical references, gonococcal infections affect millions of people worldwide and are the second most common bacterial STI in England with over 126 diagnoses per 100,000 people in 2019, up from 29 per 100,000 in 2008 (Public Health England, 2017). Although this number went down to 101 per 100,000 in 2020, PHE has attributed this decrease to the response to the COVID19 pandemic. The general overall increase in infection in recent years is in part attributed to the continual rise of antibiotic resistance in the pathogen, resulting in infections now referred to as 'super gonorrhoea'. Antibiotics have been used to treat gonococcal infections since their advent and treatments have been ever-changing as new resistant strains emerge.

The urgent nature of the antibiotic resistance crisis in gonococcal infections is illustrated in Figure 1.1. The image shows the different groups of antibiotics used in treatment over the past ~80 years and the mechanisms of resistance the pathogen has developed to circumvent drug action. Ceftriaxone is part of the cephalosporin antibiotic family which works by interrupting cell wall biosynthesis through attachment to penicillin-binding proteins (Livermore, 1987). Although Ceftriaxone was once a powerful tool to tackle increasingly resistant *N. gonorrhoeae* strains, there is now well-documented resistance to this drug too. The most common mechanism for resistance is an alteration of the *penA* gene encoding penicillin-binding protein 2 (Ohnishi et al., 2011). The current recommended treatment from the National Institute of Health and Care Excellence (NICE) is a dual antibiotic approach of ceftriaxone and azithromycin due to the level of resistance now documented in emerging strains, cementing the superbug status of *N. gonorrhoeae.* It is now a seemingly unavoidable reality that we could soon be facing untreatable gonococcal infections in large numbers, which underlines the paramount importance of developing new ways to treat or prevent infection.

Although a gonococcal infection is not usually lethal, prolonged infection can lead to life-changing consequences, such as infertility. The symptoms vary between men and women depending on the site of infection. For women, infection at the endocervix is asymptomatic in 50% of cases, though patients who do have symptoms will present altered vaginal discharge in 50% of cases and lower abdominal pain in up to 25% of cases (Bignell & Fitzgerald, 2011). Infected men will present urethral discharge in over 80% of cases and dysuria in over 50% of cases, usually within two to five days of exposure to an infected sexual partner. Pharyngeal infections for both men and women are usually asymptomatic (Bignell & Fitzgerald, 2011).

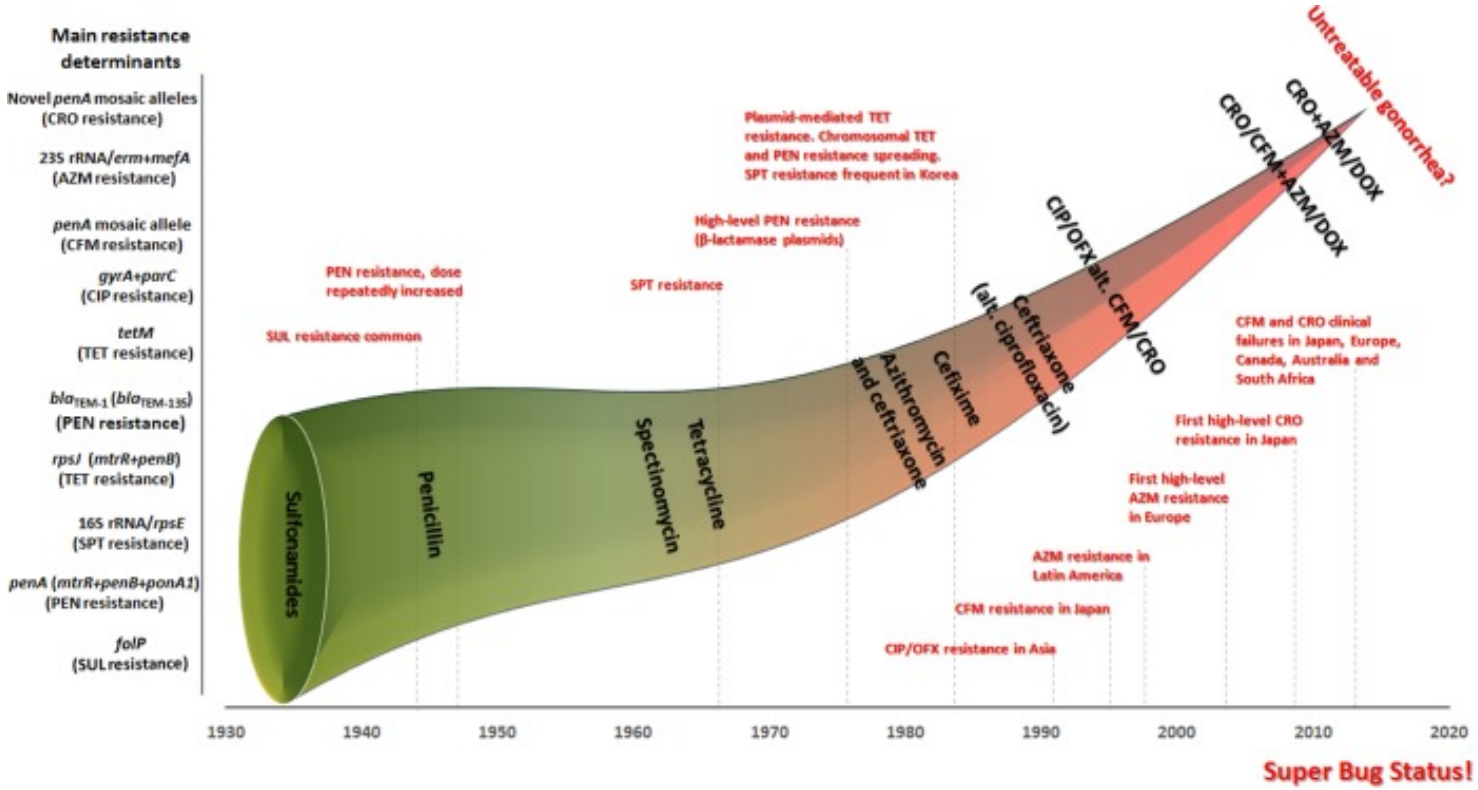

Figure 1.1: N. gonorrhoeae antibiotic resistance over time.
An image showing the history of antibiotics and antibiotic combinations used to treat gonococcal infections since the advent of antibiotics. The image also shows the resistance determinants responsible for resistance to each antibiotic (Unemo & Shafer, 2014). Permission granted by copyright holder.

1.2 – The importance of iron

As well as being the most abundant transition metal in living organisms and the environment, iron is a crucial metal for many biological processes. The vital necessity of iron is best demonstrated by its central role in the ubiquitous respiratory cytochromes, whose early discovery illustrates their pervasive importance to life (Munn & Foster, 1886; Keilin & Hardy, 1925), but it is also a co-factor for many other essential enzymes, such as class I ribonucleotide reductase, and aromatic amino acid hydroxylases (Jordan & Reichard, 1998; Fitzpatrick, 1999).

Iron's utility in biological processes is likely due to its stability in ferric (Fe^{3+}) and ferrous (Fe^{2+}) states and considerable redox potential. However, free ferric iron generally forms highly insoluble oxides and can be described as biologically inert in most cases. This great redox potential does come with some negatives, as iron ions can catalyse the production of highly reactive hydroxide radicals via the Fenton reaction. These hydroxide radicals are involved in several destructive processes when they react with biomolecules such as DNA and lipids. To mitigate this potential toxicity, a carefully balanced range of regulatory processes prevent hosts from reaching toxic concentration levels of iron. These regulatory processes are broadly referred to as iron homeostasis and include uptake, storage and excretion (Wallace, 2016).

1.3 – Bacterial iron homeostasis

Iron homeostasis allows bacteria to control the cellular concentration of iron and involves a treasure chest of regulatory mechanisms including:

1. Production of iron-chelating compounds (siderophores) to scavenge iron from the surroundings.
2. Storage of intracellular iron, allowing stores to be drawn on when external supplies are limited.
3. Downregulation of proteins that utilise or contain iron under iron-restricted conditions.
4. Redox stress response systems that respond to iron-dependent generation of reactive oxygen species.

The balancing of these regulator systems largely depends on the amount of iron available in the external environment. Although iron is abundant in most bacterial environments, it is often inaccessible due to its poor solubility in the ferric Fe^{3+} form or its sequestration by host proteins. In many bacteria, the ferric uptake regulator (Fur) protein plays a key role in controlling iron-responsive transcription of genes involved in iron homeostasis, including those involved in the production of siderophores and iron transporters (Choi & Ryu, 2019).

The Fur protein is found in most prokaryotes and binds to highly conserved 19 bp DNA sequences, known as the 'Fur box', and uses ferrous iron (Fe^{2+}) as a co-repressor to bind to the promoter region of genes related to iron acquisition (Kaushik et al., 2016). The binding of Fur to the Fur box blocks RNA polymerase from binding to the relevant promoter, repressing the transcription of one or more downstream genes. Under iron limiting conditions, Fur is unable to bind DNA which leads to the induction of gene expression (Noinaj et al., 2010).

In addition to Fur, there are other examples of Fe-dependent transcriptional regulators, including some Extra cytoplasmic Function (ECF) σ factors. ECF σ factors are ubiquitous in prokaryotes and are involved in the regulation of many genes particularly the genes which encode periplasmic and OM proteins. FecI is an ECF σ factor involved in the regulation of the *fecABCDE* operon in *E.coli* in a process that starts with responding to a signal created by the binding of ferric citrate to FecA (Ochs et al., 1995).

Although bacteria and especially bacterial human pathogens have an essential need for iron, the accumulation of excess levels of iron can be toxic so bacteria have developed to keep cellular iron levels under strict regulatory control.

1.3.1 - Intracellular iron stores

Both pathogenic and non–pathogenic bacteria deposit intracellular iron reserves within iron storage proteins (Andrews, 1998). These stores are later used to enhance growth when the availability of external iron is limited. There are three types of iron storage proteins recognised in bacteria: conventional ferritins which are also found in eukaryotes, bacterioferritins which contain haem and are only found in eubacteria and Dps proteins which are smaller. Structurally, ferritins and bacterioferritins are ~500 kDa and composed of 24 identical or similar subunits which form a protein shell with an internal cavity, functioning as a reservoir for iron storage which can accommodate 2000 – 3000 iron atoms per 24-mer. Dps protein shells, ~250 kDa, are made up of 12 identical or similar subunits which have a lower capacity of just ~500 iron atoms per 12-mer (Andrews et al., 2003).

The specific roles that these storage proteins are varied. Inactivation of the ferritin, FtnA, from *E. coli* resulted in a 50% reduction in stationary-phase cellular iron content following growth under iron-sufficient conditions and a reduction in growth rate under

iron-limiting conditions (Abdul-Tehrani et al., 1999). Conversely, Dps is understood to play a dual role. In addition to storing iron, in E. coli, Dps is also implicated in protecting DNA against the potentially damaging actions of ferrous iron and H_2O_2 in the production of hydroxyl free radicals (Zhao et al., 2002).

1.3.2 - Redox stress resistance

Just as important as acquiring iron from the local environment is the need to ensure that intracellular iron is maintained in a safe, non-toxic form. Thus, cellular iron must be prevented from unrestricted interaction with reactive oxygen species. Reactive oxygen species, which are only mildly reactive physiologically, react with iron to form the highly reactive and dangerous hydroxyl radical. An important *in vivo* mediator of iron reduction during iron-based redox stress are flavins (Woodmansee & Imlay, 2002). Flavins are a family of compounds with the basic structure of 7,8-dimethyl-10-alkylisoalloxazine (Edwards, 2014). Flavins have enormous redox potential and can alternate between three redox forms: oxidised, one-electron reduced, or two-election reduced, allowing them to mediate electron transfers and electron bifurcation processes (Sepúlveda Cisternas et al., 2018). As a result, redox stress is increased by events which favour the accumulation of reduced flavins, incapable of acting on hydroxyl radicals. An example of a ROS defence protein that is linked to iron homeostasis is the iron-dependent superoxide dismutase SodB in *E. coli*. Fur controls *sodB* indirectly via its negative regulation of a small regulatory RNA RhyB. Under iron-replete conditions Fur binds to a Fur Box to repress *rhyB* expression; under these conditions, *sodB* is expressed. However, iron depletion leads to the production of RhyB, which binds to the sodB mRNA to prevent its translation (Massé et al., 2005; Jackson et al., 2010).

1.4 – Nutritional immunity

During infection, pathogens are entirely reliant on nutrients sourced from their host. So much so, that mammalian hosts, including humans, have developed several mechanisms to sequester trace minerals to restrict the growth of infecting microorganisms. Circulating iron levels are further depleted upon infection and neutrophil granules of neutrophils contain high levels of the iron-sequestering protein lactoferrin to release at sites of inflammation. This process is referred to as nutritional immunity (Hood & Skaar, 2012; Cassat & Skaar, 2013). Both iron homeostasis and nutritional immunity create significant barriers for invading pathogens. Consistent with the Red Queen hypothesis, which suggests that direct competition is a driving force of evolution, pathogens have evolved an array of nutrient piracy mechanisms to counter nutritional immunity and to scavenge for free nutrients and even acquire nutrients from host proteins. Many human pathogens, including both clinically relevant *Neisseria* pathogens have evolved mechanisms to evade these barriers. This chapter will outline some of the systems deployed by bacterial pathogens to circumvent host nutritional immunity, specifically those that utilise haemoglobin (Hb) as an iron source. Several reviews have been written about similar topics and have focussed on the whole haem uptake process in Gram negative bacteria (Richard et al., 2019), on the system employed by *Staphylococcus aureus* and other Gram positive organisms (Skaar & Schneewind, 2004; Grigg et al., 2010; Ellis-Guardiola et al., 2021; Maresso & Schneewind, 2006; Hammer & Skaar, 2011; Haley & Skaar, 2012) on the structural aspects of the haemoprotein receptors (Hare, 2017), or give a brief overview of bacteria-haemoglobin interactions (Pishchany & Skaar, 2012). The intricacies of the diverse systems described here are unique, but the broader picture is familiar across the board: Hb is bound at the cell surface, haem is released and transported across the cell wall, haem is imported into the cell via an ABC transporter then degraded to release free iron for oxidative use by the cell.

1.5 – Haem, Haemoglobin and iron availability in humans

1.5.1 - Haemoglobin

Haemoglobin (Hb) is probably the most famous protein in the world. Knowledge of its role in transporting oxygen around our bodies and the bright red colour it gives to blood is ubiquitous. Aside from this erythrocytic role, Hb has also been found in macrophages, alveolar epithelial cells and certain kidney cells, where it is proposed to function in reducing oxidative stress, and also in oligodendrocytes and some neurones, where it may act as an oxygen store (Newton et al., 2006; Biagioli et al., 2009). Another lesser-known feature of Hb is its exploitation as a nutrient source by a substantial cohort of pathogens to support their survival, growth and virulence. Pirating essential elements from such a prominent source allows bacteria to circumvent the nutritional immunity employed as a defence mechanism by their hosts (Núñez et al., 2018).

The utilisation of Hb and other serum proteins to promote survival and virulence is well documented for many pathogens, both eukaryotic and prokaryotic, which rely on host proteins for one nutrient in particular: iron (Barber & Elde, 2015; Gunn et al., 2018). In the case of Hb, the iron comes in the form of haem. The use of this iron chelating compound ensures Hb is the largest iron source in the human body and is central to the ways in which some pathogens acquire iron within human hosts.

Structurally, Hb is a tetrameric polypeptide in erythrocytes comprising two alpha and two beta subunits, with each peptide chain containing one haem group (Perutz et al., 1960). The haem group is a prosthetic porphyrin ring and acts as an oxygen sequestering metal complex where iron is the central component. The release of Hb from erythrocytes during haemolysis increases the rate of oxidation of the Fe^{2+} centre, resulting in the oxidative change to met-haemoglobin (met-Hb). Met-Hb is the metalloprotein form in which the haem group iron is oxidised to the ferric (Fe^{3+}) state and oxy-Hb refers to Hb bound to oxygen. The most relevant form of Hb for invading pathogens is likely to be

met-Hb, because, unlike oxy-haemoglobin (oxy-Hb) which is mostly found in intact erythrocytes, met-Hb is more likely to be accessible to bacterial pathogens. The presence of four haem compounds per Hb molecule renders the protein both efficient at transporting oxygen and a very desirable target for invading pathogens with a requirement for an exogenous iron source.

1.5.2 - Haem

A large majority (70%) of the iron in the human body is bound to haem. This haem is largely inaccessible to invading pathogens due to its secluded situation in the Hb subunit. Spontaneous or induced lysis of erythrocytes releases free Hb into the serum, which, as well as the conversion to met-Hb, typically sees the tetrameric protein break up into two dimers of one alpha and one beta subunit apiece. The dissociation of Hb implicates the rate at which haem is released into solution. Haem dissociates from monomeric and dimeric Hb subunits much quicker than from the tetramer (Hargrove et al., 1997; Hargrove et al., 1994). This is one of the reasons why the Hb dimers are quickly and tightly bound by haptoglobin (Hp), in the first stage of eventual recycling by macrophages and hepatocytes (Table 1.1) (Kristiansen et al., 2001). Hp is a liver synthesized plasma glycoprotein that is reported at an average concentration of 150 mg/mL in human adults (Salvatore et al., 1987). Further degradation of Hb leads to a release of free haem, which is associated with cytotoxicity and oxidative damage. The potential toxicity of these events is mitigated in part by the proteins haemopexin and serum albumin in their role in efficiently mopping up the free haem (Table 1.1) (Tolosano et al., 2010).

Table 1.1: Concentrations and ligand affinities of serum proteins that play a role in scavenging haem and Hb.
A small amount of extraerythrocytic -Hb is present in healthy individuals, but this is rapidly bound by haptoglobin. Any haem that is released from Hb will be bound with very high affinity by haemopexin, or by the abundant albumin. Together, these proteins protect from haem-mediated oxidative damage and restrict pathogens' access to haem as an iron source

Haemoprotein	**Plasma concentration (mg/ml)** *	**Ligand**	**Dissociation constant (K_D) (M)**
Haemoglobin	0 - 0.4 (Na et al., 2005)	Haem	10^{-12} - 10^{-16} (Banerjee, 1962)
Haptoglobin	0.3 - 2.1 (Shinton et al., 1965)	Haemoglobin	$<10^{-15}$ (Hwang & Greer, 1980)
Serum albumin	34 - 54 †	Haem	10^{-8} (Muller-Eberhard et al., 1968)
Haemopexin	1-2 (Muller-Eberhard et al., 1968)	Haem	$<10^{-13}$ (Hrkal et al., 1974)

* Extraerythrocytic concentration range in healthy individuals
† Normal concentration range for serum albumin tests

1.6 – Use of haemoglobin by pathogenic Gram-positive bacteria

The single lipid bilayer and thick peptidoglycan layer of Gram-positive bacteria serve both structural and functional purposes. In the business of pirating Hb for haem, it presents unique challenges. These challenges are bypassed using transmembrane ABC transporters, which are typically made up of a haem binding protein, permease and ATPase. These proteins along with a variety of extracellular and surface-attached proteins reach beyond the cell wall for direct contact with Hb. This section will explore the details of and make comparisons between examples of these systems.

1.6.1 - *Corynebacterium diphtheriae*

Corynebacterium diphtheriae is a Gram positive, nonmotile human pathogen. It is the causative agent of the disease diphtheria and the production of the Diphtheria toxin, which is one of the most extensively studied bacteria toxins in history and is iron-regulated (Schmitt & Holmes, 1991; Pappenheimer, 1977). *C. diphtheriae* infects by colonising the mucosal surfaces of the pharynx and the toxin is responsible for symptoms such as nausea, swollen glands and difficulty breathing and swallowing. Among Gram positive bacteria, *C. diphtheriae* was the first to have a haem utilising protein characterised. HmuO was discovered via its homology with eukaryotic haem oxygenases and its ability to restore haem utilisation to *C. diphtheriae* mutants previously unable to use haem and Hb as iron sources (Schmitt, 1997). Haem oxygenase proteins, such as HmuO, are essential for accessing the iron embedded within haem once in the cytoplasm and are widespread among Hb-utilising pathogens, however, this review will focus mainly on the Hb binding events at the cell surface.

Haem acquisition in *C. diphtheriae* also depends on a haem-specific ABC transporter system named HmuTUV (Drazek et al., 2000). HmuTUV is able to transport haem acquired from a wide range of host haemoproteins as substrate, including Hb, the Hb:Hp complex and myoglobin (Bennett et al., 2015). HmuTUV is made up of 3 proteins; HmuT

which binds haem, HmuU which functions as a permease and HmuV the ATPase. These proteins work in sequence to bring haem into the cytoplasm.

The *hmuTUV* operon also includes *htaA* and neighbours the *htaB* gene both of which encode surface exposed haem binding proteins, HtaA and HtaB, of which HtaA is solely responsible for taking haem from haemoglobin, and HtaB binds free haem (Figure 1.2A) (Allen & Schmitt, 2009). HtaA has been shown to possess two functionally important domains, CR1 & CR2, both of which, when recombinantly expressed with glutathione S-transferase tags, were shown to bind haem through UV-visual spectroscopy. This work, however, did not demonstrate the ability of each domain to bind Hb itself. Using Hb-derived enzyme-linked immunosorbent (ELISA) assays, CR2 was shown to have a much higher affinity for Hb than CR1. Interestingly, it was also demonstrated through competitive binding studies that HtaA preferentially binds to Hb that is carrying haem. Alignment studies, followed by mutagenesis studies revealed two residues that are essential for CR2 domain binding to Hb; Y361 and H412. Beyond just binding Hb, *in vivo* assays involving the deletion of the Y361 residue revealed that it is essential for Hb utilisation via HtaA. These data overwhelmingly made the case for the importance of HtaA in the utilisation of Hb but it is still important to note that HtaA is able to transfer haem to HtaB (Allen & Schmitt, 2011), presumably to make the process of transport to the cell membrane more efficient.

The importance of HtaA & HtaB to haem acquisition in *C. diphtheriae* is now well documented. Additionally, the identification and characterisation of the CR domains of HtaA has been a useful tool in identifying other Hb binding proteins that are part of the *C. diphtheriae* haem acquisition system, such as ChtA, ChtB and ChtC. ChtA/ChtC are surface anchored proteins previously shown to have structural similarities to HtaA. ChtB meanwhile, although some evidence suggests that it binds Hb using a CR domain, it shows high levels of sequence similarities with the haem-binding HtaB. In fact, both ChtB and HtaB have been linked to haem transport due to significantly decreased haem

use in ChtB/HtaB double mutants (Allen et al., 2013). In 2015, Allen and Schmitt reported that double deletion mutants of ChtA and ChtC rendered *C. diphtheriae* incapable of acquiring haem from the Hb:Hp complex, although single deletion mutants of either protein resulted in wild type haem acquisition capabilities, suggesting redundancy between the proteins (Allen & Schmitt, 2015). HtaA and ChtaA/ChtC have a great deal in common. They have high sequence similarity and are similar in cellular location, size and structure. Their shared CR domains also allow all three proteins to bind both haem and Hb. These proteins however are not without their differences. Whilst HtaA is able to play a part in haem acquisition from Hb, Hb:Hp and myoglobin, ChtA/ChtC is only involved in haem acquisition from the Hb:Hp complex, suggesting these proteins must work in tandem with HtaA in Hb:Hp utilisation (Figure 1.2A) (Allen & Schmitt, 2015). In addition to the proteins possessing CR domains, *C. diphtheriae* is also able to bind Hb:Hp complex using HbpA, a recently identified surface exposed protein that is both secreted and anchored to the membrane. HbpA was identified due to proximity to a haem-responsive two-component signal transduction system and has been shown to be of significant importance in *C. diphtheriae* acquisition of haem from the Hb:Hp complex. Indeed, HbpA deletion mutants in iron-depleted media showed reduced ability to use the Hb:Hp complex as an iron source, while showing no difference in the use of Hb or haem. (Lyman et al., 2018)

In summary, HtaA, HtaB, ChtA and ChtC are surface-exposed proteins of *C. diphtheriae* and are able to bind host haemoproteins, starting the cascade of haem-passing interactions that follow; for example, HtaA to HtaB to HmuT then onto HmuUV for transmembrane transportation. The ability to use Hb as an iron source is not unique within the genus of *C. diphtheriae*. HtaA proteins can also be found in the horse pathogen *Corynebacterium pseudotuberculosis* (Ibraim et al., 2019) and the rarer cause of diphtheria in humans, *Corynebacterium ulcerans* (Drazek et al., 2000).

1.6.2 - *Staphylococcus aureus*

Staphylococcus aureus is a Gram positive bacteria found on approximately 25% of all humans as part of the skin or nasal flora (Kluytmans et al., 1997). *S. aureus* is also an opportunistic pathogen that can cause infection upon breaking through the skin barrier to cause a multitude of skin and blood infections. These include abscesses, boils, bacteraemia, endocarditis, pneumonia, empyema, osteomyelitis, toxin-mediated food poisoning, scalded skin syndrome, and toxic shock syndrome (Tong et al., 2015). *S. aureus* has an abundance of virulence factors it can use to cause infection upon invasion. It produces a variety of proteins and enzymes to aid in its survival in multiple niches.

Like most bacteria, *S. aureus* has developed systems for iron piracy in order to facilitate its survival in iron deficient environments. One of these systems comprises a series of iron-regulated surface determinant (Isd) proteins that work together to bind Hb, extract haem and transport it to the cell membrane for transport into the cytoplasm (Mazmanian et al., 2003; Skaar & Schneewind, 2004; Maresso & Schneewind, 2006; Haley & Skaar, 2012).

The Isd system of *S. aureus* is made up of four proteins which are anchored to the cell wall and work in canon - IsdA, IsdB, IsdC, IsdH (also known as HarA). Isd proteins found in the cell wall all possess a 'NEAr Transporter' otherwise known as NEAT domain (Ellis-Guardiola et al., 2021). NEAT domains are capable of binding haem and transferring it through a cascade of nearby Isd proteins toward the cell membrane. The Isd system also possesses another five proteins, IsdE, IsdF are embedded in the cell membrane and make up the ABC transporter essential for transporting haem into the cytoplasm, similar to HmuTUV of *C. diphtheriae*. IsdG and IsdI are haem oxygenases (similar to HmuO of *C. diphtheriae*) required for gaining access to the iron stored in the transported haem (Muryoi et al., 2008; Hammer & Skaar, 2011). IsdD, though previously suspected to interact with IsdE and IsdF in the ABC transporter cassette, currently has no known function (Grigg et al., 2010).

Of the haem-binding Isd proteins, IsdB was originally shown to be critical for binding Hb directly to the bacterial cell surface and for extricating the haem from it (Figure 1.2B). A 2008 study by Muryoi *et al* using magnetic circular dichroism spectra and electrospray ionization mass spectrometry data demonstrated that haem can be transferred from NEAT domains on IsdA, B or C to IsdE (Muryoi et al., 2008). It was reported that these transfer events happen in a unidirectional manner with IsdB and IsdH as potential starting points. In the IsdB pathway, IsdB is able to pass haem onto IsdA which passes it on to IsdC. The other pathway differs in that the haem can be sourced from intact Hb or the Hb:Hp complex, both of which bind the first NEAT domain of IsdH. The haem is released from the IsdH-bound Hb and is initially bound by the third NEAT domain of IsdH (Pilpa et al., 2009), which then passes haem on to IsdA, joining the same pathway as above. In both cases, the haem bound to IsdC is then passed on to IsdE - the haem binding protein of the Isd ABC transporter, responsible for transporting haem into the cytoplasm of the cell. In the scope of the experiments by Muryoi *et al*, it was reported that these haem transfers were unidirectional, where IsdE could only accept haem directly from IsdC and not IsdA. A second study confirmed the unidirectional transfer specifically using haem acquired from met-Hb; showing that IsdB strips haem from metHb via NEAT B2 and then transfers it to the membrane through the IsdA – IsdC – IsdE canon (Zhu et al., 2008). The lack of direct transfer between IsdA and IsdE, positions IsdC as an essential component of the haem transfer pathway. Interestingly, Pilpa *et al* in 2009 also observed a direct but less-efficient acquisition of haem from Hb by IsdC in vitro, suggesting that there may be additional flexibility in the system albeit the limited accessibility of IsdC would likely hamper this transfer further *in vivo* (Pilpa et al., 2009). In another interesting observation of the flexibility of the system, the two initial haem capturing proteins IsdH and IsdB could transfer haem bidirectionally exclusively amongst themselves (Figure 1.2B) (Muryoi et al., 2008). This is probably because both proteins are very closely related, and both possess at least two NEAT domains which are actively involved in the binding to Hb and stripping of haem as concluded by

crystallography analysis (Bowden et al., 2018). The transfer of haem between NEAT domains is highly specific and kinetics studies have shown that the transfer from IsdA to IsdC and IsdC to IsdE respectively happens >70,000 times faster and ~4-10 times faster than the spontaneous release of haem into a solvent, allowing for their classification as specific haem chaperones (Zhu et al., 2008; Ellis-Guardiola et al., 2021; M. Liu et al., 2008).

IsdB and its Hb utilising capabilities have also been identified as an important aspect of *S. aureus* virulence. *isdB* deletion mutants displayed a reduction in virulence in a murine model of abscess formation. This same reduction was not observed with *isdH* mutants, suggesting that IsdB facilitated haem piracy directly from Hb is crucial in full *S. aureus* virulence (Torres et al., 2006). By contrast, functional homologues of these NEAT proteins are not discernible in less virulent species of the *Staphylococcus* genus such as *S. epidermidis* and *S. saprophyticus*.

1.6.3 - *Streptococcus pyogenes*

Streptococcus pyogenes, also known as group A streptococcus, is a species of Gram positive, nonmotile cocci bacteria that is a member of the normal human nasopharyngeal flora. Immune evasion by *S. pyogenes* can lead to pathogenesis and cause local infections such as pharyngitis and scarlet fever, skin infections such as pyoderma and erysipelas, deeper soft tissue infections such as cellulitis and necrotising fasciitis (streptococcal gangrene), or systemic infections including streptococcal toxic shock syndrome (reviewed in (Walker et al., 2014)).

As a human pathogen, *S. pyogenes* is reliant on the human body for iron sources. *S. pyogenes* is able to bind and utilise free haem as well as several haem-carrying host proteins as iron sources, including Hb, myoglobin, and the Hb:Hp complex. The inability to use transferrin, lactoferrin or other iron-carrying host proteins as iron sources makes the haem utilisation of *S. pyogenes* even more significant. A 2003 study by Bates *et al* showed that haem and haemoprotein utilisation in *S. pyogenes* occurs via an ABC transporter, named SiaABC (streptococcal iron acquisition) also referred to as HtsABC (Bates et al., 2003). They demonstrated that nine clinical isolates of *S. pyogenes* bind Hb at the cell surface in a cell concentration-dependent manner by probing for Hb using a streptavidin alkaline phosphatase reporter system. The *siaABC* transporter genes are contained on an iron-regulated operon of ten genes, the first of which also encodes for a protein that is proposed to bind host haemoproteins. The researchers named this protein Shr (streptococcal haemoprotein receptor). Shr was shown to bind Hb, myoglobin and the Hb:Hp complex (but not Hp alone) through western blot analysis (Bates et al., 2003a) (Figure 1.2C). Shr deletion mutants exhibited decreased levels of growth in human blood and diminished virulence in zebrafish infection models demonstrating that the protein is paramount to *S. pyogenes* virulence (Fisher et al., 2008). Shr binds to Hb using two unique Hb interacting domains (HIDs), named HID1 and HID2. Like the Hb-binding IsdB from *S. aureus*, Shr also possesses two NEAT domains that work together to accept

haem from Hb. In the case of Shr, they are called NEAT 1 and NEAT 2 and are located in the N -terminal region of the protein (Macdonald et al., 2018). Another product of this operon, Shp (Surface exposed haem binding protein) accepts haem from Shr (Figure 1.2C). Although widely regarded as a distant relative and not a direct member of the NEAT protein family, Shp is able to bind haem using structural similarities with NEAT family proteins (Bates et al., 2003b). Once in possession of haem, Shp is able to rapidly transfer haem to SiaA, the haem binding lipoprotein of the siaABC transporter (Fisher et al., 2008). Recombinant production of the ABC transporter component SiaA allowed for solid-phase binding assays which demonstrated that SiaA could bind Hb in vitro. Although the SiaA transporter system allows *S. pyogenes* to utilise several host haemoproteins, the same experiment showed that SiaA could not bind myoglobin or the Hb:Hp complex. The other components of *siaABC* encode a membrane permease (SiaB) and an ATPase (SiaC) (Bates et al., 2003).

In addition to studies of *shr* mutants, *siaA* has also been linked with virulence. Infection of mice with *siaA* deletion mutants resulted in significantly increased survival rate, reduced skin lesion size, and reduced systemic dissemination when compared to the wild type. The reinstatement of *siaA* restored *S. pyogenes* wild-type (WT) capabilities suggesting that its ability to utilise haem is an important component for *S. pyogenes* infection (Song et al., 2018).

1.6.4 - *Bacillus anthracis*

The conserved nature of the haem- and sometimes Hb-binding NEAT domains amongst Gram positive organisms suggest the ability to pirate haem from Hb is widely distributed. *Bacillus anthracis* is the pathogen responsible for the infamous infectious disease anthrax. Anthrax infections are typically started by *B. anthracis* spores gaining access to the host via breaks in the skin or entry through the mucosa. Although the symptoms of infection differ slightly between inhalation and gastrointestinal sites; fever, nausea, vomiting and stomach pains are universal (Spencer, 2003). *B. anthracis* is able to acquire haem from Hb by secreting extracellular haemophores IsdX1/X2 which are reported via ELISA style assays to bind Hb and accept haem. The haem-saturated haemophores then make their way to the cell wall where the haem is rapidly passed to surface exposed NEAT domain protein IsdC. From IsdC, haem is transferred via the transmembrane ABC transporter into the cytoplasm (Tarlovsky et al., 2010). Although *B. anthracis* IsdC is crucial in this pathway of haem acquisition from Hb, IsdC deletion mutants did not lose their virulence in a guinea pig infection model (Gat et al., 2008). In 2012, Balderas *et al* used NEAT domain homology searches to demonstrate that the cell attached protein Hal (Haem-acquisition leucine-rich repeat) possessed a NEAT domain and was able to bind to Hb and accept its haem. Deletion mutants of Hal showed reduced growth in media in which either Hb or haem were the sole iron source (Balderas et al., 2012).

Interestingly, another human pathogen in the *Bacillus* genera, *Bacillus cereus,* is able to use Hb as an iron source and possesses NEAT domain homologs but is incapable of using other iron-carrying host proteins such as transferrin or lactoferrin (Daou et al., 2009; Sato et al., 1999). *B. cereus* is a pathogen most closely associated with food poisoning but is now also linked with serious and potentially fatal non-gastrointestinal tract infections (Bottone, 2010). There is no evidence that the non-pathogenic *Bacillus subtills* possess the NEAT domain proteins needed to use Hb as an iron source.

1.6.5 - *Listeria monocytogenes*

Listeria monocytogenes is a foodborne human pathogen. Infections with this pathogen can be responsible for gastroenteritis, meningitis, encephalitis and maternofoetal infections (Camejo et al., 2011). *L. monocytogenes* is able to pirate haem from Hb via Hbp2, a protein that is reported to exist both as a secreted haemophore as well as a surface-attached protein. Hbp2 has three NEAT domains that facilitate its binding to both haem and Hb. Secreted Hbp2 is able to bind Hb and accept its haem before transferring it to surface-bound Hbp2 or to the closely related Hbp1. Once in possession of haem, surface-bound Hbp1 or Hbp2 begin a cascade of haem transfers similar to that of the *S. aureus* Isd system toward the cell membrane, where the haem is transported into the cell by ABC transporter HupDGC. Interestingly, surface-bound Hbp2 is also able to bind Hb directly (Malmirchegini et al., 2014; Klebba et al., 2012).

1.6.6 - *Clostridium perfringens*

Clostridium perfringens is another mostly foodborne pathogen that can utilise Hb as an iron source. *C. perfringens* infections can result in gas gangrene, food poisoning, non-foodborne diarrhoea and enterocolitis (Kiu & Hall, 2018). The mechanics of Hb piracy by *C. perfringens* are still poorly understood but *C. perfringens* strain JIR325 is able to survive on Hb as a sole iron source (Choo et al., 2016). Two haem-binding, NEAT domain-possessing proteins, ChtD and ChtE can be found on the cell surface and were initially suspected to be prime candidates for Hb utilisation capabilities. Both single and double mutants of the proteins did not strip *C. perfringens* of its ability to grow on media in which Hb was the sole iron source, although the mutants did exhibit reduced virulence in mouse myonecrosis models. Downstream of the ChtD and ChtE genes, a *C. perfringens* haem ABC transporter has been identified; ChtA - a haem binding lipoprotein, ChtB – a permease and ChtC1 an ATP binding protein, all of which are needed for transport into the cytoplasm (Choo et al., 2016).

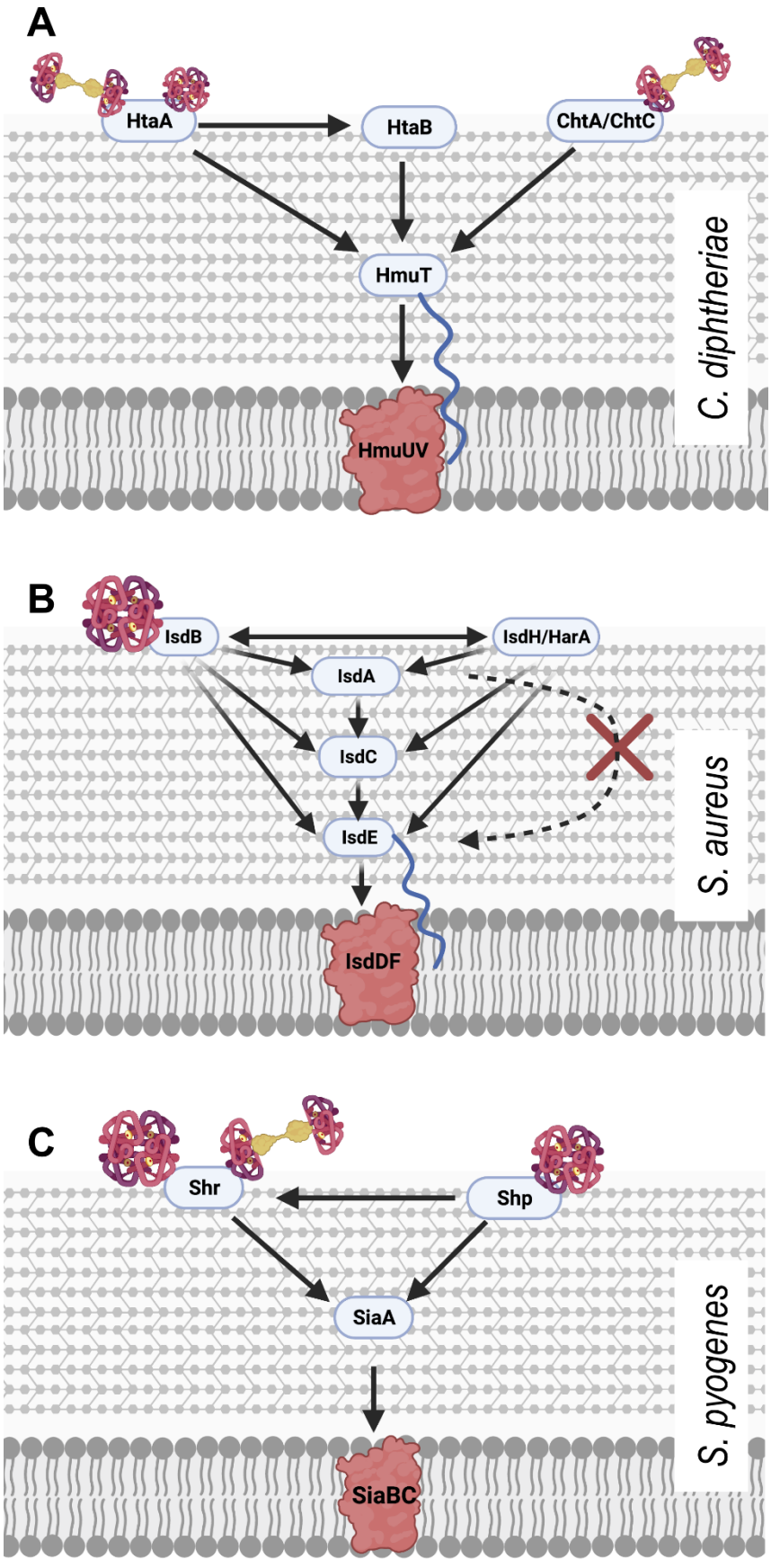
A
HtaA
HtaB
ChtA/ChtC
HmuT
HmuUV
C. diphtheriae
B
IsdB
IsdH/HarA
IsdA
IsdC
IsdE
IsdDF
S. aureus
C
Shr
Shp
SiaA
SiaBC
S. pyogenes

Figure 1.2: Schematic models of haem piracy from haemoglobin by the different Gram positive pathogens described herein.
(**A**) In *C. diphtheriae*, two groups of surface exposed proteins bind Hb and Hb:Hp. HtaA is able to bind Hb and the Hb: Hp complex while HtaB is responsible for binding free haem, meanwhile ChtA/ChtC proteins bind directly only to the Hb: Hp complex. Both groups of proteins transfer haem to HmuT, the lipoprotein component of the ABC transporter for import through the lipid bilayer. (**B**) In S. aureus, surface exposed proteins IsdB or HarA/IsdH bind haemoglobin at the cell surface and strip it's haem. The haem can them be passed to any of the proteins IsdA, IsdC and IsdE and unidirectional transfer from IsaA – IsdC – IsdE leads to transport to the cytoplasm through the IsdDEF ABC transporter for transport into the cytoplasm. (**C**) At the surface of S. pyogenes, Shp extracts haem from Hb and Shr is able to obtain haem from both Hb and the Hb:Hp complex. These proteins transfer haem to lipoprotein SiaA for transport into the cell via SiaABC. (Created with BioRender.com).

1.7 – Use of haemoglobin by mycobacteria /*Mycobacterium tuberculosis*

Bacteria of the *Mycobacterium* genus have a unique cell surface structure that does not neatly fit into either the Gram positive or Gram-negative categories. *Mycobacterium tuberculosis* can infect any tissue within a human host but often infects the respiratory system and causes the disease tuberculosis.

Access to iron is vital for *M. tuberculosis* virulence and as a result, the bacteria have evolved multiple systems to meet their needs. Iron chelating siderophores called mycobactins are produced by *M. tuberculosis* and are essential for growth in macrophages, where mycobactin synthesis genes are upregulated (De Voss et al., 2000; Tailleux et al., 2008). Siderophore use notwithstanding, the iron acquiring prowess of *M. tuberculosis* may extend to the direct utilisation of host iron and haem-carrying proteins too. Indeed, the ability to use haem iron was confirmed by experiments in which iron uptake deficient mutants were created by disruption of mycobactin/exomycobactin biosynthesis. These mutants were grown in several iron-specific environments, including those where Hb was the sole iron source (Tullius et al., 2011). The amount of iron available has been linked to the likelihood of infection, with iron overload reported to increase the risk of tuberculosis, tuberculosis treatment failure, and mortality in tuberculosis patients (Boelaert et al., 2007). On the opposite side of the iron availability spectrum, it has also been demonstrated that extended periods in an iron-deprived environment results in *M. tuberculosis* entering a persistent state, a likely characteristic of chronic tuberculosis (Kurthkoti et al., 2017).

Hb utilisation in *M. tuberculosis* involves surface-exposed proteins, which are suspected to bind Hb, and a haem-specific ABC transporter system. Hb binding by *M. tuberculosis* is facilitated by membrane proteins PPE36/PE22 and PPE62. PPE36/PE22 and PPE62 are separate systems that are both capable of binding haem and facilitating acquisition from Hb at the cell surface in order to make haem available for transport into the cytoplasm by the Dpp ABC transporter system (Figure 1.3) (Mitra et al., 2017). Although the mechanism by which haem is obtained from Hb is still unknown, largely due to the lack of published structures, we do know that PPE36 is the most essential of the surface exposed protein systems. Deletion mutant experiments showed that ΔPP36 mutants were completely halted in their growth with haem as a sole iron source, whereas ΔPP62 mutant growth was only partially impaired (Mitra et al., 2019). Another protein, PPE37, is also contested to play a role in haem acquisition by *M. tuberculosis*. There have been no experiments to suggest that PPE37 is directly involved in Hb binding and even its role in haem utilisation is disputed. Exploiting the fact that *Mycobacterium bovis* is unable to acquire haem iron, Tullius *et al* (2019) introduced the *ppe37* gene to *M. bovis* and found that the resulting mutant was able to acquire haem iron in similar levels to *M. tuberculosis*. In addition to this, Tullius et el reported that an N terminal deletion in PPE37 was responsible for the loss of the phenotype in wild type *M. bovis* and that *M. tuberculosis* strains that also possess the altered PPE37 protein (up to 60% of sequenced genomes) would be equally incapable of haem acquisition (Tullius et al., 2019). By contrast, Mitra *et al* (2019) found that deletion of PPE37 from avirulent *M. tuberculosis* strain mc^{2}6206 had no effect on growth and that this mutant grew on minimal media in the presence of 10 μM hemin or 2.5 μM human Hb identical to that of the wild type (Mitra et al., 2019). A consensus on the mechanism of haem uptake from Hb in *M. tuberculosis* therefore remains elusive.

The haem-specific ABC-like transporter of *M. tuberculosis* is named Dpp and is made up of four proteins DppA, DppB, DppC and DppD. By infecting macrophages with different iron deficient mutants including a *Δdpp* mutant, Mitra *et al* (2019) were able to

demonstrate the importance of this system for *in vivo M. tuberculosis* survival. Of the proteins in this system, DppA, specifically through its arginine 179, possesses the substrate-specific binding ability that makes it essential for Hb-free haem utilisation by the entire cell.

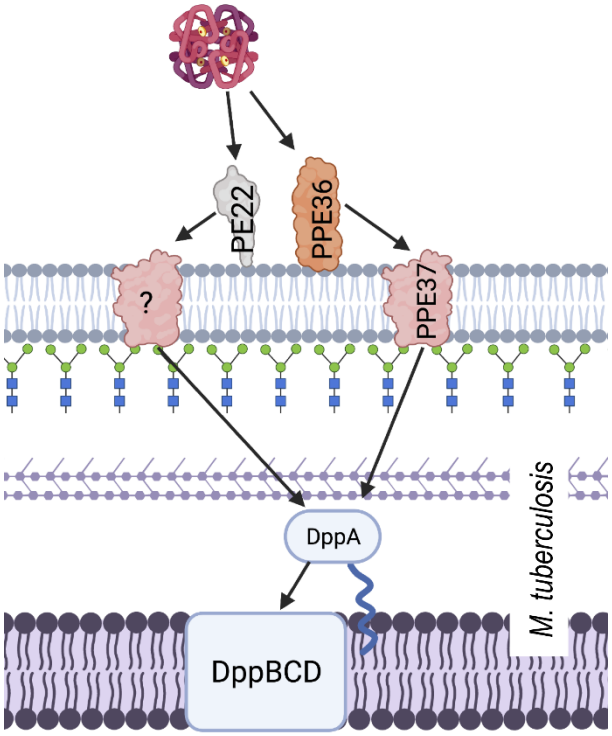

Figure 1.3: A schematic showing haem acquisition from Hb by M. tuberculosis. The cell surface proteins PPE36, PPE22 and PPE62 are able to bind haem, facilitating the use of Hb. The haem is transported into the periplasm by PPE36 or another functionally similar but unknown protein. Once in the periplasm the haem is bound by lipoprotein DppA, and transported into the cytoplasm by ABC transporter system DppBCD. (Created with BioRender.com).

1.8 – The use of Hb by pathogenic gram-negative bacteria

The cell wall structure and outer membrane of Gram-negative bacteria present additional challenges to nutrient uptake. Because of the similarity of these challenges among Gram negative bacteria, haem uptake from Hb utilises the well-conserved TonB-dependent system that is fundamental to all active iron uptake in these bacteria (Nikaido, 2003). Gram negative bacteria must not only bind to Hb but obtain the iron-containing haem from it, transport it across the outer membrane and then across the inner membrane into the cytoplasm. TonB-dependent transporters (TBDTs) are made up of a 22-strand transmembrane β-barrel protein with a globular N-terminal plug domain and eleven extracellular loops to facilitate substrate binding (Figure 1.4). The system is powered by utilising energy derived from the proton motive force transmitted from the TonB-ExbB-ExbD complex located in the inner membrane (Noinaj et al., 2010). Using the ferrichrome TBDT FhuA from *Escherichia coli* as a structural template, sequence analysis demonstrated that at least 50% of residues were conserved amongst 12 unique TBDTs. The regions of highest sequence conservation were the N-terminal plug domain and the β-strands of the barrel, indicating the core structures of the proteins are maintained, while none of the conserved residues found on the extracellular loops were reported to facilitate substrate-specific binding (Noinaj et al., 2010). Although they can be found in the outer membrane of almost all Gram negative bacteria, TBDTs are substrate-specific transporters and the conservation of the TBDT system itself does not limit the range the possible substrates, which are diverse in structure and size and include iron-carrying siderophores, carbohydrates, lignin-derived aromatic compounds or indeed host proteins such as Hb (Fujita et al., 2019; Schauer et al., 2008).

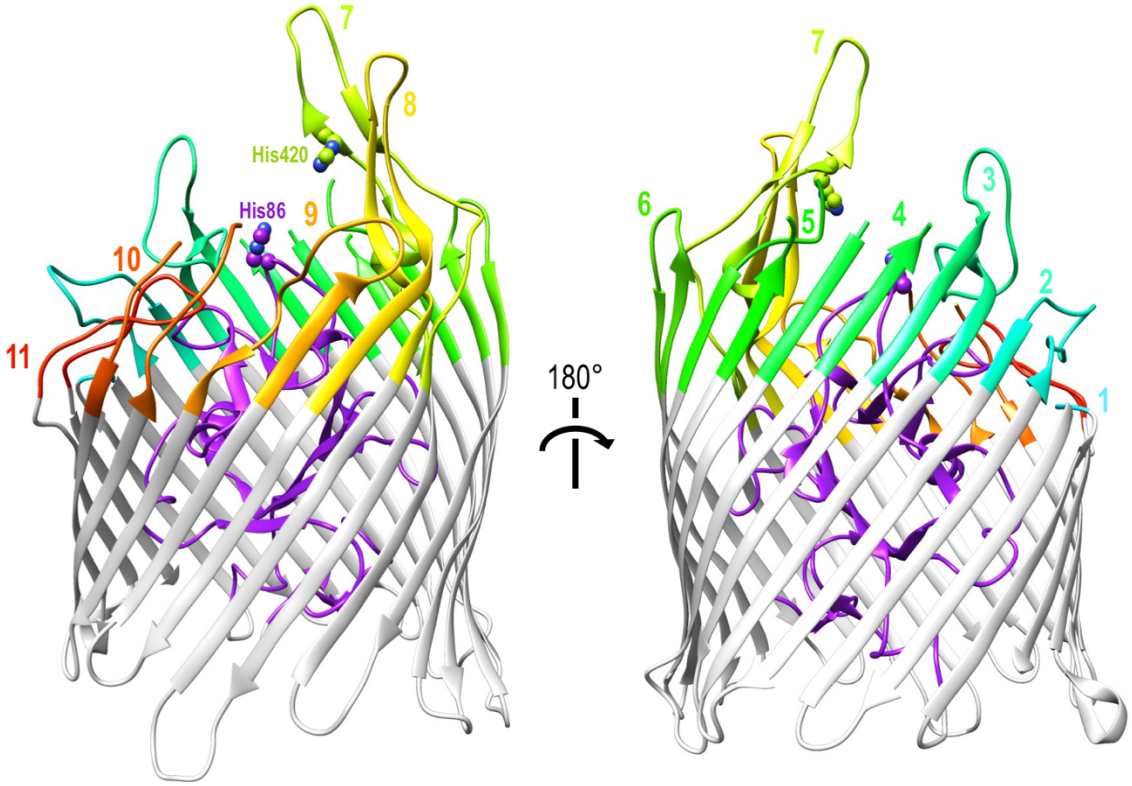

Figure 1.4: Cartoon representation of a TonB-dependent transporter involved in Hb piracy.

This is ShuA from *S. dysenterieae,* pdb id: 3fhh. The N-terminal plug domain is coloured purple, the membrane-enclosed β barrel in light grey and the extracellular loops involved in Hb recognition and haem extraction are rainbow coloured from cyan for loop one to red for loop 11. Two conserved histidine residues proposed to bind to haem are labelled and shown as balls. (Molecular analysis on UCSF Chimera).

1.8.1 - TBDTs

TBDTs have reported involvement in the binding or transport of a wide variety of substrates into the cell, including vitamin B_{12}, nickel complexes, iron-chelating siderophores, haem, carbohydrates (Noinaj et al., 2010a) and even other proteins such as proteases, out of the cell (Gómez-Santos et al., 2019). This introduction will focus on iron-specific transport and regulation of TBDTs. Transport across the outer membrane (OM) requires energy but there is no available energy source at the OM or in the periplasm. There is a twofold reason for this, ATP-hydrolysing proteins are not available in the periplasm and no proton gradient can be established across the OM lipid bilayer. It has been long understood that two additional factors to the TBDT are needed for the active transport of substrates across the OM. First is that the active transport is energised by a protonmotive force across the inner membrane. Secondly, this active transport is facilitated by a cytoplasmic transmembrane complex called the TonB complex, made up of TonB, ExbB and ExbD (Schauer et al., 2008). Although the release of the substrate into the periplasm is dependent on TonB-provided energy, TBDTs bind their substrates at the plug domain as well as using their extracellular loops with no requirement for energy. The passage of substrates through the β barrel is dependent on structural changes in the plug domain. It is hypothesised that these structural changes are initiated by substrate binding (Payne et al., 1997; Letain & Postle, 1997; Postle & Larsen, 2007).

1.8.2 - The TonB complex

The TonB complex is made up of TonB, ExbB and ExbD; in *E.coli*, 239, 141 and 244 residues respectively. All three proteins are embedded in the inner membrane (IM) and are needed to fully realise the protonmotive force that powers TBDTs. There have been many hypotheses about the mechanisms of action within the complex. The most common and supported is that the complex acts as a proton-conducting channel that passes protons from the periplasm to the cytoplasm, generating power for mechanical motion (Zeng et al., 2013).

TonB and ExbD have similar topologies with a short N-terminal domain in the cytoplasm, a single transmembrane helix and a folded C-terminal periplasmic domain connected by a flexible linker. ExbB is composed of three transmembrane helices with a short periplasmic N-terminal domain and a large cytoplasmic domain as determined by X-ray crystallography analysis (Ködding et al., 2005; Peacock et al., 2005; Garcia-Herrero et al., 2007). Celia et al (2016) presented a crystal structure of the ExbB/ExbD complex with a deleted periplasmic domain to a resolution of 2.6 Å. They proposed that the complex consists of a pentamer of ExbB, a dimer of ExbD working with at least one TonB, and that association of TonB with the other proteins does not significantly alter the structure of ExbB or ExbD within the TonB complex (Celia et al., 2016). Previous mutagenic studies identified Asp 25 of ExbD and Thr 148 / Thr 181 of ExbB as essential for protonmotive force of the complex (Braun et al., 1996) (Braun & Herrmann, 2004). Crystal structures supported this by revealing that the residues map to the interior of the ExbB pore, thought to be critical for proton translocation (Celia et al., 2016). The structural model of the complex led to the proposal of two mechanisms for action (Celia et al., 2016). First is an "electrostatic piston model', in which the transmembrane helix of ExbD creates a piston-like motion by moving translationally inside the transmembrane pore of ExbB. Second, is the 'rotational model', where the rotational motion is created by a rotating of the ExbD pore located transmembrane helix. It also acknowledged that a combination of the two is possible (Celia et al., 2016).

More recently, a cryo-EM structure of the ExbB/ExbD complex as a nanodisc to a resolution of 3.3 Å was reported (Celia et al. 2019). The cryo-EM structure confirmed many of the discoveries outlined by the crystal structure, but also revealed some new insights. The structure shows ExbB assembling as a pentamer, however, rather than one ExbD transmembrane helix, two transmembrane helices of ExbD are clearly resolved within the transmembrane pore and arranged parallel, shifted relative to one another by half a helical turn. The complex therefore appears to consist of an ExbB pentamer encircling a transmembrane dimer of ExbD. The functionally important residues of ExbD Asp 25 and ExbB Thr 148/ Thr 181 on the pore's interior are close in proximity to each other. These residues are proposed to play an important role in the conformational changes that must occur to open the channel within the pore (Celia et al., 2019).

The earliest widely accepted explanation for how TonB affects the function of TBDTs came from Letain & Postle (1997) who proposed a three-step process. Firstly, TonB is powered by the protonmotive force channelled by the ExbB/ExbD complex. Secondly, TonB either moves towards or becomes more strongly associated with the OM in order to make physical contact with the TBDT (Letain & Postle, 1997; Skare et al., 1993). Lastly, the ExbB/ExbD complex recycles the position of TonB from tight association with the OM back to tightly interacting with the IM, allowing for repetition of the process (Letain & Postle, 1997).

This model of shuttling TonB back and forth between the OM and IM is now considered inaccurate (Klebba, 2016). New models have now been proposed based on fluorescence polarisation experiments and cryo-EM structures. A "Rational Surveillance and Energy Transfer" model (ROSET) was described based on data from *in vivo* experiments with an N-terminal green fluorescence protein (GFP)-TonB construct. The ROSET model proposes that TonB functions as a dimer where it creates rotary motion in the presence of the ExbB/ExbD pentameric complex, allowing the generation of torque which opens the TBDT channel for the ligand to be transported through. The individual TonB

subunits are proposed to play separate roles, one monomer interacts with the peptidoglycan layer in the periplasm, which puts the other closer to the OM where it would interact with the TBDT (Freed et al., 2013; Klebba, 2016; Kaserer et al., 2008).

Another model, referred to as the 'pulling model' proposes that the TonB complex creates a pulling force that partially unfolds the N-terminal plug, allowing for the ligand to pass through the TBDT pore (Chimento et al., 2005). As determined by molecular dynamics simulation experiments on a BtuB/TonB complex, the movement begins with an interaction between TonB and the TBDT plug strong enough to prevent the TonB/ TBDT attachment while the force unfolds the plug domain. BtuB is a vitamin B12 transporting TBDT from *E. coli.* This was also supported by single-molecule force spectroscopy which was used to show that the BtuB/TonB interaction is strong enough to endure extension and repeated mechanical unfolding of the plug domain, before the eventual dissociation of TonB (Hickman et al., 2017)

1.8.3 - Structural analysis of TBDTs

The first published high-resolution structure of a TBDT was the crystal structure of the *E. coli* FhuA in 1998 (Ferguson et al., 1998). The structure was resolved to a resolution of 2.7 and 2.5 Å, with and without ferrochrome iron, respectively. FhuA comprises a C-terminal β-barrel domain and an N - terminal cork domain which fills the barrel interior, now more frequently referred to as a plug domain (Ferguson et al., 1998). FhuA is larger than contemporaneously well-characterised porins, 69 Å in height and cross-section of 46 by 39 Å, constituted with 22 antiparallel β strands, ten short periplasmic turns and eleven longer surface-exposed loops. In this structure, the mixed four-stranded β sheet plug domain is arranged within the barrel on a ~45°C incline and so sterically occludes most of the barrel cross-section (Ferguson et al., 1998).

The plug is connected to the barrel wall with hydrogen bonding, and it was found that the extent of hydrogen bonding in the structure of FhuA in complex with ferrochrome iron was slightly lower than in its absence, suggesting that ligand binding causes conformational changes within the plug that opens the barrel pore for transport. The binding site itself was located slightly above the OM interface and residues on the apices were shown to make direct contact with the ligand via van der waals or hydrogen bond using residues on both the barrel (Arg 81), and the plug (Gln 100 and Try 116). The extracellular loops are also implicated in ligand binding, with earlier studies showing that deletion of loop 3 (residues 236 to 248) results in the loss of ferrochrome iron uptake capabilities (Ferguson et al., 1998). Furthermore, although no loop 4 residue appears to directly bind the ligand, the conformation of the loop remains vital to the functioning binding site (Ferguson et al., 1998; Rodríguez-Ropero & Fioroni, 2012). Since the publication of the FhuA crystal structure, several other TBDT structures were published and presented very similar structural maps, including FepA and FecA from *E. coli*, (Buchanan et al., 1999; Ferguson et al., 2002) FauA from *Bordetella pertussis* (Brillet et al., 2009) and *Serratia marcescens* receptor HasR (Krieg et al., 2009).

One of the most influential studies on TBDT came from Noinaj et al (2012) who presented a comprehensive analysis of the bipartite transferrin binding TBDT system TbpAB of pathogenic *Neisseria*. TbpA is the β-barrel transporter and TbpB is an extracellular lipoprotein partner. The study included a crystal structure of the TbpA-transferrin complex, small angle X-ray scattering (SAXS) analysis of the TbpB-transferrin complex and electron microscopy analysis of the TbpA-TbpB-transferrin complex (Noinaj et al., 2012). The structures showed that TbpA binds exclusively to the C-lobe of human transferrin, which is an 80 kDa iron-carrying protein found in serum. Structurally, transferrin is divided into two lobes, the N-lobe and C-lobe that are linked together via a short spacer sequence (Gomme et al., 2005). This interaction involves significant areas of both proteins; indeed 67 transferrin residues and 81 TbpA residues participate in the interaction. During binding, there is electrostatic complementarity between TbpA and the C-lobe of transferrin which are electropositive and electronegative respectively.

Most prominently, a helix in TbpA extracellular loop 3 inserts directly into the transferrin C-lobe between its subdomains, C1and C2. There is also direct interaction of the TbpA plug with transferrin's C1-subdomain. Less prominently, peptides on loops 7 and 11 also make substantial contacts with the C-lobe of human transferrin. Corroborating previous hypotheses that both the N-terminal plug and the extracellular loops are involved in substrate binding of TBDTs. Although TbpA can bind transferrin and acquire its iron on its own, several studies have shown that this process is more efficient when performed in partnership with TbpB (Anderson et al., 1994) (Irwin et al., 1993). Data from crystal, SAXS and negative stain EM structures presented a consistent arrangement for the TbpA/TbpB/Transferrin complex. Showing that despite both proteins binding to the C-lobe, both TbpA and TbpB have exclusive transferrin binding sites and results in the formation of an enclosed chamber with a volume of 1000 $Å^3$ and sits directly about the plug domain. Noinaj et al (2012) propose

that this formation serves two purposes, firstly to prevent diffusion of iron released from transferrin and secondly to guide the iron towards the β-barrel pore for transport into the periplasm. They also propose a mechanism for iron extraction from transferrin in which the TbpA loop 3 insertion into the C-lobe cleft positions a conserved lysine (Lys359) near a transferrin trio of charged residues implicated in iron release (Lys534, Arg632, Asp634). This interaction creates a cascade of subsequent interactions which potentially results in a charge repulsion with the transferrin C-lobe which could induce cleft opening, distorting the C-lobe iron holding site, allowing for iron release (Figure 1.5B) (Noinaj et al., 2012).

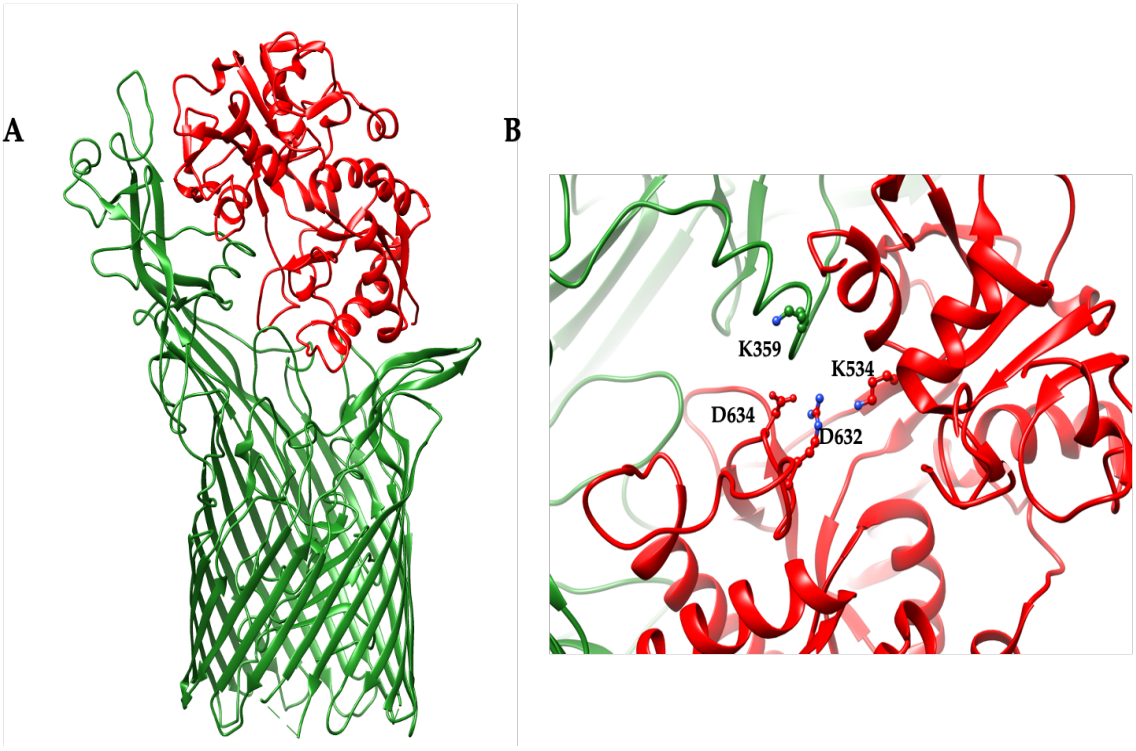

Figure 1.5: Cartoon representation of the human transferrin – TbpA complex.
This is crystal structure of TbpA *N. meningitidis* serogroup B in complex with the C-lobe of human transferrin, pdb id: 3V89. TbpA is coloured green and human transferrin is red. (**A**) Full cartoon representation of the complex. (**B**) TbpA loop 3 insertion into the transferrin C-lobe cleft. (Molecular analysis on UCSF Chimera).

There have been no resolved structures of TBDTs in complex with Hb but there are structures available for other haem extracting TBDTs in complex with their respective haemophores. *Serratia marcescens* receptor HasR in complex with its haemophore HasA is one such example. HasA is a secreted protein (19 kDa) that binds directly to haem and is necessary for growth of *S. marcescens* where haem or haemoglobin are the sole iron sources (Létoffé et al., 1994). HasA binds to haem with very tight affinity (K_d = 18 pM) with 1:1 stoichiometry. Crystal structures show that HasR is structurally similar to other TBDTs (Figure 1.6A), with a 22-strand β-barrel, N-terminal plug domain, and putative extracellular loops. Two of these loops, loops 6 and 9, make significant contact with HasA, while loops 7 and 8 play an essential role in transferring haem from its tight binding site on HasA to a much weaker site on HasR. Similarly to ShuA, a conserved Histidine residue on HasR loop 7 is involved in the liberation of haem from HasA (Létoffé et al., 1994). This interaction on its own is not sufficient to force haem away from HasA, the involvement of Ile671 on HasR loop 8 is also required. As seen in the HasRA complex, Ile671 triggers the expulsion of haem by occupying the same position relative to HasA as haem does in the HasA/haem complex (Figure 1.6B). This was confirmed with data obtained by the crystallisation of Wt HasA in complex with a mutant of HasR which exchanged Ile for Gly at position 671. The Ile-671-Gly mutant HasR could still release haem from HasA but was not able to fully remove it from the HasA binding site which also involved conserved histidine residues on both loop 7 and the plug domain of HasR.

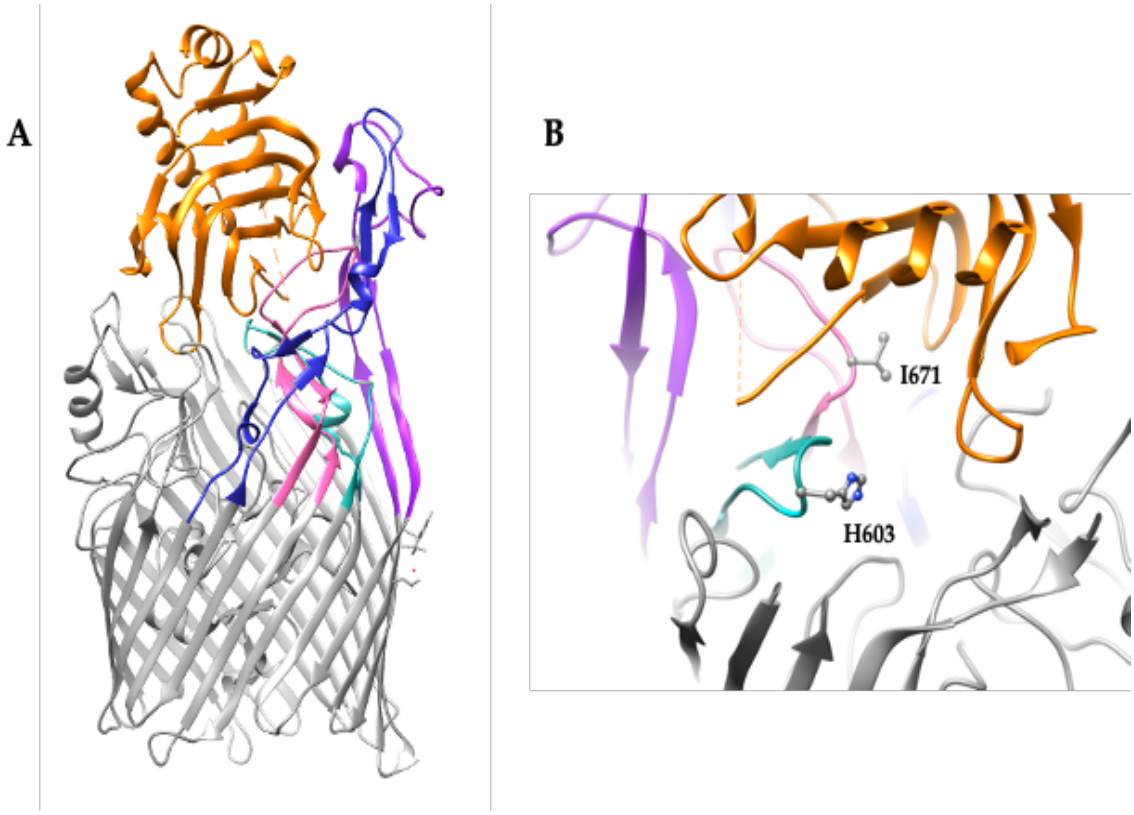

Figure 1.6: Cartoon representation of the HasA – HasR complex.

This is the crystal structure of the *Serratia marcescens* hemophore receptor HasR in complex with its hemophore HasA, pdb id: 3CSN. HasR is coloured grey with the exception of functionally important loops and HasA is orange (**A**) Full cartoon representation of the complex. Loop 6 (purple) and loop 9 (blue) make significant contact with HasA. Loop 7 (teal) and loop 8 (pink) are essential for stripping haem from HasA (**B**) Focused section a conserved His 603 (loop7) and Ile (671), confirmed to play an active role in the stripping of haem from HasR. (Molecular analysis on UCSF Chimera).

This section outlines the ways in which TBDTs are used by a range of pathogenic Gram-negative pathogens to acquire haem from Hb.

1.8.4 - *Shigella dysenteriae*

Shigella dysenteriae is a Gram negative, facultative anaerobic bacterium. It is a highly virulent pathogen and is usually transmitted by contaminated food and water invading the host via epithelial cells of the intestinal mucosa (Zaidi & Estrada-García, 2014). *S. dysenteriae* infections are associated with poor hygiene conditions resulting in a condition called shigellosis. Shigellosis commonly presents with symptoms such as diarrhoea that may be bloody, high fever and stomach cramps (Taylor, 2008).

Key to the virulence and pathogenesis of *S. dysenteriae* is the acquisition of iron, in part through the Hb-binding TBDT ShuA. Although it is important to note that *S. dysenteriae* does also produce siderophores and has TBDTs that are specific to their uptake. *S. dysenteriae* colonises the intestinal mucosa where there is an abundance of haem; due to both dietary haem intake and haemolytic damage caused by haemolytic *Shigella* toxins (Burkhard & Wilks, 2007). ShuA binds to Hb, accepts haem from it, then transports it across the outer membrane into the periplasm (Figure 1.7A). In vitro, ShuA extracts haem from met-Hb ~2000 times faster than that from oxy-Hb (Burkhard & Wilks, 2007). This suggests met-Hb is the physiological substrate of ShuA *in vivo,* although the fact that met-Hb spontaneously releases haem faster than oxyHb may have influenced the experiment (Hargrove et al., 1997). Indeed, met-Hb is the most likely available source of haem following *S. dysenteriae*-induced dysentery in the low oxygen environment of the gut.

Unique among Hb-binding TBDT homologues, the crystal structure of ShuA has been resolved (Figure 1.4) (Cobessi et al., 2010). The structure conforms to the expected 22-stranded β-barrel with an N-terminal plug domain. The importance of two conserved

histidine residues, His86 and His420, which were previously identified as crucial for the extraction of haem from Hb by observing loss of function in respective double mutants (Burkhard & Wilks, 2007), was also indicated by the crystal structure of haemophore TBDT, HasR from *Serratia marcescens*, where a haem molecule was observed coordinated between two corresponding residues (Krieg et al., 2009). Hb binding and haem transfer onto ShuA are dependent on the conserved residues His86 & His420 with other interactions also documented to play a role in haem piracy (Cobessi et al., 2010). A structural explanation of the way ShuA is able to remove haem from Hb is still elusive, but the crystal structure obtained from ShuA is now a crucial tool in modelling and understanding how other Hb-specific TBDTs work.

The role of ShuA during infection is still unclear but disrupting the *shuA* gene resulted in a strain that was incapable of using haem as an iron source, suggesting that ShuA is essential for haem utilisation in *S. dysenteriae* (Mills & Payne, 1997). In addition, very similar TBDTs can be found in the genomes of other pathogenic *Shigella* species: *S. sonnei* and *S. flexneri.*

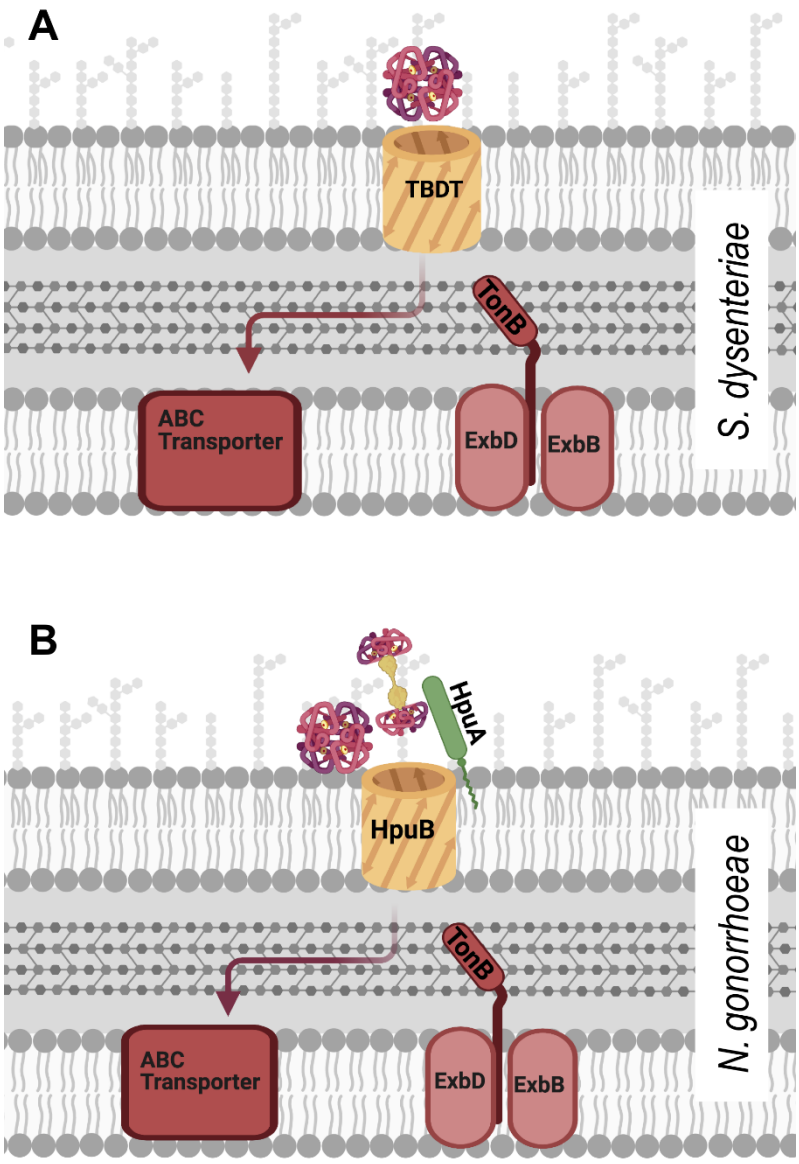

Figure 1.7: Schematic models of haem piracy from haemoglobin by the different Gram negative pathogens described herein.

(**A**) Some pathogens, such as *S. dysenteriae*, employ monopartite TonB-dependent transporters (TBDT). These β-barrel outer membrane proteins (ShuA in the case of *S. dysenteriae*), enable active transport of haem from the host haemoprotein into the periplasm from where the haem is transported into the cytoplasm by a haem specific ABC transporter. (**B**) Some TBDTs, such as the gonococcal HpuB, work in conjunction with an associated surface exposed lipoprotein (HpuA) to extract haem from Hb or Hb:Hp and transport it into the periplasm. (Created with BioRender.com).

1.8.5 - *Haemophilus*

There are several species of the *Haemophilus* genus known to cause infection in humans. Of these pathogens, *Haemophilus ducreyi* and *Haemophilus influenzae* have been reported to use Hb as an iron source. *H. ducreyi* is a Gram negative obligate human pathogen and the causative agent of the sexually transmitted disease chancroid, characterised by genital ulceration and is thought to enter through breaks in the epidermis (Spinola et al., 2002). *H. ducreyi* is mainly found in developing countries but can also be found sporadically in the 'global west'. A key comorbidity of infection is the 10 to 100-fold increase in Human Immunodeficiency Virus (HIV) transmission amongst *H. ducreyi* infected individuals (Jamie Robinson et al., 1997). The opportunistic human pathogen *H. influenzae* is nonmotile, facultatively anaerobic and its strains are broken down into two groups depending upon the absence or presence of a polysaccharide capsule (Agrawal & Murphy, 2011). *H. influenzae* is isolated predominantly from the respiratory tract of humans and is a normal part of the commensal flora in the nasopharynx (King, 2012). *H. influenzae* infections mostly manifest in conditions like pneumonia but can also result in meningitis and systemic bloodstream infections. The encapsulated *H. influenzae* type b (Hib) has been the target of a widely used conjugate vaccine which has dramatically reduced the prevalence of community-acquired pneumonia. Indeed, most invasive *H. influenzae* infections are now caused by non-typeable strains (NTHI) of the pathogen (Slack, 2015).

Like all Gram-negative bacteria that use haem from Hb as an iron source, *H. ducreyi* also has a TBDT system specifically for this purpose named HgbA, which has been demonstrated to have a vital role in the virulence of the pathogen. Unlike the Gram negative organisms from other genera described herein, *H. ducreyi* exhibits an obligate requirement for haem, at a minimum concentration of 38 μM (Lee, 1991). The organism also has a second TBDT called TdhA, which facilitates the use of free haem (Thomas et al., 1998). Interestingly, in a human infection model, HgbA-knockout *H. ducreyi* was

unable to establish an infection, suggesting that expression of TdhA alone is not sufficient for *H. ducreyi* virulence (Al-Tawfiq et al., 2000).

Due to the obligate requirement of haem by *H. ducreyi*, HgbA has been a target for successful immunisation studies against the pathogen. In a study of immunised pigs, no viable *H. ducreyi* cells were recovered following infection of HgbA-immunised pigs, whereas mock-immunised pigs were not protected from the infection. The study also showed that antibodies acquired from HgbA-immunised pigs were bactericidal and offered protection against *H. ducreyi* (Afonina et al., 2006). The swine model was chosen because of similarities in infection symptoms and also because a single experimental infection with *H. ducreyi* did not protect the animals from future infections, another shared feature with humans (Cole et al., 2003).

HgbA is modelled to be a 22-strand transmembrane β-barrel protein with 11 putative extracellular loops. *In vivo* loop deletion analysis of the protein revealed that deletion of sequences in loops 5 and 7 of HgbA rendered the protein unable to bind Hb. This elimination of Hb binding capability was not seen in deletion mutants of the other nine loops, an observation that was confirmed in two separate formats. Anti-HgbA IgG antibodies generated during the immunisation study discussed above showed show that loops 4, 5, and 7 of HgbA were immunogenic and surface exposed. Furthermore, anti-HgbA IgG specifically directed against loops 4 and 5 were shown to block Hb binding by *H. ducreyi* (Nepluev et al., 2009).

H. influenzae also cannot survive without an exogenous source of haem and different numbers and combinations of Hb- and Hb:Hp-binding TBDTs have been identified in different strains, for example, HgbA, HgbB, and HgbC in NTHI strain N182 and HhuA in NTHI strain TN106 (Maciver et al., 1996; Cope et al., 2000). These proteins all share approximately 40-50% identity with each other and with HgbA of *H. ducreyi*. Deletion mutation experiments revealed that expression of any of HgbA, HgbB or HgbC allowed *H. influenzae* N182 to retain WT level growth with Hb as the sole iron source (Cope et al.,

2001). Where the iron source was the Hb:Hp complex, mutants expressing only HgbA or HgbC grew significantly better than mutants expressing only HgbB. Interestingly, in a mutant where HgbA, HgbB and HgbC were deleted, NTHI N182 was still able to use Hb as an iron source to near wild type levels. This was in contrast to the significant impairment in the mutant's ability to utilise the Hb:Hp complex. A further *tonB* deletion mutation made to the *hgbA*, *hgbB*, *hgbC* triple mutant did strip it of its ability to grow using Hb as an iron source, indicating that there was another TBDT assisting in NTHI N182's ability to use Hb as an iron source. Proteomic analysis showed that HxuC, a TBDT previously characterised to be involved in the use of free haem and haemopexin (Cope et al., 1995) was supplementing the activity of the HgbA, HgbB and HgbC proteins. In a mutant where all four of the aforementioned TBDTs were deleted, NTHI N182 did eventually lose the ability to utilise Hb (Cope et al., 2001). Although a HxuC deletion mutant was reported to lose the ability to utilise low concentrations of free haem *in vitro,* the mutation had no observable implication on the ability of *H. influenzae* to use Hb (Cope et al., 1995), this suggests a significant amount of redundancy employed by this organism for which haem is an essential nutrient.

1.8.6 - *Pseudomonas aeruginosa*

P. aeruginosa are small Gram negative rods that survive in many niches including in soil and aquatic environments, but also infect humans by colonising the respiratory tract and can also infect the urinary tract, skin and soft tissue (Lister et al., 2009). *P. aeruginosa* is able to acquire iron using a variety of different means including secreting siderophores and haemophores. Because of its ability to infect via the respiratory tract, *P. aeruginosa* infections are prevalent in cystic fibrosis (CF) patients and can exhibit chronic long-term infections. Interestingly, *P. aeruginosa* undergoes genetic adaptation during the course of infection. In 2014, Lykke *et al* reported that one of these genetic adaptations increases the ability of *P. aeruginosa* to acquire haem from Hb, coincidental with the loss of pyoverdine production; one of its most important iron-chelating siderophores (Marvig et al., 2014). A mutation in the promoter for PhuR, a *P. aeruginosa* haem specific TBDT, conferred a significant growth advantage compared to the wild type in media in which Hb was the only iron source, an advantage not observed with other iron sources. This suggests a possible increase of reliance on haem over other iron sources during long-term chronic infections but no direct binding of Hb has been observed.

1.8.7 - *Acinetobacter baumannii*

Acinetobacter baumannii is a non-motile, gram-negative coccobacillus bacterium, which accounts for most *Acinetobacter* infections in humans and can also infect other mammals. Symptomatic human infections can be multifaceted both in infection site and severity. Infections can start in the blood, urinary tract, lungs or in open wounds around the body. *A. baumannii* is a robust pathogen, able to survive on a variety of surfaces and equipped with a genome that allows for resistance to last-line antibiotic treatments (Harding et al., 2018). Indeed, *A. baumannii* is now at the top of the World Health Organisation's list of superbugs in need of urgent development in alternative therapeutic treatments (*WHO Publishes List of Bacteria for Which New Antibiotics Are Urgently Needed*, n.d.). Aside from genomic resistance to antibiotics, *A. baumannii* is also known to demonstrate desiccation resistance, biofilm formation and notably pairs these environmental persistence features with virulence factors such as secretion systems and surface glycoconjugates. (Harding et al., 2018)

The story of *A. baumannii* infection and nutritional requirement is a familiar one: the need for crucial nutrients, like iron, has resulted in sophisticated and effective mechanisms of nutrient acquisition from the host itself. Iron acquisition via the capture of haem has been suggested as a major virulence factor in *A. baumannii* (de Léséleuc et al., 2014). Like other gram-negative bacteria seeking to import haem, *A. baumannii* utilises TBDTs to overcome the barrier of its double membrane cell wall. Two *A. baumannii* TBDTs have been observed to function as haem transporters, firstly the ubiquitous HemTR, which appears sufficient for the bacteria to survive when abundant haem is the sole iron source, and secondly, HphR, which is necessary for growth on Hb as an iron source (Bateman et al., 2021). HphR is found on a gene cluster known as the *hemO* locus alongside other proteins functionally relevant to the piracy of haem from Hb in *A. baumannii*. This review has previously described both monopartite and bipartite TBDT systems, where the TBDT itself is reported to both bind Hb and accept its haem unilaterally or with the help of an extracellular anchored lipoprotein partner respectfully. The HphR system of *A.*

baumannii is a different type of bipartite system. Downstream of the gene for *hphR* on the *hemO* locus is a gene encoding HphA (Bateman et al., 2021). HphA is a secreted protein that has been reported to bind Hb through pull down experiments, where HphA was pulled down by Hb, conjugated agarose resin and Hb was shown to bind to Apo HphA-GST immobilised to glutathione beads (Bateman et al., 2021). In contrast to lipoprotein HpuA of *Neisseria*, which is only apparently necessary for the high-affinity interaction between cells and Hb, HphA also binds to haem directly. This leads to a model where HphA is the initial Hb and haem receptor, which then passes the haem onto the TBDT HphR for import. Whether HphA is the sole protein of the system that can bind to Hb or whether HphR is also involved in Hb-binding remains to be tested.

It has been demonstrated that haem uptake via proteins encoded on the *hemO* locus is important for virulence and systemic spread with mouse infection models demonstrating that HphR mutants had the worst survival rates of *hemO* protein mutants (Bateman et al., 2021). Interesting, although HphA is the protein demonstrated to have Hb binding capabilities, it is reported to be an accessory to enhancing infection, while HphR is essential to virulence. This suggests that the essential transport of haem can occur without the Hb-binding haemophore, in which case the haem may come from other sources, albeit these would not be in such abundant quantities as Hb.

1.8.8 – *Neisseria*

N. gonorrhoeae and *N. meningitidis* have no reservoir other than humans and are thus adept at utilising host resources for their survival and pathogenesis. Pathogenic *Neisseria* obtains their iron utilising a wide range of sources; from hijacking iron-chelating siderophores made by other bacteria to host iron-carrying proteins such as transferrin. Although pathogenic Neisseria can survive solely on iron acquired from transferrin, they do pirate the metal from Hb in the form of haem via the Hb-specific TDBT systems HpuAB and, in the case of *N. meningitidis,* HmbR.

HpuAB and HmbR are both TBDTs, powered by the highly conserved TonB-ExbB-ExbD complex and are both subject to high-frequency phase variation in clinical isolates (Lewis et al., 1999), but the systems do have their distinctive differences. HmbR binds Hb and accepts haem as a monopartite system, whilst HpuAB is a bipartite system consisting of two proteins working in partnership HpuA, a lipoprotein attached to the outer membrane of the cell by its lipid anchor and HpuB, the 22-strand transmembrane β-barrel (Figure 1.7B). The ability of pathogenic *Neisseria* to use haem as an iron source is an additional arrow in the quiver of their virulence. Although strains without the Hb receptors have been isolated from patients, comparisons of receptor presence and phase variation status in disease versus carriage isolates of *N. meningitidis*, led to the suggestion that expression of one of these receptors is important for systemic infection (Tauseef et al., 2011). Therefore, although neither Hb binding receptor is essential for infection, the presence of one or the other does appear to contribute towards pathogenesis.

1.8.8.1 - *HmbR*

HmbR is a monopartite Hb-binding TBDT from *N. meningitidis* which was identified more than two decades ago but still has no published structure. Hb utilisation experiments using strains in which the *hpuB* gene was inactivated identified a poly G tract in the *hmbR* gene that is responsible for an 'on/off' phase variation switch. Strains possessing either 9 or 12 consecutive G residues were able to utilise Hb, whereas strains with any other number of consecutive G residues were not due to a resultant frameshift. The switching rates of 'phase on' to 'phase off' variation ranged from 7×10^{-6} to 2×10^{-2} in different serogroups (Richardson & Stojiljkovic, 1999).

More recently than the characterisation of phase variation in HmbR, a series of experiments identified functionally significant domains, which inevitably focused on the putative extracellular loops. Mutations in loop 2 and loop 3 affected Hb binding completely, whilst mutations in loop 6 and loop 7 did not eliminate Hb binding capability but did result in a failure to utilise Hb. Interestingly, although loop 7 was not identified to be essential for Hb binding, it is essential for Hb utilisation, theoretically due to a conserved Histidine residue and YRVP and NPNL motifs, which are found in all known Hb receptors (Perkins-Balding et al., 2003)

1.8.8.2 - *HpuAB*

HpuAB is functionally distinct from HmbR due to its ability to acquire haem from the Hb:Hp complex. It is a system used not just by *Neisseria* pathogens but by other pathogens from the wider *Neisseriaceae* family, including *Kingella kingae* and *Eikenella corrodens*. *K. kingae* is commonly found in the oropharynx of children and can lead to paediatric bacteraemia, osteomyelitis and septic arthritis (Basmaci & Bonacorsi, 2017). *E. corrodens* is a normal component of the oral flora in children and adults, but this asymptomatic colonisation can, however, lead to infections such as periodontitis, osteomyelitis, and endocarditis (Paul & Patel, 2001). Although red blood cell lysis is an important step in haem acquisition from Hb, only *E. corrodens* and *K. kingae* of the named *Neisseriaceae* family pathogens have been described to be haemolytic (Lejbkowicz et al., 1999; Mansur et al., 2017).

The earliest experiments used to investigate HpuAB Hb binding capabilities were Hb growth assays, which involved growing *Neisseria* pathogens in environments where Hb was the sole iron source. It was rationalised that the essential need for iron would require binding to Hb in order to acquire haem iron. Mickelsen and Sparling (1981) reported that 18 of 29 gonococcal strains and 20 of 21 meningococcal strains tested were able to use Hb as an iron source (Mickelsen & Sparling, 1981). Later data would also show that gonococcal and meningococcal strains can also utilise free haem.

At this point, the mechanism by which *Neisseria* pathogens were able to use haem and haemoglobin was unknown. Using batch affinity chromatography from whole cells or membranes of gonococci grown in iron-limited conditions, Lee (1992) identified two haemin binding proteins (HmBP). Competition binding experiments were used to confirm that the haemin to protein interaction was specific. Only haemin or haem carrying proteins such as cytochrome c or haemoglobin were demonstrated to bind, whereas protoporphyrin IX or iron-loaded transferrin and lactoferrin did not (Lee, 1992).

One of the unknown HmBPs was identified as HpuB by Lewis and Dyer (1994) using mutagenic analysis of *N. meningitidis* membrane proteins, and by the loss/gain function of the strain to use Hb and Hb:Hp as an iron source. The initial experiments used a whole-cell dot blot assay which indicated binding of *N. meningitidis* to Hb and Hb:Hp. *In vitro*, western blot experiments showed that HpuB did not bind Hb or Hb:Hp but was affinity purified using the Hb:Hp complex. A meningococcal mutant (DNM2E4) was created by the insertion of a transposon into the gene coding for HpuB. Analysis of all MPs yielded by the wild type (WT) and DNM2E4 mutant revealed that proteins within the respective outer membranes were identical, except that DNM2E4 did not produce HpuB. In addition, it was also observed that DNM2E4 was unable to use the Hb:Hp complex as an iron source and had an impaired ability to use free Hb (Lewis & Dyer, 1995).

Sequence analysis of *hpuB* cloned from *N. meningitidis* strain DNM2 revealed that HpuB belongs to the TonB-dependent family of outer membrane proteins, powered by trans-periplasmic proton force to transport nutrients. It was also revealed that there is a second open reading frame (ORF) located upstream from *hpuB* that encodes a ~34 kDa lipoprotein, designated HpuA. Further sequence analysis and mutagenic experiments showed that the *hpuA* and *hpuB* genes are co-transcribed and that the 3.5 kb polycistronic *hpuAB* mRNA expression is transcriptionally repressed by iron. The structure of the *hpuAB* operon led to the conclusion and designation of HpuA-HpuB as a bipartite receptor which somehow functions together in the utilisation of Hb and Hb:Hp for haem iron, similar to the analogous TbpB-TbpA receptor for the use of transferrin (Lewis et al., 1997).

Although HpuB, as the TBDT, is seen as the main feature of the HpuAB system, both proteins are needed for efficient functionality (Figure 1.7B). A 2004 flow cytometry study into the role of each protein showed that HpuB expressed alone can bind Hb and Hb:Hp (Rohde & Dyer, 2004). The study also showed that in the absence of HpuA, the binding

capacity of the system was reduced and HpuB was less able to dissociate from Hb; the speed of dissociation after nutrient extraction is an important factor in the continual acquisition of haem from Hb (Rohde & Dyer, 2004). Wild type HpuAB was shown to dissociate from Hb very rapidly and efficiently. 50% of bound Hb vacated the binding site after the addition of new Hb and that number increased to 80% for the dissociation of bound Hb:Hp. The study also reported that there was no observation of HpuA alone binding to Hb or the Hb:Hp complex through flow cytometry (Rohde & Dyer, 2004). Just over a decade later, evidence of a direct HpuA-Hb interaction was presented: a HpuA homologue from *Kingella denitrificans* was shown to independently and weakly bind Hb using pull down assays, isothermal titration calorimetry, nuclear magnetic resonance, and crystallography(Wong et al., 2015). *K. denitrificans* HpuA shares 30% sequence identity and 48% similarity with the protein in the clinically relevant relative *N. gonorrhoeae*. Due to this discovery, HpuA is secured in its description as an enigmatic, yet essential component of this iron acquisition system (Wong et al., 2015).

Structural analysis of HpuA revealed a single domain comprising a C-terminal small β-barrel and an N-terminal loose β-sandwich (Wong et al., 2015). The structure of the HpuA:Hb complex revealed some significant molecular details regarding its Hb binding capabilities: two functionally important loops involved in binding Hb (loops 1 and 5) interact with both the a and b chain of Hb, burying hydrophobic side chains and also forming several hydrogen bonds. However, these loops that are critical for substrate binding are not conserved across *Neisseriaceae* bacteria beyond the conservation of prominent hydrophobic residues (Wong et al., 2015). Although the HpuAB system has been investigated for some time, the structure of HpuB has not yet been resolved. A model of the protein has been created using the crystal structure of ShuA (which shares 16% identity with HpuB) as a template and this model comprises a β-barrel structure with an N-terminal plug domain (Harrison et al., 2013). The model is likely reliable when considering the transmembrane β-strands and the plug domain of the protein. However, as explained by Harrison *et al* (2013), it becomes unreliable when focusing on the

extracellular loops that are predicted to be involved in obtaining haem from Hb or the Hb:Hp complex. For example, loops 2 and 8 were too long to be modelled effectively and loop 9 was subject to high sequence variation (Harrison et al., 2013).

1.9 – Relevance of Hb binding

This review has focused on a wide range of pathogenic bacteria with one thing in common; the ability to use haem from Hb as an iron source through cell surface piracy, using a variety of reported Hb binding proteins (Table 1.2). The sections above have described the information available about the systems they employ to this end.

Table 1.2: Haemoglobin binding proteins in human pathogens.

Human pathogens that use Hb as an iron source usually bind Hb through specific surface-exposed membrane proteins, extracellular lipoproteins or secreted haemophores. Pathogens can have more than one Hb binding system and these proteins can have single or multiple substrates.

Hb binding organism	Hb binding protein	Functional domains	Host Haemoprotein Substrate
Corynebacterium diphtheriae	HtaA	CR domains	Hb, Hb:Hp, Myoglobin
Corynebacterium diphtheriae	ChtaA/ChtC	CR domains	Hb:Hp
Corynebacterium diphtheriae	HbpA	CR domains	Hb:Hp
Staphylococcus aureus	IsdB	NEAT domains	Hb
Staphylococcus aureus	IsdH/HarA.	NEAT domains	Hb Hb:Hp
Streptococcus pyogenes	Shr	HID & NEAT domains	Hb, Hb:Hp, Myoglobin
Bacillus anthracis	IsdX1/X2	NEAT domains	Hb
Bacillus anthracis	Hal	NEAT domains	Hb
Listeria monocytogenes	Hbp2	NEAT domains	Hb
Clostridium perfringens	ChtD/ChtE	NEAT domains	Hb
Shigella dysenteriae	ShuA	TBDT	Hb
Pathogenic *Neisseria*	HmbR	TBDT	Hb
Pathogenic *Neisseria*	HpuA	Lipoprotein	Hb, Hb:Hp
Pathogenic *Neisseria*	HpuB	TBDT	Hb, Hb:Hp
Haemophilus ducreyi* & *Haemophilus influenzae	HgbA	TBDT	Hb
Haemophilus influenzae	HgbB & HbgC	TBDT	Hb, Hb:Hp
Haemophilus influenzae	HhuA	TBDT	Hb, Hb:Hp
Pseudomonas aeruginosa	PhuR	TBDT	Hb
Acinetobacter baumannii	HphA	Lipoprotein	Hb
Mycobacterium tuberculosis	PPE36/PE22	PPE domain	Hb
Mycobacterium tuberculosis	PPE62	PPE domain	Hb

1.10 - Hb availability

The majority of pathogens covered here are capable of causing systemic infections where they will encounter free Hb from spontaneous haemolysis. Most are also known to be haemolytic, and the lysis of erythrocytes would further enhance their supply of the most abundant source of iron in the body, for which they have just the right tools to plunder. Indeed, of the pathogens listed in this review, only the organisms from the *Neisseria* and *Bacillus* genera are non-haemolytic on blood agar. However, for most of these pathogens, their usual modes of transmission involve host niches that one does not usually associate with an abundance of Hb and the selective pressure that has led to the evolution of Hb piracy systems may not be immediately obvious. The most common infection and transmission methods of these pathogens can be divided into three categories: those that involve surfaces of the respiratory system*: C. diphtheriae, S. pyogenes*, *S. aureus*, *N. meningitidis*, *M. tuberculosis*, *P. aeruginosa*, those that transmit via mucosal surfaces of genitalia*: N. gonorrhoeae, H. ducreyi*, and those that transmit via the faecal-oral route: *C. perfringens*, *S. dysenteriae*, *L. monocytogenes*. Although the concentrations of Hb encountered by these bacteria through their infection and transmission cycles are not known, these mucosal locations are not normally associated with an abundance of Hb-containing erythrocytes.

Concentrations of Hb in the oral, nasal and pharyngeal cavities that act as a niche for *S. aureus*, *S. pyogenes*, *C. diphtheriae* and *N. meningitidis* have not been directly defined, but investigations into salivary Hb as a potential diagnostic tool for periodontitis have identified an average of 6 μg/mL of Hb in the saliva of healthy individuals (Nomura et al., 2016). Whether this level is indicative of the concentrations available for these organisms in their more intimate associations with the mucosal surfaces and whether it is sufficient to support growth remains to be demonstrated. For *M. tuberculosis* and *H. influenzae* that infect deeper respiratory tissue, speculation as to the source of their targeted Hb may extend beyond erythrocytes. Although originally understood to be expressed solely by erythrocytes, expression of Hb has been detected both by activated

mouse macrophages and by alveolar epithelial cells (L. Liu et al., 1999; Newton et al., 2006; Grek et al., 2011). Whether either of these cell types could be a source of Hb for *M. tuberculosis*, whose pathogenesis is explicitly linked with alveolar macrophages, has not been directly investigated, but a dpp knockout strain of *M. tuberculosis* was impaired for survival in macrophages, suggesting that haem is an important iron source in this niche (Mitra et al., 2019)

The urogenital mucosa that supports growth of *N. gonorrhoeae* and *H. ducreyi* are also not often associated with erythrocytes and Hb. Are Hb receptors important during infection of these surfaces, or only for when these organisms spread systemically? In the case of *N. gonorrhoeae*, the dominance of iron acquisition using transferrin receptors is well documented (Cornelissen et al., 1998). Notwithstanding, there is evidence that Hb receptors are employed to benefit from the increased blood availability during menses. Hb receptor 'on' strains were far more likely to be isolated from female patients than from male patients and the receptor is expressed significantly more often by isolates from the earlier stages of the menstrual cycle (Anderson et al., 2001). In chancroid disease caused by *H. ducreyi* infection, biopsies of resulting genital ulcers have revealed a base layer of superficial necrosis that includes fibrin, leukocytes and erythrocytes, lysis of which could yield Hb as an iron source (Abeck et al., 1997).

The tissue damage that results from *S. dysenteriae* infection often leads to diarrhoea containing blood and this is a potential source of haem for these organisms during their infection cycle. The other gastrointestinal pathogens listed briefly above are less commonly associated with dysentery and for these one can only speculate that the sources of Hb could be dietary during the infection cycle, or that the Hb receptors are employed only during systemic infection.

1.11 – Aims and objectives

This project aimed to investigate the role of HpuB in the HpuAB acquisition of haem from Hb in pathogenic *Neisseria*. Whilst there is already published whole cell binding data using flow cytometry on the HpuAB system binding of Hb and the Hb:Hp complex (Rohde & Dyer, 2004), there is still much to understand about the mechanistic role of HpuB in substrate binding, haem stripping and transport. In 2015, Wong et al published a functional/structural description of HpuA *in vitro*. This included a 2.3 Å crystal structure of recombinant HpuA in complex with human Hb, pull down data using Hb and the Hb:Hp complex and binding kinetics data using ITC (Wong et al., 2015). As a membrane protein, providing similar structural and functional information for HpuB presents unique challenges. Membrane proteins are notoriously difficult to recombinantly express, solubilise and purify – leaving a structural complex of the HpuAB/Hb system as a significant missing piece of the puzzle.

This project aimed to provide a piece to this puzzle piece by:

1. Recombinantly produced HpuB using *E. coli*
2. Reconstituting and stabilising HpuB using a suitable membrane memetic
3. Using relevant structural techniques to provide a resolved structure of HpuB
4. Providing a resolved structure of HpuB in complex with Hb, Hb:Hp and its extracellular lipoprotein partner, HpuA.
5. Investigate HpuB's binding capabilities with Hb and the Hb:Hp complex using binding analysis techniques.

CHAPTER 2: METHODS AND MATERIALS

2.1 – Materials

Table 2.1: List of *E. coli* strains used in this study

Name	Genotype	Reference
PC2	BL21 (DE3), *endA::TetR, T1R, pLysS*	(Cherepanov, 2007)
DH5α	*supE44, Δ(lacZYA-argF) hsdR17, recA1, endA1 gyrA96 thi-1 relA1*	Purchased from NEB
Omp8	BL21(DE3) *ΔompA, ΔlamB, ΔompC, ΔompF*	(Meuskens et al., 2017) Addgene ID102270
BL21*	BL21 (DE3), *FhuA2::ompT,ΔhsdS*	Purchased from NEB

Table 2.2: List of protein purification columns used in this study

Name	Details	Purification Technique	Volume (mL)	Supplier
S200	Superdex 16/600 HiLoad	SEC	120	GE Healthcare
S75	Superdex 16/600 HiLoad	SEC	120	GE Healthcare
S6	Superose increase 10/300 GL	SEC	24	GE Healthcare
HisTrap HP	Ni^{2+} Sepharose HP affinity resin	IMAC	1	Cytiva
HiTrap S	CM Sepharose Fast Flow	IEX	5	Cytiva
HiTrap Q	CM Q Fast Flow	IEX	5	Cytiva

Table 2.3: List of TEM grids used in this study

Name	Film type	Technique	Provider
CF200-Cu	Carbon	Negative stain	EMS
CF150-Cu	Carbon	Negative stain	EMS
Quantifoil R1.2/1.3	Holey carbon	Cryo	EMS
Cflat 1.2/1/.3	Holey carbon	Cryo	EMS

Table 2.4: List of plasmids used in this study

Name	Details	Antibiotic resistance	Reference
pHISHKdHpuA	pET15b with added PreScission protease site *K. denitrificans HpuA*, lac inducible promoter N – terminal 6XHisTag	Ampicillin	(Wong et al., 2015b)
pHISHNgHpuA	pET15b with added PreScission protease site *N. gonorrhoeae HpuA*, lac inducible promoter N – terminal 6XHisTag	Ampicillin	(Wong et al., 2015b)
pHISHKdHpuB	pET15b with added PreScission protease site *K. denitrificans HpuB*, lac inducible promoter N – terminal 6XHisTag	Ampicillin	This study
pHISHNgHpuB	pET15b with added PreScission protease site *N. gonorrhoeae HpuB,* lac inducible promoter N – terminal 6XHisTag	Ampicillin	This study
pBASHOM2	pBAD with added PreScission protease site and ompA secretion tag N – terminal 6XHisTag	Chloramphenicol	This study
pBASHOM2NgHpuB	pBAD with added PreScission protease site and ompA secretion tag *N. gonorrhoeae* HpuB, araC inducible promoter N – terminal 6XHisTag	Chloramphenicol	This study
pBASHOM2KdHpuB	pBAD with added PreScission protease site and ompA secretion tag	Chloramphenicol	This study

	K. denitrificans HpuB, araC inducible promoter N – terminal 6XHisTag		
pBASHOM2NmHpuB	pBAD with added PreScission protease site and ompA secretion tag *N. meningitidis* HpuB, araC inducible promoter C – terminal 6XHisTag	Chloramphenicol	This study
pMSP1D1	pET28a with TEV protease site *MSP1D1*, lac inducible promoter C – terminal 6XHisTag	Kanamycin	(Denisov et al., 2004)
pMSP1E2	pET28a with TEV protease site *MSP1E2*, lac inducible promoter C – terminal 6XHisTag	Kanamycin	(Denisov et al., 2004)
pMSP1E3	pET28a with TEV protease site *MSP1E3*, lac inducible promoter C – terminal 6XHisTag	Kanamycin	(Denisov et al., 2004)

Table 2.5: List of antibiotics used in this study

Name	Stock solution	Concentration used in media (μg/mL)
Ampicillin (Amp)	100 mg/mL dissolved in 60% ethanol	100
Chloramphenicol (Cam)	34 mg/mL dissolved in 100% ethanol	34
Kanamycin (Kan)	50 mg/mL dH_20 (filter sterilised)	50

Table 2.6: List of oligonucleotide primers designed for the sub cloning of orthologous HpuBs into the pBASHOM2 expression vector.
Details of primers used to create pBASHOM2 expression vectors.

HpuB species	Forward Primer 5′ – 3′	Reverse Primer 5′ – 3′
N. gonorrhoeae	GCAGGTACCGCAGACC CGGCGCCGCAGTCTG	GCAAAGCTTTTAGAATTTC GCTTCGATGGTGAAGTTG
K. denitrificans	GCAGGTACCGCAGAAC CGGATAAAGGCACCG	GCAAAGCTTTTACCATT TGGCTTCCAGATTCAGC
N. meningitidis	GCAGGTACCGCAGAC CCCGCGCCGCAG	GGCGGATCCTTAGAACTTC GCTTCGATGGTGAAATTGTAGC

Table 2.7: List of oligonucleotide primers designed for the creation of *N. gonorrhoeae* HpuB mutants.

Details of primers used to create HpuB mutants. In loop deletions, forward primers contained an added 'GGCTCTGGG' sequence which functioned as a linker between the β sheets from which a loop was deleted. Reverse primers were designed with a dephosphorylated 5′ end to prevent self-ligation.

Mutant HpuB target location	**Mutation Detail**	**Forward Primer 5′ – 3′**	**Reverse Primer 5′ – 3′**
Loop 2	Δloop-2 (delete residues 196-244)	GGCTCTGGG TGGGTAAACAAAAGC ACCCTGTTCAAG	GCCGAAGCGGCGGGTA T AAAC
Loop 3	Δloop-3 (delete residues 274-301)	GGCTCTGGG AGCTACCGCCGCCGC ACC	GTCGGTGCGCGAGTCT TC AAAAATC
Loop 7	Δloop-7 (delete residues 515-538)	GGCTCTGGG GCGGAAAAAGCCAA AA ACTGGGAATTG	TGCGCGGAAGCCGGT GC
Loop 11	Δloop-11 (delete residues 742-755)	GGCTCTGGG GGCAGGAGCTACAAT TTCACCATCG	CTTGTTGGTAATGTTGT AC GCGGC
Loop 7	NPEL mutate to APAA	CACCCCGATTTCTACC TGA AAACCGCGCCGGCGG CGA AAGCGGAAAAAGCC AAAA ACTGG	CCAGTTTTTGGCTTTTT CCG CTTTCGCCGCCGGCGC GGT TTTCAGGTAGAAATCG GGG TG
Plug	R89 to E	GGCTGGCGCAGGCGG AAAGCGAATCTTCCG AAGCCTTCCAAG	CTTGGAAGGCTTCGGA AGATTCGCTTTCCGCCT GCGCCAGCC
Plug	K144 to E	GGCGCAGTCAATTAC CAAACCGAATCCGCA AGCGACTATGTTTC	GAAACATAGTCGCTTG CGGATTCGGTTTGGTA ATTGACTGCGCC

Table 2.8: List of all other oligonucleotides used in this study.

Name	Primer Sequence 5′ – 3′	Primer purpose
SAH737	TGGTAGCGTGAAAGAGTATC	*K. denitrificans* HpuB internal sequencing primer
SAH738	GCCCAAGTGAAACACATTGTTC	*N. gonorrhoeae* HpuB internal sequencing primer
SAH739	ATCCGCAGAATACCGAAGATCATG	*N. meningitidis* HpuB internal sequencing primer

Luria-Bertani (LB) broth: Liquid growth medium used for *E. coli*. 10 g Difco Bacto tryptone, 5 g Difco yeast extract, 5 g NaCl, 1 g glucose dissolved in 1 L dH2O. Stored in 100 ml and 500 ml aliquots.

LB agar: Solid growth medium for E. coli. 10 g Difco Bacto tryptone, 5 g Difco yeast extract, 5 g NaCl, 1 g glucose dissolved in 1 L dH2O. Aliquoted (100 ml) into flasks, stoppered with a foil and autoclaved.

Coomassie quick stain solution: 40 mg Coomassie G250 was dissolved in 500 ml dH_20 and stirred for ~ 2 hours followed by the addition of 1.5 mL concentrated HCL.

2.2 – Preparation of chemically competent *E. coli*

E. coli cells were streaked to single colonies from frozen aliquots (-80 °C) onto fresh LB agar plates and incubated overnight at 37 °C. A single colony was then used to inoculate a 5 ml of LB broth (with appropriate antibiotic) and grown overnight with shaking (250RPM) at 37 °C. Two mL of overnight culture was used to inoculate 200 mL of fresh LB broth and incubated as previously to an OD_{600} of ~0.4-0.6. Cultures were then centrifuged at 4000 x g for 10 min at 4 °C before pellets were washed with 40 ml of ice-cold 100 mM $MgCl_2$ + 10% glycerol and centrifuged again as above. Cell pellets were then resuspended in ice-cold 40 ml of 100 mM $CaCl_2$ + 10% glycerol and left on ice at 4 °C overnight. Cells were harvested by centrifugation as above and resuspended in 2 ml of 100 mM $CaCl_2$ + 10% glycerol, rapidly placed into Eppendorf tubes as 50-100 µL aliquots, and immediately flash-frozen in liquid nitrogen. Tubes were then stored at -80 °C until required.

2.3 – Plasmid extraction from *E. coli*

Plasmid DNA was extracted from DH5α cultures (transformed with relevant plasmid) grown in LB broth using a plasmid miniprep kit (Monarch), as per the manufacturer's instructions. Plasmid DNA was eluted from the column using 25-50 µL of sterile double distilled H20, with concentrations determined using a nanodrop 1000 (Thermofisher Scientific).

2.4 – Protein Expression

2.4.1 - Transformation

Transformation of the expression vector into *E. coli* expression cells was done via the standard heat shock method. The transformed cells were inoculated on separate Luria-Bertani (LB) agar with added antibiotics for the selection of positive transformants. The agar plates were incubated at 37 °C for 16 hours.

2.4.2 - Soluble protein and inclusion body expression

One colony of transformants is used to inoculate 50 mL of LB broth with added antibiotic and incubated with shaking (200 RPM) at 37 °C for 16 hours (Starter culture). 10 mL of starter culture was added to 1 L of LB broth with added antibiotic in a 2 L flask (Expression media). This culture was incubated at 37 °C with shaking (200 RPM) until it reached an OD_{600} of 0.6 – 0.8, protein expression was then induced by the addition of isopropyl β-D-1-thioglactopryranoside (IPTG) to a final concentration of 0.5 mM. The temperature was reduced to 30 °C and the protein was expressed for 4 hours. Cells were harvested from the culture by centrifugation at 4,000 x g for 15 minutes at 4 °C and the resulting pellet was resuspended in wash buffer (20 mM imidazole, 500 mM NaCl, 50 mM Tris) to be frozen at -80 °C.

2.4.3 - Membrane-bound protein expression

Expression plasmids were into *E. coli* expression cells via heat shock protocol and grown on selective LB agar. Transformants were used to inoculate a starter culture of 50 mL LB broth with added antibiotic and grown overnight at 37°C with shaking (200RPM). 10 mL of starter culture was added to 1 L of LB broth with added antibiotic in a 2 L flask. This culture was incubated at 37 °C with shaking (200 RPM) until it reached an OD600 of 0.8 – 1.0, protein expression was induced by the addition of arabinose to a final concentration of 0.001% w/v. The incubator temperature was reduced to 18°C and the protein of interest (POI) was expressed overnight. Cells were harvested from the culture by centrifugation at 4,000 x g for 15 minutes at 4 °C and the resulting pellet was resuspended in wash buffer (50 mM Tris, 20 mM imidazole, 500 mM NaCl) to be frozen at -80 °C.

2.4.4 - Protein expression for HpuB mutant dot blot experiments

The pBASHOM2 construct was used to clone a range of *N. gonorrhoeae* HpuB mutants. Plasmid pBASHOM2 HpuB was transformed into Omp8 BL21 *E. coli* cells via heat shock and grown on selective LB agar with 35 μg/ mL chloramphenicol (CAM). Transformants were used to inoculate a starter culture of 5 mL LB broth (35 μg/mL CAM) and grown overnight at 37°C with shaking (200 RPM). 1 mL of starter culture was added to 10 mL of LB broth (35 μg/mL CAM). This culture was incubated at 37 °C with shaking (200 RPM) until it reached an OD_{600} of 0.8 – 1.0, protein expression was then induced by the addition of arabinose to a final concentration of 0.001% w/v. The incubator temperature was reduced to 18°C and HpuB was expressed overnight.

2.5 – Cell lysate preparation

Cells were lysed via thawing, the addition of protease inhibitor phenylmethane sulfonyl fluoride (PMSF) (Sigma Aldrich) to 0.5 mM and sonication in short 1-second bursts for 2 minutes. Following sonication, the soluble and insoluble fractions were separated by centrifugation at high speed (27,000 x g) for 45 minutes.

2.6 – Inclusion body and outer membrane preparation

2.6.2 - Inclusion body pellet preparation

The insoluble cell lysate was resuspended in inclusion body (IB) buffer (50 mM Tris 7.5 pH 7.4, 2% v/v LDAO) at a ratio of 50 mL: 1 g and incubated for 2 hours at 4 °C with stirring. Post incubation, the insoluble material was washed three times with a wash buffer (50 mM Tris pH 7.4). The resulting inclusion body pellet was frozen at -80 °C. Small aliquots of insoluble material from each step were used to prepare samples for analysis via SDS PAGE.

2.6.3 - Inclusion body solubilisation and refolding

Inclusion body pellets were re-suspended in a solubilisation buffer (20 mM Tris pH 7.4, 6 M GuHCl, 1 mM EDTA) and incubated with stirring for 1 hour at 4°C. The insoluble material is removed by centrifugation and the solution was then added in a drop wise manner to refolding buffer (20 mM Tris pH 7.4, 5% v/v LDAO, 250 mM NaCl, 50 μM Hemin) with stirring at room temperature for 4 hours. SnakeSkin™ (5 kDa cut-off) dialysis tubing was then used to dialyse the protein mixture into a new buffer (20 mM Tris, 0.1% LDAO) at 4 °C for 16 hours.

2.6.4 - Isolating and solubilising the outer membrane

Cells were lysed as described in section 2.2.1. Following sonication, the soluble and insoluble fractions were separated by centrifugation at high speed (27,000 x g) for 20 minutes. The crude membrane was isolated by ultracentrifugation of the soluble fraction at 200,000 x g for 40 minutes at 4 °C. The isolated crude membrane was hand homogenised using a Dounce homogeniser into wash buffer with the addition of sarcosine at 2% w/v to selectively solubilise the inner membrane. This mixture was then incubated at room temperature for 1 hour with gentle agitation. The outer membrane was isolated by another ultracentrifugation step at 200,000 x g for 40 minutes at 4 °C. The outer membrane pellet was hand homogenised into wash buffer. To solubilise the outer membrane, LDAO was then added to the mixture at 2% v/v followed by incubation at room temperature for 2 hours. Insoluble material was removed by ultracentrifugation of the mixture at 200,000 x g for 30 minutes at 4 °C. The solubilised outer membrane was mixed with pre-equilibrated Ni^{2+} coated resin and incubated overnight at 4 °C with gentle agitation.

2.7 – Protein purification

2.7.1 - Immobilised Metal Affinity Chromatography

2.7.1.1 - Gravity Flow

Immobilised Metal Affinity Chromatography (IMAC) was performed using NiNTA resin on a gravity flow column. The soluble fraction of the cell lysate, refolding solution or solubilised outer membrane was incubated with the resin for 1 hour at 4 ˚C before the resin was isolated by centrifugation and washed 3 times in wash buffer. An elution buffer (50 mM Tris pH 7.4, 500 mM NaCl, 500 mM imidazole) was used to elute the POI from the column in 1 mL fractions. Small samples from each fraction were aliquoted for protein expression and purity analysis via SDS PAGE.

For the IMAC purification of refolded POIs, the refolding solution was incubated with NiNTA resin for 2 hours at 4 °C. Wash buffer here was 20 mM Tris pH 7.4, 150 mM NaCl, 0.1% LDAO, 20 mM imidazole, elution buffer was 20 mM Tris pH 7.4, 150 mM NaCl, 0.1% LDAO, 500 mM imidazole.

2.7.1.2 - AKTA

Using an ÄKTA HPLC machine, A 1 mL AKTA Ni^{2+} IMAC HP column was pre-equilibrated with wash buffer (50 mM Tris pH 7.4, 500 mM NaCl, 20 mM imidazole) with added detergent as appropriate. The solubilised outer membrane was loaded onto the column and the flowthrough was collected in 1 mL fractions. The column was washed with appropriate wash buffer and the POI was eluted with an increasing gradient of imidazole from 20 mM to 500 mM over 20 mL at a flow rate of 1 mL/min. The imidazole gradient samples were collected in 1 mL fractions and aliquoted for protein expression and purity analysis via SDS PAGE.

2.7.2 - Size Exclusion Chromatography

Size exclusion chromatography (SEC) was performed using an ÄKTA HPLC machine. Experiment appropriate columns (Table 2.2) were equilibrated with two column volumes of appropriate SEC buffer as indicated in table 2.9.

Samples were injected using volume-appropriate loops. Flow rates and elution fraction collection volumes were column specific. Following fraction collection, small aliquots of fraction corresponding to expected or significant A280 UV peaks were prepared for and analysed via SDS PAGE. Fractions containing the POI were concentrated and supplemented with 10% glycerol, frozen in liquid nitrogen and stored at -80 °C.

Table 2.9: Size Exclusion Chromatography experimental details.
Methodological details for the performance of SEC for protein purification

Protein	Column	Buffer	Flow rate (mL/min)	Fraction volume (mL)
K. denitrificans HpuA	S75	20 mM Tris pH 7.4, 150 mM NaCl	1	2
Refolded *N. gonorrhoeae* and *K. denitrificans* HpuB	S200	20 mM Tris pH 7.4, 150 mM NaCl, 0.1% LDAO	1	2
Hb:Hp complex	S6	PBS	0.5	0.5
Crosslinked Hb	S6	PBS	0.5	0.5
Membrane extracted *N. gonorrhoeae* and *K. denitrificans* HpuB	S200	20 mM Tris pH 7.4, 150 mM NaCl, 0.1% LDAO	1	2
MSP1D1, MSP1E2, MSP1E3	S75	20mM Tris pH 7.4, 150 mM NaCl	1	2
HpuB Nanodisc	S6	20 mM Tris pH 7.4, 100 mM NaCl	0.5	0.5

2.8 – Protein preparation analysis

2.8.1 - SDS PAGE

For the separation and analysis of protein purification samples by SDS-PAGE, 12% Bis-Tris polyacrylamide or 4-12% NuPAGE gradient Bis-Tris polyacrylamide gels (Invitrogen) were loaded and run for 1 hr at 120 V. Before loading protein, samples were diluted in Laemmli 2x sample buffer (Sigma Aldrich) according to manufacturer's instructions. Bands were visualised by Coomassie staining, by removing the gel from a plastic cassette and placed into a small container filled with dH_20 to submerge the gel, before heating in the microwave for 30 seconds and discarding the dH_20. This was repeated 3 more times, before submerging the gel with Coomassie quick stain and heated again for 30 seconds. The stain was discarded into a waste bottle, and gel rinsed in dH_20. The gel was either examined immediately using a light box. Coomassie stain was prepared by dissolving 40 mg Coomassie G250 500 ml dH20 with stirring for 2 hours then adding 1.5 ml of concentrated HCL

2.8.2 - Anti-His Western Blot

SDS PAGE was performed using a 10% Tris-Glycine polyacrylamide gel. A Hoefer™ TE 70 semi-dry transfer unit was used to transfer the proteins from the gel onto a nitrocellulose membrane. The membrane was blocked with blocking buffer (TBS-Tween, 3% w/v BSA) for 30 minutes with gentle agitation at room temperature. The membrane was incubated with primary antibody (anti-His Tag Antibody, pAb, Rabbit; from GenScript) overnight at 4 °C with gentle agitation then rinsed in deionised water and washed three times in PBS-Tween. The secondary antibody (anti-rabbit IgG with HRP conjugation (Sigma Aldrich) was incubated with the membrane for 2 hours at 4 °C, then rinsed in deionised water and washed three times in PBS-Tween. ECL detection was done with Pierce™ ECL Western Blotting Substrate Thermo Scientific and visualised on a digital Licor machine

2.9 – HpuB Crystallography Screen

Refolded HpuB prepared as outlined in section 2.2 was concentrated to 3.8 mg/ml. 150 nL drops of protein were used to perform MemGold™ and MemGold 2™ (Molecular Dimensions) crystal screens under oil droplets as well as without and incubated at 18 °C. The same screens were also performed with HpuB mixed with haemoglobin tetramers at a molar ratio of 1: 1.2 respectively.

2.10 – Preparation of the Haemoglobin-Haptoglobin complex

One milligram of human haptoglobin (phenotype 1-1) (Sigma Aldrich) was mixed with 1.5 mg human haemoglobin (Purified from blood acquired from malaria research lab at Imperial college London) in 10 mL phosphate buffered saline (PBS). The mixture was then concentrated down to 500 μl and loaded onto a Superose™ 6 10/300 GL SEC column from GE Healthcare. A SEC protocol was run using an ÄKTA to separate the Hb:Hp complex from free haemoglobin. Fractions were collected in 0.5 mL volumes, concentrated, and supplemented with 10% glycerol then stored at -80 °C. Fractions were aliquoted for purity and separation analysis using SDS PAGE.

2.11 – Pull down experiments

Haemoglobin and bovine serum albumin (BSA) were prepared to 0.5 mg/ml in PBS, added to 150 mg of hydrated Pierce™ NHS-Activated Agarose and incubated at 4 °C overnight with agitation. The resin was removed via centrifugation (4000 xg for 15 minutes) and washed with PBS to remove unbound protein. After washing, the agarose beads were incubated in 1 M Tris-HCl pH 7.4 at room temperature for 30 minutes with agitation to block unbound sites. Aliquots of 40 μL of activated beads for both HpuB and BSA were added to 500 μL of PBS with 50 μg of HpuB and then incubated at 4 °C for two hours with agitation. The agarose beads were removed by centrifugation (4000 xg for 15 minutes) and washed three times in PBS then added to Laemmli buffer in preparation for SDS PAGE. For HpuB mutant pull down experiments, 100 μg of purified HpuB mutants were incubated with activated beads.

2.12 – Cross-linking experiments

2.12.1 - Cross-linking HpuA to Hb:Hp

HpuA was cross-linked to Hb:Hp using glutaraldehyde at a final concentration of 0.2%. HpuA was added to a molar excess of Hb:Hp which was at 15 μM: 10 μM respectively. The reaction was performed on ice for 30 minutes and stopped by adding 10 μL of 1M Tris-HCl pH 7.4. Small samples were aliquoted and analysed via SDS PAGE.

2.12.2 - Cross-linking of Hb

Haemoglobin was diluted to 1.25 mg/mL in PBS before the cross-linker was added to the desired concentration and a final volume of 500 μL. The reactions were performed on ice for 15 minutes using glutaraldehyde concentrations ranging from 0.1% to 0.4% after which the reaction was stopped with 10 μL of 1M Tris-HCl pH 7.4. The state of the haemoglobin was then checked via SEC using a Superose 6 Increase 10/300 GL column. 0.5 mL fractions were collected and aliquoted for analysis via SDS PAGE.

2.13 – Assembly of HpuB into Nanodisc

HpuB nanodiscs were prepared using HpuB refolded from inclusion bodies and solubilised in LDAO. The lipid of choice, 1-palmitoyl-2-oleoyl-glycero-3-phosphocholine (POPC) from Avanti® was prepared for use by evaporation of excess solvent using a gentle stream of N_2. Nanodisc buffer B (20 mM Tris-HCl, 100 mM NaCl, 80mM $C_{24}H_{39}NaO_5$) (NBB) was added to the dried lipid to a final POPC concentration of 40 mM. NNB was incubated with the dried lipid for two hours in a sonicating water bath. It is vital to ensure the concentration of $C_{24}H_{39}NaO_5$ (Sodium Cholate) is double that of POPC lipid at this stage.

Membrane Scaffold Protein (MSP(1D1,1E2,1E3)) from Sigma-Aldrich was made up to 5 mg/ml solution as per manufacturer instructions. For empty Nanodisc assembly, sodium cholate solubilised POPC lipid was added to MSP at a molar ratio of 65:1. The mixture was topped up with Nanodisc buffer A (20 mM Tris-HCl, 100 mM NaCl) whilst ensuring the sodium cholate concentration did not fall below 25 mM. The mixture was then incubated at 4°C for 60 minutes with gentle agitation.

Refolded or membrane extracted HpuB was added to the empty Nanodisc mixture at a varying ratio of HpuB to MSP (4:1, 10:1 & 20:1). In order to remove the amphipathic molecules in the mixture, Bio Beads™ SM resin (BioRad) was added at a ratio of 0.5g per ml. HpuB Nanodisc self-assembly was prepared by incubating with HpuB and empty Nanodisc overnight at 4°C with gentle agitation. Bio Beads™ SM resin was removed from the mixture using centrifugation at 4000 xg for 10 minutes and the resulting solution was further filtered.

HpuB nanodisc was purified via SEC using a superose 6 01/300 column, at a flow rate of 0.5 mL/min collecting 0.5 mL fractions.

2.14 – MSP (1D1,1E2, 1E3) Preparation.

The MSP constructs (Addgene) were transformed into *E.coli* expression cells via standard heat shock method (section 2.2.1). MSP proteins were expressed as described in section 2.1.2.

Expression cultures were lysed and prepared for purification as outlined in 2.2.1. MSP proteins were first purified from the soluble cell lysate using Ni^{2+} gravity flow IMAC section 2.3.1 with 50 mM Tris-HCl 7.4, 500 mM NaCl, 20mM Imidazole as the wash buffer and 50 mM Tris-HCl 7.4, 500 mM NaCl, 500mM Imidazole as the elution buffer.

Following His-Trap IMAC, Ion Exchange Chromatography (IEX) was used to further purify MPS1D1. IEX was performed using an ÄKTA HPLC. Pooled fractions from IMAC were diluted 10-fold in order to reduce the NaCl concentration to 50 mM. The diluted protein solution was injected onto a HiTrap® Q column (GE HealthCare), washed with buffer (50 mM Tris pH 7.4) and eluted using a gradient of increasing NaCl concentration up to 500 mM NaCl. The protein was eluted in 1 ml fractions and the fractions were aliquoted for analysis via SDS PAGE. Fractions containing MSP1D1 were pooled and concentrated before further purification using SEC.

SEC was performed using an S75 SEC column and a 20mM Tris pH 7.4, 150 mM NaCl buffer. Fractions containing MSP1D1 were pooled and concentrated then supplemented to a final concentration of 10% glycerol and frozen at -80 °C.

2.15 – Cloning experiments

2.15.1 - Restriction cloning of HpuB for recombinant outer membrane expression

Restriction digestions were done using KpnI and HindIII enzymes from New England Biolabs (NEB). Following the manufacturer's protocol, a double digest of both the pHISHNgHpuB and the empty pBASHOM2 vectors was performed and then run on a 0.7% agarose gel. After visualising the gel, the correct bands were cut from the gel and the DNA was extracted using a Monarch DNA gel extraction kit from NEB.

A ligation reaction combined 2X ligation buffer, T4 DNA ligase, 50ng of vector DNA and the insert DNA was added at a ratio of 3:1, as per the manufacturer's instructions. The ligation reaction was incubated at room temperature for 1 hour. Ligated plasmid DNA was transformed into DH5α *E. coli* cells and grown on selective LB agar plates (35 μg/ mL CAM). Colony PCR using HpuB insert-specific primer sets was employed to check that the correct insert was present.

GeneJET Plasmid Miniprep Kit (Thermofisher) protocol was used to extract plasmids from colonies shown to contain the desired plasmid. The plasmids were sequenced using sequencing primers for the pBASHOM2 vector. This protocol was repeated to clone pBASHOM2 plasmids for the expression of the *K. denitrificans* and *N. meningitidis* HpuB.

2.15.2 - Inverse PCR mutagenesis for recombinant HpuB mutant expression

HpuB mutants were constructed via inverse PCR mutagenesis using primers (Table 2.7) designed to introduce a mutation. The KOD hot start DNA polymerase kit (Novagen) and specific primers were used to amplify the pBASHOM2NgHpuB PLASMID which functioned as the template DNA, the PCR experiment was performed as per the manufacturer's protocol. Each PCR reaction was made up to a final volume of 50 µL and performed using the thermocycler protocol outlined in table 2.10 repeating steps 2 to 4 for 20 cycles.

Table 2.10: The components and volumes for inverse PCR.

Components were added as per the manufacturer's protocol to a final reaction volume of 50 µL.

Component	**Volume (µL)**
10X buffer for KOD DNA pol	5
25 mM $MgSO_4$	3
dNTPs (2mM each)	5
PCR grade water	32
Forward primer (10µM)	1.5
Reverse primer (10µM)	1.5
Template DNA (85ng/µL)	1
KOD DNA polymerase (1 U/µL)	1

Table 2.11: The thermocycler steps for inverse PCR in HpuB mutagenesis.

Annealing temperatures for oligonucleotide primers were specific to each primer set. Steps 2 to 4 were repeated for 20 cycles.

PCR Step	Temperature (°C)	Time (Secs)
1) Polymerase Activation	95	120
2) Denature	95	20
3) Annealing	Primer specific	10
4) Extension	70	200

2.16 – Preparation of HpuB Peptidisc

N. gonorrhoeae HpuB was recombinantly expressed directly into the *E.coli* membrane as described in section 2.9.2 and not as IBs. The outer membrane was then solubilised as described in sections 2.9.3. The solubilised outer membrane was incubated with NiNTA resin for two hours at 4 °C

The HpuB bound Ni^{2+} coated resin was washed with Peptidisc wash buffer (50 mM Tris, 50 mM NaCl, 10% w/v glycerol, 0.04% LDAO, 5mM imidazole) and loaded onto a gravity flow column for the beads to settle. One-fifth column volume of concentrated 10mg/ml Peptidisc peptide solution (50 mM Tris, 50 mM NaCl) was added to the resin and incubated for five minutes at room temperature. 10 times column volume of dilute 1 mg/ml peptidisc solution in TSG buffer (50 mM Tris, 50 mM NaCl, 10% w/v glycerol) was then added to the resin and incubated for a further five minutes. The excess Peptidisc peptide solutions were drained by gravity flow and the resin was washed with 20 column volumes of TSG buffer. HpuB peptidisc was eluted with 10 mL of Peptidisc elution buffer (50 mM Tris, 50 mM NaCl, 10% w/v glycerol, 600mM imidazole) and collected in 1 mL fractions. Small aliquots from each fraction were aliquoted to check for protein expression and purity on SDS PAGE.

2.17 – HpuB mutant Dot blot experiments

N. gonorrhoeae HpuB and mutants were recombinantly expressed directly into the *E.coli* membrane as described in section 2.9.2 in 50 mL LB cultures. Cells were harvested from the culture by centrifugation, 4,000 x g for 15 minutes at 4 °C and the resulting pellet was resuspended in 1 mL of PBS. The OD_{600} of each resuspended pellet was normalised by dilution to an OD_{600} of 1 in a final volume of 1 mL using PBS. Hb was added to the suspension at a final concentration of 5 μM and incubated for 1 hour at room temperature with gentle agitation. Following incubation, the pellet suspension was washed three times by centrifugation and resuspension in PBS. A 1 μL sample of each expression pellet was dotted onto a PVDF membrane with additional samples from each wash step. The membrane was blocked with blocking buffer (PBS tween, 3% BSA) and washed three times in PBS tween this was followed by overnight incubation with rabbit anti-haemoglobin primary (Sigma Aldrich) antibody at 4 °C. The primary antibody was removed with three washes in PBS tween, followed by incubation with secondary antibody (IRDye 800CW Goat anti-rabbit) for 1 hour at room temperature. Secondary antibody incubation was followed by an additional three washes in PBS tween before membrane exposure. Detection was done with Pierce™ ECL Western Blotting Substrate Thermo Scientific.

2.18 – HpuB amphipol assembly

Isolated and LDAO solubilised outer membrane was loaded onto a 1 mL HisTrap high-pressure column from Cytiva Life Sciences pre-equilibrated with DDM wash buffer (50 mM Tris, 500 mM NaCl, 0.05% DDM). The sample was injected via a super loop on an AKTA protein purifier, at a flow rate of 0.5 mL/min using DDM wash buffer. Once fully loaded, the column was washed with 20 column volumes of DDM wash buffer, then HpuB was eluted via an increasing imidazole gradient from 20 mM to 500 mM, in 1 mL fractions. Fractions corresponding with a significant A280 absorbance peak were prepared for SDS PAGE analysis and fractions confirmed to contain HpuB were pooled. HpuB was reconstituted into amphipol particles via the addition of Amphipol A8-35 at a ratio of 1:3 w/w protein to amphipol. This mixture was incubated with gentle agitation for 4 hours at 4°C. DDM detergent was removed by the addition of BioBeads at 30 mg per 1mL of protein/amphipol mixture and incubated again with gentle agitation for 16 hours at 4°C. BioBeads were removed ahead of further SEC HpuB purification using amphipol buffer (50 mM Tris, 150 mM NaCl) on an S200 (16/600) column. Peak SEC fractions were analysed via SDS PAGE.

2.19 – Negative Stain Electron Microscopy (NSEM)

2.19.1 - Table of grid types

2.19.2 - Grid preparation

Grids were glow discharged (Easy glow, Agar Scientific) to create a hydrophilic surface. 3.5 μL samples of varying concentrations of each POI were adsorbed on grids before blotting with filter paper to remove excess liquid. Grids were washed twice with the buffer in which each protein is stored then coated with a thin layer (20 μL) of 2% (v/v) Uranyl acetate for 20 seconds. Excess uranyl acetate was blotted off the grid until it was completely dry.

2.19.3 – Grid imaging

Grids were imaged using a JEOL JEM1400-Plus transmission electron microscope. The microscope was equipped with a Gatan 4k x 4k OneView camera operating at 25 fps. Micrographs were collected using the GMS3 Gatan microscopy suite with 1-second final exposure and defocus ranging from – 0.5 um to - 2 um. Drift correction was automated with the GMS3 electron microscopy suite. Micrograph data collection was done manually at x50 000 (0.22 nm/pixel) or x60 000 (0.18 nm/pixel) for HpuB reconstituted in amphipols.

2.19.4 - Single particle data processing.

Single particle data processing was done using the Regularized Likelihood Optimization (RELION) suite from the MRC Laboratory for molecular biology. RELION 2.0 was used for refolded HpuB nanodiscs and all other analysis was done using RELION 3.0

2.19.5 - Particle picking

Using RELION, particle picking was performed by initially picking a small number of particles (800 – 1500). The particles are then extracted using a particle-appropriate box size (Å) and then grouped into 2D classes (6-10) based on the number of particles picked. These 2D classes were then used as a reference for automated particle picking with a low pass filer of 20 Å. Oher parameters were set at RELION 2 or RELION 3 default values.

2.19.6 - 2D Classification

The RELION program uses a reference-free maximum likelihood methodology for the alignment and averaging of 2D images. Extracted particles are randomly separated into a user-defined number of groups and averaged together. Over several iterations, each particle is compared with each averaged group and a unique probability weighting is calculated for each one. New averages are then calculated using the weighted averages, i.e. a single unique particle may initially contribute to multiple classes but with different weightings. This process is repeated until similar particles have typically been amalgamated into a single 2D class. Within this study, all 2D classifications were performed over 25 iterations using a particle-appropriate mask diameter (Å). The number of classes varied between 8 and 30 dependent on the number of particles being classified (Scheres, 2010).

2.19.7 - Initial Model

Initial models were processed to act as a reference map in 3D classification. A small subset (3-5) of representative 2D classes were chosen as input data. Model processing was low pass filtered at 60 Å, sampling performed at RELION 2.1 or RELION 3 default values.

2.19.8 - 3D Classification

Like 2D classification, 3D classification is also performed using a maximum likelihood methodology. A significant difference is in the generation of the initial averages. The dataset is split into a user-defined number of groups then each particle is refined against the initial model which is low pass filtered to avoid high-resolution noise. This results in multiple differing models forming the basis for the initial classification. Each particle is then compared to each reference with user-defined angular sampling and probabilities, this process is repeated until the particles converge into individual classes (Scheres, 2016). All 3D classifications were performed over 25 iterations with 4 classes. All references were low pass filtered to 60 Å and sampling performed at RELION 2.1 or RELION 3 default values.

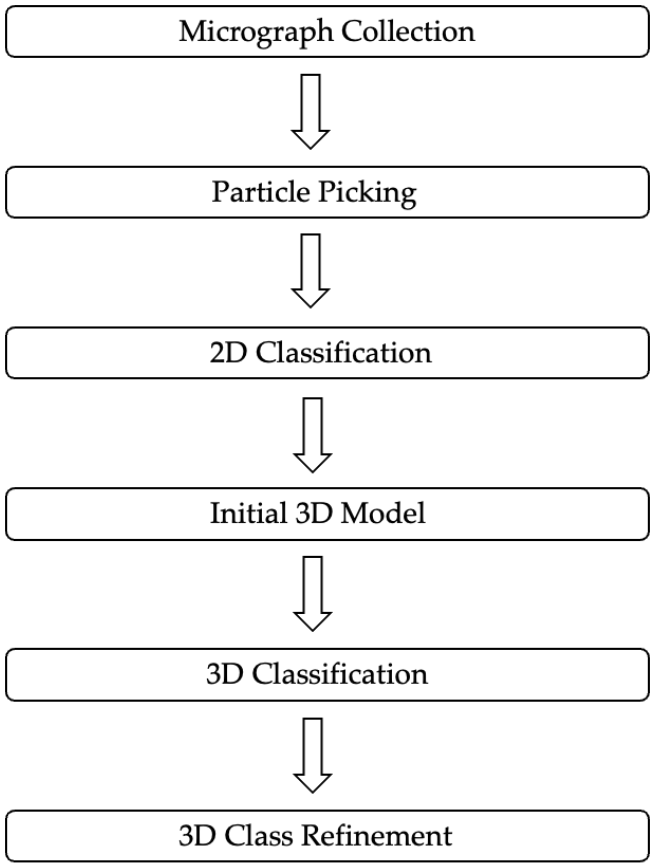

Figure 2.1: A flowchart schematic showing general workflow for single particle processing of HpuB particles.

2.20 – Cryo Electron Microscopy

2.20.1 - Grid preparation and Plunge freezing

Cryo-EM sample preparation was done by Dr Pascale Schellenberger. Grids were plasma cleaned and discharged (Tergo-EM, PIE Scientific) to create a hydrophilic surface. 3.5 μL samples of maximum HpuB sample concentration were adsorbed on grids before back blotting (3.5, 4 & 4.5 secs) to remove excess liquid and create a very thin layer of protein suspension on the grid. The grids used were Quantifoil 1.2/1.3 and Cflat 1.2/1.3 grids from EMS. The grids were then rapidly frozen in a mix of liquid ethane/propane using a Leica GP3 automatic plunge freezer. Chamber conditions were 10 °C with 95% humidity.

2.20.2 – Grid screening

Cryo-EM grid screening was done by Dr Pascale Schellenberger using a CryoARM200 microscope. The JEOL CryoARM operates at 200kV (Cold FEG) and is equipped with a Gatan K2 DDE camera, Omega energy in-column filter. Atlas images were collected at low magnification to determine the thickness and quality of the ice and then higher magnification images at x80 000 (0.6 A/pixel) were taken in holes from promising grid squares.

CHAPTER 3: HOW TO MAKE HPUB

3.1 – Introduction

Membrane proteins (MP) are omnipresent fixtures of cell membranes. In addition to lipids, they make up the fluid-mosaic bilayer that surrounds cells and intracellular organelles (Karr et al., 2017). The genes that encode MPs make up around 30% of all sequenced genomes, and indeed 25% of all proteins (Mulkidjanian & Galperin, 2010; Carpenter et al., 2008). The roles performed by MPs are broad and often essential, from the facilitation of solute exchange to signal transduction and the catalytic functions in enzymatic reactions. These are some of the reasons why MPs make up 40% of drug and therapeutic targets (Overington et al., 2006).

The importance of MPs in cellular function might lead to the assumption that they are amongst the most studied and structurally characterised proteins in the field of structural biology. On the contrary, of the over 50 000 entries of protein structure in the Protein Data Bank (PDB), less than 1% are structures of MPs; the number is even smaller when looking specifically at unique monotopic and multi-spanning MPs (Overington et al., 2006).

Amongst the few MP structures that are available in the PDB, there is extensive variation in methodologies used to isolate and purify the proteins, including from natural sources, recombinant production and chemical synthesis of short peptides. In cases where isolation from natural sources is not possible or advantageous, standard overexpression systems are routinely used to recombinantly make MPs. *E .coli* and *Lactococcus lactis* have been staple choices for prokaryotic expression whilst Pichia pastoris, Saccharomyces cerevisiae, insect cells and mammalian cell lines have been used for eukaryotic protein expression (Junge et al., 2008).

The main obstacles to the structural characterisation of MPs via foundational structural determination techniques such as X-ray crystallography or Nuclear magnetic resonance (NMR) are twofold. First is the fact that MP insertion and housing in the lipid bilayer means that those integral parts of the protein are inherently hydrophobic, resulting in instability or insolubility in standard solutions, impacting the ability to produce sufficiently pure MP samples at the high concentrations required for X-ray crystallography or NMR analysis; extensive optimization, sometimes over years, is often required (Rawlings, 2016). To overcome issues of solubility, MPs must be kept in environments that can mimic the amphipathic environment of the membrane.

Recombinant expression of MPs can be done both in the form of inclusion body (IB) expression or direct insertion into the native or host cell membrane. Inclusion bodies can be described as aggregated insoluble material that is produced as a result of the partial or complete misfolding of proteins that have been expressed from an inducible or strong promoter (Carrió & Villaverde, 2005). MPs can be recovered from inclusion bodies through denaturation to disrupt the aggregation of the peptide chains, followed by refolding to allow for the peptide chains to return to their intended tertiary structure (Singh et al., 2015). Alternatively, the recombinant expression vector encoding the protein of interest (POI) could also possess a signal tag that informs the cell to insert the protein into the outer or inner membrane.

3.1.1 - Detergents

Detergents are amphipathic surface-acting reagents that have the general structure of a hydrophilic polar head group and a hydrophobic non-polar tail group. In aqueous solution, the hydrophobic tail of detergent molecules orients itself to reduce its contact with water molecules, and the inverse is observed for the hydrophilic head. While the detergent nonpolar tail is repelled from the aqueous solvent, the polar head group's properties can vary. Polar head groups can be ionic, non-ionic or zwitterionic, and tend to have strong attraction for aqueous solvents (Anandan & Vrielink, 2016).

The form taken by detergents in solution is dependent on the concentration of detergent molecules as well as the other components of the solution. At low concentrations, detergents can exist in solution as monomers. However, unique to each detergent, within specific physiological conditions and at a higher concentration referred to as the critical micelle concentration (CMC), detergent molecules aggregate to form micelles. The size and shape of the micelle is determined by the number of detergent monomers per micelle, also known as the aggregation number (Cardi et al., 2010). Since the amphipathic nature of detergents is reminiscent of those same properties found in MPs and lipids, they can be used as a disruptive force within the membrane to replace the lipid bilayer's function of shielding the hydrophobic regions of MPs. The practical process of solubilising MPs with detergents is relatively simple. The detergent of choice is added to isolated membranes or denatured isolated IBs and incubated for enough time to allow the detergent molecules to disrupt the membrane and associate with the hydrophobic surfaces of the MP (Figure 3.1)

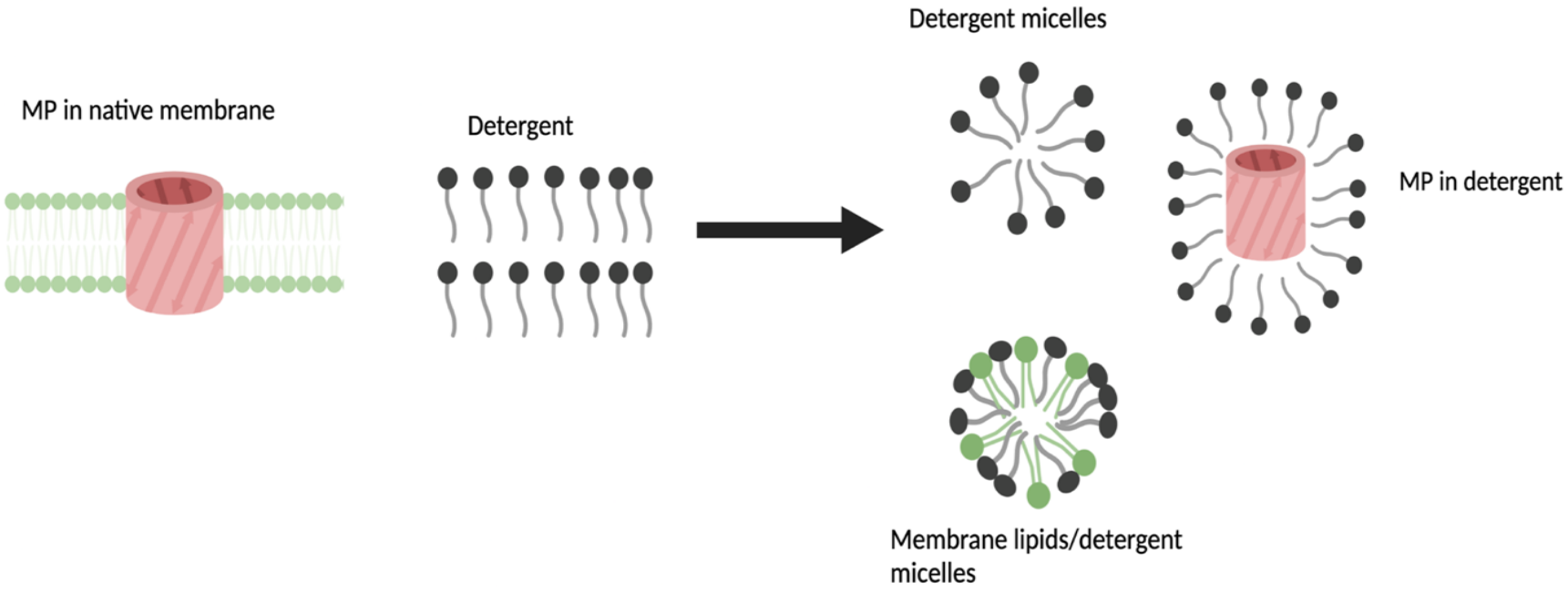

Figure 3.1: Detergent solubilisation of membrane proteins from an embedded native membrane.
The stability of MPs is dependent on their environment. In the membrane, phospholipids protect the hydrophobic regions from water, keeping them stable, flexible and function. This schematic depicts the process of using detergents to disrupt the membrane and create MP/detergent complexes. After solubilization, other by products of this process are empty detergent micelles and membrane lipid/detergent micelles. (Created with BioRender.com).

Different groups of detergents have historically had different uses in biochemical research. Whist ionic detergents such as sodium dodecyl sulphate (SDS) has uses in electrophoresis, non-ionic detergents have been preferred for MP solubilisation and manipulation. Indeed, some have been successfully used for protein structure determination using X-ray crystallography and occasionally cryo electron microscopy (cryo-EM). These include n-octyl-b-D-glucopyranoside (OG), n-decyl-b-D-maltopyranoside (DM), n-dodecyl-b-D-maltomaltpyranoside (DDM) and lauryl dimethylamine oxide (LDAO). Due to their amphipathic properties, detergents can effectively extract MPs direct from isolated membranes as well as facilitate the refolding of MPs that have been denatured from inclusion bodies (Seddon et al., 2004; Anandan & Vrielink, 2016).

The use of detergents in MP study is ubiquitous and essential but they do have significant drawbacks. Of the most significant is the general instability of detergent solubilised MPs. In the natural lipid membrane environment, the unique lipid MP complexes provide curvature stress and lateral pressure that are essential for the maintenance of MP structural stability and topology (Booth, 2005). Detergent micelles are much more rigid than the native membrane and can obscure functionally important regions of MPs. This instability can be exacerbated by the frequent failure of the detergent micelles to completely cover the hydrophobic regions of the MP resulting in aggregation; a common foil of progress in MP biochemistry (Bowie, 2005). More specifically, MP protein aggregation occurs where there is protein unfolding activity in the detergent/MP complex, which could uncover typically concealed hydrophobic domains, or via the exposing of hydrophobic regions which non-specifically interact with each other resulting in precipitation (Privé, 2007).

The flaws of detergents in keeping MPs soluble are well documented but even beyond these issues are the practicalities of finding the most suitable detergent for structural characterisation in each context. In a laboratory setting, there is a need to screen to identify the detergents that most effectively refold the protein or solubilise the membrane for MP extraction. This screening process can be lengthy and expensive, which has led to the development of alternative approaches for the biochemical study of MPs; these include the application of nanodiscs, peptidiscs, amphipols, and Styrene Maleic Acid Lipid Particles.

3.1.2 - Nanodiscs

Nanodiscs are a non-covalent assembly of phospholipid and a genetically modified membrane scaffold protein (MSP) which is based on human serum apolipoprotein A-I. The MSP wraps around the phospholipids, which associates as a bilayer domain, mimicking the native membrane. This wrapping occurs in a belt-like configuration, with one MSP covering the hydrophobic chains of each bilayer leaflet (Bayburt & Sligar, 2010). Similarly with detergents, there are advantages, disadvantages, and obstacles to navigate when working with nanodiscs. Notably, MP reassembly into nanodiscs is not a detergent-free process. Prior to reassembly, MPs must first be isolated and purified in a solution stabilised by detergent micelles (Figure 3.2). The most recently engineered MSP constructs include synthetic tags for protein purification. These include a range of MSP lengths beyond the standard 10 nm and affinity purification tags such as 6xHis, FLAG, Strep-tag etc. The literature has demonstrated that nanodisc reconstituted MPs are stable and monodispersed, which are two of the most important features for structural determination (Efremov et al., 2015; Yoshiura et al., 2010; Abosharaf et al., 2021).

The emergence of nanodiscs has coincided with the popularisation of cryo-EM as a reliable and effective technique for the structural determination of single particle proteins and complexes (Efremov et al., 2017). The final product of a detergent extracted, but nanodisc reconstituted, MP sample is free of detergent micelles, which enables the reduction of background noise and makes the sample far more suitable for cryo-EM studies (Yokogawa et al., 2019). Nanodiscs offer an alternative to detergents that allows for a more 'native' configuration of the hydrophobic regions of the MP with the lipids in the disc. Although not usually identical to the lipids in the native lipid membrane, these are much more similar than detergent molecules. This tends to improve the biochemical function of MP solutions, in addition to increased suitability for techniques such as cryo-EM and small angle solution X-ray (SAXS)/ neutron (SANS) (Bengtsen et al., 2020)

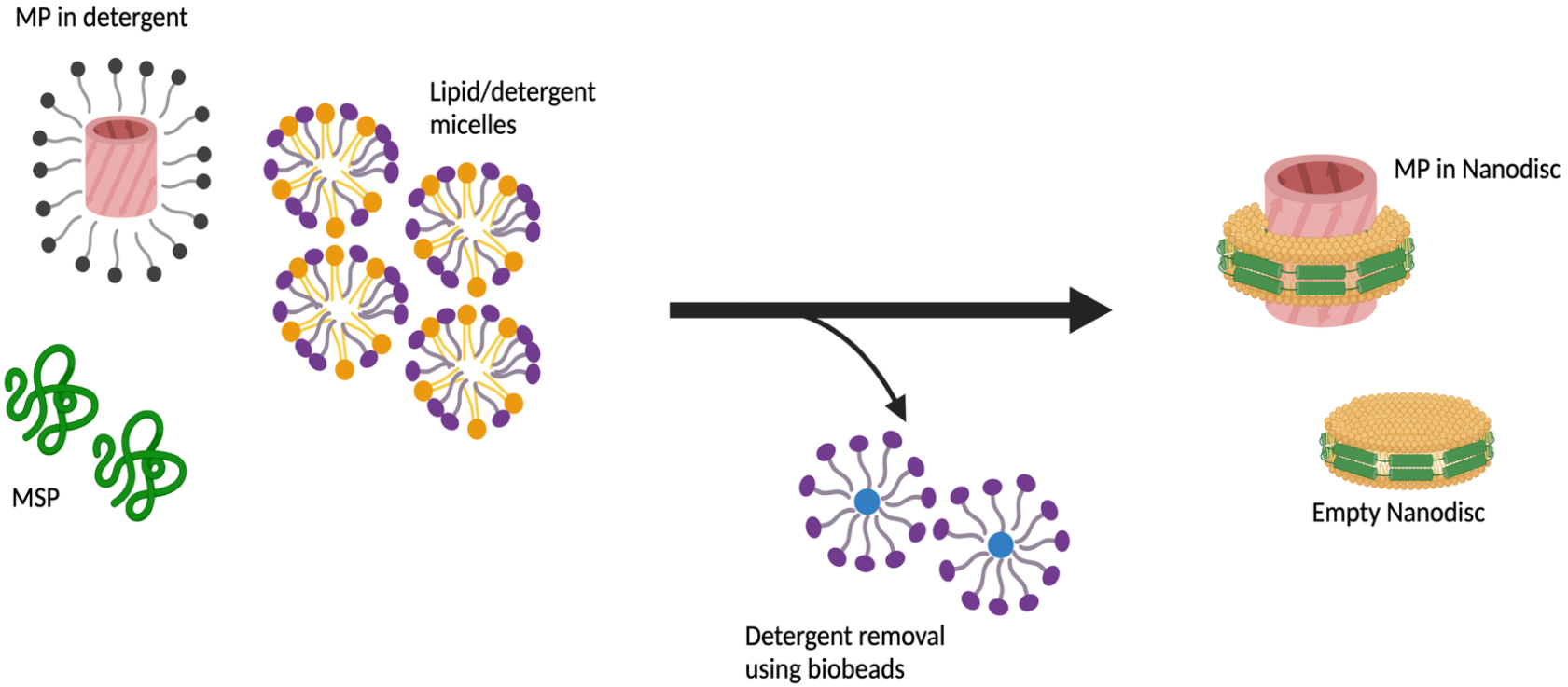

Figure 3.2: Assembly of detergent solubilised membrane proteins into nanodiscs.
Nanodiscs are one of several modern membrane memetics. MPs solubilised in nanodiscs are housed within small individual membrane cassettes. This is achieved using an engineered helical amphipathic protein (the MSP) and exogenous lipids to mimic the lipids from the membrane. In nanodisc assembly, the MP is already solubilised in detergents before addition to a solution comprised of MSP and exogenous lipids. These components are added at specific ratios to reduce the concentration of detergent to below the CMC, forcing MPs into nanodisc assembly. Bio beads are used to remove the detergent molecules before further purification in buffers that lack detergents. (Created with BioRender.com).

MlaFEDB, which is an ABC transporter implicated in phospholipid trafficking into the outer membrane of Gram negative bacteria, was solved to a resolution of 3.05 Å after being reconstituted into nanodiscs (Coudray et al., 2020). While the benefits of nanodiscs are plentiful, the disadvantages are not insignificant. One of these is that nanodisc MPs are not fully compatible with X-ray crystallography. Although more stable than detergent-solubilised MPs, nanodisc MPs possess traits that make crystallisation difficult. First is that the MP is azimuthally disordered in the disc's lipid bilayer and, depending on the temperature, this can make the MP mobile. Second is that the MSPs organise themselves anti-parallel to each other, and their stabilisation by inter-helical salt bridges in addition to the similarity in amino acid sequences contributing to repeat topology can result in rotational disorder in the MSP configuration (Denisov & Sligar, 2017).

In theory, the general nanodisc assembly protocol can be adapted to any MP. However, there are several compatibility issues to contend with. A great deal of optimisation is often needed to find the right ratio of MSP: Lipid as well as MSP: MP in nanodisc assembly (Puthenveetil & Vinogradova, 2013). Prior knowledge of the MP's size, side chain charges, its oligomers, and the lipid composition of the particular membrane it will be extracted from are also required. There is also the thermodynamic stability of the MP to consider. The transfer of a MP from a detergent buffer to the nanodisc lipid environment is dependent on the stability of the protein which is closely linked with the propensity for precipitation, which can occur during the process of nanodisc/MP assembly (Hagn et al., 2018). In short, nanodisc MP assembly is not a trivial task and small deviations from optimal conditions can lead to low-efficiency reconstitution or disastrous levels of protein aggregation (Carlson et al., 2018).

3.1.3 - Peptidiscs

Nanodiscs are not the only memetic that make use of engineered proteins for the stabilisation and reconstitution of MPs. As the name suggests, the peptidisc system uses small, amphipathic peptides to reconstitute MPs for downstream studies. Although previous similar systems had not been widely adopted, the potential of peptides in MP studies had long been considered. For example, 'Peptergents' were introduced as short designer lipid-like peptide detergents used to functionally solubilise 12 unique olfactory receptors (Corin et al., 2011). It was demonstrated that the peptide detergents were able to stabilise the receptors, had confirmed secondary structure by circular dichroism (CD) and could bind to their respective ligands by microscale thermophoresis (MST). However, blot intensity measurements only indicated milligram quantities of MP reconstitution using just one of the designed peptides (Corin et al., 2011).

An advantageous property of the peptergent system is that it allows the user to solubilise the desired MP directly from the membrane. However, similarly to detergents, these peptides form mixed micelles that readily aggregate and precipitate below a certain CMC (Carlson et al., 2018). In addition, peptergents, and their similar peptide-based counterparts such as beltides (Larsen et al., 2016) and nanostructured β-sheet peptides (Tao et al., 2013), can be costly and complex to make and use. Peptergents are insoluble in aqueous solutions and require titration of a base to achieve solubility (Corin et al., 2011). Nanostructured b-sheet peptides can form undesirable extended filament clusters without detergent (Privé, 2009).

The peptidisc system emerged as a way to harness the positives of peptide-based membrane mimetic design while mitigating against the typical drawbacks (Yeh et al., 2005). A novel peptidisc peptide was launched in 2018 and was designed to keep MPs soluble and stable in solution in the absence of detergent micelles (Carlson et al., 2018). This peptide was based on the original apolipoprotein A-I peptide initially identified for membrane memetic use by the Segrest group (Epand et al., 1987). According to the

designers, peptidisc peptides form 'two amphipathic stretched helices that are separated by a proline residue'. In practical terms, when the peptidisc peptide is mixed with an already detergent-extracted and solubilised MP, the micelles are removed and multiple copies of the peptide bind to the hydrophobic transmembrane portions of the MP, which might also incorporate any lipids that had remained bound to the MP. (Carlson et al., 2019). It has been demonstrated that peptidisc are capable of reconstituting both a-helical and b-barrel MPs in a way that is efficient, relatively simple and with less optimisation than its counterparts. An example is the reconstitution of the PlexinC1/A39R in peptidiscs and subsequently solved to a resolution of 3.1 Å using cryo-EM (Kuo et al., 2020)

Within structural determination of MPs using in the peptidisc system, cryoEM has been favoured over other methods because even though the peptidisc peptide is still expensive, cryoEM requires very small amounts of sample for data collection. Cryo-EM has been used to present and confirm the structures of a number of proteins using the peptidisc system, including a 3.3 Å resolution structure of the E. coli homo-heptametric mechanosensitive channel MscS (Angiulli et al., 2020).

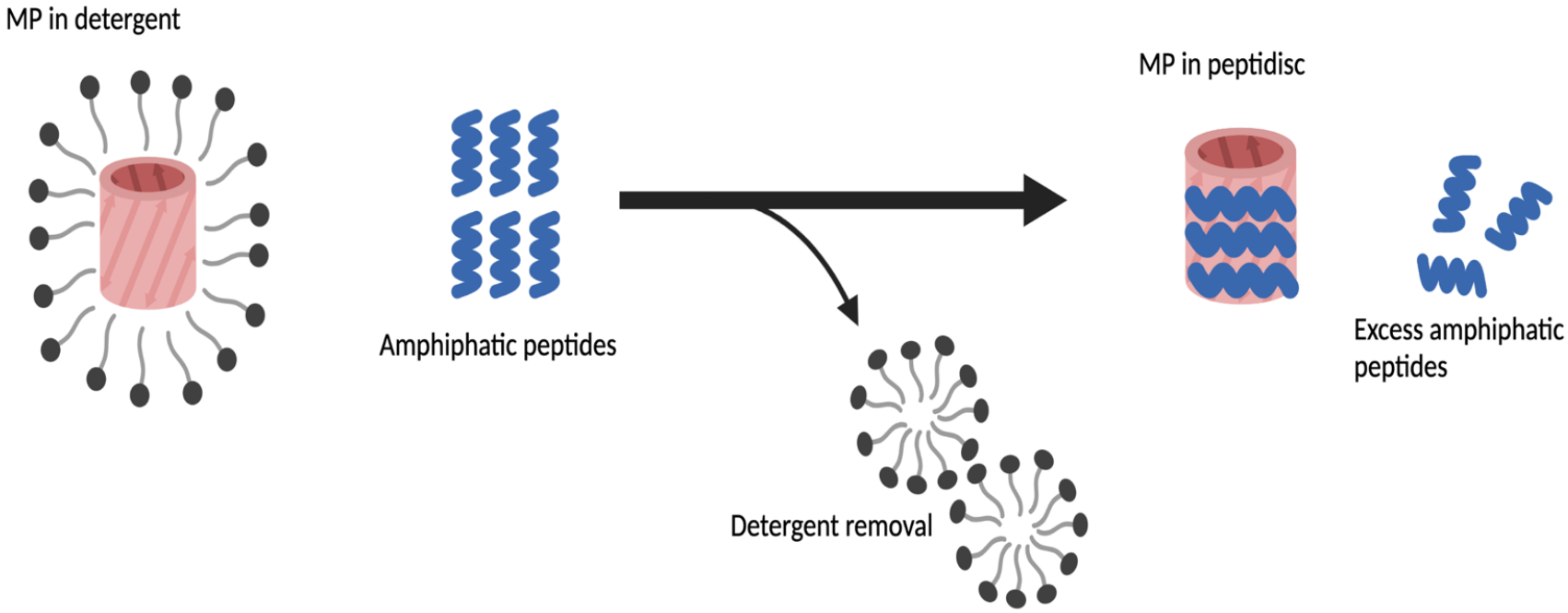

Figure 3.3: Assembly of detergent solubilised membrane proteins into peptidiscs.
Peptidiscs are one of many modern membrane memetics. Peptidiscs make use of small engineered amphipathic peptides that can associate with the hydrophobic regions of the MP for stabilisation in solution. In the 'on-bead' peptidisc assembly strategy, the MP is already solubilised in detergents before addition to a solution comprised with MSP and exogenous lipids. These components are added at specific ratios to reduce the concentration of detergent to below the CMC, forcing MPs into nanodisc assembly. Detergents are removed by on bead dilution and elution using a buffer without detergents. (Created with BioRender.com).

3.1.4 - Amphipols

Amphipols are short amphipathic polymers that possess a large number of hydrophobic chains allowing them to associate at multiple contact points with the transmembrane region of MPs (Tribet et al., 1996). Amphipols need to be very water soluble, flexible and contain a dense distribution of hydrophobic chains in order to create stable and soluble MP complexes. The term amphipol is derived from 'Amphipathic Polymers'. Amphipols were designed to be polymers that would have a high affinity for the hydrophobic regions of MPs and thereby keep the MP stable and soluble. The developers suggested that an MP transferred into an amphipol would be able to retain its associated lipids, cofactors and subunits (Popot, 2010).

As with other membrane memetics discussed here, the reconstitution of MPs into amphipols is not a detergent-free process. The MP of interest must first be extracted and solubilised, and even partially purified, in a non-ionic detergent, before transfer into the amphipol for downstream studies (Figure 3.4). Once in detergent, the MP is mixed with a solution containing amphipols, where the solution is diluted to below the CMC of detergent. Although at this stage the detergent is not physically removed from the solution, most of it disperses in the aqueous phases as monomers, leaving room for the polymer to take its place on the hydrophobic surfaces of the MP (Popot et al., 2011). The removal of detergent molecules can also be expedited with the use of biobeads. Biobeads are non-polar polystyrene adsorbent resins composed of neutral, microporous polymeric beads for use in hydrophobic interaction experiments as described by Bio-Rad Laboratories Inc. Although the use of amphipols had been known to occasionally result in aggregation of MPs under certain conditions, the use of more minimalist buffers has helped to mitigate against this potential road block (Picard et al., 2006).

Of the initially designed polymers, A8-35 has been the most successful amphipol in the structural biology of MPs. A8-35 has been used to solubilise a wide range of MPs including many integral MPs. Unlike other membrane memetics, molecular size does not appear to be so crucial a factor in the use of amphipols. For example, A8-35 has been used for the reconstitution of small single transmembrane helices and large complexes with over 70 transmembrane helices nearly 2 MDa in size. An example is the ~1.7 MDa mitochondrial super complex, which possesses over 120 transmembrane helices (Vonck & Schäfer, 2009).

A8-35 has also been instrumental in the structural determination of MPs using amphipols. Although suitable for almost all the major techniques, progress in X-ray crystallography data from amphipol reconstituted MPs has been lacking and unsuccessful. The reasons are complicated, from the limitations of MP production in sufficient concentrations for crystallography to the unique issues presented by amphipols themselves (Popot, 2018). The increasing use and popularity of single particle cryo-EM has allowed for the re-evaluation of amphipols for MP structural studies. For example, the STRA6 receptor for retinol uptake in zebrafish fish was solved in its entirety and in complex with binding partners to a resolution of 3.9 A by transfer into A8-35, after initially purifying the protein in lauryl maltose-neopentyl glycol (LMNG). At 74 kDa and only ~150 kDa as a complex, this MP is a good example of the potential of amphipols in cryo-EM, even for smaller proteins (Chen et al., 2016)

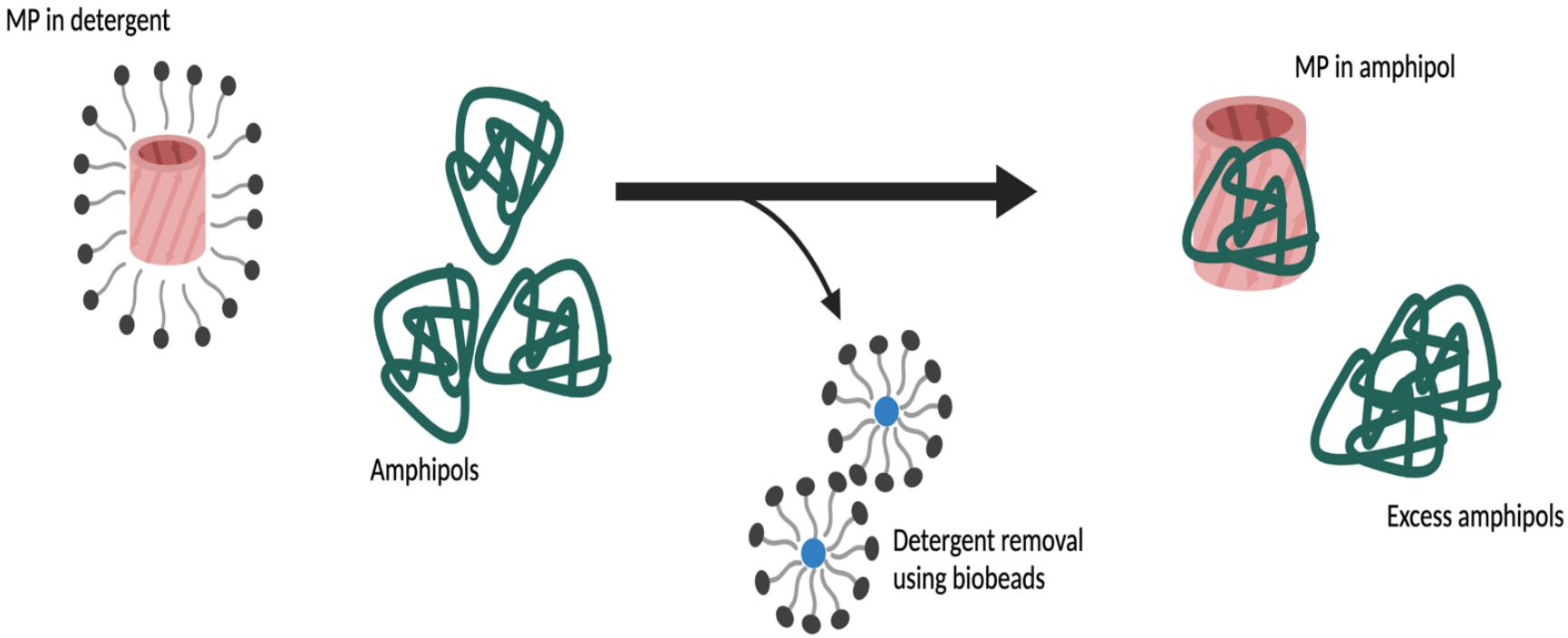

Figure 3.4: Assembly of detergent solubilised membrane proteins into amphipols.

Amphipols are one of the earliest non detergent membrane memetics. Unlike nanodiscs or peptidiscs, the amphipol system centres amphipathic polymers which associate with the hydrophobic surfaces of the MP. MPs already solubilised and IMAC purified in detergent are mixed and incubated with and excess of amphipol. Detergent molecules are removed using Biobeads and excess amphipols are removed using SEC. (Created with BioRender.com).

3.1.5 - Styrene Maleic Acid Lipid Particles

Virtually all the membrane memetics described here rely on the initial use of detergents to extract and solubilise the MP from its native environment before later reconstitution into a detergent-free membrane memetic. Which prompts the question, if detergents are an obstacle to structural determination and functionality of the extracted and purified MP, is there a way to avoid using them at all? Styrene Maleic Acid Lipid Particles (SMALPs) are a membrane mimetic that essentially create a nanodisc but rather than using MSPs and exogenous lipids in reassembly, SMALPs extract the MP directly from its native environment and makes them immediately stable and soluble in a completely detergent-free process (Jamshad et al., 2011).

Styrene maleic acid (SMA) is the hydrolysed form of styrene-maleic anhydride (SMAnh) copolymer. SMA is synthesised by the copolymerisation of styrene and maleic anhydride monomers. Both polymers have signification industrial uses as well as historical uses within the life sciences (Dörr et al., 2016). Although initially identified as conjugates for cancer drugs, it was later discovered that the ability of SMAs to interact with phospholipids and incorporate hydrophobic molecules could make them useful as a drug delivery system (Tonge & Tighe, 2001). These properties led to the use of the SMA copolymer as a tool to extract and solubilise membrane proteins, as initially reported by the Dafforn and Overduin groups (Knowles et al., 2009).

In the SMALP making process, SMA is the main ingredient. It has been described as a 'cookie cutter' which extracts MPs in the form of a lipid/protein nanodisc. The copolymer can be added to isolated membranes from prokaryotic and eukaryotic organisms to extract MPs, forming discs in the range of 10 – 15 nm and incorporating 11 – 150 lipids. Because the SMA co-polymer cuts from the membrane indiscriminately, the use of a purification tag is useful to separate the MP of interest from the heterogeneous mixture of proteins (Dörr et al., 2016 ; Swainsbury et al., 2017). A major benefit of the SMALP system is that the extracted MP is removed with its correct composition of native lipids intact and is therefore more likely to be functionally active. SMA has also

demonstrated unique promise of solubilising multi-component MP complexes, including large complexes that could not be solubilised using detergents (Baeta et al., 2021). However, size can be a limiting factor. Analysis of extraction using the diameter of the large 15 nm SMA has suggested that MPs with more than 40 transmembrane a-helices may not be solubilised by SMA copolymer. Although promisingly, the existence of up to 25 nm nanodiscs is suggestive that SMALPs too could be expanded to increase in maximum size over time (Laursen et al., 2016).

Structural biology of MPs extracted and solubilised by SMALPs is in ascendancy, with a steady increase of published structures acquired using this memetic. Both solution and solid-state NMR have been used to obtain structures of MPs inside SMALPs. For example, following solubilisation from *E. coli* membranes using SMALPs, the zinc diffusion facilitator CzcD retained its dimeric structure and its associated lipid molecules allowing for structure resolution using solid-state NMR via its assignable amide and methyl group peaks in ^{13}C and ^{15}N spectra. Similarly, the coat protein of the Pf1 bacteriophage, also solubilised by SMALP, showed shaper solid-state NMR spectra than the same protein in bicelles or peptide-based nanodiscs (Radoicic et al., 2018; Brown et al., 2021).

SMALP solubilised MPs are also very compatible with structural determination via electron microscopy, both low-resolution screening and structures with negative stain EM and high-resolution structures with cryo-EM. From the relatively small 136 kDa KimA homodimer of *E. coli*, which was solved to a resolution of 3.7 Å, to the 344 kDa AcrB homotrimer of *E. coli* which was solved to a resolution of 3.0 Å. (Tascón et al., 2020; Qiu et al., 2018).

5.1.6 - Aims

The following chapter describes a programme of experimentation and optimisation towards the purification of HpuB for structural and functional biochemical studies. The aim was to produce a HpuB sample that was structurally stable and functionally active, suitable for structural determination and to optimise purification for mutagenic studies.

IB expression and refolding as well as membrane-bound expression of HpuB would be major strategies. It was considered that the use of a modern membrane memetic would be crucial to the success of HpuB structural studies. To that end, HpuB will be reconstituted in a variety of membrane memetics, including, nanodiscs, SMALPs, peptidiscs and amphipols.

3.2 – Results

3.2.1 – HpuB refolded from inclusion bodies (IB)

Initial experiments to optimise HpuB overexpression and purification focused on the orthologues (49% identity) from *Neisseria gonorrhoeae* and *Kingella denitrificans*. Each gene had previously been cloned into the expression vector pHISHNgHpuB and pHISHKdentHpuB respectfully and introduced into the *E. coli* expression host BL21 ((DE3), *endA::TetR, T1R, pLysS*) (Figure 3.5).

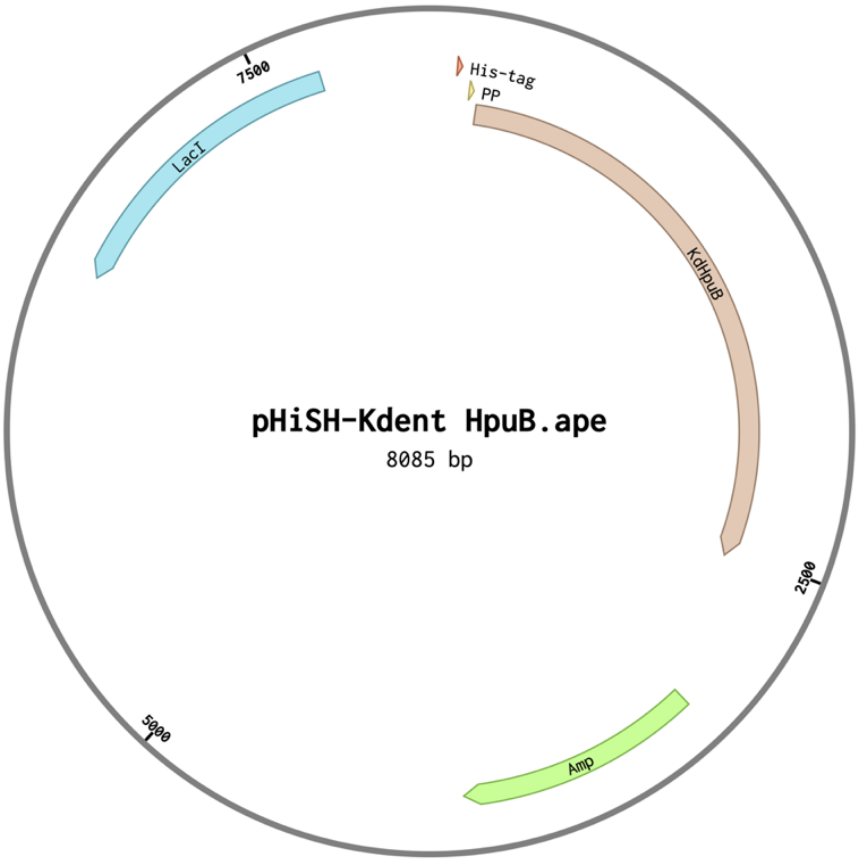

Figure 3.5: The pHISH-KdentHpuB plasmid map.

This map includes the position of the LacI repressor (blue), the gene encoding *K. denitrificans* HpuB from strain B6992, 2349 base pairs (brown), an N-terminal 6xHisTag (orange), a precision protease cleavage cite (yellow) and the ampicillin resistance gene (green) to allow to selective growing of *E.coli* containing the plasmid. (Created with Benchling.com)

Standard expression conditions involved growth in LB broth to an OD_{600} of 0.8, followed by induction using IPTG and continued growth for 4 hours at 37 °C. Under these conditions, and as is the case for many integral membrane proteins, the HpuB protein was produced as insoluble IBs that could be easily separated from soluble cell components to provide the initial starting material. Although expression was confirmed for both homologues of the protein, SDS PAGE analysis showed *N. gonorrhoeae* HpuB was produced at higher levels (data not shown), and so further studies focused on this protein. In order to purify HpuB IBs from other insoluble components, washing steps were performed by repeated resuspension in buffer and centrifugation (Figure 3.6A). There is a clear and gradual purification of HpuB from the insoluble fraction to the pre-washed and then washed IBs. The final product (Figure 3.6A) includes pure HpuB IBs and appears to lack significant levels of contaminants. Pure HpuB IBs were denatured with GuHCl, refolded in the presence of haem and LDAO, and further purified by IMAC in 1 mL fractions from a gravity flow column (Figure 3.6B). SDS PAGE analysis revealed a band that corresponds to the ~90 kDa HpuB as well as a larger band present at the top of the gel, which is likely to be aggregated protein. For downstream studies, a purer, more monodispersed sample of HpuB was required and so SEC was used to separate the ~90 kDa HpuB band from the aggregate (Figure 3.6C&D). The A280 chromatogram (Figure 3D) shows an imperfect separation of the refolded HpuB from its suspected aggregate at 54 – 66 mL elution volume. The peaks are not completely separated from each other, and this overlap is also visible on the SDS PAGE gel, although the gel does also show that there are fractions in which the proteins are more definitively separated (Figure 3.6C).

Western blot analysis (Figure 3.7) was used to confirm the identity of the ~90 kDa band as HpuB. HpuB is expressed with an N-terminal His-tag allowing an anti-His antibody to be used as the primary antibody. Samples corresponding to the separated HpuB and suspected aggregate obtained by SEC (Figure 3.7) were analysed. Although the samples were normalised for protein quantity, a stronger signal was detected for the lane containing the ~90 kDa HpuB protein. The weak signal detected for the larger proposed aggregate suggested that this aggregate protein is not HpuB, although it is possible that the aggregation persists during boiling and exposure to denaturants in SDS-PAGE and this shields the 6X His tag from antibody binding (den Engelsman et al., 2011). Alternatively, it is possible that the aggregate does not transfer as efficiently to the PVDF membrane. A sample of the aggerate was prepared for mass spectrometry analysis in an attempt to identify the protein, although the results were inconclusive (data not shown).

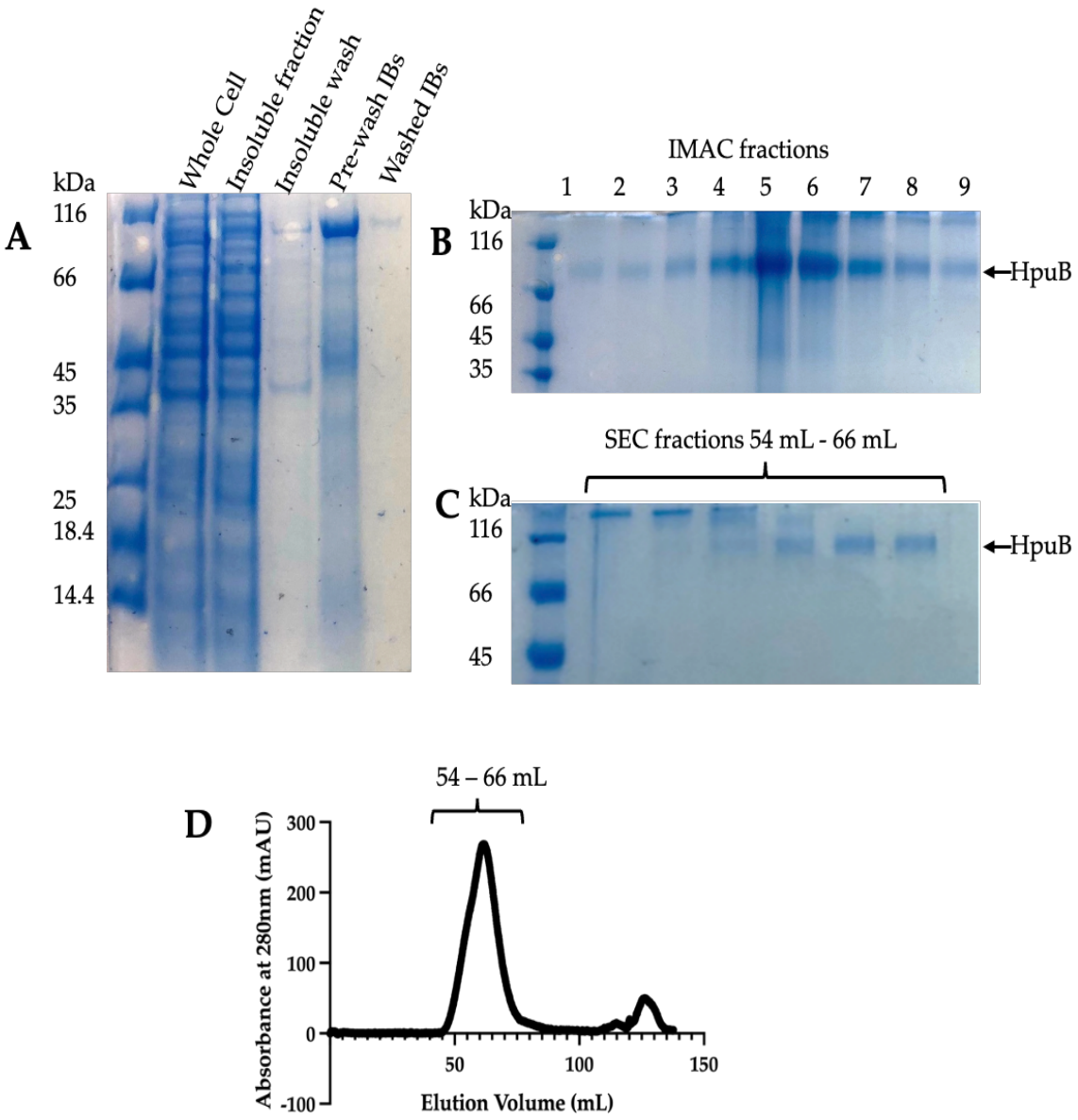

Figure 3.6: Preparation and purification of HpuB from inclusion bodies.

HpuB was expressed as IBs. IBs were denatured and HpuB refolded in the presence of LDAO and haem. (**A**) Preparation of inclusion bodies using the insoluble fraction of the cell lysate. (**B**) IMAC purification of HpuB from refolded inclusion bodies. 1 mL fractions were collected from a gravity flow NiNTA column were aliquoted for SDS PAGE (**C**) SDS PAGE from SEC purification of pooled IMAC fractions. SDS samples were aliquoted from 2 mL SEC fractions at 54 – 66 mL elution volume. (**D**) A280 chromatogram of SEC purification of HpuB IMAC pooled fractions in LDAO using a Superdex 200 16/600 column.

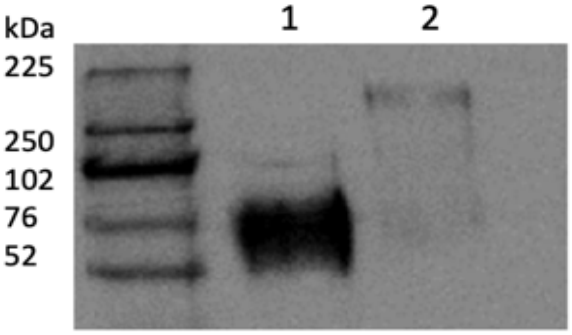

Figure 3.7: Western Blot probing for 6x His tag on HpuB.

SEC Fractions corresponding with the two peaks from SEC HpuB purifications were pooled and concentrated for western blot. Lane 1 = ~90 kDa protein, Lane 2 = suspected aggregate. Anti-his antibodies were used to probe the proteins and showed a much more intense band for the ~90 kDa protein confirming its identity as HpuB.

Figures 3.6 and 3.7 together demonstrate that HpuB was isolated in the final washed IBs. IBs that were denatured and refolded were used to produce HpuB through successful solubilisation and purification in LDAO, albeit with a suspected aggregate contaminant. The SEC A280 chromatogram suggested a large broad peak but SDS PAGE showed sufficient separation to produce a single HpuB band on the gel. Western blot confirmed HpuB identity, but the identity of the suspected aggregate was not revealed by mass spectrometry analyses. The successfully prepared HpuB sample was used for downstream biochemical studies. These included Hb pull downs, X-ray crystallography screens, and was also used to prepare grids for negative stain electron microscopy studies. Due to a range of factors illuminated by these biochemical techniques, it was ultimately determined that simple refolded HpuB was not the best sample to meet this project's aims.

3.2.2 - Assembling refolded HpuB into nanodiscs

The denaturing and refolding of HpuB in LDAO produced a purified sample of HpuB as seen in SDS PAGE and western blot. This HpuB sample was taken forward to structural techniques using X-ray crystallography and negative stain EM. During crystallography trails, there was a successive hit (0.05M citric acid, 0.1M lithium sulphate, 19% PEG 1000) which produced protein crystals using the 'MemGold™' screening tray from Molecular Dimensions with HpuB at a concentration of 3.8 mg/ml. However, a substantial number of these crystals were damaged during removal and those extracted undamaged were poorly diffracting (data not shown). Several attempts were made to repeat and optimise HpuB crystallisation, but the crystals proved to be unreproducible. During negative stain EM screening, the HpuB LDAO sample was not suitable for data collection due to the formation of large micelle complexes, probably both with and without HpuB, making it difficult to identify HpuB particles.

The nanodisc membrane memetic was selected as an alternative to LDAO solubilisation of HpuB due to the issues LDAO posed in structural studies (X-ray crystallography and TEM). The assembly of a MP nanodisc is a multi-step process and involves the preparation of lipids into a sodium cholate buffer, then assembly of lipids into empty nanodiscs using MSP, and then incubation of empty nanodiscs with the POI to initiate self-assembly. HpuB was expressed into inclusion bodies as described in section 2.4.2, and then refolded from inclusion bodies and assembled into nanodiscs made up of the 25 kDa scaffold protein MSP1D1 and POPC lipids. MSP1D1 was chosen as the standard scaffold protein used in nanodisc assemblies. Although HpuB was successfully refolded in LDAO and demonstrated stability during pull down experiments performed at 4°C, previous experiments performed with this HpuB sample showed that HpuB refolded in LDAO was unstable after long periods at room temperature (data not shown). As a result, POPC lipids were chosen for nanodisc assembly through a process of optimisation and because the POPC optimal assembly temperature of 4°C is more

compatible with the LDAO refolded HpuB. Other lipids used in nanodisc assemblies such as Dipalmitoylphosphatidylcholine(DPPC) and dimyristoylphosphatidylcholine (DMPC) have optimal assembly temperatures of 37°C and 25°C respectively and are thus incompatible with LDAO refolded HpuB

Following SEC purification, two A280 chromatogram peaks were expected: a high MWt (earlier) peak aligning with the HpuB nanodisc and a lower MWt (later) peak, aligning with any excess empty nanodisc scaffold protein. However, in this assembly, the A280 chromatogram only revealed one notable peak (Figure 3.8A).

This was surprising because the molar ratio of MSP1D1 was four times that of HpuB, and excess empty nanodiscs should remain in solution even if all HpuB was successfully assembled into nanodiscs. SDS-PAGE analysis of the major peak (Figure 3.8B) revealed that HpuB and MSP proteins co-eluted, suggesting but not confirming the assembly of HpuB nanodiscs. However, compared to the load sample, the intensity of the HpuB band was significantly diminished during SEC suggesting that much of the protein remained on the SEC resin, possibly due to precipitation. It was therefore decided not to proceed further with this approach.

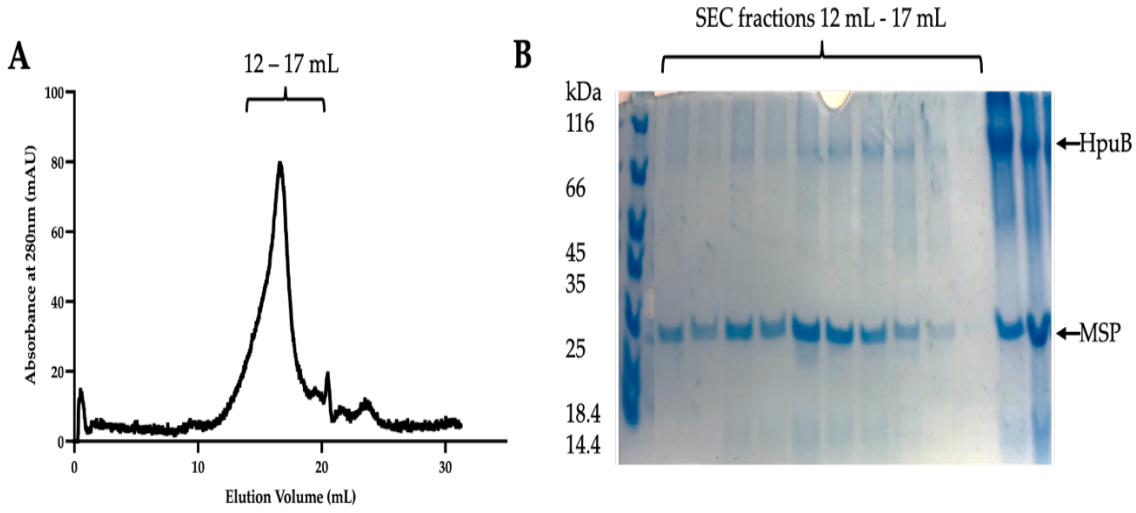

Figure 3.8: Assembly of refolded, detergent solubilised HpuB into nanodiscs.

HpuB was assembled into nanodiscs using the MSP1D1 scaffold protein and POPC lipids at a ratio of 4:1 MSP: HpuB and 65:1 POPC :MSP. (**A**) A280 chromatogram of the SEC purification step separating HpuB nanodiscs from empty nanodiscs on a superose 6 10/300 GL column (**B**) SDS PAGE gel using fractions corresponding to the peak elution volumes 12 – 17 mL from SEC. The A280 presents one major peak, SDS PAGE shows that HpuB and MSP1D1 are co-eluting however the HpuB band shows higher intensity in the load sample than in fractions following SEC.

3.2.3 - Producing HpuB by recombinant expression into the *E. coli* outer-membrane

Refolding any MP from IBs has its disadvantages and the refolding of HpuB is no exception. It is well understood that IBs need long and extensive processing before they can be purified into functionally active proteins. The process requires the denaturation and subsequent refolding of proteins and often leads to poor recovery of functional protein (Singh et al., 2015). In addition, refolded protein samples are more likely to be heterogenous. When preparing a recombinant protein for structural analysis, a sample as close to native as possible is most desirable.

In order to circumvent the refolding process, an overexpression plasmid (pBASHOM2.HpuB) was constructed in which an N-terminal *OmpA* secretion signal tag was fused to *HpuB* from gonococcal strain FA19 and meningococcal strain 8047 causing HpuB to express directly into the *E. coli* membrane, under the control of an arabinose-inducible promoter (Figure 3.9). A specialised host *E. coli* BL21 omp8, was used, in which some of its most populous outer membrane protein genes had been deleted (i.e., *OmpF, OmpC, OmpA, and LamB*) (Qiao et al., 2014) (Eren et al., 2012) to allow for more room in the membrane and reduce interference in downstream purification steps. Initial tests showed that the *K. denitrificans* homolog showed higher expression levels than *N. gonorrhoeae*, and so further studies were performed on the *N. gonorrhoeae* HpuB. Expression of *N. gonorrhoeae* OmpA-fused HpuB was optimized for expression time, incubation temperature and concentration of arabinose. Poor growth, even in the absence of an inducer, indicated that HpuB expression was toxic to the expression cells. Therefore, optimal expression conditions were chosen in order to allow for HpuB production, while also mitigating against the toxicity of expression, resulting in a relatively low yield of HpuB. Nonetheless, successful expression of HpuB was confirmed and IMAC purification fractions of the LDAO solubilised membrane revealed the ~90 kDa HpuB (Figure 3.10A). Solubilisation of the membrane material was also

subject to lengthy optimisation with several detergents and methods. A critical optimisation step was the addition of a step to selectively solubilise the inner membrane using 2% w/v sarcosine prior to OM solubilisation and IMAC purification of HpuB. Several attempts were made to concentrate these IMAC fractions for further purification via SEC, but all were unsuccessful. In each attempt, HpuB extracted from the membrane and solubilised in LDAO was not recovered from SEC columns. Indeed, when pooled and concentrated IMAC fractions were run on SDS PAGE gels prior to SEC, there was extensive contamination with diminished levels of HpuB. In an attempt to improve HpuB purity without SEC, an imidazole gradient was used, which successfully purified HpuB in the absence of contaminants as seen in the peak fractions (Figure 3.10B). Imidazole gradients produced samples that were much more suitable for downstream studies such as assembly into membrane memetics; nanodisc, peptidiscs and amphipols, albeit sometimes inconsistently.

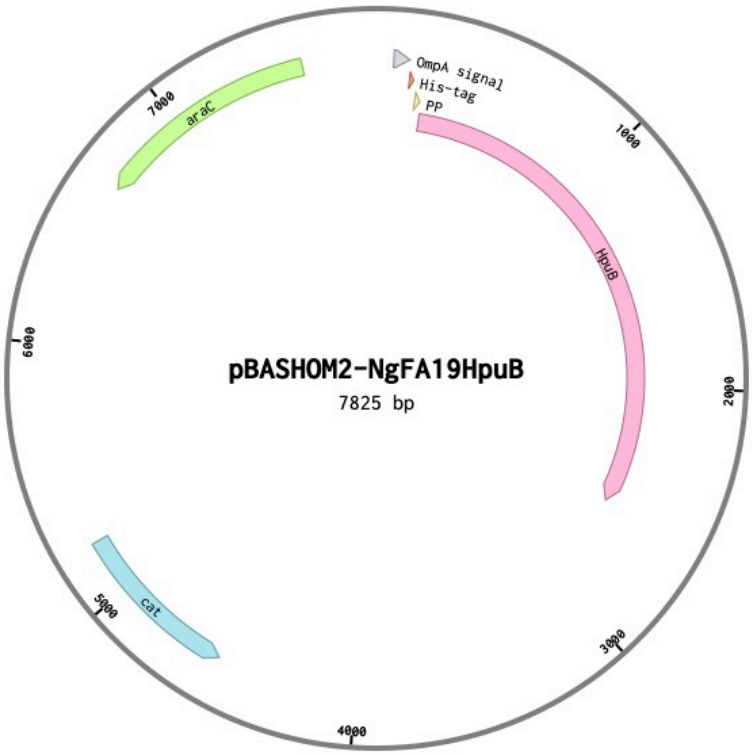

Figure 3.9: The pBASHOM2NgHpuB plasmid map.

pBASHOM2NgHpuB cloned for the purpose of inserting HpuB into the outer membrane after expression using an OmpA signal (grey). This map also includes the position of the araC repressor (green), the gene encoding *N. gonorrhoeae* FA19 HpuB, 2364 base pairs (pink), a 6xHisTag (orange), a precision protease cleavage cite (yellow) and the cat of chloramphenicol acetyltransferase resistance gene (blue) to allow to selective growing of *E.coli* containing the plasmid. (Created with Benchling.com).

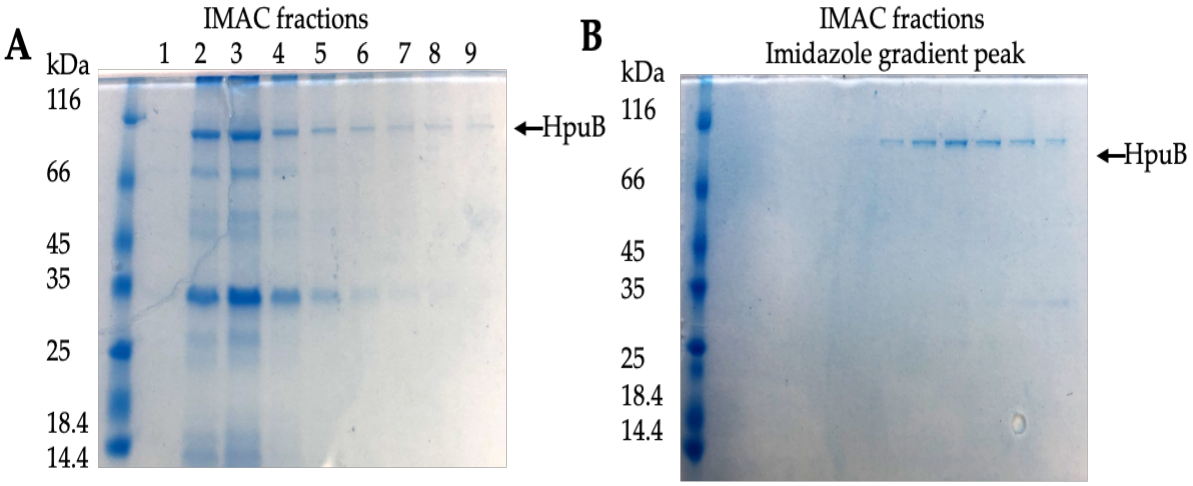

Figure 3.10: IMAC purification of HpuB expressed into the *E. coli* outer membrane.

HpuB expressed into the *E. coli* membrane using the pBASHOM2NgHpuB construct with an OmpA secretion tag. The outer membrane was isolated and solubilised in LDAO buffer purification via IMAC. (**A**) gravity flow IMAC purification of HpuB showing successful expression of HpuB, collected in 1 mL fractions and aliquoted for SDS PAGE but with many contaminants visible by coomassie staining (**B**) imidazole gradient purification of HpuB collected in 1 mL fractions using a 1ml HisTrap HP column on an ÄKTA and shows successful expression and a significantly purer sample of HpuB

3.2.4 - Assembling outer-membrane extracted HpuB into nanodiscs

As described in section 3.2.2, HpuB, even when extracted directly from the outer membrane in its native form, is incompatible with X-ray crystallography and EM studies. As a result, recombinant HpuB extracted directly from the *E.coli* membrane in LDAO was therefore assembled into nanodiscs using the extended MSP, MSP1E3.

Negative stain EM micrographs and analysis of a HpuB model suggested that HpuB has a diameter of ~9.8 nm and as such is too wide for nanodisc assembly in the 10 nm diameter of MSP1D1. As a result, the extended scaffold protein MSP1E3 (~13 nm) was chosen as an alternative. For comparison, an empty nanodisc was assembled and purified alongside HpuB nanodisc. However, SEC of both empty and HpuB nanodisc purifications revealed little difference in elution volume of the two major peaks, whereas a correctly assembled HpuB nanodisc should confer at least a ~90 kDa molecular weight difference and commensurate elution volume; this suggested that HpuB had not been successfully assembled into a nanodisc (Figure 3.11A).

SDS PAGE analysis of peak fractions for the empty nanodisc revealed a band of ~27 kDa, as expected for MSP1E3 (Figure 3.11B). However, analysis of the expected HpuB nanodisc also revealed only the ~27 kDa band, with no HpuB present. Since the load sample, contains the ~90 kDa HpuB (Figure 3.11C), this suggests an unsuccessful assembly, which might have led to HpuB instability in the detergent-free buffer.

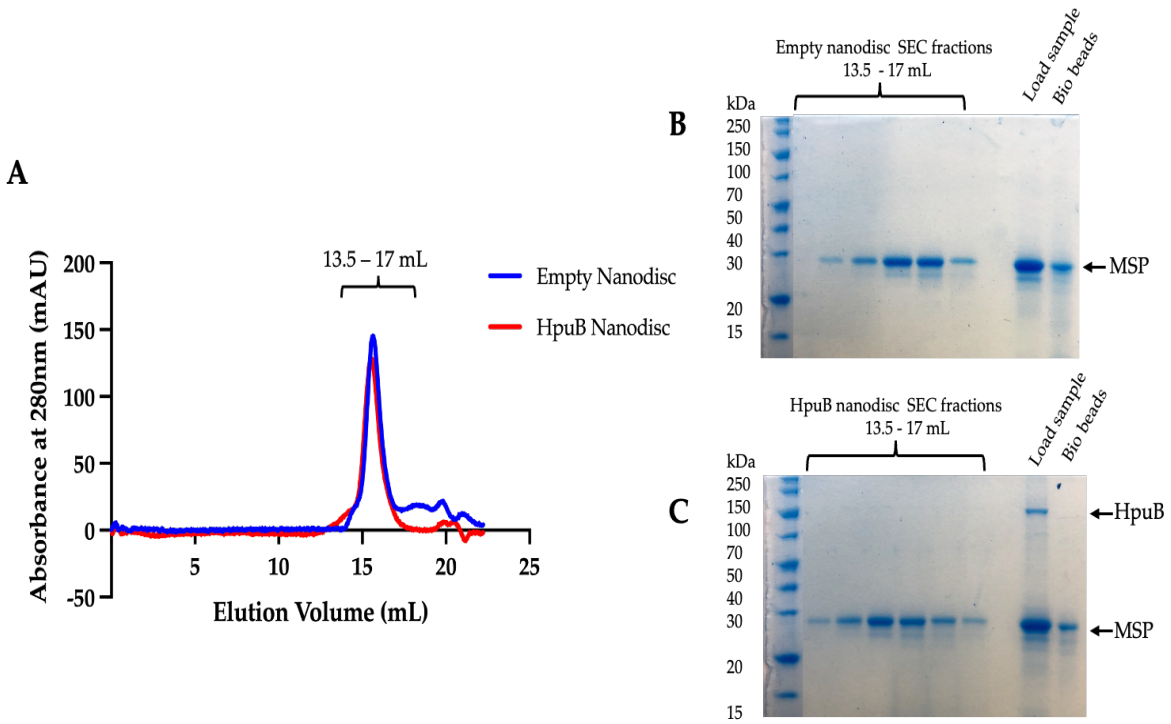

Figure 3.11: Assembly of membrane extracted, detergent solubilised HpuB into nanodiscs.

HpuB was assembled into nanodiscs using the MSP1E3 scaffold protein and POPC lipids at a ratio of 4:1 MSP: HpuB and 85:1 MSP: POPC. (**A**) A280 chromatogram of the SEC purification empty nanodiscs (blue) and HpuB nanodiscs (red) on a superose 6 10/300 GL column. (**B**) SDS PAGE gel using fractions corresponding to 0.5 mL fractions taken elution volumes 13.5 – 17 mL from empty nanodisc SEC. (**C**) SDS PAGE gel using fractions corresponding to 0.5 mL fractions taken elution volumes 13.5 – 17 mL from HpuB nanodisc SEC. A280 chromatograms present one major peak, untypical of nanodisc SEC purifications, which should show a commensurate peak shift with the additional 90 kDa MWt of HpuB. SDS PAGE shows that MSP1E3 is the only protein in the peak fractions for both chromatograms. HpuB is present in the load sample after the assembly and detergent removal by Biobeads, but disappears during SEC.

3.2.5 - Reconstituting membrane extracted HpuB into peptidiscs

Peptidiscs were identified as an alternative to nanodiscs and detergents because of the relative simplicity in their assembly, and their advantages in solubilising a wide range of membrane proteins. Assembly of HpuB was achieved via the 'on-bead' method (Carlson et al., 2018), where HpuB was first extracted and solubilised in LDAO, then mobilised on affinity beads before the addition of the small peptides that form the peptidisc as acquired from 'Peptidisc Lab'. 1 mL fractions collected from the on-bead substitution and subsequent IMAC purifications were analysed by SDS-PAGE (Figure 3.12A) and showed a successful and relatively pure HpuB, stable in solution in a buffer that lacks detergent. This was confirmed by repeated SDS-PAGE analysis 48 h after purification and delayed SEC purification steps after IMAC (data not shown). To prepare the HpuB peptidisc complex for downstream structural and functional studies, the IMAC fractions were pooled and concentrated for further purification via SEC. However, SDS PAGE analysis showed that the load sample contained contaminating bands (Figure 3.12C) and, although a major peak at 55 – 65 mL was detected by SEC (Figure 3.12B), HpuB levels were low and contaminant levels increased. This suggested that the HpuB peptidisc sample was either not suitable for concentration or the IMAC sample was significantly less pure than initially assumed. These results taken together suggest that the HpuB peptidisc sample is not suitable for purification. As the IMAC fractions are too diluted to be purified by SEC without concentration, IEX was used as an alternative to SEC. However, this approach failed possibly due to peptides changing the PI of HpuB and thereby affecting column binding characteristics.

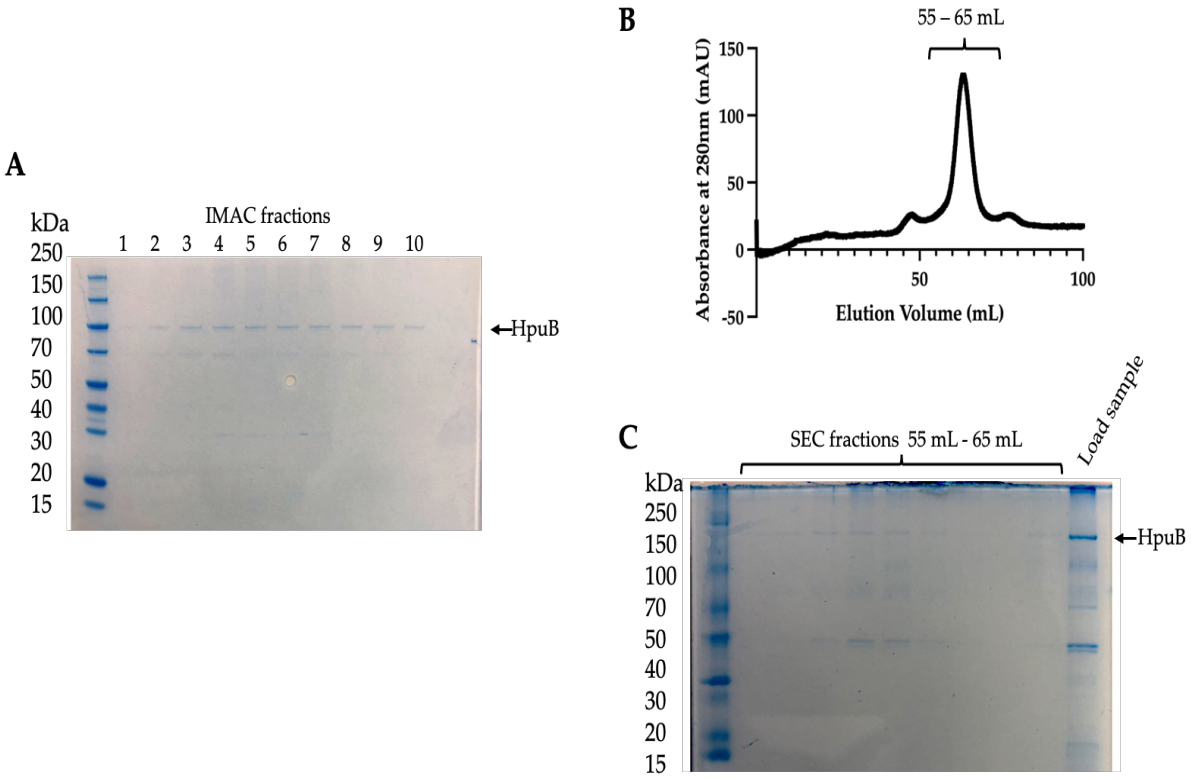

.

Figure 3.12: 'On-bead' assembly of membrane expressed HpuB into peptidisc and SEC purification of HpuB peptidisc.

The outer membrane was isolated and solubilised in LDAO buffer before 'on-bead' peptidisc assembly and IMAC/SEC purifications (**A**) SDS PAGE gel using IMAC samples collected as 1 mL fractions from a gravity flow NiNTA column. (**B**) A280 chromatogram of HpuB peptidisc SEC purification using concentrated IMAC fractions on a 10/300 GL column. (**C**) SDS PAGE gel using 0.5 mL SEC fractions taken from elution volumes 55 – 65 mL. IMAC shows successful purification of HpuB peptidisc eluted in a buffer with no detergents. Fractions 2-10 were concentrated before SEC purification. A280 trace shows a promising major peak however, the resultant SDS PAGE gel shows that the peak fractions contain contaminants as well as HpuB.

3.2.6 - Reconstituting membrane extracted HpuB into amphipols

The peptidisc and nanodisc systems are membrane memetics that involve the use of other peptides. The amphipol system makes use of an amphipathic polymer to replace detergents on the hydrophobic surface of the MP. In this case, MPs are extracted and IMAC purified in detergents before the exchange to amphipol can proceed. In initial experiments, an imidazole gradient method was used to purify LDAO solubilised HpuB from the membrane in preparation for exchanging with the amphipol (Figure 3.13A); however, it was later discovered that LDAO is incompatible with detergent extraction using biobeads, which is used in a subsequent step. To overcome this obstacle, following LDAO solubilisation of HpuB from *E. coli* membranes, exchange to DDM was performed during the IMAC purification via SEC. DDM was chosen for exchange after LDAO extraction due to its lower CMC. DDM was also reported to demonstrate better compatibility with bio bead removal in correspondence with other research groups. The buffers used for this experiment were 0.05% and 0.1% respectively, as described in section 2.18.

Following the IMAC purification of HpuB into DDM, amphipol A8-35 was added and the detergent molecules were subsequently removed using Biobeads. Several attempts to concentrate the sample after this step failed, so the sample was directly loaded for SEC purification in a buffer lacking detergents. SDS PAGE analysis of the peak fractions (Figure 3.13C) showed separation of HpuB from its contaminants and qualitatively demonstrated that HpuB remained stable and in solution through the process of SEC purification in a buffer lacking detergents. Attempts to concentrate HpuB amphipol following this step were largely unsuccessful, an obstacle that would further limit the use of the sample for downstream functional analysis. The solution to this problem was the upscaling of the purification method, increasing the starting amount of membrane material from which HpuB would be purified by increasing the expression volume of *E. coli*, ultimately to 12 L. This resulted in samples that were pure and sufficiently concentrated for EM studies.

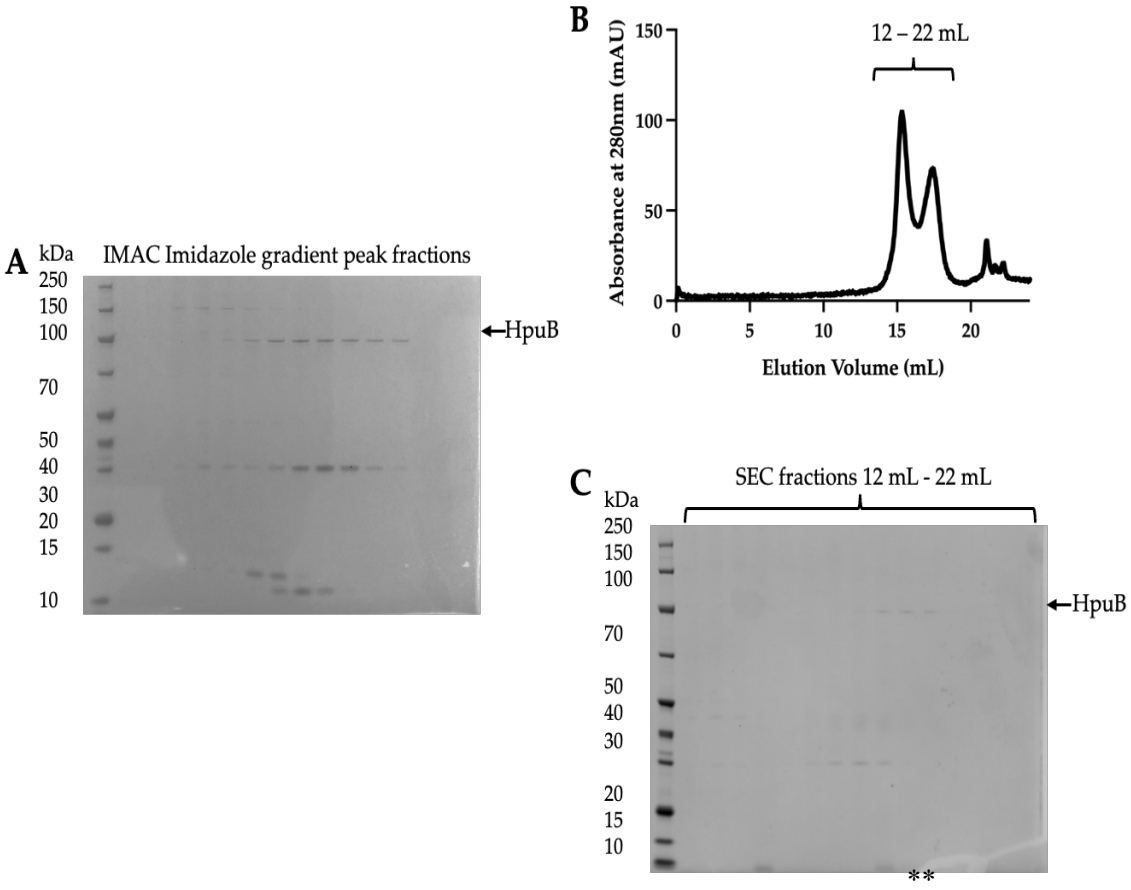

Figure 3.13: Imidazole gradient IMAC purification of HpuB in DDM. HpuB amphipol assembly and SEC purification.

The outer membrane was isolated and solubilised in LDAO before transfer to (**A**) SDS PAGE gel using IMAC fractions. (**B**) A280 chromatogram of HpuB peptidisc SEC purification using concentrated IMAC fractions. (**C**) SDS PAGE gel using SEC peak elution volume fractions. IMAC shows successful purification of HpuB peptidisc eluted in a buffer with no detergents. Fractions 2-10 were concentrated from 9 mL to 1 mL before SEC purification. The A280 trace shows a promising major peak, however, the resultant SDS PAGE gel shows that the peak fractions contain contaminants as well as HpuB.

* = pure HpuB amphipol fractions used for downstream EM studies.

5.3 - Summary

Isolating MPs, whether from natural environments or recombinant IBs and membrane expression has always been a difficult task. Studying those isolated MPs functionally and structurally has historically been even more difficult. The emergence of a wide range of modern membrane memetics has offered reprieve to the efforts of membrane protein scientists. However, other issues, such as overcoming toxic expression and optimisation to find the most appropriate membrane memetic remain obstacles.

HpuB was first isolated for downstream studies using a detergent solubilisation method from inclusion bodies. It was confirmed that HpuB had successfully been expressed in the form of IBs and purified using LDAO. This HpuB sample was shown to bind Hb via pull down studies and was crystalised, albeit crystallisation was unreproducible and thus not optimised.

Due to the incompatibility of LDAO-refolded HpuB with negative stain EM, the sample was reconstituted into nanodiscs with mixed success. Refolded HpuB was eventually abandoned in favour of the expression of HpuB into the *E. coli* outer membrane for near-native expression conditions. Membrane expressed HpuB was extracted using LDAO and sequentially reconstituted into membrane memetics: nanodiscs, peptidiscs, SMALPs (data not shown) and amphipols.

Of the range of membrane memetics, amphipols produced the most consistently effective method to produce a pure HpuB sample which was stable and functional without the presence of detergents. Unfortunately, the low yield of HpuB preparations was an ever-present challenge and indeed even scaling up the expression culture volumes would not produce milligram quantities of the POI, particularly because concentration of the sample seemed to encourage aggregation of HpuB.

CHAPTER 4: HPUB BINDING

4.1 – Introduction

4.1.1 - Substrate use by HpuAB

Although pathogenic *Neisseria* are able to survive solely using transferrin-acquired iron, they do still acquire and use haem iron. Furthermore, through the HpuAB system, pathogenic *Neisseria* can use Hb:Hp complex as well as Hb for haem iron *in vivo*. The HpuAB system was first molecularly described in 1997 by Lewis et al. HpuB was initially discovered as one of two outer membrane proteins involved in Hb use by *N. meningitidis* which also included HmbR (Lewis & Dyer, 1995); the identification of HpuA came shortly afterwards (Lewis et al., 1997).

Following the identification of HpuA, growth assays confirmed that the meningococci HpuAB utilises Hb:Hp more efficiently than Hb when the respective proteins were the sole iron source (Rohde & Dyer, 2004). A liquid phase binding assay using meningococci strain DNM140 and radioisotope [^{125}I]-Hb showed that the HpuAB receptor has a single binding site for Hb and that the dissociation constant (K_d) for binding is 150 nM (Rohde et al., 2002). Reinterpretation of this data would lead the authors to increase this number by a factor of two; the original data was calculated using the molecular weight of Hb as a tetramer ($\alpha^2\beta^2$) but upon release from erythrocytes, Hb exists as a dimer ($\alpha\beta$) before potential sequestering by other proteins An updated K_d was presented as 298.4 nM (Rohde & Dyer, 2004b). As outlined in table 1.1, the blood plasma concentration of Hb in humans is 0 – 0.4 mg/mL.

A repeat of the radio-labelled experiment was attempted to produce a K_d for HpuAB binding to Hb:Hp. However, the [^{125}I]-labelled Hb:Hp produced erratic and irreproducible isotherms and was rendered unsuitable. As a result, the Dyer group developed a non-radioactive assay for flowcytometric analysis of HpuAB binding, including to different phenotypic Hb:Hp complexes. Indeed, not all haptoglobins are made equal and there are several polymorphic phenotypes possible within human

serum (Kasvosve et al., 2010) (Delanghe et al., 2011). This revealed that HpuAB showed a preference for binding human-specific 2-2 or 2-1 Hb:Hp phenotypic complexes compared to Hb alone. Indeed, HpuAB was shown to have a 4.7-fold, 6.6-fold, and 14-fold greater affinity to Hb:Hp types 1-1(4.2 μM), 2-2 (808 nM) and 2-1 (486 nM), respectively, compared to Hb. (Rohde & Dyer, 2004).

As a bipartite system, there have been investigations into the essentiality of each component in the HpuAB system for Hb utilisation and binding. Although the transmembrane HpuB is essential to haem transport from outside the cell to the cytoplasm, HpuA also plays an important role and contributes to the differential capability of *Neisseria* pathogens to bind and use different Hb ligands. An early observation was that HpuA is required for growth with Hb as the sole iron source (Rohde et al., 2002). This conclusion was reached with the construction of an *hpuA* deletion mutant using the meningococci strain DNM143 which expressed wild-type levels of HpuB but could not grow in media in which Hb or Hb:Hp was the sole iron source (Rohde et al., 2002). Despite being essential for growth using Hb proteins, initial flowcytometric studies suggested that an $HpuA^{+}HpuB^{-}$ DNM143 strain did not bind Hb, apoHp or Hb:Hp significantly greater than nonspecific binding to the negative control (Rohde & Dyer, 2004).

There has been no published analysis of the *in vitro* binding of HpuB to Hb or Hb:Hp. This void creates a need for more biochemical information on HpuB binding and remedying this was a major aim of this project. There is however binding data available for another bipartite iron acquisition TBDT system from *Neisseria,* which uses transferrin instead of Hb. TbpA, like HpuB, is a 22-strand beta barrel transporter with putative extracellular loops and TbpB is a lipid-anchored lipoprotein similar to HpuA. During the initial *in vitro* analysis of the TbpAB system, both proteins were co-purified from *N. meningitidis* using affinity chromatography (Boulton et al., 1998). Using surface plasmon resonance (SPR), it was demonstrated that both TbpA and TbpB bind to human

transferrin in distinct regions of the iron-carrying serum protein. The SPR experiments also showed that TbpA preferentially binds to diferric transferrin when compared to iron-free transferrin. This preferential binding between forms of transferrin was not observed with TbpB alone, but rather during studies of transferrin binding to the co-purified TbpAB (Boulton et al., 1998). And although TbpA has been shown to bind, extract and import iron from transferrin in the absence of TbpB, the process is much more efficient when both proteins are present (Noinaj et al., 2012).

4.1.2 - HpuA substrate binding

The whole-cell flowcytometric analysis of cell surface binding by HpuAB was followed up with *in vitro* analysis of recombinantly produced HpuA by the Hare group (Wong et al., 2015b). The *hpuA* gene was cloned from gonococcal strain FA1090 and used to create a HpuA expressing construct in *E.coli*; similarly, synthetically produced *K. denitrificans* and *Eikenella corrodens* HpuA homologue constructs were also created for *E.coli* expression. Using these purified recombinant HpuA homologs, Wong et al (2015) performed co - affinity pull-downs using Hb and Hb:Hp crosslinked agarose resin and showed that all respective HpuA homologs were pulled down by Hb and Hb:Hp whilst failing to be pulled down by the BSA crosslinked negative control. This *in vitro* analysis of HpuA also included isothermal titration calorimetry (ITC), titrating Hb into the *K. denitrificans* HpuA which gave a dissociation constant of 6.1 μM for Hb in its dimeric form and 10.9 μM in its tetrameric form, dimeric Hb is the more clinically relevant of the two. ITC was also used to determine the dissociation constant of HpuA to the Hb:Hp complex which was described as an endothermic binding event with a dissociation constant of 2.9 μM (Wong et al., 2015).

Significant residues, motifs and domains for HpuA binding were identified and then tested. Mutant binding experiments were guided from data acquired from the crystal

structure of the *K. denitrificans* HpuA/Hb complex used as follow-ups to structural information. Wong et al (2015) constructed several deletion and substitution mutants to study binding interfaces with Hb identified during X-ray crystallography analysis and there were many interesting findings. The independent deletion of loop 1 & loop 2 (both containing important binding residues) reduced the amount of HpuA pulled down by Hb but did not cause significant alterations to the folding of the protein as analysed by one-dimensional NMR spectroscopy. Substitution of key aromatic residues in loop 5 also dramatically reduced the amount of HpuA pulled down by Hb (Wong et al., 2015).

Although there is no high-resolution crystal structure for the *N. gonorrhoeae* HpuA in complex with Hb, pull-down experiments using equivalent deletion and substitution mutants to those studied for the *K. denitrificans* protein revealed similar results, suggesting that the HpuA homologues share the same Hb binding interface. Specifically, deleting *N. gonorrhoeae* HpuA loop 1 residues 77–82 (*K. denitrificans* equivalent 60–65), loop 2 residues 111–116 (*K. denitrificans* equivalent 94–99) and loop 4 residues 225–231 (*K. denitrificans* equivalent 201–204) and replacing them with Gly–Ser–Gly residues disrupted binding. The loop 1 deletion had the most significant impact on binding. As expected from x-ray crystallography analysis of *K. denitrificans* HpuA that indicated that loop 4 was not involved in direct binding, deletion of this loop had minimal effect on Hb binding (Wong et al., 2015).

4.1.3 - A HpuB structural homology model

In the absence of a high-resolution structure of HpuB, Harrison et al (2013) created a model of the MP during their studies into the distribution and diversity of the HpuAB system in pathogenic and non-pathogenic *Neisseria*. The model was created using SWISS-MODEL, a 'web-based environment for protein structure homology modelling' (Arnold et al., 2006). The iron scavenging TBDT from *S. dysenteriae,* ShuA, was used as the template for the structural modelling of HpuB. Whilst ShuA and HpuB are expected to have many 3D structural similarities, the overall amino acid sequence identity is

relatively low (16%), preventing the incorporation of some loops with low homology from the model (Harrison et al., 2013). Although ShuA was used as the model template because of its available high-resolution crystal structure, the comparisons of the model functionality were made with HmbR, a monopartite Hb binding TBDT from *Neisseria* pathogens for which there was no structure available, but detailed functional studies were available for the protein. HpuB and HmbR share 28% sequence similarity (Lewis et al., 1997), and determined structural characteristics of HmbR were used to identify potentially important motifs, residues and loops for HpuB.

The 22-strand β - barrel structure of HpuB is very well conserved across TBDTs; the barrel, with its N - terminal plug domain is known to be the pore through which haem is transported. TBDTs are known to bind their ligands using their often-variable surface-exposed loops. HpuB has 11 surface-exposed loops and are numbered based on their position on the β - barrel. According to Harrison et al (2013), the loops with the highest degree of sequence variation among *Neisseria* HpuBs were loops 2, 8 and 9, and this prevented loop 2 from being modelled correctly. Indeed, of these most variable loops, only loop 9 was modelled fully and loop 8 was settled with only a partial construction (Harrison et al., 2013b). Additionally, loop 2 from HpuB is in a similar position to loop 2 from HmbR and the loop 3 sequences have less length variation than most other loops on both HmnR and HpuB. Mutagenesis functional studies of HmbR showed that both loops 2 and 3 are vital for Hb binding and utilisation (Evans et al., 2010).

In contrast to the variable loops, other surface-exposed loops showed a strong degree of conservation. Loops 6 and 7 possessed a high degree of conservation, similar to conservation analysis of the equivalent loops in HmbR. In addition to analysing the degree of conservation within each loop, the Harrison et al (2013) analysis also sought to identify conserved motifs and residues which had already been demonstrated to be important for binding in other haem or Hb binding TBDTs. For example, the conserved ShuA FRAP/NPNL motif, which is characteristic of haem transporters, is aligned with

well conserved FRAP/NPEL motifs in all HpuBs and, interestingly, is conserved on loop 7 of both HmbR and HpuB (Perkins-Balding et al., 2004). Furthermore, both loops 6 and 7 have been demonstrated to be important in the use of Hb for iron; deletion mutations of these loops reduced Hb utilisation via HmbR (Perkins-Balding et al., 2003).

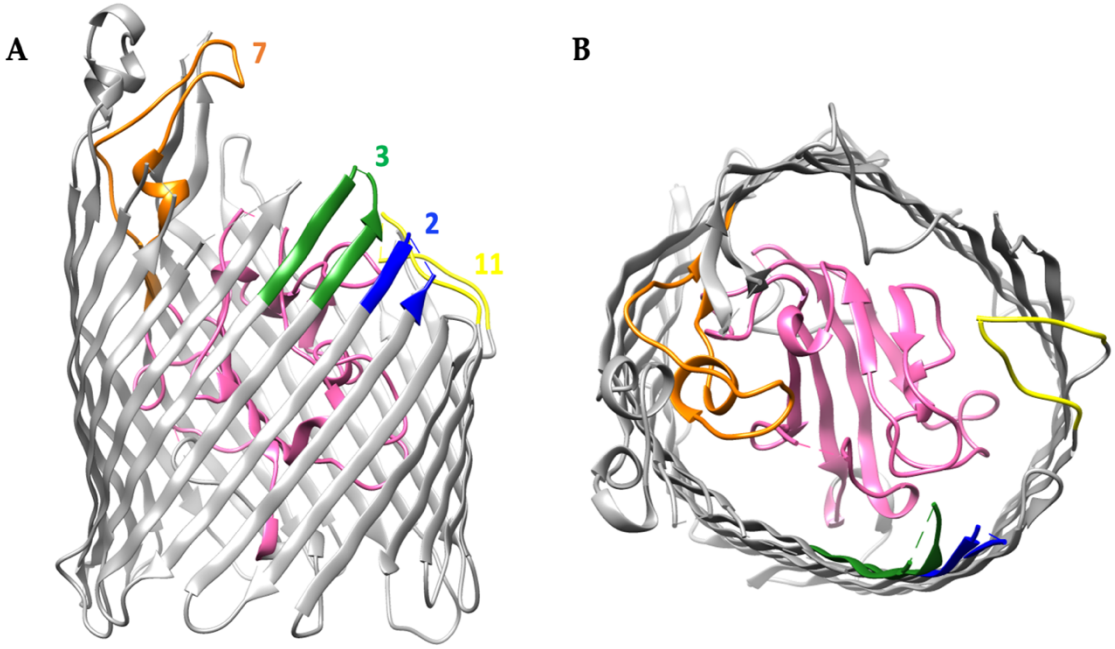

Figure 4.1: Cartoon representation of a HpuB homology model.

This is the HpuB from N. gonorrhoeae as modelled by Harrison et al (2013). (**A**) Side view of HpuB model, unmodelled loop 2 position = blue, partially modelled loop 3 = green, loop 7 = orange, partially modelled loop 11 = yellow. (**B**) Top view of HpuB model, N-terminal plug domain = pink. Not all loops are not fully modelled due to length, only loops 1, 7 and 9 are fully modelled and loops 3, 8 and 11 are partially modelled

.

4.1.4 - Aims

The molecular and biochemical details of the binding of HpuB to Hb or the Hb:Hp complex is fundamental to our understanding of the HpuAB system. However, binding this far has only been demonstrated using flow cytometric analysis of whole cell binding experiments and *in vitro* binding studies of the proteins confirming the binding have not been published. In this chapter *in vitro* biochemical methods are applied in an attempt to relate predicted structure to function, towards understanding how HpuB contributes to the Hb and Hb:Hp utilisation capabilities. To achieve these aims, the WT HpuB proteins would be recombinantly expressed in *E.coli*, solubilised and purified in order to be used in binding experiments such as pull-down assays. Using the homology model of HpuB and the past mutagenic studies of HmbR, a selection of HpuB mutant proteins would be designed, cloned and recombinantly produced to investigate proposed functionally important loops, residues and domains.

4.2 – Results

4.2.1 - Refolded WT HpuB shows binding to Hb

Initially, the ability of recombinant overexpressed *N. gonorrhoeae* HpuB to bind to Hb was investigated using a pull-down assay. As described in Section 2.2, HpuB was cloned for recombinant expression in *E. coli* as inclusion bodies before being denatured, refolded and purified via IMAC and SEC. The purified refolded HpuB was used in pull down experiments in which Hb was crosslinked to agarose resin. BSA crosslinked resin was used as a negative control (Figure 4.2). In these pull downs, the N-Hydroxysuccinimide (NHS)-activated agarose beads were separately incubated with 0.5 mg/ml of BSA and Hb. Additionally, 50 μg of HpuB was incubated with each set of crosslinked beads prior to pull-down and analysis of co-purification by SDS-PAGE.

The data revealed that Hb-crosslinked to agarose beads pulled-down HpuB while BSA-crosslinked beads did not. This experiment was repeated with similar results and was the first evidence that HpuB binds Hb *in vitro,* suggesting that HpuB purified via IB denaturation and refolding in detergent is functionally viable for Hb binding. An omission in this experiment is the lack of a load lane which would allow for comparisons between the amount of HpuB added to the beads and the amount pull down by the Hb crosslinked beads.

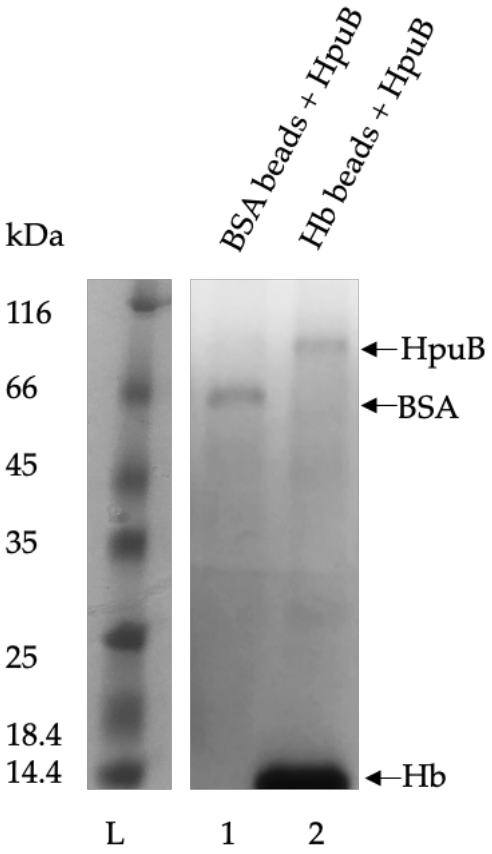

Figure 4.2: Figure 4.2: Refolded HpuB pull down using Hb crosslinked agarose resin.

N. gonorrhoeae HpuB (90 kDa) was expressed into inclusion bodies then refolded in the presence of LDAO and purified via IMAC and SEC. Hb (14 kDa)(Lane 1) and BSA (66 kDa)(Lane 2) were separately crosslinked to agarose resin then each incubated with 50 mg of HpuB. 12% bis-tris SDS PAGE gels using boiled agarose beads show that there is a HpuB band pulled down by the Hb crosslinked resin and no HpuB band with the BSA resin. L is a molecular weight ladder from another gel run in identical conditions.

4.2.2 - Investigating functional binding of HpuB to Hb using HpuB mutants

The HpuB model created by Harrison et al (2013) and the *N. meningitidis* mutagenic functional analysis of HmbR conducted by Perkins-Balding et al (2003) was used to guide the creation of HpuB mutants for this analysis.

The initial focus was on the construction of four loop deletions that were chosen based on factors including the degree of conservation and similarity with equivalent loops on HmbR. This study focused on the deletions of loops 2, 3 7 and 11, as well as the substitution of two conserved plug-based residues. Deleted loop mutants were replaced with a Gly-Ser-Gly sequence which functions as a linker between the two β-sheets. This linker was chosen because small non-polar residues such as Gly allows the linker to be flexible, whilst a polar Ser functions to prevent linker/POI interactions and preserves protein function (Klein et al., 2014). Although loop 2 was too long to be modelled by Harrison et al, HmbR binding studies demonstrated that loop 2 is important to the binding and utilisation of Hb; as such a Δloop-2 mutant was selected for construction. A Δloop-3 mutant was also selected due to the importance of the loop to HmbR Hb binding. Loop 7 was reported to be highly conserved among *Neisseria* HpuB homologs and possesses the NPEL motif that is conserved even amongst non-*Neisseria* Hb or haem binding TBDTs. As a result, a Δloop-7 mutant was selected for construction as well as more specifically, a NPEL substitution mutant. NPEL was substituted to APAA, adding amino acids which had similar-sized side chains with uncharged properties. Loop 11 was selected as a mutational control because comparative analysis suggested it was likely to be a functionally unimportant loop. In addition to loop mutations, two plug-based, potentially functionally important residues to Hb binding, Arg 89 and Lys 144, were substituted to Glu, exchanging basic residues for acidic ones. Altogether, seven mutants were designed that specifically targeted the regions of the plug domain and extracellular loops for their proposed implication in Hb binding (Table 4.1, Figure 4.3). Sequence alignment of HpuB orthologues (Figure 4.3) demonstrated a high degree of

conservation throughout including the loops and residues chosen for mutagenesis. For the following experiments, the *N. gonorrhoea* protein was chosen since it yielded the highest level of HpuB, and the conservation means that these results could be applied to HpuB in all *Neisseria* pathogens.

4.2.3 - Construction and analysis of the Hb-binding activity of HpuB mutations

HpuB mutants were constructed via inverse PCR mutagenesis using the mutagenic primers outlined in table 2.6 and the WT pBASHOM2NgHpuB plasmid as the template DNA. The inverse PCR method employed the use of a forward primer containing the desired mutation and a dephosphorylated reverse primer to prevent self-ligation of the amplified of a linear, double-stranded, mutated PCR product. The restriction enzyme DpnI was used to digest and remove the methylated template DNA, allowing the unmethylated linear PCR product to be self-ligated T4 DNA ligase and transformed into *E. coli.*

Figure 4.3: Alignment of the HpuB amino acid sequences from *K. denitrificans* (B6992), *N. gonorrhoeae* (FA19) and *N. meningitidis* (8047).

HpuB sequences were aligned using Clustal Omega to demonstrate the high conservation between the orthologues. Several mutants were designed to investigate the role of specific determinants in HpuB's Hb binding capabilities. The areas of mutagenesis are highlighted sperate colours. Purple = R89, Yellow = K144, Pink = Loop 2, Loop 3 = Brown, Loop 7 = Green, NPEL = Red, Loop 11 = Blue.

Table 4.1: HpuB mutants designed to investigate Hb binding determinants.
Based on the modelling of HpuB by Harrison et al (2013) and mutagenetic analysis of haem utilizing TBDT HmbR, a list of mutants was designed to investigate the roles of predicted functionally important motifs, residues and extracellular loops on Hb binding by *N. gonorrhoeae* HpuB. Mutants were cloned via inverse PCR mutagenesis using primers listed in table 2.4. In loop deletion mutants the removed loop sequences were replaced with a short Gly-Ser-Gly linker between the two beta strands from which they emanate.

Mutant HpuB target location	**Mutation Detail**
loop2	Δloop-2 (delete residues 196-244)
loop3	Δloop-3 (delete residues 274-301)
loop7	Δloop-7 (delete residues 515-538)
loop11	Δloop-11 (delete residues 742-755)
loop7	NPEL mutate to APAA
Plug	R89 to E
Plug	K144 to E

Following the successful construction of the HpuB mutants listed in (Table 4.1, Figure 4.3), a whole-cell dot blot assay was used to speedily determine which mutants, if any, would show functional deficiencies in binding Hb. The dot blot assay is a method in which protein to protein interactions are determined via the deposition of a protein solution directly onto a polyvinylidene fluoride (PVDF) or nitrocellulose membrane. Whole-cell dot blot assays have long been used to identify protein interactions on cell surfaces, and indeed both HpuB and HmbR were initially identified using this assay (Lewis & Dyer, 1995). In addition, a version of dot blot experiments was used in the mutagenic analysis of HmbR. In This case, HmbR mutants were recombinantly expressed on the *E. coli* OM, the OM was isolated and samples were deposited onto the PVDF or nitrocellulose membrane for incubation with Hb (Perkins-Balding et al., 2003b).

Here, the mutant proteins were recombinantly expressed into the *E.coli* membrane via the arabinose induction on the pBASHOM2 expression system. Successful expression of each mutant was previously confirmed by SDS PAGE following small-scale expression and isolation of the OM fractions (data not shown). For these dot blot experiments, following expression as described in section 2.17, small volumes of PBS-washed cell culture were blotted onto a nitrocellulose membrane before incubation with Hb and later probing with anti-Hb antibodies. After several washes, a secondary antibody was used to detect the presence of anti-Hb antibodies remaining on the membrane. Two iterations of the experiment were conducted, one in which the cells were blotted on the membrane unfixed and another in which the cells were fixed to the membrane using paraformaldehyde (PFA). This was done due to a concern that repeated washes might affect the amount of Hb incubated cells remaining on the PVDF membrane. PFA has previously been used to fix biological materials such as proteins to PVDF membranes (Newman et al., 2013) (Sasaki et al., 2015).

Although some pathogenic *E. coli* strains such as EB1 produce Hb proteases to pirate its haem, there are no reported *E. coli* OM Hb binding proteins exposed on the cell surface. Therefore, *E. coli* containing the empty vector was used as a negative control and was expected to exhibit minimal to no Hb binding. However, the empty vector expression cells did exhibit Hb binding (Figure 2). This could be because the amount of Hb added was too high, allowing for non-specific binding or that the *E.coli* strain used has native Hb-binding activity, possibly through an outer membrane protein. Therefore, although there was some variation between binding activity for the different mutant constructs, the lack of a functioning negative control invalidated the experiment.

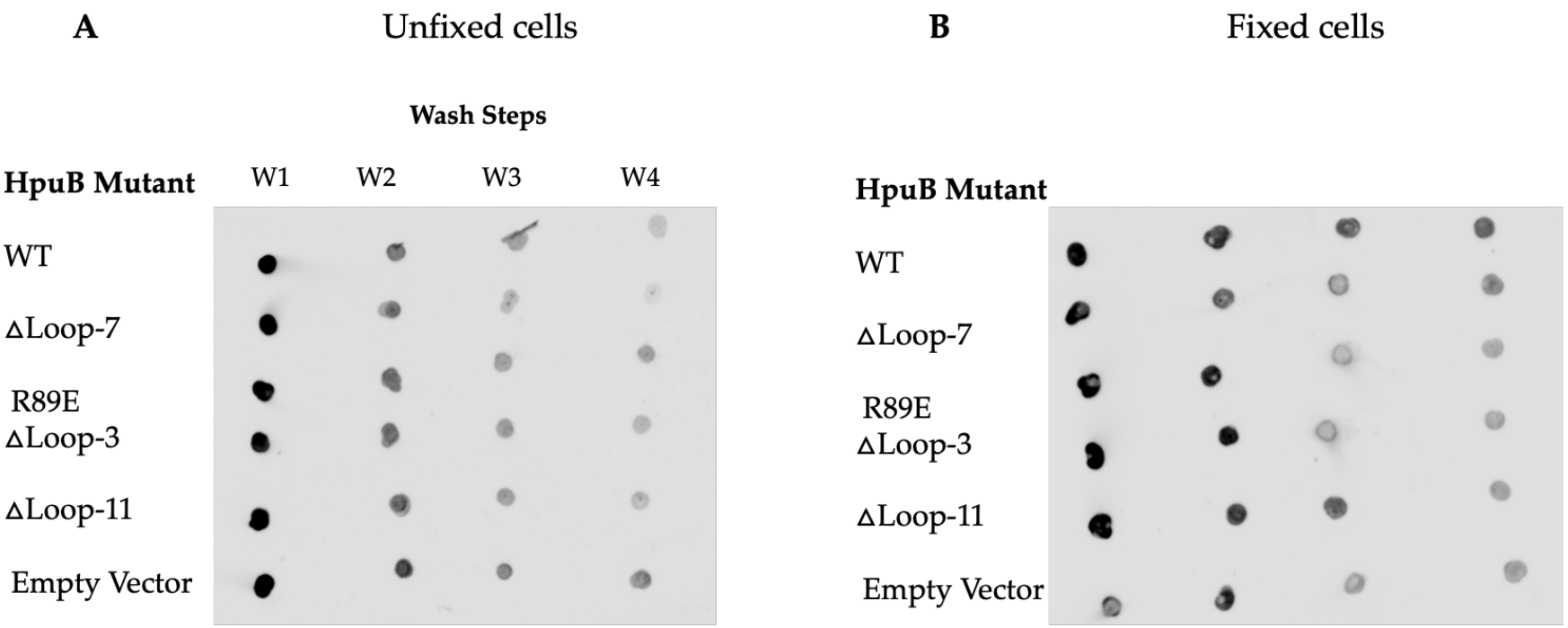

Figure 4.4: Dot blot PVDF membranes investigating cell surface binding of HpuB mutants to Hb.

N. gonorrhoeae WT HpuB and HpuB mutants were individually recombinantly expressed into the *E. coli* outer membrane. Protein expression was induced at OD600 1.0 and 0.5 mL of cell cultures were aliquoted and washed. Washed cells were incubated with 200 mg of Hb, washed and probed for with anti-Hb antibodies to detect Hb binding. (**A**) PVDF membrane blotted with 5 mL of cell culture in PBS following each wash step (**B**) cells prepared as in panel A, and fixed with 4% PFA.

4.2.3 - HpuB mutants show variance in binding capabilities to Hb via pull down assays

Following the inconclusive results obtained by the dot blot experiments, pull-down experiments were attempted to determine the ability of HpuB mutants to bind Hb. The WT and mutant HpuBs were overexpressed, isolated, and purified as described in sections 2.6.2 and 2.7. Once purified, the pull downs were performed as described in section 2.11 and analysed by SDS PAGE. Briefly, this involves incubation of the purified HpuB mutant proteins with Hb and BSA crosslinked agarose beads. Unfortunately, the expression yield of the Δloop-2 mutant was too low to allow further analysis. As a negative control, HpuB proteins were incubated with BSA beads and as expected, there was little to no binding detectable by Coomassie staining (Figure 4.5A). In contrast, WT HpuB was pulled down effectively by the Hb beads suggesting that the binding was specific. Assays with the HpuB mutants revealed that each was pulled down by Hb beads to some degree, with none appearing to completely lose the ability to bind Hb. Analysis of the Coomassie-stained gel data using 'ImageStudioLite' was used to provide qualitative information on the binding of HpuB mutants normalised to the load sample (Figure 4.5B)

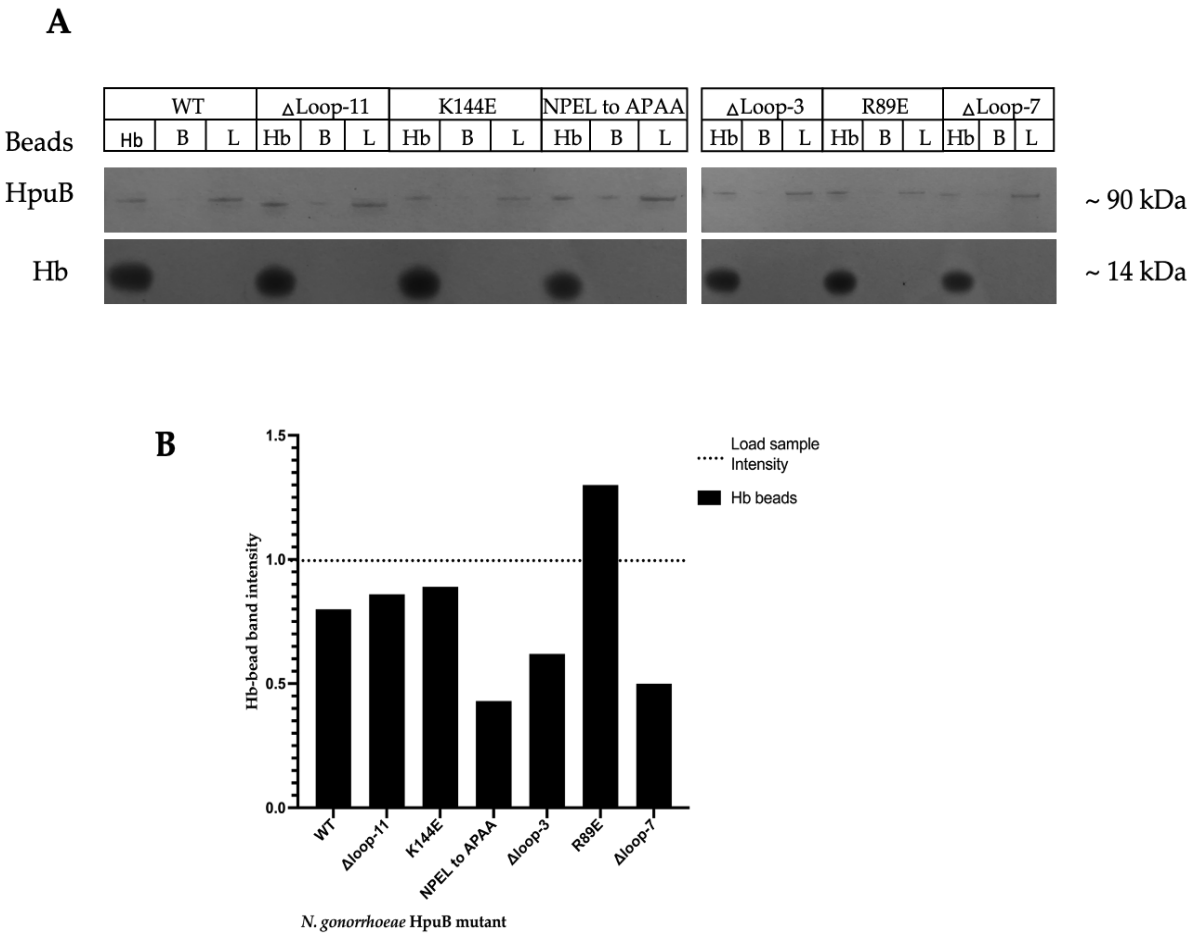

Figure 4.5: Membrane expressed HpuB mutant pull downs on Hb crosslinked agarose resin.
WT HpuB and HpuB mutants were individually recombinantly expressed into the *E. coli* outer membrane then extracted and purified in LDAO. (**A**) 12% bis tris SDS PAGE gels, 100mg of HpuB proteins were used to perform pull downs on Hb and BSA agarose beads. Hb = Hb beads, B = BSA beads, L = load sample. (**B**) Relative intensity of Hb bead bands compared to the intensity of respective load band as calculated using 'ImageStudioLite'. In cases where there is a faint but visible HpuB band in the BSA lanes, that reading was regarded as background and subtracted from the reading acquired from Hb beads.

In comparison to WT HpuB, which showed a binding ratio of 0.8, the Δloop-11 mutant and K144E also showed high levels of binding to the Hb beads, with a ratio of 0.86 and 0.89, respectively. This is consistent with their expected minor role in Hb binding; according to modelling, loop 11 is unlikely to be involved in Hb utilisation and the lysine at position 114 is a conserved positively charged residue in the plug domain predicted to face the periplasm where surface Hb binding is unlikely. On the other hand, HpuB mutated in Loops 3, 7 and NPEL exhibited the lowest binding ratios, at 0.62, 0.43 and 0.5 respectively, suggesting a lower affinity. This is consistent with the predicted importance in the binding of these determinants through conservation among HpuB homologues and other haem and Hb binding TBDTs.

4.3 - Summary

This chapter sought to investigate the ability of recombinantly produced HpuB to bind Hb *in vitro.*

Firstly, *N. gonorrhoeae* HpuB refolded from inclusion bodies was shown to bind Hb via pull down assays. The refolded detergent solubilised HpuB sample was not taken forward for further binding studies partly due to its incompatibility with structural determination techniques such as X-ray crystallography and electron microscopy. The IB refolding method for HpuB reconstitution was also abandoned due to a lack of trust in the refolding process. The literature considers native membrane expression more reliable in producing a correctly folded protein than IB denaturation and refolding (Bhatwa et al., 2021) (Gutiérrez-González et al., 2019).

Secondly, HpuB was cloned for membrane expression via the pASHOM2 vector; successful expression and purification were confirmed by SDS PAGE. To further understand the roles of functionally implicated areas, HpuB mutants were created via inverse PCR based on the Harrison et al (2013) homology model of HpuB and HmbR mutagenesis studies. Whole-cell dot blot assays were done to quickly ascertain HpuB mutant binding capabilities. Dot blot experiments were deemed unsuccessful because although there was some variation between binding activity for the different mutant constructs, the lack of a functioning negative control invalidated the experiment.

Thirdly, *N. gonorrhoeae* HpuB mutants were produced, purified, and used for Hb pull downs. Pull downs showed that HpuB mutated in Loops 3, 7 and NPEL exhibited the lowest binding affinity to Hb, although a lack of biological replicates prevents the drawing of strong conclusions here. In particular, Loop 7 has repeatedly been shown to be an important functional loop for haem and Hb binding TBDTs (Perkins-Balding et al., 2003a) (Perkins-Balding et al., 2004) (Stojiljkovic & Perkins-Balding, 2002). It has been demonstrated that all haem or Hb binding TBDT loop 7s contain a FRAP/NPEL motif which is known to facilitate substrate binding. There is no direct split in which version

of the FRAP/NPEL motif correlates to a higher propensity for Hb or haem in other TBDTs. Interestingly, although these pull downs show significant loss of Hb binding function commensurate with the NPEL substitution, its role is still in question. Deletion of this conserved motif in HmbR loop 7 showed that the motif was not required for Hb binding but is essential for Hb utilisation. Prompting the suggestion of a more mechanistic role for the motif in the removal of haem from Hb (Perkins-Balding et al., 2004). It is however important to note that HpuB works in tandem with its bipartite partner HpuA whilst HmbR functions alone. This key difference might prompt slight functionality differences in seemingly highly conserved regions too. The loop 3 deletion mutant, which also demonstrated significant function loss is interesting because loop 3 is amongst the most variable loops in HmbR and HpuB sequence analysis. In HmbR mutagenesis studies, unlike the NPEL motif, loop 3 was demonstrated to be involved in Hb binding (Perkins-Balding et al., 2003b)

Throughout the process of studying HpuB binding to Hb, other techniques were considered as alternatives to pull downs but were not pursued due to issues in the compatibility of different HpuB samples. The most promising of which was the switchSENSE platform, designed for the investigation of protein-protein or protein-nucleic acid interactions. The use of this platform required the covalent conjugation of HpuB to a DNA nanolever. Significantly, the switchSENSE platform is incompatible with detergents and so HpuB must be reconstituted into a detergent-free membrane memetic first. As outlined in chapter 3, HpuB nanodiscs were never produced with enough assembly confidence to take forward for switchSENSE assays and although several attempts were made, HpuB peptidiscs could not be sufficiently purified and concentrated for conjugation.

CHAPTER 5: ELECTRON MICROSCOPY STUDIES OF HPUB

5.1 – Introduction

5.1.1 - Transmission Electron Microscopy background

Electron microscopy is a broad and versatile technique used to obtain high-resolution images of biological and non-biological specimens invented in the early 20th century (Knoll & Ruska, 1932). It has long been used in the biological sciences to study the structures of cells and cell organelles in detail. In basic terms, electron microscopy takes advantage of the short wavelengths of elections, which can be up to 100,000 times shorter than visible light photons (Erni et al., 2009), in using them as a source of illuminating radiation on the specimen. There are two types of electron microscopy, scanning electron microscopy (SEM) and transition electron microscopy (TEM). In TEM, an electron gun fires a beam of electrons accelerated towards an ultrathin specimen which produces an image through a projection onto a phosphorescent screen or camera. TEM has long been used to study cells and tissues allowing for the production of 3D tissue and cell reconstructions from virtual slices up to 1.4 nm thick (X. Chen et al., 2008; Graham & Orenstein, 2007). As technology in software and hardware has advanced over time, the targets of TEM use have become smaller and more complex, reaching 3D reconstruction of isolated complexes of below 50 kDa in recent applications. An example is the 2017 3.2 Å structure of Hb (Khoshouei et al., 2017)

X-ray crystallography has historically been the most commonly used technique in the determination of protein structures if well diffracting crystals can be reliably obtained. However, studying protein structures via TEM has several advantages that neutralise the disadvantages of other structural determination techniques like X-ray crystallography. In TEM, the sample does not need to be crystalised, requires very low sample concentrations, and can be studied in dynamic forms as opposed to the static positions associated with X-ray crystallography (Boekema et al., 2009).

5.1.2 - Negative staining

Before a sample is progressed to cryo electron microscopy (Cryo-EM) where high magnification images are collected as a precursor to high-resolution protein structures, the sample is usually screened and analysed by negative staining. Negative staining uses heavy metal solutions such as uranyl acetate to increase the contrast of samples when imaged by the electron microscope. Whilst this contrast only allows for visualisation up to around 18 Å due to the microcrystals formed by the drying of heavy metals (Ohi et al., 2004; Scarff et al., 2018), this level of resolution can offer crucial information about the sample's homogeneity, purity, ideal concentration and complex formation.

Negative stain is usually performed with thin carbon grids with each grid requiring 2 to 4 μL of sample in low salt buffer. Working with the most homogenous samples, 2000-5000 individual particles can be enough to generate informative 2D class averages. This number can be significantly greater with less homogenous samples. The individual particles can be used to produce 2D class averages and even low-resolution 3D models. Experimenting with conditions at this stage can provide substantial guiding information on the best conditions when preparing grids for cryo-EM (De Carlo & Harris, 2011; Ohi et al., 2004; Burgess et al., 2004). Although considered a crude technique when compared to Cryo-EM, negative staining has been instrumental to the study of MPs. In the initial stages of MP structural determination using SMALPs, negative staining was used to demonstrate the capabilities of the membrane memetic. *E. coli* secondary transporter AcrB was extracted with SMALPs and using several techniques including negative stain, TEM was demonstrated to be significantly more active than the equivalent DDM extracted form (Postis et al., 2015). A 3D reconstruction of ArcB which showed a clear 3-fold symmetry model was also produced to a resolution of 18 Å. There was sufficient clarity in the model to distinguish between the polymer, the surrounding lipids and the protein itself (Postis et al., 2015).

5.1.3 - Cryo Electron Microscopy

Cryo-EM is regarded as one of the most exciting techniques in biochemistry and is considered revolutionary in the world of structural biology. Indeed, three scientists were awarded the 2017 Nobel prize for chemistry in recognition of their contribution in developing the technology as a technique for 'high-resolution structure determination of biomolecules in solution' and bringing humankind to the 'resolution revolution' (*NIH Grantee Wins 2017 Nobel Prize in Chemistry*, 2017; Neumann et al., 2017). Cryo-EM is an umbrella term for more specific sub-disciplines such as cryo-electron tomography, electron crystallography and most commonly used, single particle cryo-EM (Milne et al., 2013). Cryo-EM addresses two of the most significant early limitations that hindered the early progress of specimen and protein analysis by TEM. The first was that it was considered impossible to collect images of biological samples under the vacuum which is required for TEM function. The second is that the interactions between electrons and matter causes damage and can be completely destructive. To address both these issues, microscopists introduced the rapid freezing of single molecules in vitrified amorphous water to form a thin layer of ice which functions as both protective and preservative (Renaud et al., 2018).

The use and popularity of cryo-EM have increased exponentially over the last two decades and have now replaced other techniques as the primary technique for the structural determination of samples like viruses, ribosomes and MPs (Nogales, 2016). Advancements in the capabilities of cryo-EM and in the methods used to solubilise and stabilise MP has created a fruitful environment for MP structural studies. MPs have now been imaged via cryo-EM as solubilised detergent-MP and bicelle/detergent – MP complexes (Ujwal & Bowie, 2011), as MP/nanodisc complexes (Denisov & Sligar, 2016) (Bayburt & Sligar, 2010), as SMALP/MP complexes (Parmar et al., 2018; Schmidt & Sturgis, 2018) and as amphipol/MP complexes (Y. Chen et al., 2016; Zubcevic et al., 2016). The speed and resolution to which the MP structure can be solved depends on

sample quality, and so the expression, solubilization, and purification protocol must be optimized for each MP (Carvalho et al., 2018).

5.1.4 - Modern membrane memetics and cryo-EM

Many of the game-changing membrane mimetics discussed in chapter 3 have been influential in the MP field because of their compatibility with TEM and cryo-EM. Nanodiscs have now been instrumental in the solving of several cryo-EM MP structures, including the ~4 Å transmembrane domain of voltage-activated potassium (Kv) channel solubilised using MSP1E3D1 and a mixture of POPC: POPG: POPE lipids. Although the cytoplasmic regions of the protein were resolved to a higher resolution than the transmembrane regions (~3 Å), the authors of the work were able to use cryo-EM to solve the complex as a whole and investigate the channel's structural dimerism (Matthies et al., 2018). Similarly to nanodiscs, peptidiscs use amphipathic peptides as a membrane mimicking component and an example of their use in cryo-EM structural biology is the PlexinC1/A39R complex which is the receptor for semaphorins that transduce signals for regulating neuronal development and other processes. Peptidiscs were used to stabilise the transmembrane regions of the complex for cryo-EM resolution of 3.1 Å. allowing the study of the complex and its many interesting configurations and using subunits expressed and purified in different physiological contexts (Kuo et al., 2020). An example where amphipols were used for cryo-EM work is TRPV2, which is a transient receptor potential (TRP) channel MP. The protein was expressed in insect cells and ultimately solubilised and stabilised for cryo-EM studies using the amphipol A8-35 to a resolution of ~4 Å, with some regions resolved to 3.3 Å. The use of both amphipols and cryo-EM meant that the authors of this work were able to provide detailed structural information regarding the function of the channel in its many dynamic modes and in complex with its ligand with and without the presence of exogenous and native lipids (Zubcevic et al., 2016).

SMALPS have also proven to be an excellent membrane memetic for the study of MPs. They are unique in that they do not involve the use of traditional detergents at any stage, the MP is cut out of the membrane intact with its native lipids. SMALPs have been used to solubilise and stabilise these important MPs for structural and functional studies using SAXS/SANS as well as cryo-EM. Cryo-EM was able to offer distinct structural information for the binding of a MP that is often not surface exposed, adding an extra layer of complexity (Pollock et al., 2022). An example is the transmembrane domain of the mechanosensitive-like channel, YnaI which was solved to a resolution of 2.4 Å with eluded details of MP and endogenous lipid interactions (Catalano et al., 2021). And also, a 3.8 Å structure of the *C. perfringens* β-toxin using the SMA200 polymer (Bruggisser et al., 2021)

5.1.5 - Aims

A major aim of this project is the structural resolution of HpuB alone and in complex with its substrates. X-ray crystallography screens produced unreproducible, poorly diffracting crystals. The problems associated with the crystallography of MPs led to the focus on TEM as a more suitable technique to achieve this aim.

HpuB samples, reconstituted into a range of membrane memetics, as described in chapter 3, were prepared on grids for NSEM data collection and subsequent data processing of 2D and 3D classifications. These classifications would then be used to make assessments regarding the quality of the sample and particles to derive useful structural information and as triage for progression to cryo-EM.

5.2 – Results

5.2.1 - Single particle analysis HpuB in detergents

Negative stain EM (NSEM) was chosen as a technique to screen the purity and homogeneity of HpuB samples ahead of cryo-EM and for low-resolution structural determination. The initial HpuB samples, produced by the denaturing and refolding of recombinantly produced *N. gonorrhoeae* HpuB IBs in the presence of detergent and then purified by IMAC and SEC showed large micelles inhibiting the identification of smaller particles (Figure 5.1). This sample was prepared for NSEM on carbon-coated grids (section 2.19.2) at a range of protein concentrations which all displayed a constant background of micelles across the carbon. 2D projections collected at the TEM demonstrated that the LDAO detergent was not suitable for NSEM analysis (Figure 5.1). Although this HpuB buffer kept the LDAO concentration (0.1%) close to the CMC, it was difficult to distinguish possible HpuB particles from HpuB/micelle complexes or empty micelle complexes. Micelles themselves had a heterogenous size. The micrographs presented in figure 5.1 show insufficient contrast between potential particles and the grid background. There is little indication of the presence of individual protein particles and indeed, although each micrograph was taken from the same grid using the same magnification, there is significant difference in size and patterns of the visible material. A potential solution to this is experimental optimisation with other detergents to stabilise HpuB. However, LDAO was repeatedly demonstrated as the best detergent for HpuB extraction, and dialysis exchange to more EM-friendly detergents such as LMNG resulted in precipitation of the protein (data not shown).

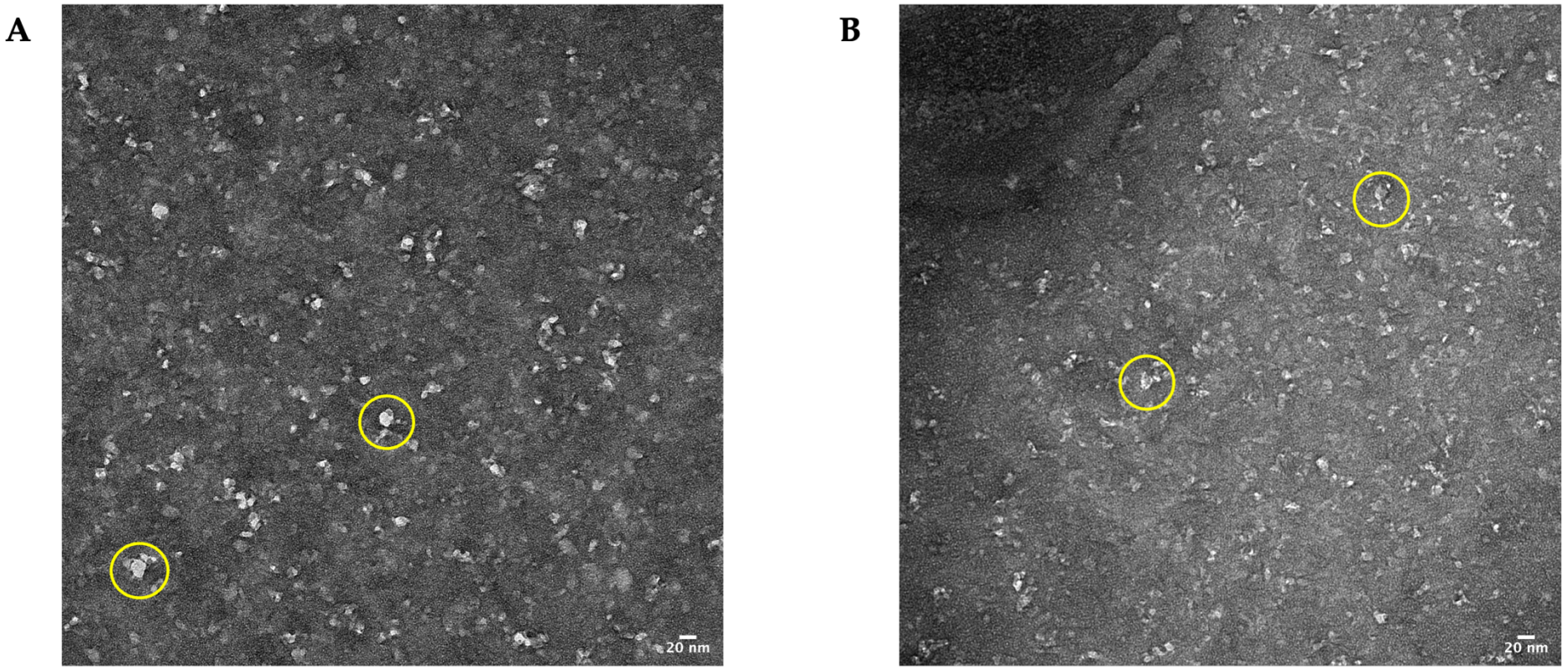

Figure 5.1: Negative staining EM images of refolded HpuB reconstituted in LDAO.

Two representative 2D projection images show the presence of *N. gonorrhoeae* HpuB indifferent size micelles (examples in yellow circles). Images were taken from a carbon-coated grid prepared with HpuB at 0.2 mg/ml, at 100 kV and x60 000 magnification. Scale bar is 20 nm.

5.2.2 - Single particle analysis of HpuB in Nanodiscs

To address the difficulties posed by detergent reconstituted HpuB in NSEM samples, nanodiscs were first chosen as an alternative membrane memetic.

5.2.2.1 - TEM analysis of LDAO-Refolded HpuB in nanodiscs

Initially, HpuB nanodiscs were assembled using refolded *N. gonorrhoeae* HpuB, the type MSP1D1 of MSP and POPC lipids giving a theoretical reconstituted nanodisc diameter of 10 nm. During assembly optimisation, a range of MSP:HpuB ratios were trialled, and SDS-PAGE and SEC analysis demonstrated that the best co-elution of MSP and HpuB was with a ratio of 4:1 (Figure 3.6). This sample was prepared for NSEM on carbon-coated grids in a range of concentrations following standard protocols to ascertain the optimal protein concentration for data collection. TEM images showed relatively homogenous size particles across the grid of the estimated size.

For single particle analysis of refolded HpuB in nanodiscs, 8742 single particles were manually picked from 98 micrographs and grouped into 30 initial 2D classes. Following three rounds of exclusions and reclassifications based on the quality of particles within each class and the estimated resolution, the 2D classification of these particles was finalised showing different potential orientations of the HpuB nanodisc particle (Figure 5.2B). The final grouping of 19 final 2D classes presents an overrepresentation of circular potential top view particles in the classifications. In these top view classes, there is a dominant 'pore-like' feature, visible in classes 4, 9, 11, 12 and 17. These classes are amongst the most populous particle distribution compared to the total 2Ds particles (appendix table 7.1) Although the presence of this pore might not be an absolute absence of material, it does indicate lower density than elsewhere in the particles within those classes. It is possible that these features correspond to the centre of the HpuB β-barrel, although this HpuB construct was expected to contain an intact N-terminal plug domain, which should obscure the barrel.

An initial 3D model was built to function as a reference map to the subsequent 3D classification of the data set. To this end, a subset selection of particles which represented a mixture of potential HpuB orientations were selected as the particle input (Figure 5.2C, classes 2, 5, 7, 13, 15), amounting to 21.8% of 2D classes shown in Figure 5.2B. Classes in which the 'pore-like' feature is visible were excluded from the 3D initial model to avoid the biasing of the data set in favour of this feature during 3D classification. The initial 3D model (Figure 5.2D) was built with a resolution limitation of 50 Å. Despite the low-resolution filter stipulated in building this model, the sideview of the model is bulged which could indicate the MSP protein surrounding HpuB. More striking is the persistent presence of a pore as seen in the top view panel (Figure 5.2D), even when not visible in the input 2D classes.

The initial 3D model was used as a reference map for the processing of four 3D classes using all particles in the final set of 2D classes. All the 3D classes are disc-shaped which is expected from a nanodisc HpuB particle, with varying but similar bulging features seen on the side views. Classes 1 and 4, the classes with the lowest number of input particles and lowest resolution were excluded and are not shown in figure 2. Classes 2 and 3 were processed to the highest resolution and contained large shares of the total particle input, 46.2% and 31.6% respectively. Classes 2 (Figure 5.2E) and 3 (Figure 5.2F), the major 3D classes out of the four similarly share variations of a 'pore-like' feature in the centre of top views. There is also a barrel-like shape in the side views of these classes which is expected of β-barrel HpuB. It is also possible that the bulges are an outline of the MSP surrounding the protein. The further refinement of the 3D classes built from refolded HpuB nanodisc particles was halted due to a change experimental method for the production of HpuB samples. Indeed HpuB would subsequently be produced by expression directly into the *E.coli* membrane to avoid uncertainty regarding the reliability of the refolding process.

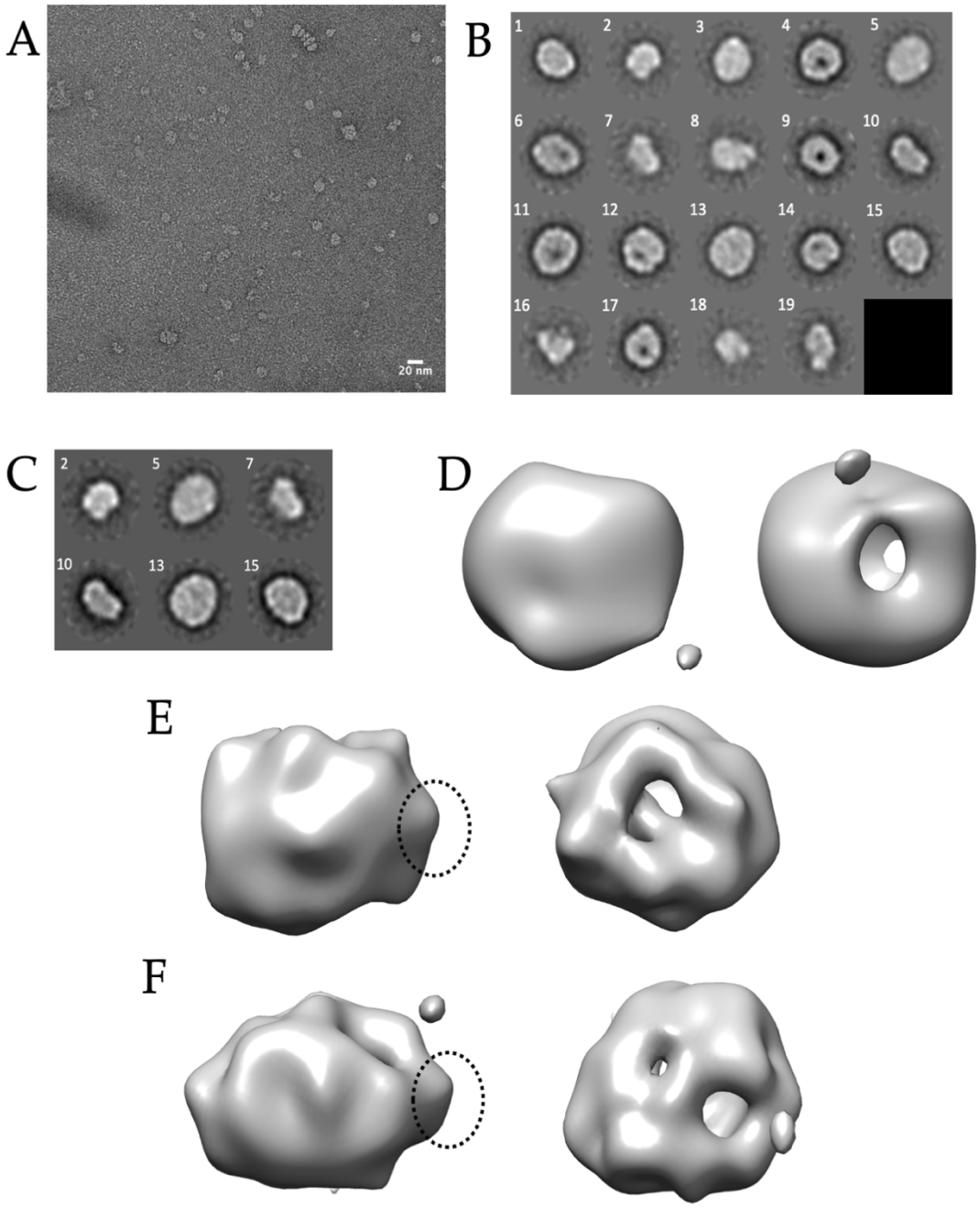

Figure 5.2: Single particle analysis of refolded HpuB nanodisc using TEM.

Recombinantly produced *N. gonorrhoeae* HpuB IBs were denatured, refolded, and reconstituted into nanodiscs. Samples were analysed using negative stain TEM (A) A cropped representative micrograph of HpuB nanodiscs (0.2 mg/mL). Images were taken from carbon coated grid at 100 kV, x50 000 magnification. Scale bar is 20 nm. (B) Final 2D classification of 8742 extracted particles (particles distribution per class) (Appendix table 7.1). (C) Subset selection of diverse 2D class orientations for initial 3D model build. (D) Initial 3D model, limited to 50 Å. Left = side view, Right = top view (E) 3D class 2, 23.6 Å, 46.2% of total particles. Left = side view of barrel-like shape showing a bulge extension (black dotted circle), Right = top view showing a hollow pore in the middle of the model. (F) 3D class 3, 21.5 Å, 31.6% of total particles. Left = side view, Right = top view.

5.2.2.2 - TEM analysis of Membrane expressed HpuB reconstituted in nanodiscs

In order to further optimize the assembly of HpuB into nanodiscs, two key changes were made. Firstly, to mitigate the extensive and harsh processing required to solubilise HpuB IBs, the pBASHOM2.HpuB constructs were cloned to express HpuB directly into the *E. coli* membrane, under the control of an arabinose-inducible promoter. Secondly, since NSEM analysis of refolded HpuB nanodiscs revealed that the diameter of the MSP1D1 MSP (10 nm) could be restrictive to effective HpuB (9.5 nm) nanodisc assembly, it was decided to trial an extended nanodisc type MSP1E3. This would be expected to provide more space within the MSP belt for the assembly of HpuB and POPC lipids at a ratio of 4:1 and POPC to MSP at 85:1. To allow for comparisons between HpuB nanodiscs and empty nanodiscs, this HpuB nanodisc assembly was conducted in parallel with an empty nanodisc assembly. As outlined in section 2.3.4, this comparison showed that the SEC A280 chromatograms of both assemblies (Figure 5.3A) was near identical and both HpuB nanodisc and empty nanodisc were eluting at the same volume for both experiments. This implied that HpuB was not correctly assembled into nanodiscs, and this assessment was confirmed using NSEM. Samples taken from the SEC purifications of both assemblies at the same elution volume and protein concentration were used to prepare grids for NSEM micrograph collection (Figure 3.11B&C). The micrographs show an almost identical shape and orientation of the particles on both HpuB nanodisc and empty nanodisc (Figure 5.3B&C). In addition, although the diameter of particles was expected to be similar due to the rigid diameter of the MSP1E3, there is no visual differentiation of particles between empty nanodiscs and HpuB nanodisc. As a result of this assessment, this HpuB nanodisc sample was not taken forward for 2D and 3D classification.

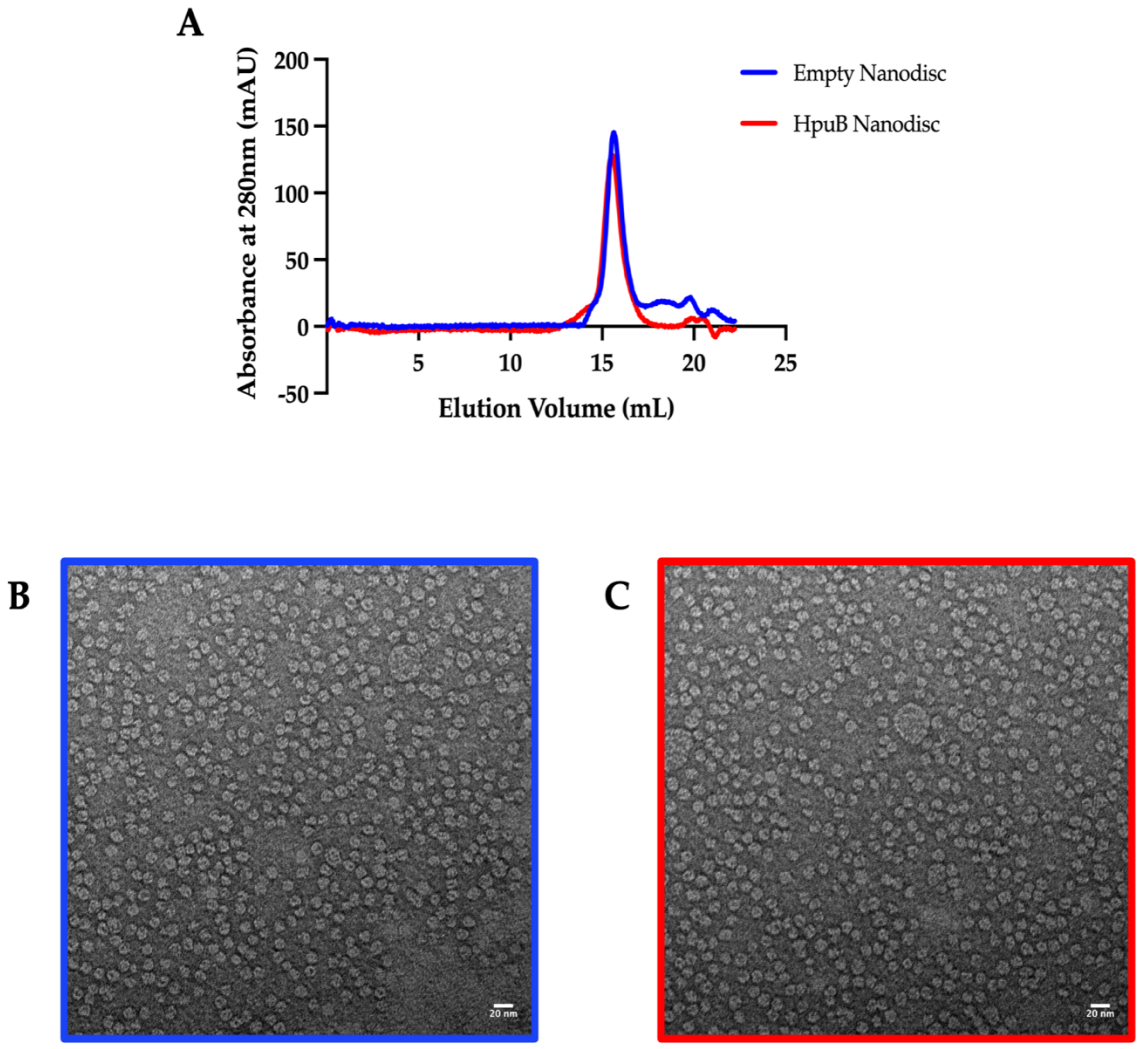

Figure 5.3: Comparison of Empty nanodisc and HpuB nanodiscs using TEM and size exclusion chromatography.

N. gonorrhoeae HpuB, recombinantly produced by expression directly into the *E.coli* membrane was reconstituted into nanodiscs using MSP1E3 and POPC. Representative micrographs of negatively stained particles Images were taken from carbon coated grid at 100 kV, x60 000 magnification using samples taken from the SEC purifications of empty and HpuB nanodiscs. Both samples were prepared at the same concentration (0.15 mg/mL). (**A**) A280 chromatogram of the SEC purification empty nanodiscs (blue) and HpuB nanodiscs (red) on a superose 6 10/300 GL column. (**B**) cropped representative micrograph of empty nanodisc particles (blue). (**C**) cropped representative micrograph of empty nanodisc particles (red) showing the same type of particles. Scale bar is 20 nm.

5.2.3 - TEM analysis of Membrane expressed HpuB reconstituted in peptidiscs

The failure to reconstitute HpuB into nanodiscs prompted the exploration of another membrane memetic, peptidiscs. HpuB peptidiscs were prepared using *N. gonorrhoeae* HpuB extracted and purified from the *E.coli* membrane in LDAO then substituted for peptidiscs following the 'on-bead' method (Figure 3.12) and prepared for NSEM on carbon-coated grids in a range of concentrations.

TEM imaging of the HpuB peptidisc revealed a distinctively heterogenous sample consisting of particles that varied significantly in size and shape (Figure 5.4B). This is likely due to the poor SEC purification as SDS PAGE analysis showed that there were contaminants present in the sample following SEC purification. SPA using RELION was used to further analyse particles observed. 25 655 particles were automatically picked from a total of 91 micrographs. Following six rounds of refinement by exclusion and reclassifications, 20 final classes were calculated, including 16 246 particles. As expected, the 2D classes produced from this heterogenous HpuB peptidisc sample dramatically differed in size and shape, ranging from 7 nm, smaller than the ~13 nm expected particle size to 21 nm which is significantly larger. The final set of 2D classes were categorised by size for downstream processing. Six small classes ranging from 7 - 10 nm were grouped together (42.3% of particles, Figure 5.4C). Another six classes ranging from 11 – 16 nm were grouped together as 'medium classes' (20.6% of particles, Figure 5.4D). Finally, the 8 large classes, 17 – 21 nm (37.1% of particles, Figure 5.4E). Particles within the small and large classes were excluded from downstream analysis because their class diameter was significantly different from the expected size (~13 nm). As a result, particles from the medium classes were taken forward for 3D reconstruction.

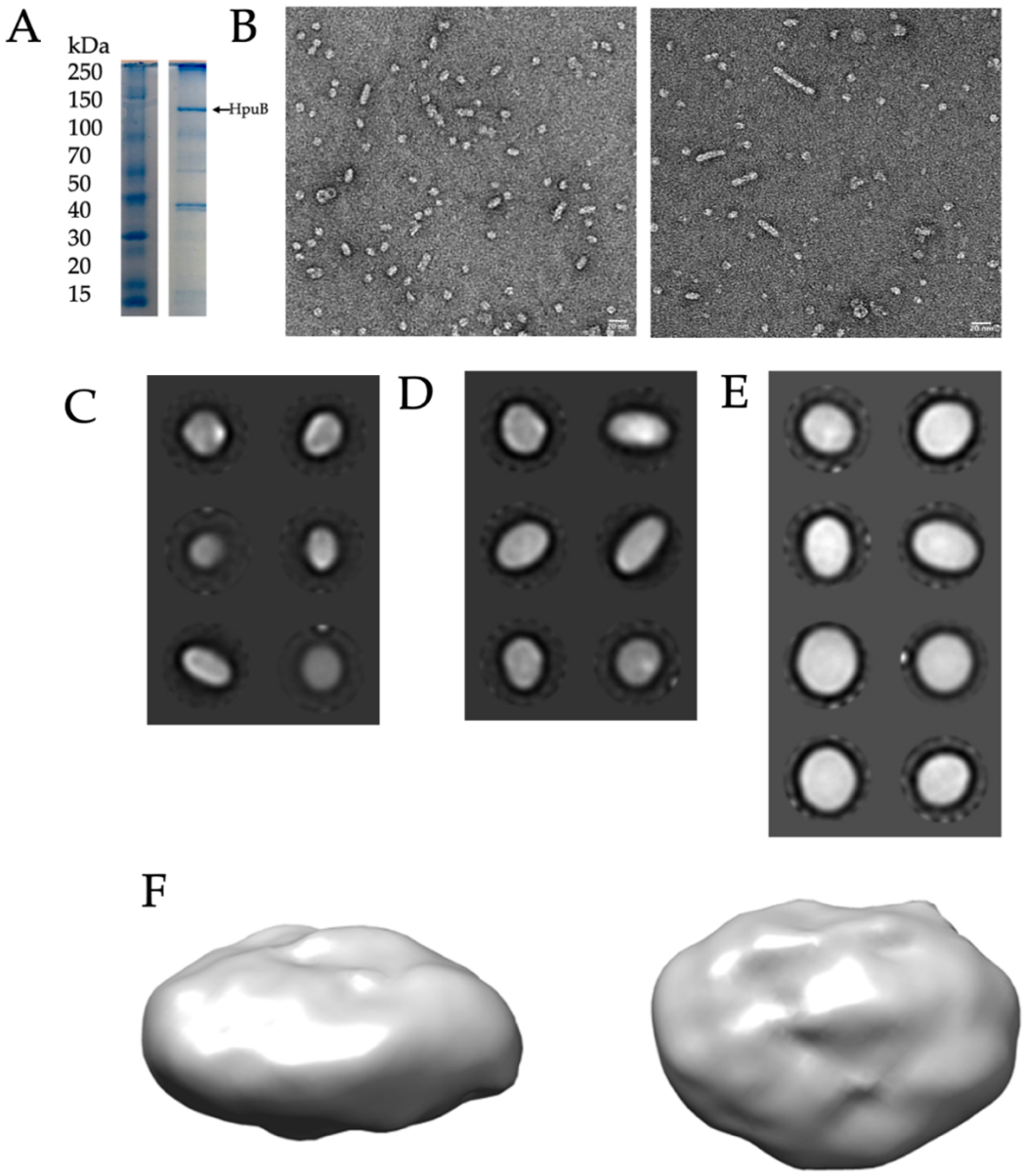

Figure 5.4: HpuB reconstituted in peptidisc characterised using TEM: from negative stained 2D projections to 3D model.

N. gonorrhoeae HpuB, recombinantly produced by expression directly into the *E.coli* membrane was reconstituted into peptidiscs following the 'on-bead' method. (A) SDS PAGE gel showing purity of HpuB peptidiscs (B) Left and right are cropped representative micrographs of negatively stained HpuB peptidiscs (0.2 mg/mL). Images were taken from a carbon-coated grid at 100 kV, x60 000 magnification. Scale bar is 20 nm. B-D = class groupings from final 2D classification. (C) Six 'small' classes, 7 - 10 nm. (D) Six 'medium' classes, 11 – 16 nm. (E) Eight 'large' classes, 17 – 21 nm. (F) The final 3D model of HpuB peptidisc was processed using a 3D initial model and particles within the 'medium' diameter distribution of 2D classes. The input particles for this final 3D model are a minority (20.6%) of all particles within the total final 2D classes and is at 12.3 Å resolution. Left = side view, right = top view.

A subset of particles grouped as medium 2D classes were used to build an initial *ab-initio* 3D model which was subsequently used as a reference map for the creation of two 3D classes. The class, which had the highest particle number and highest estimated resolution of the two, was taken forward for further refinement. As a result, Class 1 was used as a new reference map in addition with all medium 2D class particles to guide the processing of a final 3D HpuB peptidisc. The final 3D HpuB peptidisc was processed to a resolution of 12.3 Å and has a distinct disc-like structure (Figure 5.4F).

The particles taken as the input data for 3D reconstructions are a minority (20.6%) of total particles extracted from the very heterogenous HpuB peptidisc micrographs. Although diameter measurements suggested that these particles are closest to the expected size, their minority status in a highly heterogeneous population calls the reliability of the model into question. In addition, the lack of distinct features and the lack of 'barrel-like' depth in the side view of the 3D model is attributed to the over-representation of top views within the 2D classification in large parts as a result of significant impurities in the sample. Together, this contributed to the decision to progress to another membrane mimetic for the reconstitution of HpuB.

5.2.4 - Negative stain TEM analysis of HpuB reconstituted into amphipols.

The significant heterogenicity of the HpuB peptidisc sample cast doubt on the identity of particles visualised by NSEM. Attempts to optimise the use of the peptidisc membrane memetic on HpuB did not yield sufficiently pure and homogenous samples to be retrieved by SEC and the use of IEX was incompatible due to the use of peptidisc peptides. Amphipols were used as another alternative membrane memetic to solubilise and stabilise HpuB. Here *N. gonorrhoeae* HpuB was extracted and purified from the *E.coli* membrane in LDAO and then exchanged for a different detergent, DMM, which was suspected to be more compatible with the use of biobeads. Following this exchange, biobeads were used to remove detergent molecules in a solution of DDM solubilised HpuB and A8-35 amphipol (Figure 3.2.6). The HpuB amphipol sample was successfully purified using SEC and prepared for NSEM on carbon-coated grids in a range of concentrations.

Micrographs taken of HpuB amphipols (Figure 5.5B) show a more homogenous sample than previous iterations of HpuB reconstitution into other membrane mimetics. For single particle processing of HpuB amphipols, 48 550 particles were picked from 129 micrographs and grouped into 30 2D classes. Following seven rounds of exclusions and reclassifications based on the quality of particles within each class and the estimated resolution, the 2D classification of these particles was finalised with 20 classes of the HpuB amphipol particle made up of 20 410 particles (Figure 5.5C). The final 2D classes show different potential orientations of the HpuB particles. Notably, classes 17 and 18 exhibit a 'pore-like' feature in the top view reminiscent of the same features seen in the 2D classification of refolded HpuB nanodiscs (Figure 5.2B). A small subset of three classes (Figure 5.5D) totalling 18% of total particles in the final 2D classes was used to build an initial 3D model of HpuB amphipol (Figure 5.5E).

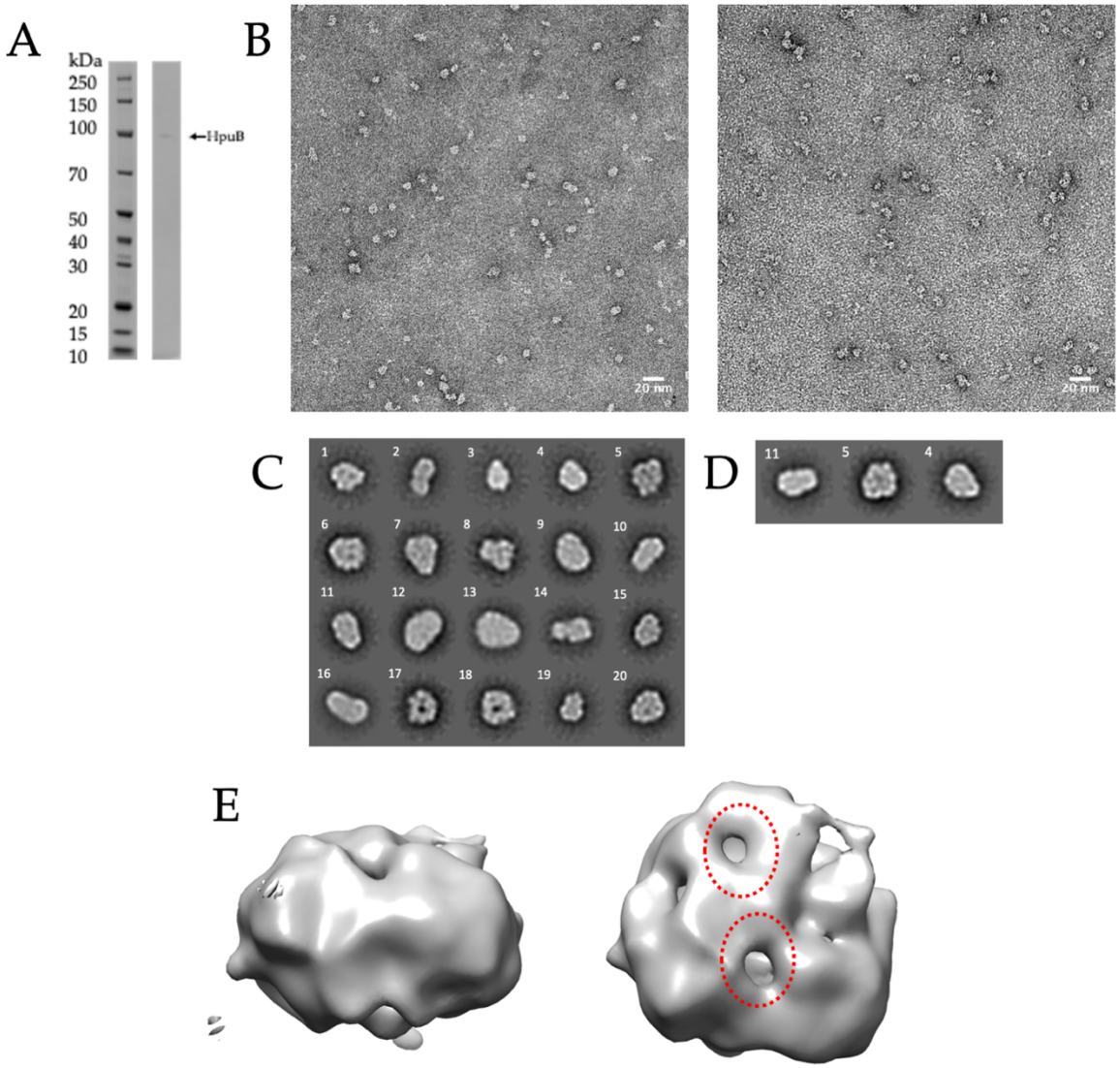

Figure 5.5: HpuB reconstituted in amphipol structural characterisation, from micrographs to initial ab-initio 3D model.

N. gonorrhoeae HpuB, recombinantly produced by expression directly into the E. coli membrane was reconstituted into amphipols. (**A**) SDS PAGE gel showing purity of HpuB amphipol sample. (**B**) Cropped representative micrographs of negatively stained HpuB amphipol (0.1 mg/mL). Images were taken from carbon coated grid at 80 kV, x50 000. (**C**) Final 2D classification of HpuB amphipol particles. (**D**) Subset selection of final 2D classes as input for initial 3D model processing. (**E**) Initial 3D model at 21.2 Å from an 18% subset of final 2D class particles. Left = side view showing barrel like structure, right = top view showing 3 cavities in structure (dotted red circles).

The initial 3D model of HpuB amphipol (Figure 5.5E) shows many distinct features including bulging on the side view which could be indicative of the projection of the A8-35 polymer surrounding the HpuB β - barrel. In addition, there are holes on the top view that are suggestive of low density or no density, which may indicate a pore, but the low resolution (21.2 Å) of the model and small particle input means that these features could be artefacts.

For the 3D classification of HpuB amphipols, the initial 3D model was used as a reference map to process all particles within the final 2D classification to produce four 3D classes (Table 5.1). Of the four classes, classes 1 and 3 contained the highest number of input particles and had the highest resolution and as a result, were chosen for further refinement. 3D refinement was done by using the first model as a reference map to guide the processing of a more refined model using the particles which made up the model. This process was repeated three times until it became clear that the resolution limit had been reached.

Table 5.1: HpuB amphipol 3D classes particle distribution and estimated resolution.

RELION 3 metadata outputs for the 3D classifications of HpuB amphipols. Particle input from final 2D classification

Class Number	Number of Particles Within Class	Estimated Resolution (Å)
1	6006	16.2
2	3710	17.6
3	5168	16.2
4	2977	29.6

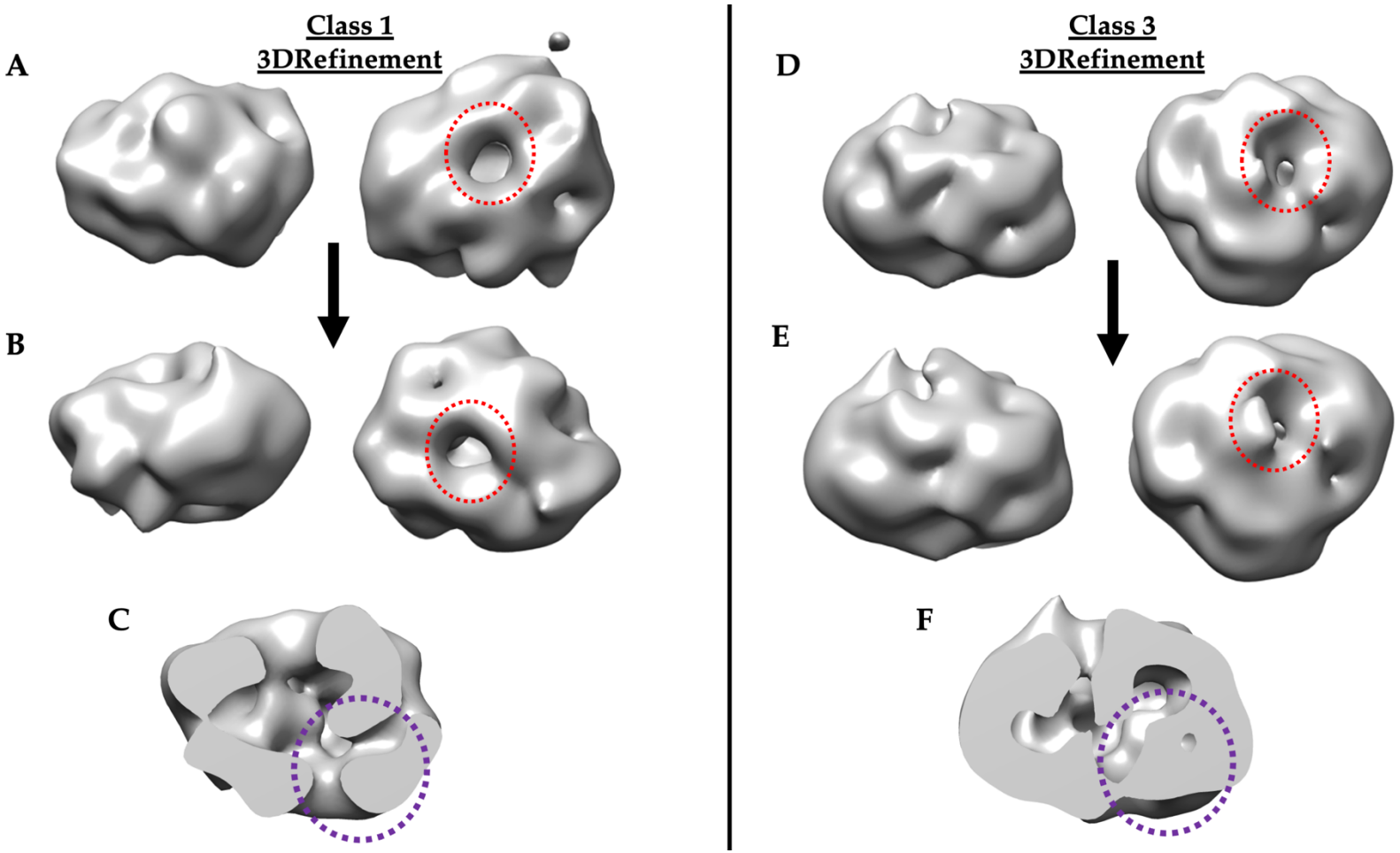

Figure 5.6: Refinement of the 3D classes processed from HpuB particles reconstituted in amphipols.
An initial 3D model for HpuB amphipols was used to build four 3D classes. Classes 1 and 3 were chosen for further refinement due to comparatively higher resolution and particle distribution. Left = side view, right = top view. All top views reveal structural cavities though the model (red dotted circle). (**A**) First round class 1 model (16.2Å) (**B**) Final class 1 model (16.2Å) (**C**) Final class 1 model, cross section of the side view with high density lower portion (purple dotted circle). (**D**) First round class 3 model (16.2Å) (**E**) Final class 3 model (16.2Å). Left = side view, right = top view (F) Final class 3 model, cross section of the side view.

The 3D classes chosen for further refinement in total make up 62.5% of final 2D class particles. In early refinement of both classes 1 and 3, RELION was programmed to create two new subclasses in an attempt to remove particles which did not fit the majority. However, in both cases, the classes continued to be evenly split in terms of particle number and the resolution remain the same. Ultimately, the subclasses were merged into one model after the third round of 3D refinement. 3D Class refinement of classes 1 and 3 revealed distinct features within the model and although the resolution limit (16.2Å) was reached on the first models, the 3D refinement process improved the visual quality of the models. HpuB peptidisc class 1 and 3 models show a familiar 'pore-like' feature on the top views which could be indicative of the lower density inside the HpuB β - barrel with detruding high-density features on top which could indicate the presence of extracellular loops. Additionally, cross sections of both final models (Figure 5.6C&F) demonstrate that whilst there are cavities in the model, they are not completely hollow and indeed there is significant density in the lower portions of the models which could be indicative of the presence of the N-terminal plug domain.

5.2.5 - Cryo-EM screening of HpuB reconstituted in amphipols

HpuB samples were prepared and plunge frozen for cryo-EM screening using Quantifoil 1.2/1.3 and Cflat 1.2/1.3 grids from EMS and various blotting times. Through several preparations, it was clear that ultrafiltration concentration of the samples by centrifugation resulted in aggregation of HpuB and increased levels of heterogeneity as seen on SDS PAGE and NSEM. As a result, HpuB amphipol samples were prepared for cryo-EM freezing directly from SEC purification fractions, which typically had a very low yield of the pure protein (Figure 3.13), particularly for a relatively small particle like HpuB (90 kDa). However, initial screening of HpuB amphipol grids cryo-EM showed that the yield from 4 L expression cultures resulted in <0.1 mg/ml protein solution, which was not sufficiently high to show particles in the ice. To remedy this, HpuB expression volumes were steadily increased until a 12 L expression volume produced a sample of 0.13 mg/mL of pure HpuB amphipols.

HpuB amphipol samples were plunge frozen and screened by Dr Pascale Schellenberger using a CryoARM200 microscope at 200kV. Adequate vitrification and ice thickness were obtained as shown by the atlas image of a Quantifoil HpuB amphipol grid blotted at 3.5 seconds (Figure 5.7A). The atlas image demonstrates a gradient of ice thickness but overall good ice for data collection. Screening of all grids showed that even at the improved concentration of 0.13 mg/mL, only rare potential particles were identifiable in the ice (Figure 5.7B&C, white circle). Of the potential particles, not all are the expected size of ~11 nm HpuB amphipols, with some larger particles of about 20 nm also present (black circle). An even higher sample concentration is likely needed for a better populating of the grid with particles before high magnification data collection can commence. In addition, it is possible that the presence of the amphipathic polymer might be affecting the particle affinity for ice.

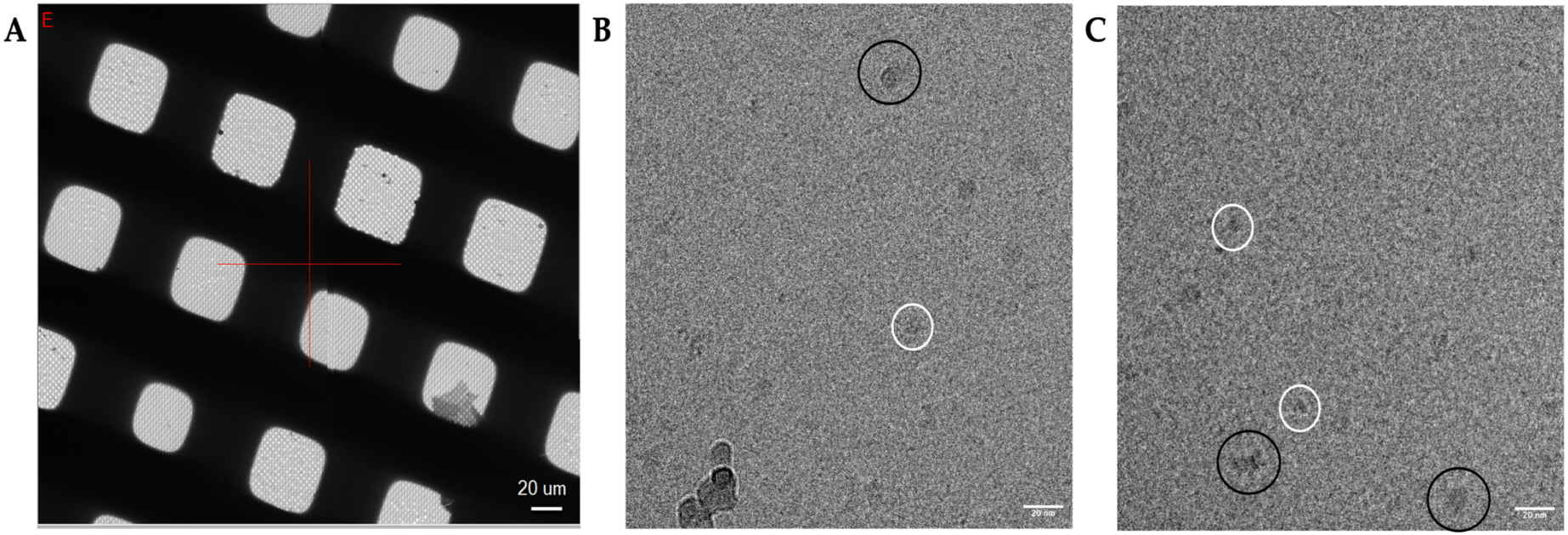

Figure 5.7: Cryo-EM screening of HpuB reconstituted in amphipols.
HpuB amphipol samples were prepared for cryo-EM screening at 0.15 mg/mL. (A) Grid atlas for Quantifoil 1.2/1.3 mm grid back blotted at 3.5 seconds. (B & C) Images taken at 200kV, x80 000. Potential HpuB amphipol particles densities as determined by diameter are circled white. Larger, potentially aggregated HpuB amphipol samples are circled black. Scale bar is 20 nm.

5.3 - Summary

A key aim of this project is the structural characterisation of HpuB on its own, as well as in complex with its substrates using cryo-EM. Following the recombinant production of HpuB and its reconstitution into a stabilising membrane memetic, each version of HpuB was prepared for NSEM screening and data collection.

HpuB refolded and stabilised in LDAO was the first iteration of sample screened and it was immediately clear that LDAO was not a suitable detergent for TEM studies. Attempts to screen in detergents more friendly to TEM showed that HpuB was not stable in these detergents and was prone to aggregation and precipitation. Nanodiscs were used to address this in the production of a detergent-free refolded HpuB sample in a more 'membrane-like' environment. Refolded HpuB nanodiscs produced much better NSEM grids and micrographs collected were used for single particle data processing. Promising sets of 3D classes were produced from this data set which showed a distinct pore-like feature through the 3D reconstruction. However, heterogeneity in the extracted particles, concerns regarding the efficiency of assembly of HpuB into nanodiscs and the reliability of the refolding process prompted a change to HpuB production through recombinant expression into the *E. coli* outer membrane.

Membrane-expressed HpuB was reconstituted into nanodiscs using an extended MSP. However, SEC A280 trace comparisons in addition with NSEM micrographs showed that the nanodisc assembly was inefficient; empty and HpuB nanodiscs eluted as the same elution volume and looked the same on EM grids. Next, peptidiscs were used as a new membrane memetic to reconstitute HpuB. NSEM analysis showed that this sample was highly heterogenous and produced 2D classifications which a large range of diameters. A minority portion of the data set was taken forward for 3D classification and refinement based on size comparisons with the expected particle size.

Lastly, amphipols were used as a membrane mimetic to reconstitute HpuB. This system improved the purity of the sample and was successful in producing homogenous particles in sizes of ~11 nm, as shown by NSEM analysis. All 3D reconstructions built from this data set revealed a familiar globular structure, with the distinct feature of pore-like cavities on the top views and bulging densities on side views. Two classes (1 & 3) were manually refined and although the refined models remained at the same resolution (16.2 Å), they did visually improve whilst keeping the distinct features seen in the first 3D classifications. Both share common features described above, with slight density variations around the top and bottom views, and cavity densities. These features could be indications of the N terminal plug and extracellular loops of HpuB (Figure 5.7), altogether being consistent with the homology model described in Chapter 4 and the structures of other TBDTs.

The HpuB amphipol sample was taken forward for cryo-EM but did not progress beyond grid screening due to an insufficient number of distinguishable potential HpuB particles. The likely cause is a low protein concentration. Research papers and prescriptive cryo-EM manuals routinely recommend that protein concentrations for data collection should be ~1 mg/mL (Bhella, 2019) (Schmidli et al., 2019) (Passmore & Russo, 2016) and despite scale-up efforts, this HpuB sample was significantly less concentrated (0.13 mg/mL). In addition to this, there is the matter of HpuB's size. Although some small proteins structures such as Hb have been resolved using cryo-EM (Khoshouei et al., 2017), this is typically difficult and proteins smaller than 100 kDa make up a small proportion of cryo-EM structures. To remedy this, protein scaffolds have now been designed to support the study of small proteins using cryo-EM. The system makes use of 12 symmetrically arranged copies of the 26 kDa green fluorescent protein (GFP) to ask as a platform for the attached meant of any POI. The scaffold itself has been resolved to a resolution of 3.8 Å by cryo-EM and is modular and hospitable to modest amino acid changes for POI-specific optimisation (Y. Liu et al., 2019).

CHAPTER 6: DISCUSSION

6.1 – Overview

As described in Chapter 1, the two human *Neisseria* pathogens have a critical need for iron in their survival and pathogenesis. However, as obligate human pathogens that do not produce iron-chelating siderophores, they must acquire their iron directly from their human host; iron acquisition is therefore a vital aspect of their virulence. Although the human host also has an essential need for iron, its toxicity at high concentrations and potential to be exploited by invading pathogens means humans sequester the metal nutrient by depleting free iron levels, producing iron-sequestering proteins and keeping iron-containing compounds such as haem tightly bound to host proteins such as hemopexin, Hb and the Hb:Hp complex. Using two known TBDT systems, HmbR and HpuAB, both *N. meningitidis* and *N. gonorrhoeae* utilise Hb to acquire haem iron, the largest iron reservoir in humans. Unlike the TbpAB TBDT system through which pathogenic *Neisseria* acquire iron from transferrin, there is no high-resolution structure or structural description of Hb binding and haem extraction by either HmbR or HpuAB.

Although several studies had previously demonstrated that HpuAB is required for growth using Hb as the sole iron source (Rohde et al., 2002; Rohde & Dyer, 2004), only HpuA has a high-resolution structure of its binding to Hb (Wong et al., 2015). HpuB has been shown to bind Hb but there is no structural information about how this happens. This project aimed to structurally and functionally understand the role that HpuB plays in the acquisition of haem iron from Hb. The importance of Hb utilisation for meningococcal and gonococcal strains makes the protein systems by which they acquire the nutrient attractive targets for therapeutic intervention. Furthermore, TBDTs in general have been singled out as promising vaccine targets due to their role in essential nutrient transportation (Baliga et al., 2018).

6.2 – Recombinantly produced HpuB demonstrates Hb binding functionality.

HpuB expression and production in this project was achieved via two distinct strategies. First was the cytoplasmic recombinant expression of HpuB in *E. coli* which resulted in the production of insoluble inclusion bodies, that were then denatured and refolded in the presence of LDAO. Second was the recombinant expression of HpuB, aided by an *OmpA* secretion signal directly into the *E. coli* outer membrane, which was also subsequently extracted and solubilised using LDAO.

Although previous work had reported a K_d of 298.4 nM and 409 nM for binding of the HpuAB system and HpuB alone, respectively, to dimeric Hb using whole cell flow cytometry (Rohde & Dyer, 2004), HpuA binding to Hb was not detected in this way. Later, it was shown through pull down assays and ITC that HpuA does indeed Hb, at 6.1 μM K_d (Wong et al., 2015). This demonstrated that *in vitro* confirmation is needed to corroborate or challenge flowcytometric binding. Consistent with previous analysis, both refolded and membrane extracted WT HpuB were shown to bind Hb via pull down assays. This is the first time this interaction has been demonstrated *in vitro* (Figures 4.2 and 4.5*)*. Further attempts to employ more quantitative techniques to provide a K_d for *in vitro* HpuB binding were hampered by the limitations of the HpuB samples. The yield was insufficient for ITC studies and the use of detergents was deemed non-ideal for use with techniques such as MST and switchSENSE. However, when reconstituted into other, detergent free membrane memetics, purity, yield and concentration were significant barriers to conjugation on the switchSENSE platform DNA nanolever and fluorescence labelling for MST (data not shown). There are also ongoing discussions in the literature regarding the consistency of affinity values determined for MPs reconstituted in membrane mimetics. In their critical assessment of MP biophysical studies, Chipot et al (2018) noted that differences in structure, dynamics and interactions can clearly be seen even in highly stable MPs studied in different membrane mimetic environments (Chipot et al., 2018).

6.3 – Key HpuB loops and determinants are likely implicated in Hb binding.

A key aim of this project was to investigate HpuB's substrate binding capabilities and determinants by using a combination of binding analysis techniques. Once recombinantly produced WT HpuB was demonstrated to bind Hb via pull downs (Figure 4.2), HpuB mutations in potentially functionally important loops and determinants were identified, constructed, and expressed. This was guided by HmbR mutagenesis analysis by Perkins-Balding et al (2003) and the structural homology by Harrison et al (2013).

Varied Hb binding by the HpuB mutants demonstrated that extracellular loops likely have different roles in Hb binding (Figure 4.5). Consistent with their expected minor role in Hb binding, the Δloop-11 mutant and plug K144E exhibited little loss of binding when compared to the WT. Conversely, HpuB mutated in Loops 3, 7 and the NPEL motif exhibited significant binding loss compared to the WT. While promising and correlating with a predicted role in Hb binding, these data remain preliminary, requiring further experimental repeats.

The experimental techniques used to determine the ability of haem acquisition systems to bind directly to Hb as their substrate have typically been ELISAs and pull downs, and the reliability of some of these techniques has now been called into question. For some of the gram-positive pathogens mentioned in chapter 1, the binding of their surface exposed proteins to Hb is facilitated by NEAT domains, often more than one. Specific motifs have been identified within NEAT domains that are indicative of either haem (S/YXXXY) or Hb (F/Y)YH(Y/F) binding capabilities (Pilpa et al., 2009). While some NEAT domains have been proposed to bind both haem and Hb, the lack of domains containing both motifs makes this unlikely. NEAT domain proteins identified as capable of binding both haem and Hb possess distinct NEAT domains for binding each substrate. Experimentally, haem binding of NEAT domains is well evidenced by solved structures of NEAT domains bound to haem and UV-vis spectroscopy. For Hb binding, ELISA and

pull down experiments have been the main demonstrative tool. *C. diphtheriae* proteins HtaA and ChtB (Allen & Schmitt, 2011; Schmitt, 1997), *B. anthracis* proteins IsdX1/X2 (Gat et al., 2008) and *L. monocytogenes* protein Hbp2 (Malmirchegini et al., 2014) are examples ELISA or pull down demonstrated Hb binding, but follow up NMR experiments aimed at detecting haem binding directly failed to detect Hb interaction for *B. anthracis* IsdX1/X2 (Macdonald et al., 2019). One plausible explanation for this discrepancy is that in most ELISA and pull-down experiments, the Hb used, usually commercially bought, contains a variety of breakdown products including multiple oligomeric and oxidation states and that immobilisation of these products with more readily accessible haem produces false positive results (Macdonald et al., 2019; Akinbosede et al., 2022).

6.4 – *In vitro* HpuB studies requires the use of modern membrane mimetics.

The MP biochemistry discipline is currently going through somewhat of a revolution, turbo-charged by the development of modern membrane memetics and recent advancements in structural characterisation techniques such as cryo-EM and SAXS/SANS. Although well known to be notoriously difficult (Kermani, 2021), LDAO reconstituted HpuB crystallography trails did initially yield some crystals. The fact that the crystals were poorly diffracting and irreproducible prompted a permanent shift to TEM. NSEM images demonstrated that HpuB in LDAO would not be suitable for single particle analysis and structural resolution and indeed, even TEM-friendly detergents failed to both stabilise HpuB and allow for the collection of processable datasets. A recent review discussing the implications of MPs studies using detergents reiterated the significant disadvantages, including the propensity of MP denaturation but most importantly for this study, the often-high chances of non-physiological MP conformations due to mismatched MP/micelle complexes (Majeed et al., 2021). Membrane memetic alternatives were immediately more compatible with TEM and indeed NSEM data sets collected of HpuB nanodisc, HpuB peptidisc and HpuB amphipol samples would be processed into 3D models, albeit at relatively low resolution. Together this demonstrates the critical need to move beyond detergents in studying HpuB.

6.5 – Amphipols are most compatible with these *in vitro* HpuB studies

Of the membrane memetics used to reconstitute HpuB as an alternative to detergents, amphipols were the most successful. This success is highlighted in a number of ways. Firstly, the HpuB sample reconstituted into amphipols was extracted directly from the membrane and as such is assumed to be more structurally reliable. Secondly, unlike other HpuB samples in modern memetics, HpuB amphipols remained stable during SEC and produced a pure sample without visible contaminants as determined by Coomassie-stained PAGE gels (Figure 3.13). This was also demonstrated by the relatively high

degree of homogeneity in the particles collected from NSEM micrographs (Figure 5.5). HpuB peptidiscs and HpuB amphipols were sub-optimal in these regards (Figures 3.8, 3.11, 5.3, 5.4).

6.6 – Electron microscopy is the key to a more complete understanding of the HpuAB system.

Electron microscopy was used for single particle analysis of HpuB. Although cryo-EM is necessary for the high-resolution reconstruction, 2D and 3D modelling by NSEM is a prerequisite step which provides significant insights regarding the sample quality and structural important information about the particles. In this study, 3D models were presented for HpuB nanodiscs (21.5 Å, Figure 5.2), HpuB peptidiscs (12.3 Å, Figure 5.4) and HpuB amphipols (16.2 Å, Figure 5.6). It is important to note that the sample quality as determined by the degree of homogeneity on micrographs varied based on the membrane memetic used. HpuB reconstituted in peptidisc was least pure, most heterogeneous on NSEM and in turn provided a comparatively structurally distinctive 3D model (Figures 3.12 & 5.4). Unlike, HpuB nanodisc and HpuB amphipol 3D models which all revealed 'pore-like' cavities in their top views, HpuB peptidisc is sealed all the way around and was resolved to the highest resolution of the three. However, the use of a minority population in building this model and a significant overrepresentation of top views questions its validity when compared to HpuB amphipols. Processed with the largest data set, 2D classified with the largest number of particles and 3D resolved to the effective resolution limit of NSEM (Scarff et al., 2018), the HpuB amphipol models present interesting structural insights. The protruding densities on the top of the model corresponding with areas of density lower than the bulk of the model could indicate the presence of HpuB extracellular loops. If real and not artefactual, this could have profound implications on the ability of higher resolution cryo-EM studies to provide in-depth information into loop activity, corroborating the initial data acquired from HpuB mutant pull down assays. There is also the cross-section of the two models (Figure

5.6C&F), which indicates the presence of the plug domain. If prepared in the presence of hemin, higher resolution cryo-EM studies could also show the specific positioning of the iron-carrying compound within the barrel and determine if it is indeed the binding of Hb or haem that causes the conformational change within the β barrel as the first step in the mechanical transfer of haem into the periplasm.

6.7 – Future studies

Altogether, this study has made progress in the structural and functional characterisation of HpuB and has also identified the best path to full characterisation. A priority in future studies would be a return to the optimisation of HpuB yields to maximise the sample potential in both structural and functional studies. There are numerous steps along the pipeline of MP production that could be optimised to this end. A first step should be the improvement of MP production per expression culture. Recombinant MP production is hampered by poor cellular accumulation and fatal toxicity for the host, leading to low levels of final biomass and purified protein (Michou et al., 2019). Although in this study, the Omp8 *E. coli* strain was used to successfully improve the recombinant expression of HpuB directly into the outer membrane, there are new and improved strains recently made commercially available to improve yield outcomes. SuptoxD and SuptoxR are new *E. coli* strains that express two very potent effectors to improve MP production. Co-expression of the membrane-bound DnaK co-chaperone protein DjlA, and RraA the inhibitor of the mRNA-degrading activity of the *E. coli* RNase E showed significantly higher final biomass and significantly improved yields for a range of prokaryotic and eukaryotic recombinant membrane proteins (Gialama et al., 2016). An improved yield would be extremely beneficial for the end yield after reconstitution into membrane mimetics. This would in turn expand the number of functional analysis techniques available for binding studies such as ITC and switchSENSE and allow for higher concentrations and indeed dilution ranges in the preparation of cryo-EM grids.

Although there was significant success here in using amphipols to reconstitute HpuB, amphipols are amongst the least 'membrane-like' membrane mimetics. There is scope to revisit the use of SMALPs for HpuB studies. Unsuccessful here due to limited resources and lack of affordable commercially available variants for optimisation, revisiting SMALPs would allow for a completely detergent-free reconstitution of HpuB and add more possibilities to the information acquirable by cryo-EM. SMALP extracted MPs have been used not only to resolve MP structures and protein-protein interactions within small and large complexes but also details of annular lipids and the nature of lipids within central cavities, binding pockets, regions involved in stabilising complexes, identification of physiologically relevant states and details of terminal residues that usually left unresolved (Unger et al., 2021). The understanding of endogenous lipids and their interactions with MPs are now a major component of high-resolution MP studies. Scientists now value the importance of lipids for MP function, particularly how specific lipid interactions can regulate some functions in ion channels, transporters, and receptors (Corradi et al., 2019). SMALP extraction could even remove the need for a recombinant expression system altogether, extracting HpuB directly from the outer membrane of *Neisseria.*

6.8 – Potential therapeutic considerations for HpuAB

Once a high-resolution structure of HpuB and complexes are achieved, there is also the question of whether or not HpuAB would make a sensible vaccine target in the battle against bacterial meningitis or super-resistant gonorrhoea. The ability of pathogens to circumvent host nutritional immunity and to exploit the host proteins involved has long been touted as a possible focus for therapeutic intervention (Boelaert, 1996; Yadav et al., 2020; Cornelissen, 2018; Murdoch & Skaar, 2022). With respect to therapeutic potential, the most significant question in the case of the systems described above is whether haem acquisition from Hb makes up a large enough proportion of the total iron needs of the pathogen to constitute a worthwhile target.

The degree to which the Hb utilising pathogens are reliant on Hb acquired haem for iron is variable. The elimination of haem piracy systems restricts bacterial growth to varying degrees, and in some cases abolishes pathogenicity or even proves lethal. Obligate human pathogen and haem utiliser *H. dureyi* requires a minimum haemin concentration of 38 μM for growth and, whilst it is able to pirate this haem from Hb using Hb receptor HgbA, it also possesses TdhA, a free haem receptor that allows it to utilise free haem (Lee, 1991). However, haem acquisition via TdhA is not sufficient to support infection, as demonstrated by a human model of infection where pustules did not develop in adults infected with HgbA-knockout *H. dureyi* (Al-Tawfiq et al., 2000). This requirement for haem iron, combined with the lack of other iron sources, means that the *H. ducreyi* Hb receptor HgbA is a promising candidate for a vaccine antigen (Nepluev et al., 2009). Outer membrane proteins have already been used in the creation of bactericidal antibodies against *N. meningitidis.* However, the potential of the HpuAB system in new vaccines or as drug targets deserves further investigation, similar to the one discussed for *H. dureyi.*

CHAPTER 7: APPENDICES

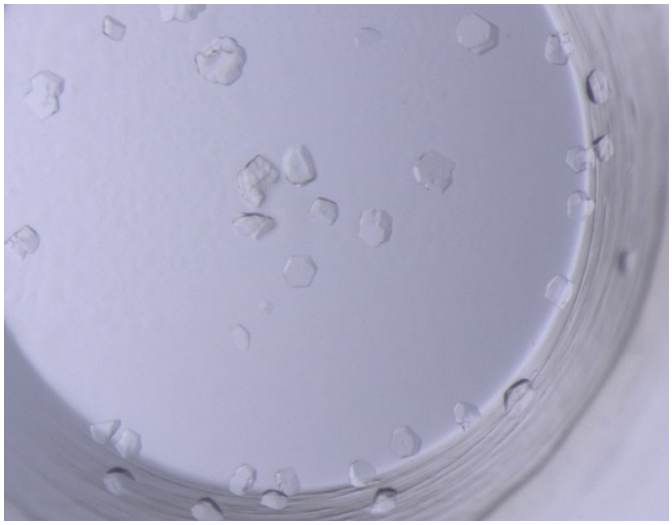

Figure 7.1: Successful crystallisation of refolded *N. gonorrhoeae* HpuB.

Mem-Gold crystal screens were used to identify crystallisation conditions for HpuB. A successful hit was found using the conditions 0.05 M citric acid, 0.1 M lithium sulphate and 19% PCG 1000.

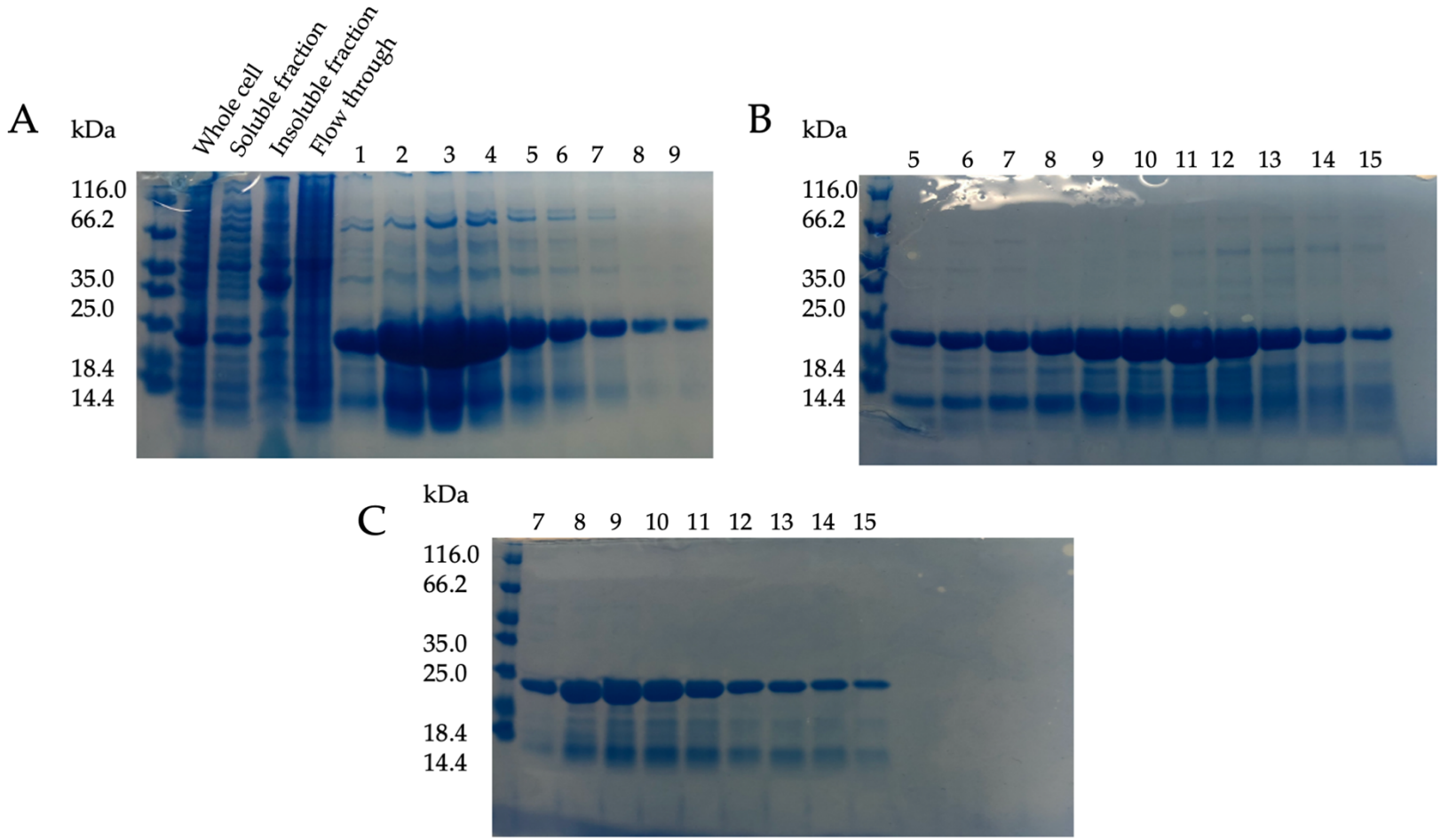

Figure 7.2: Purification pipeline for homemade MSP1D1.

SDS PAGE gels showing the IMAC – IEX – SEC purification pipeline for MSP1D1 and other MSP proteins. (**A**) IMAC purification from soluble cell lysate with NiNTA gravity flow column, elution collected in 1 mL fractions. (**B**) IEX purification of pooled IMAC fraction using a HiTrap Q column. Fraction numbers correlate to elution from AKTA HPLC. (**C**) SEC purification on an S75 column using pooled samples from IEX purification step. Fraction numbers correlate to elution from AKTA HPLC.

Table 7.1: Metadata details of the final set of 2D classes produced from NSEM analysis of refolded HpuB nanodiscs.
This table outlines the number of particles and the estimated resolution of each class as determined by RELION 2.0.

Class Number	Number of Particles Within Class	Estimated Resolution (Å)
1	428	10.8
2	308	10.8
3	182	12.5
4	442	10.3
5	144	11.3
6	276	10.8
7	134	11.3
8	168	15.7
9	302	9.9
10	494	9.9
11	602	9.9
12	214	11.3
13	364	11.8
14	492	9.9
15	254	10.8
16	120	13.9
17	378	10.3
18	128	10.8
19	116	11.3

Table 7.2: Table: Metadata details of the 3D classes produced from NSEM analysis of refolded HpuB nanodiscs.
This table outlines the number of particles and the estimated resolution of each class as determined by RELION 2.0.

Class Number	Number of Particles Within Class	Estimated Resolution (Å)
1	482	26.3
2	2553	23.6
3	1748	21.5
4	743	29.6

Table 7.3: Metadata details of the 'medium' 2D classes produced from NSEM analysis of HpuB peptidiscs.
This table outlines the number of particles and the estimated resolution of each class as determined by RELION 3.0.

Class Number	Number of Particles Within Class	Estimated Resolution (Å)
1	297	11.8
2	441	10.4
3	727	8.1
4	641	8.9
5	349	10.0
6	887	8.9

Table 7.4: Metadata details of the 3D classes produced from NSEM analysis of 'medium' HpuB peptidiscs.
This table outlines the number of particles and the estimated resolution of each class as determined by RELION 3.0.

Class Number	Number of Particles Within Class	Estimated Resolution (Å)
1	2073	13.6
2	1269	15.2

.

Table 7.5: Metadata details of the final set of 2D classes produced from NSEM analysis of refolded HpuB amphipols.
This table outlines the number of particles and the estimated resolution of each class as determined by RELION 3.0.

Class Number	Number of Particles Within Class	Estimated Resolution (Å)
1	663	11.7
2	2030	10.1
3	512	11.7
4	635	10.6
5	808	12.4
6	647	12.4
7	548	14.1
8	387	13.2
9	804	11.7
10	941	11.1
11	1306	10.6
12	834	11.2
13	688	12.4
14	519	15.1
15	2305	10.1
16	1934	11.1
17	834	10.6
18	517	11.7
19	2368	10.1
20	1130	10.1

CHAPTER 8: REFERENCES

Abdul-Tehrani, H., Hudson, A. J., Chang, Y.-S., Timms, A. R., Hawkins, C., Williams, J. M., Harrison, P. M., Guest, J. R., & Andrews, S. C. (1999). Ferritin Mutants of Escherichia coli Are Iron Deficient and Growth Impaired, and fur Mutants are Iron Deficient. *Journal of Bacteriology*, *181*(5), 1415–1428.

Abeck, D., Freinkel, A. L., Korting, H. C., Szeimis, R. M., & Ballard, R. C. (1997). Immunohistochemical investigations of genital ulcers caused by Haemophilus ducreyi. *International Journal of STD & AIDS*, *8*(9), 585–588. https://doi.org/10.1258/0956462971920839

Abosharaf, H. A., Sakamoto, Y., Radwan, A. M., Yuzu, K., Fujimura, M., Diab, T., Mohamed, T. M., Chatani, E., Kimura, T., & Tsubaki, M. (2021). Functional Assembly of Caenorhabditis elegans Cytochrome b-2 (Cecytb-2) into Phospholipid Bilayer Nanodisc with Enhanced Iron Reductase Activity. *Biomolecules*, *11*(1), 96. https://doi.org/10.3390/biom11010096

Afonina, G., Leduc, I., Nepluev, I., Jeter, C., Routh, P., Almond, G., Orndorff, P. E., Hobbs, M., & Elkins, C. (2006). Immunization with the Haemophilus ducreyi Hemoglobin Receptor HgbA Protects against Infection in the Swine Model of Chancroid. *INFECTION AND IMMUNITY*, *74*(4), 2224–2232. https://doi.org/10.1128/IAI.74.4.2224-2232.2006

Agrawal, A., & Murphy, T. F. (2011). Haemophilus influenzae Infections in the H. influenzae Type b Conjugate Vaccine Era ▿. *Journal of Clinical Microbiology*, *49*(11), 3728–3732. https://doi.org/10.1128/JCM.05476-11

Akinbosede, D., Chizea, R., & Hare, S. A. (2022). Pirates of the haemoglobin. *Microbial Cell (Graz, Austria)*, *9*(4), 84–102. https://doi.org/10.15698/mic2022.04.775

Allen, C. E., Burgos, J. M., & Schmitt, M. P. (2013). Analysis of novel iron-regulated, surface-anchored hemin-binding proteins in Corynebacterium diphtheriae. *Journal of Bacteriology*, *195*(12), 2852–2863. https://doi.org/10.1128/JB.00244-13

Allen, C. E., & Schmitt, M. P. (2009). HtaA is an iron-regulated hemin binding protein involved in the utilization of heme iron in Corynebacterium diphtherial. *Journal of Bacteriology*, *191*(8), 2638–2648. https://doi.org/10.1128/JB.01784-08

Allen, C. E., & Schmitt, M. P. (2011). Novel Hemin Binding Domains in the Corynebacterium diphtheriae HtaA Protein Interact with Hemoglobin and Are Critical for Heme Iron Utilization by HtaA. *JOURNAL OF BACTERIOLOGY*, *193*(19), 5374–5385. https://doi.org/10.1128/JB.05508-11

Allen, C. E., & Schmitt, M. P. (2015). Utilization of host iron sources by Corynebacterium diphtheriae: Multiple hemoglobin-binding proteins are essential for the use of iron from the hemoglobin-haptoglobin complex. *Journal of Bacteriology*, *197*(3), 553–562. https://doi.org/10.1128/JB.02413-14

Al-Tawfiq, J. A., Fortney, K. R., Katz, B. P., Hood, A. F., Elkins, C., & Spinola, S. M. (2000). An isogenic hemoglobin receptor-deficient mutant of Haemophilus ducreyi is attenuated in the human model of experimental infection. *The Journal of Infectious Diseases*, *181*(3), 1049–1054. https://doi.org/10.1086/315309

Anandan, A., & Vrielink, A. (2016). Detergents in Membrane Protein Purification and Crystallisation. In I. Moraes (Ed.), *The Next Generation in Membrane Protein Structure Determination* (Vol. 922, pp. 13–28). Springer International Publishing. https://doi.org/10.1007/978-3-319-35072-1_2

Anderson, J. E., Leone, P. A., Miller, W. C., Chen, C.-J., Hobbs, M. M., & Sparling, P. F. (2001). Selection for expression of the gonococcal hemoglobin receptor

during menses. *The Journal of Infectious Diseases*, *184*(12), 1621–1623. https://doi.org/10.1086/324564

Anderson, J. E., Sparling, P. F., & Cornelissen, C. N. (1994). Gonococcal transferrin-binding protein 2 facilitates but is not essential for transferrin utilization. *Journal of Bacteriology*, *176*(11), 3162–3170.

Andrews, S. C. (1998). Iron storage in bacteria. *Advances in Microbial Physiology*, *40*, 281–351. https://doi.org/10.1016/s0065-2911(08)60134-4

Andrews, S. C., Robinson, A. K., & Rodríguez-Quiñones, F. (2003). Bacterial iron homeostasis. *FEMS Microbiology Reviews*, *27*(2–3), 215–237. https://doi.org/10.1016/S0168-6445(03)00055-X

Angiulli, G., Dhupar, H. S., Suzuki, H., Wason, I. S., Duong Van Hoa, F., & Walz, T. (2020). New approach for membrane protein reconstitution into peptidiscs and basis for their adaptability to different proteins. *ELife*, *9*, e53530. https://doi.org/10.7554/eLife.53530

Arnold, K., Bordoli, L., Kopp, J., & Schwede, T. (2006). The SWISS-MODEL workspace: A web-based environment for protein structure homology modelling. *Bioinformatics (Oxford, England)*, *22*(2), 195–201. https://doi.org/10.1093/bioinformatics/bti770

Baeta, T., Giandoreggio-Barranco, K., Ayala, I., Moura, E. C. C. M., Sperandeo, P., Polissi, A., Simorre, J.-P., & Laguri, C. (2021). The lipopolysaccharide-transporter complex LptB2FG also displays adenylate kinase activity in vitro dependent on the binding partners LptC/LptA. *Journal of Biological Chemistry*, *297*(6). https://doi.org/10.1016/j.jbc.2021.101313

Balderas, M. A., Nobles, C. L., Honsa, E. S., Alicki, E. R., & Maresso, A. W. (2012). Hal is a Bacillus anthracis heme acquisition protein. *Journal of Bacteriology*, *194*(20), 5513–5521. https://doi.org/10.1128/JB.00685-12

Baliga, P., Shekar, M., & Venugopal, M. N. (2018). Potential Outer Membrane Protein Candidates for Vaccine Development Against the Pathogen Vibrio anguillarum: A Reverse Vaccinology Based Identification. *Current Microbiology*, *75*(3), 368–377. https://doi.org/10.1007/s00284-017-1390-z

Banerjee, R. (1962). [Thermodynamic study of the heme-globin association. II. Methemoglobin]. *Biochimica Et Biophysica Acta*, *64*, 385–395. https://doi.org/10.1016/0006-3002(62)90747-3

Barber, M. F., & Elde, N. C. (2015). Buried Treasure: Evolutionary Perspectives on Microbial Iron Piracy. In *Trends in Genetics* (Vol. 31, Issue 11, pp. 627–636). Elsevier Ltd. https://doi.org/10.1016/j.tig.2015.09.001

Basmaci, R., & Bonacorsi, S. (2017). Kingella kingae: From carriage to infection. In *CMAJ* (Vol. 189, Issue 35, pp. E1105–E1106). Canadian Medical Association. https://doi.org/10.1503/cmaj.170843

Bateman, T. J., Shah, M., Ho, T. P., Shin, H. E., Pan, C., Harris, G., Fegan, J. E., Islam, E. A., Ahn, S. K., Hooda, Y., Gray-Owen, S. D., Chen, W., & Moraes, T. F. (2021). A Slam-dependent hemophore contributes to heme acquisition in the bacterial pathogen Acinetobacter baumannii. *Nature Communications*, *12*, 6270. https://doi.org/10.1038/s41467-021-26545-9

Bates, C. S., Montañez, G. E., Woods, C. R., Vincent, R. M., & Eichenbaum, Z. (2003a). Identification and Characterization of a Streptococcus pyogenes Operon Involved in Binding of Hemoproteins and Acquisition of Iron.

INFECTION AND IMMUNITY, *71*(3), 1042–1055. https://doi.org/10.1128/IAI.71.3.1042-1055.2003

Bates, C. S., Montañez, G. E., Woods, C. R., Vincent, R. M., & Eichenbaum, Z. (2003b). Identification and Characterization of a Streptococcus pyogenes Operon Involved in Binding of Hemoproteins and Acquisition of Iron. *INFECTION AND IMMUNITY*, *71*(3), 1042–1055. https://doi.org/10.1128/IAI.71.3.1042-1055.2003

Bayburt, T. H., & Sligar, S. G. (2010). Membrane Protein Assembly into Nanodiscs. *FEBS Letters*, *584*(9), 1721–1727. https://doi.org/10.1016/j.febslet.2009.10.024

Bengtsen, T., Holm, V. L., Kjølbye, L. R., Midtgaard, S. R., Johansen, N. T., Tesei, G., Bottaro, S., Schiøtt, B., Arleth, L., & Lindorff-Larsen, K. (2020). Structure and dynamics of a nanodisc by integrating NMR, SAXS and SANS experiments with molecular dynamics simulations. *ELife*, *9*, e56518. https://doi.org/10.7554/eLife.56518

Bennett, E. H., Akbas, N., Adrian, S. A., Lukat-Rodgers, G. S., Collins, D. P., Dawson, J. H., Allen Δ, C. E., Schmitt Δ, M. P., Rodgers, K. R., Dixon, D. W., & Abstract, G. (2015). Heme binding by Corynebacterium diphtheriae HmuT: Function and heme environment HHS Public Access. *Biochemistry*, *54*(43), 6598–6609. https://doi.org/10.1021/acs.biochem.5b00666

Bhatwa, A., Wang, W., Hassan, Y. I., Abraham, N., Li, X.-Z., & Zhou, T. (2021). Challenges Associated With the Formation of Recombinant Protein Inclusion Bodies in Escherichia coli and Strategies to Address Them for Industrial Applications. *Frontiers in Bioengineering and Biotechnology*, *9*, 630551. https://doi.org/10.3389/fbioe.2021.630551

Bhella, D. (2019). Cryo-electron microscopy: An introduction to the technique, and considerations when working to establish a national facility. *Biophysical Reviews*, *11*(4), 515–519. https://doi.org/10.1007/s12551-019-00571-w

Biagioli, M., Pinto, M., Cesselli, D., Zaninello, M., Lazarevic, D., Roncaglia, P., Simone, R., Vlachouli, C., Plessy, C., Bertin, N., Beltrami, A., Kobayashi, K., Gallo, V., Santoro, C., Ferrer, I., Rivella, S., Beltrami, C. A., Carninci, P., Raviola, E., & Gustincich, S. (2009). Unexpected expression of alpha- and beta-globin in mesencephalic dopaminergic neurons and glial cells. *Proceedings of the National Academy of Sciences of the United States of America*, *106*(36), 15454–15459. https://doi.org/10.1073/pnas.0813216106

Bignell, C., & Fitzgerald, M. (2011). UK national guideline for the management of gonorrhoea in adults, 2011. *International Journal of STD and AIDS*, *22*(10), 541–547. https://doi.org/10.1258/ijsa.2011.011267

Bodie, M., Gale-Rowe, M., Alexandre, S., Auguste, U., Tomas, K., & Martin, I. (2019). Addressing the rising rates of gonorrhea and drug-resistant gonorrhea: There is no time like the present. *Canada Communicable Disease Report*, *45*(2–3), 54–62. https://doi.org/10.14745/ccdr.v45i23a02

Boekema, E. J., Folea, M., & Kouřil, R. (2009). Single particle electron microscopy. *Photosynthesis Research*, *102*(2), 189–196. https://doi.org/10.1007/s11120-009-9443-1

Boelaert, J. R. (1996). Iron and Infection. *Acta Clinica Belgica*, *51*(4), 213–221. https://doi.org/10.1080/22953337.1996.11718513

Boelaert, J. R., Vandecasteele, S. J., Appelberg, R., & Gordeuk, V. R. (2007). The effect of the host's iron status on tuberculosis. *The Journal of Infectious Diseases*, *195*(12), 1745–1753. https://doi.org/10.1086/518040

Booth, P. (2005). Sane in the membrane: Designing systems to modulate membrane proteins. *Current Opinion in Structural Biology*, *15*(4), 435–440. https://doi.org/10.1016/j.sbi.2005.06.002

Bottone, E. J. (2010). Bacillus cereus, a Volatile Human Pathogen. *Clinical Microbiology Reviews*, *23*(2), 382–398. https://doi.org/10.1128/CMR.00073-09

Boulton, I. C., Gorringe, A. R., Allison, N., Robinson, A., Gorinsky, B., Joannou, C. L., & Evans, R. W. (1998). Transferrin-binding protein B isolated from Neisseria meningitidis discriminates between apo and diferric human transferrin. *Biochemical Journal*, *334*(1), 269–273. https://doi.org/10.1042/bj3340269

Bowden, C. F. M., Chan, A. C. K., Li, E. J. W., Arrieta, A. L., Eltis, L. D., & Murphy, M. E. P. (2018). Structure–function analyses reveal key features in Staphylococcus aureus IsdB-associated unfolding of the heme-binding pocket of human hemoglobin. *The Journal of Biological Chemistry*, *293*(1), 177–190. https://doi.org/10.1074/jbc.M117.806562

Bowie, J. U. (2005). Solving the membrane protein folding problem. *Nature*, *438*(7068), 581–589. https://doi.org/10.1038/nature04395

Braun, V., Gaisser, S., Herrmann, C., Kampfenkel, K., Killmann, H., & Traub, I. (1996). Energy-coupled transport across the outer membrane of Escherichia coli: ExbB binds ExbD and TonB in vitro, and leucine 132 in the periplasmic region and aspartate 25 in the transmembrane region are important for ExbD activity. *Journal of Bacteriology*, *178*(10), 2836–2845. https://doi.org/10.1128/jb.178.10.2836-2845.1996

Braun, V., & Herrmann, C. (2004). Point mutations in transmembrane helices 2 and 3 of ExbB and TolQ affect their activities in Escherichia coli K-12. *Journal of*

Bacteriology, *186*(13), 4402–4406. https://doi.org/10.1128/JB.186.13.4402-4406.2004

Brillet, K., Meksem, A., Lauber, E., Reimmann, C., & Cobessi, D. (2009). Use of an in-house approach to study the three-dimensional structures of various outer membrane proteins: Structure of the alcaligin outer membrane transporter FauA from Bordetella pertussis. *Acta Crystallographica. Section D, Biological Crystallography*, *65*(Pt 4), 326–331. https://doi.org/10.1107/S0907444909002200

Brown, C. J., Trieber, C., & Overduin, M. (2021). Structural biology of endogenous membrane protein assemblies in native nanodiscs. *Current Opinion in Structural Biology*, *69*, 70–77. https://doi.org/10.1016/j.sbi.2021.03.008

Bruggisser, J., Iacovache, I., Musson, S. C., Degiacomi, M. T., Posthaus, H., & Zuber, B. (2021). *Cryo-EM structure of the octameric pore of Clostridium perfringens β-toxin*. 2021.11.23.469684. https://doi.org/10.1101/2021.11.23.469684

Buchanan, S. K., Smith, B. S., Venkatramani, L., Xia, D., Esser, L., Palnitkar, M., Chakraborty, R., van der Helm, D., & Deisenhofer, J. (1999). Crystal structure of the outer membrane active transporter FepA from Escherichia coli. *Nature Structural Biology*, *6*(1), 56–63. https://doi.org/10.1038/4931

Burgess, S. A., Walker, M. L., Thirumurugan, K., Trinick, J., & Knight, P. J. (2004). Use of negative stain and single-particle image processing to explore dynamic properties of flexible macromolecules. *Journal of Structural Biology*, *147*(3), 247–258. https://doi.org/10.1016/j.jsb.2004.04.004

Burkhard, K. A., & Wilks, A. (2007). Characterization of the outer membrane receptor ShuA from the heme uptake system of Shigella dysenteriae: Substrate specificity

and identification of the heme protein ligands. *Journal of Biological Chemistry*, *282*(20), 15126–15136. https://doi.org/10.1074/jbc.M611121200

Camejo, A., Carvalho, F., Reis, O., Leitão, E., Sousa, S., & Cabanes, D. (2011). The arsenal of virulence factors deployed by Listeria monocytogenes to promote its cell infection cycle. In *Virulence* (Vol. 2, Issue 5, pp. 379–394). Taylor and Francis Inc. https://doi.org/10.4161/viru.2.5.17703

Cardi, D., Montigny, C., Arnou, B., Jidenko, M., Marchal, E., Maire, M., & Jaxel, C. (2010). Heterologous Expression and Affinity Purification of Eukaryotic Membrane Proteins in View of Functional and Structural Studies: The Example of the Sarcoplasmic Reticulum Ca2+-ATPase. In I. Mus-Veteau (Ed.), *Heterologous Expression of Membrane Proteins* (Vol. 601, pp. 247–267). Humana Press. https://doi.org/10.1007/978-1-60761-344-2_15

Carlson, M. L., Stacey, R. G., Young, J. W., Wason, I. S., Zhao, Z., Rattray, D. G., Scott, N., Kerr, C. H., Babu, M., Foster, L. J., & Duong Van Hoa, F. (2019). Profiling the Escherichia coli membrane protein interactome captured in Peptidisc libraries. *ELife*, *8*, e46615. https://doi.org/10.7554/eLife.46615

Carlson, M. L., Young, J. W., Zhao, Z., Fabre, L., Jun, D., Li, J., Li, J., Dhupar, H. S., Wason, I., Mills, A. T., Beatty, J. T., Klassen, J. S., Rouiller, I., & Duong, F. (2018). The Peptidisc, a simple method for stabilizing membrane proteins in detergent-free solution. *ELife*, *7*, e34085. https://doi.org/10.7554/eLife.34085

Carpenter, E. P., Beis, K., Cameron, A. D., & Iwata, S. (2008). Overcoming the challenges of membrane protein crystallography. *Current Opinion in Structural Biology*, *18*(5), 581–586. https://doi.org/10.1016/j.sbi.2008.07.001

Carrió, M. M., & Villaverde, A. (2005). Localization of Chaperones DnaK and GroEL in Bacterial Inclusion Bodies. *Journal of Bacteriology*, *187*(10), 3599–3601. https://doi.org/10.1128/JB.187.10.3599-3601.2005

Carvalho, V., Pronk, J. W., & Engel, A. H. (2018). Characterization of Membrane Proteins Using Cryo-Electron Microscopy. *Current Protocols in Protein Science*, *94*(1), e72. https://doi.org/10.1002/cpps.72

Cassat, J. E., & Skaar, E. P. (2013). Iron in infection and immunity. In *Cell Host and Microbe* (Vol. 13, Issue 5, pp. 509–519). Cell Press. https://doi.org/10.1016/j.chom.2013.04.010

Catalano, C., Ben-Hail, D., Qiu, W., Blount, P., des Georges, A., & Guo, Y. (2021). Cryo-EM Structure of Mechanosensitive Channel YnaI Using SMA2000: Challenges and Opportunities. *Membranes*, *11*(11), 849. https://doi.org/10.3390/membranes11110849

Celia, H., Botos, I., Ni, X., Fox, T., De Val, N., Lloubes, R., Jiang, J., & Buchanan, S. K. (2019). Cryo-EM structure of the bacterial Ton motor subcomplex ExbB–ExbD provides information on structure and stoichiometry. *Communications Biology*, *2*(1), 358. https://doi.org/10.1038/s42003-019-0604-2

Celia, H., Noinaj, N., Zakharov, S. D., Bordignon, E., Botos, I., Santamaria, M., Barnard, T. J., Cramer, W. A., Lloubes, R., & Buchanan, S. K. (2016). Structural insight into the role of the Ton complex in energy transduction. *Nature*, *538*(7623), 60–65. https://doi.org/10.1038/nature19757

Chen, X., Winters, C. A., & Reese, T. S. (2008). Life Inside a Thin Section: Tomography. *The Journal of Neuroscience*, *28*(38), 9321–9327. https://doi.org/10.1523/JNEUROSCI.2992-08.2008

Chen, Y., Clarke, O. B., Kim, J., Stowe, S., Kim, Y.-K., Assur, Z., Cavalier, M., Godoy-Ruiz, R., von Alpen, D. C., Manzini, C., Blaner, W. S., Frank, J., Quadro, L., Weber, D. J., Shapiro, L., Hendrickson, W. A., & Mancia, F. (2016). Structure of the STRA6 receptor for retinol uptake. *Science (New York, N.Y.)*, *353*(6302), aad8266. https://doi.org/10.1126/science.aad8266

Cherepanov, P. (2007). LEDGF/p75 interacts with divergent lentiviral integrases and modulates their enzymatic activity in vitro. *Nucleic Acids Research*, *35*(1), 113–124. https://doi.org/10.1093/nar/gkl885

Chimento, D. P., Kadner, R. J., & Wiener, M. C. (2005). Comparative structural analysis of TonB-dependent outer membrane transporters: Implications for the transport cycle. *Proteins: Structure, Function, and Bioinformatics*, *59*(2), 240–251. https://doi.org/10.1002/prot.20416

Chipot, C., Dehez, F., Schnell, J. R., Zitzmann, N., Pebay-Peyroula, E., Catoire, L. J., Miroux, B., Kunji, E. R. S., Veglia, G., Cross, T. A., & Schanda, P. (2018). Perturbations of Native Membrane Protein Structure in Alkyl Phosphocholine Detergents: A Critical Assessment of NMR and Biophysical Studies. *Chemical Reviews*, *118*(7), 3559–3607. https://doi.org/10.1021/acs.chemrev.7b00570

Choi, J., & Ryu, S. (2019). Regulation of Iron Uptake by Fine-Tuning the Iron Responsiveness of the Iron Sensor Fur. *Applied and Environmental Microbiology*, *85*(9), e03026-18. https://doi.org/10.1128/AEM.03026-18

Choo, J. M., Cheung, J. K., Wisniewski, J. A., Steer, D. L., Bulach, D. M., Hiscox, T. J., Chakravorty, A., Smith, A. I., Gell, D. A., Rood, J. I., & Awad, M. M. (2016). The NEAT Domain-Containing Proteins of Clostridium perfringens Bind Heme. *PLOS ONE*, *11*(9), e0162981. https://doi.org/10.1371/journal.pone.0162981

Cobessi, D., Meksem, A., & Brillet, K. (2010). Structure of the heme/hemoglobin outer membrane receptor ShuA from shigella dysenteriae: Heme binding by an induced fit mechanism. *Proteins: Structure, Function and Bioinformatics*, *78*(2), 286–294. https://doi.org/10.1002/prot.22539

Cole, L. E., Toffer, K. L., Fulcher, R. A., San Mateo, L. R., Orndorff, P. E., & Kawula, T. H. (2003). A Humoral Immune Response Confers Protection against Haemophilus ducreyi Infection. *INFECTION AND IMMUNITY*, *71*(12), 6971–6977. https://doi.org/10.1128/IAI.71.12.6971-6977.2003

Cope, L. D., Hrkal, Z., & Hansen, E. J. (2000). Detection of phase variation in expression of proteins involved in hemoglobin and hemoglobin-haptoglobin binding by nontypeable Haemophilus influenzae. *Infection and Immunity*, *68*(7), 4092–4101. https://doi.org/10.1128/iai.68.7.4092-4101.2000

Cope, L. D., Love, R. P., Guinn, S. E., Gilep, A., Usanov, S., Estabrook, R. W., Hrkal, Z., & Hansen, E. J. (2001). Involvement of HxuC Outer Membrane Protein in Utilization of Hemoglobin by Haemophilus influenzae. *Infection and Immunity*, *69*(4), 2353–2363. https://doi.org/10.1128/IAI.69.4.2353-2363.2001

Cope, L. D., Yogev, R., Muller-Eberhard, U., & Hansen, E. J. (1995). A gene cluster involved in the utilization of both free heme and heme:hemopexin by Haemophilus influenzae type b. *Journal of Bacteriology*, *177*(10), 2644–2653. https://doi.org/10.1128/jb.177.10.2644-2653.1995

Corin, K., Baaske, P., Ravel, D. B., Song, J., Brown, E., Wang, X., Wienken, C. J., Jerabek-Willemsen, M., Duhr, S., Luo, Y., Braun, D., & Zhang, S. (2011). Designer Lipid-Like Peptides: A Class of Detergents for Studying Functional Olfactory Receptors Using Commercial Cell-Free Systems. *PLoS ONE*, *6*(11), e25067. https://doi.org/10.1371/journal.pone.0025067

Cornelissen, C. N. (2018). Subversion of nutritional immunity by the pathogenic Neisseriae. *Pathogens and Disease*, *76*(1), ftx112. https://doi.org/10.1093/femspd/ftx112

Cornelissen, C. N., Kelley, M., Hobbs, M. M., Anderson, J. E., Cannon, J. G., Cohen, M. S., & Sparling, P. F. (1998). The transferrin receptor expressed by gonococcal strain FA1090 is required for the experimental infection of human male volunteers. *Molecular Microbiology*, *27*(3), 611–616. https://doi.org/10.1046/j.1365-2958.1998.00710.x

Corradi, V., Sejdiu, B. I., Mesa-Galloso, H., Abdizadeh, H., Noskov, S. Yu., Marrink, S. J., & Tieleman, D. P. (2019). Emerging Diversity in Lipid–Protein Interactions. *Chemical Reviews*, *119*(9), 5775–5848. https://doi.org/10.1021/acs.chemrev.8b00451

Coudray, N., Isom, G. L., MacRae, M. R., Saiduddin, M. N., Bhabha, G., & Ekiert, D. C. (2020). Structure of bacterial phospholipid transporter MlaFEDB with substrate bound. *ELife*, *9*, e62518. https://doi.org/10.7554/eLife.62518

Coureuil, M., Join-Lambert, O., Lécuyer, H., Bourdoulous, S., Marullo, S., & Nassif, X. (2012). Mechanism of meningeal invasion by Neisseria meningitidis. *Virulence*, *3*(2), 164–172. https://doi.org/10.4161/viru.18639

Daou, N., Buisson, C., Gohar, M., Vidic, J., Bierne, H., Kallassy, M., Lereclus, D., & Nielsen-LeRoux, C. (2009). IlsA, A Unique Surface Protein of Bacillus cereus Required for Iron Acquisition from Heme, Hemoglobin and Ferritin. *PLoS Pathogens*, *5*(11), e1000675. https://doi.org/10.1371/journal.ppat.1000675

De Carlo, S., & Harris, J. R. (2011). Negative staining and Cryo-negative Staining of Macromolecules and Viruses for TEM. *Micron (Oxford, England : 1993)*, *42*(2), 117–131. https://doi.org/10.1016/j.micron.2010.06.003

de Léséleuc, L., Harris, G., KuoLee, R., Xu, H. H., & Chen, W. (2014). Serum resistance, gallium nitrate tolerance and extrapulmonary dissemination are linked to heme consumption in a bacteremic strain of Acinetobacter baumannii. *International Journal of Medical Microbiology: IJMM*, *304*(3–4), 360–369. https://doi.org/10.1016/j.ijmm.2013.12.002

De Voss, J. J., Rutter, K., Schroeder, B. G., Su, H., Zhu, Y., & Barry, C. E. (2000). The salicylate-derived mycobactin siderophores of Mycobacterium tuberculosis are essential for growth in macrophages. *Proceedings of the National Academy of Sciences of the United States of America*, *97*(3), 1252–1257. https://doi.org/10.1073/pnas.97.3.1252

Delanghe, J. R., Langlois, M. R., & De Buyzere, M. L. (2011). Haptoglobin polymorphism: A key factor in the proatherogenic role of B cells? *Atherosclerosis*, *217*(1), 80–82. https://doi.org/10.1016/j.atherosclerosis.2011.03.031

Denisov, I. G., Grinkova, Y. V., Lazarides, A. A., & Sligar, S. G. (2004). Directed Self-Assembly of Monodisperse Phospholipid Bilayer Nanodiscs with Controlled Size. *Journal of the American Chemical Society*, *126*(11), 3477–3487. https://doi.org/10.1021/ja0393574

Denisov, I. G., & Sligar, S. G. (2016). Nanodiscs for structural and functional studies of membrane proteins. *Nature Structural & Molecular Biology*, *23*(6), 481–486. https://doi.org/10.1038/nsmb.3195

Denisov, I. G., & Sligar, S. G. (2017). NANODISCS IN MEMBRANE BIOCHEMISTRY AND BIOPHYSICS. *Chemical Reviews*, *117*(6), 4669–4713. https://doi.org/10.1021/acs.chemrev.6b00690

Dörr, J. M., Scheidelaar, S., Koorengevel, M. C., Dominguez, J. J., Schäfer, M., van Walree, C. A., & Killian, J. A. (2016). The styrene–maleic acid copolymer: A versatile tool in membrane research. *European Biophysics Journal*, *45*(1), 3–21. https://doi.org/10.1007/s00249-015-1093-y

Drazek, E. S., Hammack, C. A., & Schmitt, M. P. (2000a). Corynebacterium diphtheriae genes required for acquisition of iron from haemin and haemoglobin are homologous to ABC haemin transporters. *Molecular Microbiology*, *36*(1), 68–84. https://doi.org/10.1046/j.1365-2958.2000.01818.x

Drazek, E. S., Hammack, C. A., & Schmitt, M. P. (2000b). Corynebacterium diphtheriae genes required for acquisition of iron from haemin and haemoglobin are homologous to ABC haemin transporters. *Molecular Microbiology*, *36*(1), 68–84. https://doi.org/10.1046/j.1365-2958.2000.01818.x

Edwards, A. M. (2014). Structure and general properties of flavins. *Methods in Molecular Biology (Clifton, N.J.)*, *1146*, 3–13. https://doi.org/10.1007/978-1-4939-0452-5_1

Efremov, R. G., Gatsogiannis, C., & Raunser, S. (2017). Lipid Nanodiscs as a Tool for High-Resolution Structure Determination of Membrane Proteins by Single-Particle Cryo-EM. *Methods in Enzymology*, *594*, 1–30. https://doi.org/10.1016/bs.mie.2017.05.007

Efremov, R. G., Leitner, A., Aebersold, R., & Raunser, S. (2015). Architecture and conformational switch mechanism of the ryanodine receptor. *Nature*, *517*(7532), 39–43. https://doi.org/10.1038/nature13916

Ellis-Guardiola, K., Mahoney, B. J., & Clubb, R. T. (2021). NEAr Transporter (NEAT) Domains: Unique Surface Displayed Heme Chaperones That Enable Gram-

Positive Bacteria to Capture Heme-Iron From Hemoglobin. *Frontiers in Microbiology*, *11*, 3346. https://doi.org/10.3389/fmicb.2020.607679

Epand, R. M., Gawish, A., Iqbal, M., Gupta, K. B., Chen, C. H., Segrest, J. P., & Anantharamaiah, G. M. (1987). Studies of synthetic peptide analogs of the amphipathic helix. Effect of charge distribution, hydrophobicity, and secondary structure on lipid association and lecithin:cholesterol acyltransferase activation. *The Journal of Biological Chemistry*, *262*(19), 9389–9396.

Eren, E., Vijayaraghavan, J., Liu, J., Cheneke, B. R., Touw, D. S., Lepore, B. W., Indic, M., Movileanu, L., & Berg, B. van den. (2012). Substrate Specificity within a Family of Outer Membrane Carboxylate Channels. *PLOS Biology*, *10*(1), e1001242. https://doi.org/10.1371/journal.pbio.1001242

Erni, R., Rossell, M. D., Kisielowski, C., & Dahmen, U. (2009). Atomic-resolution imaging with a sub-50-pm electron probe. *Physical Review Letters*, *102*(9), 096101. https://doi.org/10.1103/PhysRevLett.102.096101

Evans, N. J., Harrison, O. B., Clow, K., Derrick, J. P., Feavers, I. M., & Maiden, M. C. J. Y. 2010. (2010). Variation and molecular evolution of HmbR, the Neisseria meningitidis haemoglobin receptor. *Microbiology*, *156*(5), 1384–1393. https://doi.org/10.1099/mic.0.036475-0

Ferguson, A. D., Chakraborty, R., Smith, B. S., Esser, L., van der Helm, D., & Deisenhofer, J. (2002). Structural basis of gating by the outer membrane transporter FecA. *Science (New York, N.Y.)*, *295*(5560), 1715–1719. https://doi.org/10.1126/science.1067313

Ferguson, A. D., Hofmann, E., Coulton, J. W., Diederichs, K., & Welte, W. (1998). Siderophore-Mediated Iron Transport: Crystal Structure of FhuA with Bound

Lipopolysaccharide. *Science*, *282*(5397), 2215–2220. https://doi.org/10.1126/science.282.5397.2215

Fisher, M., Huang, Y. S., Li, X., McIver, K. S., Toukoki, C., & Eichenbaum, Z. (2008). Shr is a broad-spectrum surface receptor that contributes to adherence and virulence in group A streptococcus. *Infection and Immunity*, *76*(11), 5006–5015. https://doi.org/10.1128/IAI.00300-08

Fitzpatrick, P. F. (1999). Tetrahydropterin-dependent amino acid hydroxylases. *Annual Review of Biochemistry*, *68*, 355–381. https://doi.org/10.1146/annurev.biochem.68.1.355

Freed, D. M., Lukasik, S. M., Sikora, A., Mokdad, A., & Cafiso, D. S. (2013). Monomeric TonB and the Ton box are required for the Formation of a High-Affinity Transporter-TonB Complex. *Biochemistry*, *52*(15), 2638–2648. https://doi.org/10.1021/bi3016108

Fujita, M., Mori, K., Hara, H., Hishiyama, S., Kamimura, N., & Masai, E. (2019). A TonB-dependent receptor constitutes the outer membrane transport system for a lignin-derived aromatic compound. *Communications Biology*, *2*(1), 1–10. https://doi.org/10.1038/s42003-019-0676-z

Garcia-Herrero, A., Peacock, R. S., Howard, S. P., & Vogel, H. J. (2007). The solution structure of the periplasmic domain of the TonB system ExbD protein reveals an unexpected structural homology with siderophore-binding proteins. *Molecular Microbiology*, *66*(4), 872–889. https://doi.org/10.1111/j.1365-2958.2007.05957.x

Gat, O., Zaide, G., Inbar, I., Grosfeld, H., Chitlaru, T., Levy, H., & Shafferman, A. (2008). Characterization of Bacillus anthracis iron-regulated surface determinant

(Isd) proteins containing NEAT domains. *Molecular Microbiology*, *70*(4), 983–999. https://doi.org/10.1111/j.1365-2958.2008.06460.x

Gialama, D., Kostelidou, K., Michou, M., Delivoria, D. C., Kolisis, F. N., & Skretas, G. (2016, November 17). *Development of Escherichia coli Strains That Withstand Membrane Protein-Induced Toxicity and Achieve High-Level Recombinant Membrane Protein Production* (world) [Research-article]. ACS Publications; American Chemical Society. https://doi.org/10.1021/acssynbio.6b00174

Gómez-Santos, N., Glatter, T., Koebnik, R., Świątek-Połatyńska, M. A., & Søgaard-Andersen, L. (2019). A TonB-dependent transporter is required for secretion of protease PopC across the bacterial outer membrane. *Nature Communications*, *10*(1), 1360. https://doi.org/10.1038/s41467-019-09366-9

Gomme, P. T., McCann, K. B., & Bertolini, J. (2005). Transferrin: Structure, function and potential therapeutic actions. *Drug Discovery Today*, *10*(4), 267–273. https://doi.org/10.1016/S1359-6446(04)03333-1

Graham, L., & Orenstein, J. M. (2007). Processing tissue and cells for transmission electron microscopy in diagnostic pathology and research. *Nature Protocols*, *2*(10), 2439–2450. https://doi.org/10.1038/nprot.2007.304

Grek, C. L., Newton, D. A., Spyropoulos, D. D., & Baatz, J. E. (2011). Hypoxia up-regulates expression of hemoglobin in alveolar epithelial cells. *American Journal of Respiratory Cell and Molecular Biology*, *44*(4), 439–447. https://doi.org/10.1165/rcmb.2009-0307OC

Grigg, J. C., Ukpabi, G., Gaudin, C. F. M., & Murphy, M. E. P. (2010). Structural biology of heme binding in the Staphylococcus aureus Isd system. *Journal of Inorganic Biochemistry*, *104*(3), 341–348. https://doi.org/10.1016/j.jinorgbio.2009.09.012

Guedes, S., Bricout, H., Langevin, E., Tong, S., & Bertrand-Gerentes, I. (2022). Epidemiology of invasive meningococcal disease and sequelae in the United Kingdom during the period 2008 to 2017 – a secondary database analysis. *BMC Public Health*, *22*(1), 521. https://doi.org/10.1186/s12889-022-12933-3

Gunn, J. S., Mason, K., Zughaier, S. M., & Cornelis, P. (2018). Editorial: Role of Iron in Bacterial Pathogenesis. *Front. Cell. Infect. Microbiol*, *8*, 344. https://doi.org/10.3389/fcimb.2018.00344

Gutiérrez-González, M., Farías, C., Tello, S., Pérez-Etcheverry, D., Romero, A., Zúñiga, R., Ribeiro, C. H., Lorenzo-Ferreiro, C., & Molina, M. C. (2019). Optimization of culture conditions for the expression of three different insoluble proteins in Escherichia coli. *Scientific Reports*, *9*(1), 16850. https://doi.org/10.1038/s41598-019-53200-7

Hagn, F., Nasr, M. L., & Wagner, G. (2018). Assembly of phospholipid nanodiscs of controlled size for structural studies of membrane proteins by NMR. *Nature Protocols*, *13*(1), 79–98. https://doi.org/10.1038/nprot.2017.094

Haley, K. P., & Skaar, E. P. (2012). A battle for iron: Host sequestration and Staphylococcus aureus acquisition. *Microbes and Infection*, *14*(3), 217–227. https://doi.org/10.1016/j.micinf.2011.11.001

Hammer, N. D., & Skaar, E. P. (2011). Molecular mechanisms of Staphylococcus aureus iron acquisition. *Annual Review of Microbiology*, *65*, 10.1146/annurev-micro-090110–102851. https://doi.org/10.1146/annurev-micro-090110-102851

Harding, C. M., Hennon, S. W., & Feldman, M. F. (2018). Uncovering the mechanisms of Acinetobacter baumannii virulence. *Nature Reviews. Microbiology*, *16*(2), 91–102. https://doi.org/10.1038/nrmicro.2017.148

Hare, S. A. (2017). Diverse structural approaches to haem appropriation by pathogenic bacteria. *Biochimica Et Biophysica Acta. Proteins and Proteomics*, *1865*(4), 422–433. https://doi.org/10.1016/j.bbapap.2017.01.006

Hargrove, M. S., Singleton, E. W., Quillin, M. L., Ortiz, L. A., Phillips, G. N., Olson, J. S., & Mathews, A. J. (1994). His64(E7)—>Tyr apomyoglobin as a reagent for measuring rates of hemin dissociation. *The Journal of Biological Chemistry*, *269*(6), 4207–4214. https://doi.org/10.2210/pdb1mgn/pdb

Hargrove, M. S., Whitaker, T., Olson, J. S., Vali, R. J., & Mathews, A. J. (1997). Quaternary structure regulates hemin dissociation from human hemoglobin. *The Journal of Biological Chemistry*, *272*(28), 17385–17389. https://doi.org/10.1074/jbc.272.28.17385

Harrison, O. B., Bennett, J. S., Derrick, J. P., Maiden, M. C. J., & Bayliss, C. D. (2013a). Distribution and diversity of the haemoglobin-haptoglobin iron-acquisition systems in pathogenic and non-pathogenic Neisseria. *Microbiology (United Kingdom)*, *159*(PART 9), 1920–1930. https://doi.org/10.1099/mic.0.068874-0

Harrison, O. B., Bennett, J. S., Derrick, J. P., Maiden, M. C. J., & Bayliss, C. D. (2013b). Distribution and diversity of the haemoglobin–haptoglobin iron-acquisition systems in pathogenic and non-pathogenic Neisseria. *Microbiology*, *159*(Pt_9), 1920–1930. https://doi.org/10.1099/mic.0.068874-0

Hickman, S. J., Cooper, R. E. M., Bellucci, L., Paci, E., & Brockwell, D. J. (2017). Gating of TonB-dependent transporters by substrate-specific forced remodelling. *Nature Communications*, *8*(1), 14804. https://doi.org/10.1038/ncomms14804

Hood, M. I., & Skaar, E. P. (2012). Nutritional immunity: Transition metals at the pathogen-host interface. In *Nature Reviews Microbiology* (Vol. 10, Issue 8, pp. 525–537). NIH Public Access. https://doi.org/10.1038/nrmicro2836

Hrkal, Z., Vodrázka, Z., & Kalousek, I. (1974). Transfer of heme from ferrihemoglobin and ferrihemoglobin isolated chains to hemopexin. *European Journal of Biochemistry*, *43*(1), 73–78. https://doi.org/10.1111/j.1432-1033.1974.tb03386.x

Hwang, P. K., & Greer, J. (1980). Interaction between hemoglobin subunits in the hemoglobin. Haptoglobin complex. *The Journal of Biological Chemistry*, *255*(7), 3038–3041.

Ibraim, I. C., Parise, M. T. D., Parise, D., Sfeir, M. Z. T., de Paula Castro, T. L., Wattam, A. R., Ghosh, P., Barh, D., Souza, E. M., Góes-Neto, A., Gomide, A. C. P., & Azevedo, V. (2019). Transcriptome profile of Corynebacterium pseudotuberculosis in response to iron limitation. *BMC Genomics*, *20*(1), 663. https://doi.org/10.1186/s12864-019-6018-1

Irwin, S. W., Averil, N., Cheng, C. Y., & Schryvers, A. B. (1993). Preparation and analysis of isogenic mutants in the transferrin receptor protein genes, tbpA and tbpB, from Neisseria meningitidis. *Molecular Microbiology*, *8*(6), 1125–1133. https://doi.org/10.1111/j.1365-2958.1993.tb01657.x

Jackson, L. A., Ducey, T. F., Day, M. W., Zaitshik, J. B., Orvis, J., & Dyer, D. W. (2010). Transcriptional and Functional Analysis of the Neisseria gonorrhoeae Fur Regulon. *Journal of Bacteriology*, *192*(1), 77–85. https://doi.org/10.1128/JB.00741-09

Jamie Robinson, N., Mulder, D. W., Auvert, B., Hayes, R. J., & J, R. N. (1997). Proportion of HIV Infections Attributable to Other Sexually Transmitted

Diseases in a Rural Ugandan Population: Simulation Model Estimates. In *International Journal of Epidemiology* (Vol. 26, Issue 1).

Jamshad, M., Lin, Y.-P., Knowles, T. J., Parslow, R. A., Harris, C., Wheatley, M., Poyner, D. R., Bill, R. M., Thomas, O. R. T., Overduin, M., & Dafforn, T. R. (2011). Surfactant-free purification of membrane proteins with intact native membrane environment. *Biochemical Society Transactions*, *39*(3), 813–818. https://doi.org/10.1042/BST0390813

Jordan, A., & Reichard, P. (1998). Ribonucleotide reductases. *Annual Review of Biochemistry*, *67*, 71–98. https://doi.org/10.1146/annurev.biochem.67.1.71

Junge, F., Schneider, B., Reckel, S., Schwarz, D., Dötsch, V., & Bernhard, F. (2008). Large-scale production of functional membrane proteins. *Cellular and Molecular Life Sciences: CMLS*, *65*(11), 1729–1755. https://doi.org/10.1007/s00018-008-8067-5

Kamwendo, F., Forslin, L., Bodin, L., & Danielsson, D. (1996). Decreasing Incidences of Gonorrhea- and Chlamydia-Associated Acute Pelvic Inflammatory Disease: A 25-Year Study From an Urban Area of Central Sweden. *Sexually Transmitted Diseases*, *23*(5), 384–391. https://doi.org/10.1097/00007435-199609000-00007

Karr, U., Simonian, M., & Whitelegge, J. P. (2017). Integral membrane proteins: Bottom-up, top-down and structural proteomics. *Expert Review of Proteomics*, *14*(8), 715–723. https://doi.org/10.1080/14789450.2017.1359545

Kaserer, W. A., Jiang, X., Xiao, Q., Scott, D. C., Bauler, M., Copeland, D., Newton, S. M. C., & Klebba, P. E. (2008). Insight from TonB hybrid proteins into the mechanism of iron transport through the outer membrane. *Journal of Bacteriology*, *190*(11), 4001–4016. https://doi.org/10.1128/jb.00135-08

Kasvosve, I., Speeckaert, M. M., Speeckaert, R., Masukume, G., & Delanghe, J. R. (2010). Haptoglobin polymorphism and infection. *Advances in Clinical Chemistry*, *50*, 23–46. https://doi.org/10.1016/s0065-2423(10)50002-7

Kaushik, M. S., Singh, P., Tiwari, B., & Mishra, A. K. (2016). Ferric Uptake Regulator (FUR) protein: Properties and implications in cyanobacteria. *Annals of Microbiology*, *66*(1), 61–75. https://doi.org/10.1007/s13213-015-1134-x

Keilin, D., & Hardy, W. B. (1925). On cytochrome, a respiratory pigment, common to animals, yeast, and higher plants. *Proceedings of the Royal Society of London. Series B, Containing Papers of a Biological Character*, *98*(690), 312–339. https://doi.org/10.1098/rspb.1925.0039

Kermani, A. A. (2021). A guide to membrane protein X-ray crystallography. *The FEBS Journal*, *288*(20), 5788–5804. https://doi.org/10.1111/febs.15676

Khoshouei, M., Radjainia, M., Baumeister, W., & Danev, R. (2017). Cryo-EM structure of haemoglobin at 3.2 Å determined with the Volta phase plate. *Nature Communications*, *8*(1), 16099. https://doi.org/10.1038/ncomms16099

King, P. (2012). Haemophilus influenzae and the lung (Haemophilus and the lung). *Clinical and Translational Medicine*, *1*, 10. https://doi.org/10.1186/2001-1326-1-10

Kiu, R., & Hall, L. J. (2018). An update on the human and animal enteric pathogen Clostridium perfringens. In *Emerging Microbes and Infections* (Vol. 7, Issue 1). Nature Publishing Group. https://doi.org/10.1038/s41426-018-0144-8

Klebba, P. E. (2016). ROSET Model of TonB Action in Gram-Negative Bacterial Iron Acquisition. *Journal of Bacteriology*, *198*(7), 1013–1021. https://doi.org/10.1128/JB.00823-15

Klebba, P. E., Charbit, A., Xiao, Q., Jiang, X., & Newton, S. M. (2012). Mechanisms of iron and haem transport by Listeria monocytogenes. In *Molecular Membrane Biology* (Vol. 29, Issues 3–4, pp. 69–86). Mol Membr Biol. https://doi.org/10.3109/09687688.2012.694485

Klein, J. S., Jiang, S., Galimidi, R. P., Keeffe, J. R., & Bjorkman, P. J. (2014). Design and characterization of structured protein linkers with differing flexibilities. *Protein Engineering Design and Selection*, *27*(10), 325–330. https://doi.org/10.1093/protein/gzu043

Kluytmans, J., Van Belkum, A., & Verbrugh, H. (1997). Nasal carriage of Staphylococcus aureus: Epidemiology, underlying mechanisms, and associated risks. In *Clinical Microbiology Reviews* (Vol. 10, Issue 3, pp. 505–520). American Society for Microbiology. https://doi.org/10.1128/cmr.10.3.505-520.1997

Knoll, M., & Ruska, E. (1932). Das Elektronenmikroskop. *Zeitschrift für Physik*, *78*(5), 318–339. https://doi.org/10.1007/BF01342199

Knowles, T. J., Finka, R., Smith, C., Lin, Y.-P., Dafforn, T., & Overduin, M. (2009). Membrane Proteins Solubilized Intact in Lipid Containing Nanoparticles Bounded by Styrene Maleic Acid Copolymer. *Journal of the American Chemical Society*, *131*(22), 7484–7485. https://doi.org/10.1021/ja810046q

Ködding, J., Killig, F., Polzer, P., Howard, S. P., Diederichs, K., & Welte, W. (2005). Crystal structure of a 92-residue C-terminal fragment of TonB from Escherichia coli reveals significant conformational changes compared to structures of smaller TonB fragments. *The Journal of Biological Chemistry*, *280*(4), 3022–3028. https://doi.org/10.1074/jbc.M411155200

Krieg, S., Huché, F., Diederichs, K., Izadi-Pruneyre, N., Lecroisey, A., Wandersman, C., Delepelaire, P., & Welte, W. (2009). Heme uptake across the outer membrane as revealed by crystal structures of the receptor-hemophore complex. *Proceedings of the National Academy of Sciences of the United States of America*, *106*(4), 1045–1050. https://doi.org/10.1073/pnas.0809406106

Kristiansen, M., Graversen, J. H., Jacobsen, C., Sonne, O., Hoffman, H. J., Law, S. K. A., & Moestrup, S. K. (2001). Identification of the haemoglobin scavenger receptor. *Nature*, *409*(6817), 198–201. https://doi.org/10.1038/35051594

Kuo, Y.-C., Chen, H., Shang, G., Uchikawa, E., Tian, H., Bai, X.-C., & Zhang, X. (2020). Cryo-EM structure of the PlexinC1/A39R complex reveals inter-domain interactions critical for ligand-induced activation. *Nature Communications*, *11*(1), 1953. https://doi.org/10.1038/s41467-020-15862-0

Kurthkoti, K., Amin, H., Marakalala, M. J., Ghanny, S., Subbian, S., Sakatos, A., Livny, J., Fortune, S. M., Berney, M., & Rodriguez, G. M. (2017). The capacity of mycobacterium tuberculosis to survive iron starvation might enable it to persist in iron- deprived microenvironments of human granulomas. *MBio*, *8*(4). https://doi.org/10.1128/mBio.01092-17

Larsen, A. N., Sørensen, K. K., Johansen, N. T., Martel, A., Kirkensgaard, J. J. K., Jensen, K. J., Arleth, L., & Midtgaard, S. R. (2016). Dimeric peptides with three different linkers self-assemble with phospholipids to form peptide nanodiscs that stabilize membrane proteins. *Soft Matter*, *12*(27), 5937–5949. https://doi.org/10.1039/c6sm00495d

Laursen, T., Borch, J., Knudsen, C., Bavishi, K., Torta, F., Martens, H. J., Silvestro, D., Hatzakis, N. S., Wenk, M. R., Dafforn, T. R., Olsen, C. E., Motawia, M. S., Hamberger, B., Møller, B. L., & Bassard, J.-E. (2016). Characterization of a

dynamic metabolon producing the defense compound dhurrin in sorghum. *Science*, *354*(6314), 890–893. https://doi.org/10.1126/science.aag2347

Lee, B. C. (1991). Iron sources for Haemophilus ducreyi. *Journal of Medical Microbiology*, *34*(6), 317–322. https://doi.org/10.1099/00222615-34-6-317

Lee, B. C. (1992). Isolation of haemin-binding proteins of Neisseria gonorrhoeae. -. *Medical Microbiology*, *36*, 121–127. https://doi.org/10.1099/00222615-36-2-121

Lejbkowicz, F., Cohn, L., Hashman, N., & Kassis, I. (1999). Recovery of Kingella kingae from blood and synovial fluid of two pediatric patients by using the BacT/Alert system [3]. In *Journal of Clinical Microbiology* (Vol. 37, Issue 3, p. 878). American Society for Microbiology. https://doi.org/10.1128/jcm.37.3.878-878.1999

Letain, T. E., & Postle, K. (1997). TonB protein appears to transduce energy by shuttling between the cytoplasmic membrane and the outer membrane in Escherichia coli. *Molecular Microbiology*, *24*(2), 271–283. https://doi.org/10.1046/j.1365-2958.1997.3331703.x

Létoffé, S., Ghigo, J. M., & Wandersman, C. (1994). Iron acquisition from heme and hemoglobin by a Serratia marcescens extracellular protein. *Proceedings of the National Academy of Sciences of the United States of America*, *91*(21), 9876–9880. https://doi.org/10.1073/pnas.91.21.9876

Lewis, L. A., & Dyer, D. W. (1995). Identification of an iron-regulated outer membrane protein of Neisseria meningitidis involved in the utilization of hemoglobin complexed to haptoglobin. *Journal of Bacteriology*, *177*(5), 1299–1306.

Lewis, L. A., Gipson, M., Hartman, K., Ownbey, T., Vaughn, J., & Dyer, D. W. (1999). Phase variation of HpuAB and HmbR, two distinct haemoglobin receptors of

Neisseria meningitidis DNM2. *Molecular Microbiology*, *32*(5), 977–989. https://doi.org/10.1046/j.1365-2958.1999.01409.x

Lewis, L. A., Gray, E., Wang, Y.-P., Roe, B. A., & Dyer, D. W. (1997). Molecular characterization of hpuAB, the haemoglobin–haptoglobin-utilization operon of Neisseria meningitidis. *Molecular Microbiology*, *23*(4), 737–749. https://doi.org/10.1046/j.1365-2958.1997.2501619.x

Lister, P. D., Wolter, D. J., & Hanson, N. D. (2009). Antibacterial-resistant Pseudomonas aeruginosa: Clinical impact and complex regulation of chromosomally encoded resistance mechanisms. In *Clinical Microbiology Reviews* (Vol. 22, Issue 4, pp. 582–610). American Society for Microbiology (ASM). https://doi.org/10.1128/CMR.00040-09

Liu, G., Tang, C. M., & Exley, R. M. (2015). Non-pathogenic neisseria: Members of an abundant, multi-habitat, diverse genus. *Microbiology (United Kingdom)*, *161*(7), 1297–1312. https://doi.org/10.1099/mic.0.000086

Liu, L., Zeng, M., & Stamler, J. S. (1999). Hemoglobin induction in mouse macrophages. *Proceedings of the National Academy of Sciences of the United States of America*, *96*(12), 6643–6647. https://doi.org/10.1073/pnas.96.12.6643

Liu, M., Tanaka, W. N., Zhu, H., Xie, G., Dooley, D. M., & Lei, B. (2008). Direct Hemin Transfer from IsdA to IsdC in the Iron-regulated Surface Determinant (Isd) Heme Acquisition System of Staphylococcus aureus. *Journal of Biological Chemistry*, *283*(11), 6668–6676. https://doi.org/10.1074/jbc.M708372200

Liu, Y., Huynh, D. T., & Yeates, T. O. (2019). A 3.8 Å resolution cryo-EM structure of a small protein bound to an imaging scaffold. *Nature Communications*, *10*(1), 1864. https://doi.org/10.1038/s41467-019-09836-0

Livermore, D. M. (1987). Mechanisms of resistance to cephalosporin antibiotics. *Drugs*, *34 Suppl 2*, 64–88. https://doi.org/10.2165/00003495-198700342-00007

Lyman, L. R., Peng, E. D., & Schmitt, M. P. (2018). Corynebacterium diphtheriae Iron-Regulated Surface Protein HbpA Is Involved in the Utilization of the Hemoglobin-Haptoglobin Complex as an Iron Source. *Journal of Bacteriology*, *200*(7), e00676-17. https://doi.org/10.1128/JB.00676-17

Macdonald, R., Cascio, D., Collazo, M. J., Phillips, M., & Clubb, R. T. (2018). The Streptococcus pyogenes Shr protein captures human hemoglobin using two structurally unique binding domains. *Journal of Biological Chemistry*, *293*(47), 18365–18377. https://doi.org/10.1074/jbc.RA118.005261

Macdonald, R., Mahoney, B. J., Ellis-Guardiola, K., Maresso, A., & Clubb, R. T. (2019). NMR experiments redefine the hemoglobin binding properties of bacterial NEAr-iron Transporter domains. *Protein Science*, *28*(8), 1513–1523. https://doi.org/10.1002/pro.3662

Maciver, I., Latimer, J. L., Liem, H. H., Muller-Eberhard, U., Hrkal, Z., & Hansen, E. J. (1996). Identification of an outer membrane protein involved in utilization of hemoglobin-haptoglobin complexes by nontypeable Haemophilus influenzae. *Infection and Immunity*, *64*(9), 3703–3712. https://doi.org/10.1128/IAI.64.9.3703-3712.1996

Majeed, S., Ahmad, A. B., Sehar, U., & Georgieva, E. R. (2021). Lipid Membrane Mimetics in Functional and Structural Studies of Integral Membrane Proteins. *Membranes*, *11*(9), 685. https://doi.org/10.3390/membranes11090685

Malmirchegini, G. R., Sjodt, M., Shnitkind, S., Sawaya, M. R., Rosinski, J., Newton, S. M., Klebba, P. E., & Clubb, R. T. (2014). Novel mechanism of hemin capture by Hbp2, the hemoglobin-binding hemophore from Listeria monocytogenes.

Journal of Biological Chemistry, *289*(50), 34886–34899. https://doi.org/10.1074/jbc.M114.583013

Mansur, F. J., Takahara, S., Yamamoto, M., Shimatani, M., Karim, M. M., Noiri, Y., Ebisu, S., & Azakami, H. (2017). Purification and characterization of hemolysin from periodontopathogenic bacterium Eikenella corrodens strain 1073. *Bioscience, Biotechnology and Biochemistry*, *81*(6), 1246–1253. https://doi.org/10.1080/09168451.2017.1295807

Maresso, A. W., & Schneewind, O. (2006). Iron acquisition and transport in Staphylococcus aureus. *Biometals: An International Journal on the Role of Metal Ions in Biology, Biochemistry, and Medicine*, *19*(2), 193–203. https://doi.org/10.1007/s10534-005-4863-7

Marvig, R. L., Damkiær, S., Hossein Khademi, S. M., Markussen, T. M., Molin, S., & Jelsbak, L. (2014). Within-host evolution of pseudomonas aeruginosa reveals adaptation toward iron acquisition from hemoglobin. *MBio*, *5*(3). https://doi.org/10.1128/mBio.00966-14

Massé, E., Vanderpool, C. K., & Gottesman, S. (2005). Effect of RyhB Small RNA on Global Iron Use in Escherichia coli. *Journal of Bacteriology*, *187*(20), 6962–6971. https://doi.org/10.1128/JB.187.20.6962-6971.2005

Matthies, D., Bae, C., Toombes, G. E., Fox, T., Bartesaghi, A., Subramaniam, S., & Swartz, K. J. (2018). Single-particle cryo-EM structure of a voltage-activated potassium channel in lipid nanodiscs. *ELife*, *7*, e37558. https://doi.org/10.7554/eLife.37558

Mazmanian, S. K., Skaar, E. P., Gaspar, A. H., Humayun, M., Gornicki, P., Jelenska, J., Joachmiak, A., Missiakas, D. M., & Schneewind, O. (2003). Passage of heme-

iron across the envelope of Staphylococcus aureus. *Science (New York, N.Y.)*, *299*(5608), 906–909. https://doi.org/10.1126/science.1081147

Meuskens, I., Michalik, M., Chauhan, N., Linke, D., & Leo, J. C. (2017). A New Strain Collection for Improved Expression of Outer Membrane Proteins. *Frontiers in Cellular and Infection Microbiology*, *7*. https://www.frontiersin.org/article/10.3389/fcimb.2017.00464

Michou, M., Kapsalis, C., Pliotas, C., & Skretas, G. (2019). Optimization of Recombinant Membrane Protein Production in the Engineered Escherichia coli Strains SuptoxD and SuptoxR. *ACS Synthetic Biology*, *8*(7), 1631–1641. https://doi.org/10.1021/acssynbio.9b00120

Mickelsen, P. A., & Sparling, P. F. (1981). Ability of Neisseria gonorrhoeae, Neisseria meningitidis, and commensal Neisseria species to obtain iron from transferrin and iron compounds. *INFECTION AND IMMUNITY*, *33*(2), 555–564. https://doi.org/10.1128/iai.33.2.555-564.1981

Mills, M., & Payne, S. M. (1997). Identification of shuA, the gene encoding the heme receptor of Shigella dysenteriae, and analysis of invasion and intracellular multiplication of a shuA mutant. *Infection and Immunity*, *65*(12), 5358–5363. https://doi.org/10.1128/iai.65.12.5358-5363.1997

Milne, J. L. S., Borgnia, M. J., Bartesaghi, A., Tran, E. E. H., Earl, L. A., Schauder, D. M., Lengyel, J., Pierson, J., Patwardhan, A., & Subramaniam, S. (2013). Cryo-electron microscopy: A primer for the non-microscopist. *The FEBS Journal*, *280*(1), 28–45. https://doi.org/10.1111/febs.12078

Mitra, A., Ko, Y. H., Cingolani, G., & Niederweis, M. (2019). Heme and hemoglobin utilization by Mycobacterium tuberculosis. *Nature Communications*, *10*(1), 1–14. https://doi.org/10.1038/s41467-019-12109-5

Mitra, A., Speer, A., Lin, K., Ehrt, S., & Niederweis, M. (2017). PPE surface proteins are required for heme utilization by Mycobacterium tuberculosis. *MBio*, *8*(1). https://doi.org/10.1128/mBio.01720-16

Mulkidjanian, A. Y., & Galperin, M. Y. (2010). Evolutionary origins of membrane proteins. In D. Frishman (Ed.), *Structural Bioinformatics of Membrane Proteins* (pp. 1–28). Springer. https://doi.org/10.1007/978-3-7091-0045-5_1

Muller-Eberhard, U., Javid, J., Liem, H. H., Hanstein, A., & Hanna, M. (1968). Plasma concentrations of hemopexin, haptoglobin and heme in patients with various hemolytic diseases. *Blood*, *32*(5), 811–815.

Munn, C. A. M., & Foster, M. (1886). VI. Researches on myohamatin and the histohæmatins. *Philosophical Transactions of the Royal Society of London*, *177*, 267–298. https://doi.org/10.1098/rstl.1886.0007

Murdoch, C. C., & Skaar, E. P. (2022). Nutritional immunity: The battle for nutrient metals at the host–pathogen interface. *Nature Reviews Microbiology*, 1–14. https://doi.org/10.1038/s41579-022-00745-6

Muryoi, N., Tiedemann, M. T., Pluym, M., Cheung, J., Heinrichs, D. E., & Stillman, M. J. (2008). Demonstration of the iron-regulated surface determinant (Isd) heme transfer pathway in Staphylococcus aureus. *Journal of Biological Chemistry*, *283*(42), 28125–28136. https://doi.org/10.1074/jbc.M802171200

Na, N., Ouyang, J., Taes, Y. E. C., & Delanghe, J. R. (2005). Serum free hemoglobin concentrations in healthy individuals are related to haptoglobin type [5]. *Clinical Chemistry*, *51*(9), 1754–1755. https://doi.org/10.1373/clinchem.2005.055657

Nepluev, I., Afonina, G., Fusco, W. G., Leduc, I., Olsen, B., Temple, B., & Elkins, C. (2009). An immunogenic, surface-exposed domain of Haemophilus ducreyi

outer membrane protein HgbA is involved in hemoglobin binding. *Infection and Immunity*, *77*(7), 3065–3074. https://doi.org/10.1128/IAI.00034-09

Neumann, E., Estrozi, L. F., Effantin, G., Breyton, C., & Schoehn, G. (2017). Prix Nobel de Chimie 2017: Jacques Dubochet, Joachim Frank et Richard Henderson - La révolution de la résolution en cryo-microscopie électronique. *médecine/sciences*, *33*(12), 1111–1117. https://doi.org/10.1051/medsci/20173212019

Newman, A. J., Selkoe, D., & Dettmer, U. (2013). A New Method for Quantitative Immunoblotting of Endogenous α-Synuclein. *PLoS ONE*, *8*(11), e81314. https://doi.org/10.1371/journal.pone.0081314

Newton, D. A., Rao, K. M. K., Dluhy, R. A., & Baatz, J. E. (2006). Hemoglobin is expressed by alveolar epithelial cells. *The Journal of Biological Chemistry*, *281*(9), 5668–5676. https://doi.org/10.1074/jbc.M509314200

NIH Grantee Wins 2017 Nobel Prize in Chemistry. (2017, October 4). National Institutes of Health (NIH). https://www.nih.gov/news-events/news-releases/nih-grantee-wins-2017-nobel-prize-chemistry

Nikaido, H. (2003). Molecular Basis of Bacterial Outer Membrane Permeability Revisited. *Microbiology and Molecular Biology Reviews*, *67*(4), 593–656. https://doi.org/10.1128/mmbr.67.4.593-656.2003

Nogales, E. (2016). The development of cryo-EM into a mainstream structural biology technique. *Nature Methods*, *13*(1), 24–27. https://doi.org/10.1038/nmeth.3694

Noinaj, N., Easley, N. C., Oke, M., Mizuno, N., Gumbart, J., Boura, E., Steere, A. N., Zak, O., Aisen, P., Tajkhorshid, E., Evans, R. W., Gorringe, A. R., Mason, A. B., Steven, A. C., & Buchanan, S. K. (2012). Structural basis for iron piracy by

pathogenic Neisseria. *Nature*, *483*(7387), 53–58. https://doi.org/10.1038/nature10823

Noinaj, N., Guillier, M., Barnard, T. J., & Buchanan, S. K. (2010a). TonB-dependent transporters: Regulation, structure, and function. *Annual Review of Microbiology*, *64*, 43–60. https://doi.org/10.1146/annurev.micro.112408.134247

Noinaj, N., Guillier, M., Barnard, T. J., & Buchanan, S. K. (2010b). TonB-dependent transporters: Regulation, structure, and function. In *Annual Review of Microbiology* (Vol. 64, pp. 43–60). Annu Rev Microbiol. https://doi.org/10.1146/annurev.micro.112408.134247

Nomura, Y., Okada, A., Kakuta, E., Gunji, T., Kajiura, S., & Hanada, N. (2016). A new screening method for periodontitis: An alternative to the community periodontal index. *BMC Oral Health*, *16*(1), 64. https://doi.org/10.1186/s12903-016-0216-x

Núñez, G., Sakamoto, K., & Soares, M. P. (2018). Innate Nutritional Immunity. *Journal of Immunology (Baltimore, Md.: 1950)*, *201*(1), 11–18. https://doi.org/10.4049/jimmunol.1800325

Ochs, M., Veitinger, S., Kim, I., Weiz, D., Angerer, A., & Braun, V. (1995). Regulation of citrate-dependent iron transport of Escherichia coli: FecR is required for transcription activation by FeeI. *Molecular Microbiology*, *15*(1), 119–132. https://doi.org/10.1111/j.1365-2958.1995.tb02226.x

Ohi, M., Li, Y., Cheng, Y., & Walz, T. (2004). Negative Staining and Image Classification – Powerful Tools in Modern Electron Microscopy. *Biological Procedures Online*, *6*, 23–34. https://doi.org/10.1251/bpo70

Ohnishi, M., Golparian, D., Shimuta, K., Saika, T., Hoshina, S., Iwasaku, K., Nakayama, S. I., Kitawaki, J., & Unemo, M. (2011). Is Neisseria gonorrhoeae initiating a future era of untreatable gonorrhea?: Detailed characterization of the

first strain with high-level resistance to ceftriaxone. *Antimicrobial Agents and Chemotherapy*, *55*(7), 3538–3545. https://doi.org/10.1128/AAC.00325-11

Overington, J. P., Al-Lazikani, B., & Hopkins, A. L. (2006). How many drug targets are there? *Nature Reviews. Drug Discovery*, *5*(12), 993–996. https://doi.org/10.1038/nrd2199

Pappenheimer, A. M. (1977). Diphtheria toxin. *Annual Review of Biochemistry*, *Vol. 46*, 69–94. https://doi.org/10.1146/annurev.bi.46.070177.000441

Parmar, M., Rawson, S., Scarff, C. A., Goldman, A., Dafforn, T. R., Muench, S. P., & Postis, V. L. G. (2018). Using a SMALP platform to determine a sub-nm single particle cryo-EM membrane protein structure. *Biochimica et Biophysica Acta (BBA) - Biomembranes*, *1860*(2), 378–383. https://doi.org/10.1016/j.bbamem.2017.10.005

Passmore, L. A., & Russo, C. J. (2016). Specimen preparation for high-resolution cryo-EM. *Methods in Enzymology*, *579*, 51–86. https://doi.org/10.1016/bs.mie.2016.04.011

Paul, K., & Patel, S. S. (2001). Eikenella corrodens infections in children and adolescents: Case reports and review of the literature. *Clinical Infectious Diseases*, *33*(1), 54–61. https://doi.org/10.1086/320883

Payne, M. A., Igo, J. D., Cao, Z., Foster, S. B., Newton, S. M. C., & Klebba, P. E. (1997). Biphasic Binding Kinetics between FepA and Its Ligands. *Journal of Biological Chemistry*, *272*(35), 21950–21955. https://doi.org/10.1074/jbc.272.35.21950

Peacock, S. R., Weljie, A. M., Peter Howard, S., Price, F. D., & Vogel, H. J. (2005). The solution structure of the C-terminal domain of TonB and interaction studies

with TonB box peptides. *Journal of Molecular Biology*, *345*(5), 1185–1197. https://doi.org/10.1016/j.jmb.2004.11.026

Perkins-Balding, D., Baer, M. T., & Stojiljkovic, I. (2003a). Identification of functionally important regions of a haemoglobin receptor from Neisseria meningitidis. *Microbiology*, *149*(12), 3423–3435. https://doi.org/10.1099/mic.0.26448-0

Perkins-Balding, D., Baer, M. T., & Stojiljkovic, I. (2003b). Identification of functionally important regions of a haemoglobin receptor from Neisseria meningitidis. *Microbiology*, *149*(12), 3423–3435. https://doi.org/10.1099/mic.0.26448-0

Perkins-Balding, D., Ratliff-Griffin, M., & Stojiljkovic, I. (2004). Iron transport systems in Neisseria meningitidis. *Microbiology and Molecular Biology Reviews: MMBR*, *68*(1), 154–171. https://doi.org/10.1128/MMBR.68.1.154-171.2004

Perutz, M. F., Rossmann, M. G., Cullis, A. F., Muirhead, H., Will, G., & North, A. C. (1960). Structure of haemoglobin: A three-dimensional Fourier synthesis at 5.5-A. resolution, obtained by X-ray analysis. *Nature*, *185*(4711), 416–422. https://doi.org/10.1038/185416a0

Picard, M., Dahmane, T., Garrigos, M., Gauron, C., Giusti, F., le Maire, M., Popot, J.-L., & Champeil, P. (2006). Protective and Inhibitory Effects of Various Types of Amphipols on the Ca^{2+} -ATPase from Sarcoplasmic Reticulum: A Comparative Study. *Biochemistry*, *45*(6), 1861–1869. https://doi.org/10.1021/bi051954a

Pilpa, R. M., Robson, S. A., Villareal, V. A., Wong, M. L., Phillips, M., & Clubb, R. T. (2009). Functionally distinct NEAT (NEAr Transporter) domains within the staphylococcus aureus IsdH/HarA protein extract heme from methemoglobin.

Journal of Biological Chemistry, *284*(2), 1166–1176. https://doi.org/10.1074/jbc.M806007200

Pishchany, G., & Skaar, E. P. (2012). Taste for Blood: Hemoglobin as a Nutrient Source for Pathogens. *PLoS Pathogens*, *8*(3), e1002535. https://doi.org/10.1371/journal.ppat.1002535

Pollock, N. L., Lloyd, J., Montinaro, C., Rai, M., & Dafforn, T. R. (2022). Conformational trapping of an ABC transporter in polymer lipid nanoparticles. *Biochemical Journal*, *479*(2), 145–159. https://doi.org/10.1042/BCJ20210312

Popot, J.-L. (2010). Amphipols, Nanodiscs, and Fluorinated Surfactants: Three Nonconventional Approaches to Studying Membrane Proteins in Aqueous Solutions. *Annual Review of Biochemistry*, *79*(1), 737–775. https://doi.org/10.1146/annurev.biochem.052208.114057

Popot, J.-L. (2018). Amphipols and Membrane Protein Crystallization. In J.-L. Popot, *Membrane Proteins in Aqueous Solutions* (pp. 497–531). Springer International Publishing. https://doi.org/10.1007/978-3-319-73148-3_11

Popot, J.-L., Althoff, T., Bagnard, D., Banères, J.-L., Bazzacco, P., Billon-Denis, E., Catoire, L. J., Champeil, P., Charvolin, D., Cocco, M. J., Crémel, G., Dahmane, T., de la Maza, L. M., Ebel, C., Gabel, F., Giusti, F., Gohon, Y., Goormaghtigh, E., Guittet, E., … Zoonens, M. (2011). Amphipols From A to Z. *Annual Review of Biophysics*, *40*(1), 379–408. https://doi.org/10.1146/annurev-biophys-042910-155219

Postis, V., Rawson, S., Mitchell, J. K., Lee, S. C., Parslow, R. A., Dafforn, T. R., Baldwin, S. A., & Muench, S. P. (2015). The use of SMALPs as a novel membrane protein scaffold for structure study by negative stain electron

microscopy. *Biochimica et Biophysica Acta*, *1848*(2), 496–501. https://doi.org/10.1016/j.bbamem.2014.10.018

Postle, K., & Larsen, R. A. (2007). TonB-dependent energy transduction between outer and cytoplasmic membranes. *Biometals: An International Journal on the Role of Metal Ions in Biology, Biochemistry, and Medicine*, *20*(3–4), 453–465. https://doi.org/10.1007/s10534-006-9071-6

Privé, G. G. (2007). Detergents for the stabilization and crystallization of membrane proteins. *Methods (San Diego, Calif.)*, *41*(4), 388–397. https://doi.org/10.1016/j.ymeth.2007.01.007

Privé, G. G. (2009). Lipopeptide detergents for membrane protein studies. *Current Opinion in Structural Biology*, *19*(4), 379–385. https://doi.org/10.1016/j.sbi.2009.07.008

Public Health England. (2017). Invasive meningococcal disease in England: Annual laboratory confirmed reports for epidemiological year 2016 to 2017. *Health Protection Report*, *11*(38).

Puthenveetil, R., & Vinogradova, O. (2013). Optimization of the design and preparation of nanoscale phospholipid bilayers for its application to solution NMR. *Proteins: Structure, Function, and Bioinformatics*, *81*(7), 1222–1231. https://doi.org/10.1002/prot.24271

Qiao, S., Luo, Q., Zhao, Y., Zhang, X. C., & Huang, Y. (2014). Structural basis for lipopolysaccharide insertion in the bacterial outer membrane. *Nature*, *511*(7507), 108–111. https://doi.org/10.1038/nature13484

Qiu, W., Fu, Z., Xu, G. G., Grassucci, R. A., Zhang, Y., Frank, J., Hendrickson, W. A., & Guo, Y. (2018). Structure and activity of lipid bilayer within a membrane-

protein transporter. *Proceedings of the National Academy of Sciences*, *115*(51), 12985–12990. https://doi.org/10.1073/pnas.1812526115

Radoicic, J., Park, S. H., & Opella, S. J. (2018). Macrodiscs Comprising SMALPs for Oriented Sample Solid-State NMR Spectroscopy of Membrane Proteins. *Biophysical Journal*, *115*(1), 22–25. https://doi.org/10.1016/j.bpj.2018.05.024

Rawlings, A. E. (2016). Membrane proteins: Always an insoluble problem? *Biochemical Society Transactions*, *44*(3), 790–795. https://doi.org/10.1042/BST20160025

Renaud, J.-P., Chari, A., Ciferri, C., Liu, W., Rémigy, H.-W., Stark, H., & Wiesmann, C. (2018). Cryo-EM in drug discovery: Achievements, limitations and prospects. *Nature Reviews Drug Discovery*, *17*(7), 471–492. https://doi.org/10.1038/nrd.2018.77

Richard, K. L., Kelley, B. R., & Johnson, J. G. (2019). Heme Uptake and Utilization by Gram-Negative Bacterial Pathogens. *Frontiers in Cellular and Infection Microbiology*, *9*, 81. https://doi.org/10.3389/fcimb.2019.00081

Richardson, A. R., & Stojiljkovic, I. (1999). HmbR, a Hemoglobin-Binding Outer Membrane Protein of Neisseria meningitidis, Undergoes Phase Variation. In *JOURNAL OF BACTERIOLOGY* (Vol. 181, Issue 7).

Rodríguez-Ropero, F., & Fioroni, M. (2012). Structural and dynamical analysis of an engineered FhuA channel protein embedded into a lipid bilayer or a detergent belt. *Journal of Structural Biology*, *177*(2), 291–301. https://doi.org/10.1016/j.jsb.2011.12.021

Rohde, K. H., & Dyer, D. W. (2004a). Analysis of Haptoglobin and Hemoglobin-Haptoglobin Interactions with the Neisseria meningitidis TonB-Dependent

Receptor HpuAB by Flow Cytometry. *INFECTION AND IMMUNITY*, *72*(5), 2494–2506. https://doi.org/10.1128/IAI.72.5.2494-2506.2004

Rohde, K. H., & Dyer, D. W. (2004b). Analysis of Haptoglobin and Hemoglobin-Haptoglobin Interactions with the Neisseria meningitidis TonB-Dependent Receptor HpuAB by Flow Cytometry. *INFECTION AND IMMUNITY*, *72*(5), 2494–2506. https://doi.org/10.1128/IAI.72.5.2494-2506.2004

Rohde, K. H., Gillaspy, A. F., Hatfield, M. D., Lewis, L. A., & Dyer, D. W. (2002). Interactions of haemoglobin with the Neisseria meningitidis receptor HpuAB: The role of TonB and an intact proton motive force. *Molecular Microbiology*, *43*(2), 335–354. https://doi.org/10.1046/j.1365-2958.2002.02745.x

Rouphael, N. G., & Stephens, D. S. (2014). Neisseria meningitidis. *Molecular Medical Microbiology: Second Edition*, *3*(3), 1729–1750. https://doi.org/10.1016/B978-0-12-397169-2.00098-6

Salvatore, O., Morrone, G., & Cortese, R. (1987). The human haptoglobin gene: Transcriptional regulation during development and acute phase induction. *The EMBO Journal*, *vol.6*(no.7), 1905–1912.

Sasaki, A., Arawaka, S., Sato, H., & Kato, T. (2015). Sensitive western blotting for detection of endogenous Ser129-phosphorylated α-synuclein in intracellular and extracellular spaces. *Scientific Reports*, *5*(1), 14211. https://doi.org/10.1038/srep14211

Sato, N., Ikeda, S., Mikami, T., & Matsumoto, T. (1999). Bacillus cereus dissociates hemoglobin and uses released heme as an iron source. *Biological & Pharmaceutical Bulletin*, *22*(10), 1118–1121. https://doi.org/10.1248/bpb.22.1118

Scarff, C. A., Fuller, M. J. G., Thompson, R. F., & Iadaza, M. G. (2018). Variations on Negative Stain Electron Microscopy Methods: Tools for Tackling Challenging Systems. *Journal of Visualized Experiments : JoVE*, *132*, 57199. https://doi.org/10.3791/57199

Schauer, K., Rodionov, D. A., & de Reuse, H. (2008). New substrates for TonB-dependent transport: Do we only see the 'tip of the iceberg'? *Trends in Biochemical Sciences*, *33*(7), 330–338. https://doi.org/10.1016/j.tibs.2008.04.012

Scheres, S. H. W. (2010). Classification of structural heterogeneity by maximum-likelihood methods. *Methods in Enzymology*, *482*, 295–320. https://doi.org/10.1016/S0076-6879(10)82012-9

Scheres, S. H. W. (2016). Processing of Structurally Heterogeneous Cryo-EM Data in RELION. *Methods in Enzymology*, *579*, 125–157. https://doi.org/10.1016/bs.mie.2016.04.012

Schmidli, C., Albiez, S., Rima, L., Righetto, R., Mohammed, I., Oliva, P., Kovacik, L., Stahlberg, H., & Braun, T. (2019). Microfluidic protein isolation and sample preparation for high-resolution cryo-EM. *Proceedings of the National Academy of Sciences*, *116*(30), 15007–15012. https://doi.org/10.1073/pnas.1907214116

Schmidt, V., & Sturgis, J. N. (2018). Modifying styrene-maleic acid co-polymer for studying lipid nanodiscs. *Biochimica et Biophysica Acta (BBA) - Biomembranes*, *1860*(3), 777–783. https://doi.org/10.1016/j.bbamem.2017.12.012

Schmitt, M. P. (1997). Utilization of host iron sources by Corynebacterium diphtheriae: Identification of a gene whose product is homologous to eukaryotic heme oxygenases and is required for acquisition of iron from heme and hemoglobin.

Journal of Bacteriology, *179*(3), 838–845. https://doi.org/10.1128/jb.179.3.838-845.1997

Schmitt, M. P., & Holmes, R. K. (1991). Iron-dependent regulation of diphtheria toxin and siderophore expression by the cloned Corynebacterium diphtheriae repressor gene dtxR in C. diphtheriae C7 strains. *Infection and Immunity*, *59*(6).

Seddon, A. M., Curnow, P., & Booth, P. J. (2004). Membrane proteins, lipids and detergents: Not just a soap opera. *Biochimica et Biophysica Acta (BBA) - Biomembranes*, *1666*(1–2), 105–117. https://doi.org/10.1016/j.bbamem.2004.04.011

Sepúlveda Cisternas, I., Salazar, J. C., & García-Angulo, V. A. (2018). Overview on the Bacterial Iron-Riboflavin Metabolic Axis. *Frontiers in Microbiology*, *9*, 1478. https://doi.org/10.3389/fmicb.2018.01478

Shinton, N. K., Richardson, R. W., & Williams, J. D. (1965). DIAGNOSTIC VALUE OF SERUM HAPTOGLOBIN. *Journal of Clinical Pathology*, *18*, 114–118. https://doi.org/10.1136/jcp.18.1.114

Singh, A., Upadhyay, V., Upadhyay, A. K., Singh, S. M., & Panda, A. K. (2015). Protein recovery from inclusion bodies of Escherichia coli using mild solubilization process. *Microbial Cell Factories*, *14*(1), 41. https://doi.org/10.1186/s12934-015-0222-8

Skaar, E. P., & Schneewind, O. (2004). Iron-regulated surface determinants (Isd) of Staphylococcus aureus: Stealing iron from heme. *Microbes and Infection*, *6*(4), 390–397. https://doi.org/10.1016/j.micinf.2003.12.008

Skare, J. T., Ahmer, B. M., Seachord, C. L., Darveau, R. P., & Postle, K. (1993). Energy transduction between membranes. TonB, a cytoplasmic membrane

protein, can be chemically cross-linked *in vivo* to the outer membrane receptor FepA. *The Journal of Biological Chemistry*, *268*(22), 16302–16308.

Slack, M. P. E. (2015). A review of the role of Haemophilus influenzae in community-acquired pneumonia. *Pneumonia*, *6*(1), 26–43. https://doi.org/10.15172/pneu.2015.6/520

Song, Y., Zhang, X., Cai, M., Lv, C., Zhao, Y., Wei, D., & Zhu, H. (2018). The heme transporter HtsABC of group a Streptococcus contributes to virulence and innate immune evasion in murine skin infections. *Frontiers in Microbiology*, *9*(MAY). https://doi.org/10.3389/fmicb.2018.01105

Spencer, R. C. (2003). Bacillus anthracis. *Journal of Clinical Pathology*, *56*(3), 182–187.

Spinola, S. M., Bauer, M. E., & Munson, R. S. (2002). Immunopathogenesis of Haemophilus ducreyi infection (chancroid). In *Infection and Immunity* (Vol. 70, Issue 4, pp. 1667–1676). American Society for Microbiology (ASM). https://doi.org/10.1128/IAI.70.4.1667-1676.2002

Stojiljkovic, I., & Perkins-Balding, D. (2002). Processing of heme and heme-containing proteins by bacteria. *DNA and Cell Biology*, *21*(4), 281–295. https://doi.org/10.1089/104454902753759708

Swainsbury, D. J. K., Scheidelaar, S., Foster, N., van Grondelle, R., Killian, J. A., & Jones, M. R. (2017). The effectiveness of styrene-maleic acid (SMA) copolymers for solubilisation of integral membrane proteins from SMA-accessible and SMA-resistant membranes. *Biochimica et Biophysica Acta (BBA) - Biomembranes*, *1859*(10), 2133–2143. https://doi.org/10.1016/j.bbamem.2017.07.011

Tailleux, L., Waddell, S. J., Pelizzola, M., Mortellaro, A., Withers, M., Tanne, A., Castagnoli, P. R., Gicquel, B., Stoker, N. G., Butcher, P. D., Foti, M., & Neyrolles, O. (2008). Probing host pathogen cross-talk by transcriptional profiling of both Mycobacterium tuberculosis and infected human dendritic cells and macrophages. *PloS One*, *3*(1), e1403. https://doi.org/10.1371/journal.pone.0001403

Tao, H., Lee, S. C., Moeller, A., Roy, R. S., Siu, F. Y., Zimmermann, J., Stevens, R. C., Potter, C. S., Carragher, B., & Zhang, Q. (2013). Engineered Nanostructured β-Sheet Peptides Protect Membrane Proteins. *Nature Methods*, *10*(8), 759–761. https://doi.org/10.1038/nmeth.2533

Tarlovsky, Y., Fabian, M., Solomaha, E., Honsa, E., Olson, J. S., & Maresso, A. W. (2010). A Bacillus anthracis S-Layer Homology Protein That Binds Heme and Mediates Heme Delivery to IsdC. *JOURNAL OF BACTERIOLOGY*, *192*(13), 3503–3511. https://doi.org/10.1128/JB.00054-10

Tascón, I., Sousa, J. S., Corey, R. A., Mills, D. J., Griwatz, D., Aumüller, N., Mikusevic, V., Stansfeld, P. J., Vonck, J., & Hänelt, I. (2020). Structural basis of proton-coupled potassium transport in the KUP family. *Nature Communications*, *11*(1), 626. https://doi.org/10.1038/s41467-020-14441-7

Tauseef, I., Harrison, O. B., Wooldridge, K. G., Feavers, I. M., Neal, K. R., Gray, S. J., Kriz, P., Turner, D. P. J., Ala'Aldeen, D. A. A., Maiden, M. C. J., & Bayliss, C. D. (2011). Influence of the combination and phase variation status of the haemoglobin receptors HmbR and HpuAB on meningococcal virulence. *Microbiology*, *157*(5), 1446–1456. https://doi.org/10.1099/mic.0.046946-0

Taylor, C. M. (2008). Enterohaemorrhagic Escherichia coli and Shigella dysenteriae type 1-induced haemolytic uraemic syndrome. In *Pediatric Nephrology* (Vol.

23, Issue 9, pp. 1425–1431). Springer. https://doi.org/10.1007/s00467-008-0820-3

Thomas, C. E., Olsen, B., & Elkins, C. (1998). Cloning and characterization of tdhA, a locus encoding a TonB-dependent heme receptor from Haemophilus ducreyi. *Infection and Immunity*, *66*(9), 4254–4262.

Tinsley, C. R., & Nassif, X. (1996). Analysis of the genetic differences between Neisseria meningitidis and Neisseria gonorrhoeae: Two closely related bacteria expressing two different pathogenicities. *Proc Natl Acad Sci U S A*, *93*(20), 11109–11114. https://doi.org/10.1073/pnas.93.20.11109

Tolosano, E., Fagoonee, S., Morello, N., Vinchi, F., & Fiorito, V. (2010). Heme scavenging and the other facets of hemopexin. *Antioxidants and Redox Signaling*, *12*(2), 305–320. https://doi.org/10.1089/ars.2009.2787

Tong, S. Y. C., Davis, J. S., Eichenberger, E., Holland, T. L., & Fowler, V. G. (2015). Staphylococcus aureus infections: Epidemiology, pathophysiology, clinical manifestations, and management. *Clinical Microbiology Reviews*, *28*(3), 603–661. https://doi.org/10.1128/CMR.00134-14

Tonge, S. R., & Tighe, B. J. (2001). Responsive hydrophobically associating polymers: A review of structure and properties. *Advanced Drug Delivery Reviews*, *53*(1), 109–122. https://doi.org/10.1016/S0169-409X(01)00223-X

Torres, V. J., Pishchany, G., Humayun, M., Schneewind, O., & Skaar, E. P. (2006). Staphylococcus aureus IsdB is a hemoglobin receptor required for heme iron utilization. *Journal of Bacteriology*, *188*(24), 8421–8429. https://doi.org/10.1128/JB.01335-06

Tribet, C., Audebert, R., & Popot, J.-L. (1996). Amphipols: Polymers that keep membrane proteins soluble in aqueous solutions. *Proceedings of the National Academy of Sciences of the United States of America*, *93*(26), 15047–15050.

Tullius, M. V., Harmston, C. A., Owens, C. P., Chim, N., Morse, R. P., McMath, L. M., Iniguez, A., Kimmey, J. M., Sawaya, M. R., Whitelegge, J. P., Horwitz, M. A., & Goulding, C. W. (2011). Discovery and characterization of a unique mycobacterial heme acquisition system. *Proceedings of the National Academy of Sciences*, *108*(12), 5051–5056. https://doi.org/10.1073/pnas.1009516108

Tullius, M. V., Nava, S., & Horwitz, M. A. (2019). PPE37 Is Essential for Mycobacterium tuberculosis Heme-Iron Acquisition (HIA), and a Defective PPE37 in Mycobacterium bovis BCG Prevents HIA. *Infection and Immunity*, *87*(2). https://doi.org/10.1128/IAI.00540-18

Ujwal, R., & Bowie, J. U. (2011). Crystallizing membrane proteins using lipidic bicelles. *Methods (San Diego, Calif.)*, *55*(4), 337–341. https://doi.org/10.1016/j.ymeth.2011.09.020

Unger, L., Ronco-Campaña, A., Kitchen, P., Bill, R. M., & Rothnie, A. J. (2021). Biological insights from SMA-extracted proteins. *Biochemical Society Transactions*, *49*(3), 1349–1359. https://doi.org/10.1042/BST20201067

Vonck, J., & Schäfer, E. (2009). Supramolecular organization of protein complexes in the mitochondrial inner membrane. *Biochimica Et Biophysica Acta*, *1793*(1), 117–124. https://doi.org/10.1016/j.bbamcr.2008.05.019

Walker, M. J., Barnett, T. C., McArthur, J. D., Cole, J. N., Gillen, C. M., Henningham, A., Sriprakash, K. S., Sanderson-Smith, M. L., & Nizet, V. (2014). Disease manifestations and pathogenic mechanisms of Group A Streptococcus. *Clinical Microbiology Reviews*, *27*(2), 264–301. https://doi.org/10.1128/CMR.00101-13

Wallace, D. F. (2016). The Regulation of Iron Absorption and Homeostasis. *The Clinical Biochemist. Reviews*, *37*(2), 51–62.

Whittaker, R., Dias, J. G., Ramliden, M., Ködmön, C., Economopoulou, A., Beer, N., & Pastore Celentano, L. (2017). The epidemiology of invasive meningococcal disease in EU/EEA countries, 2004–2014. *Vaccine*, *35*(16), 2034–2041. https://doi.org/10.1016/j.vaccine.2017.03.007

WHO publishes list of bacteria for which new antibiotics are urgently needed. (n.d.). Retrieved 26 November 2021, from https://www.who.int/news/item/27-02-2017-who-publishes-list-of-bacteria-for-which-new-antibiotics-are-urgently-needed

Wong, C. T., Xu, Y., Gupta, A., Garnett, J. A., Matthews, S. J., & Hare, S. A. (2015a). Structural analysis of haemoglobin binding by HpuA from the Neisseriaceae family. *Nature Communications*, *6*, 1–11. https://doi.org/10.1038/ncomms10172

Wong, C. T., Xu, Y., Gupta, A., Garnett, J. A., Matthews, S. J., & Hare, S. A. (2015b). Structural analysis of haemoglobin binding by HpuA from the Neisseriaceae family. *Nature Communications*, *6*, 10172. https://doi.org/10.1038/ncomms10172

Woodmansee, A. N., & Imlay, J. A. (2002). Reduced flavins promote oxidative DNA damage in non-respiring Escherichia coli by delivering electrons to intracellular free iron. *The Journal of Biological Chemistry*, *277*(37), 34055–34066. https://doi.org/10.1074/jbc.M203977200

Yadav, R., Noinaj, N., Ostan, N., Moraes, T., Stoudenmire, J., Maurakis, S., & Cornelissen, C. N. (2020). Structural Basis for Evasion of Nutritional Immunity by the Pathogenic Neisseriae. *Frontiers in Microbiology*, *10*. https://www.frontiersin.org/articles/10.3389/fmicb.2019.02981

Yeh, J. I., Du, S., Tortajada, A., Paulo, J., & Zhang, S. (2005). Peptergents: Peptide detergents that improve stability and functionality of a membrane protein, glycerol-3-phosphate dehydrogenase. *Biochemistry*, *44*(51), 16912–16919. https://doi.org/10.1021/bi051357o

Yokogawa, M., Fukuda, M., & Osawa, M. (2019). Nanodiscs for Structural Biology in a Membranous Environment. *Chemical and Pharmaceutical Bulletin*, *67*(4), 321–326. https://doi.org/10.1248/cpb.c18-00941

Yoshiura, C., Kofuku, Y., Ueda, T., Mase, Y., Yokogawa, M., Osawa, M., Terashima, Y., Matsushima, K., & Shimada, I. (2010). NMR Analyses of the Interaction between CCR5 and Its Ligand Using Functional Reconstitution of CCR5 in Lipid Bilayers. *Journal of the American Chemical Society*, *132*(19), 6768–6777. https://doi.org/10.1021/ja100830f

Zaidi, M. B., & Estrada-García, T. (2014). Shigella: A Highly Virulent and Elusive Pathogen. In *Current Tropical Medicine Reports* (Vol. 1, Issue 2, pp. 81–87). Springer Verlag. https://doi.org/10.1007/s40475-014-0019-6

Zeng, X., Xu, F., & Lin, J. (2013). Specific TonB-ExbB-ExbD energy transduction systems required for ferric enterobactin acquisition in Campylobacter. *FEMS Microbiology Letters*, *347*(1), 83–91. https://doi.org/10.1111/1574-6968.12221

Zhao, G., Ceci, P., Ilari, A., Giangiacomo, L., Laue, T. M., Chiancone, E., & Chasteen, N. D. (2002). Iron and hydrogen peroxide detoxification properties of DNA-binding protein from starved cells. A ferritin-like DNA-binding protein of Escherichia coli. *The Journal of Biological Chemistry*, *277*(31), 27689–27696. https://doi.org/10.1074/jbc.M202094200

Zhu, H., Xie, G., Liu, M., Olson, J. S., Fabian, M., Dooley, D. M., & Lei, B. (2008). Pathway for heme uptake from human methemoglobin by the iron-regulated

surface determinants system of Staphylococcus aureus. *Journal of Biological Chemistry*, *283*(26), 18450–18460. https://doi.org/10.1074/jbc.M801466200

Zubcevic, L., Herzik, M. A., Chung, B. C., Liu, Z., Lander, G. C., & Lee, S.-Y. (2016). Cryo-electron microscopy structure of the TRPV2 ion channel. *Nature Structural & Molecular Biology*, *23*(2), 180–186. https://doi.org/10.1038/nsmb.3159